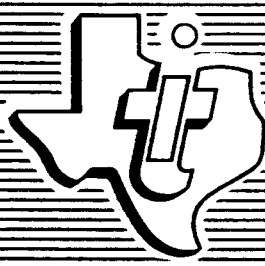


GPO PRICE \$ \_\_\_\_\_  
 CFSTI PRICE(S) \$ \_\_\_\_\_  
 Hard copy (HC) \$ 5.00  
 Microfiche (MF) L

ff 653 July 65

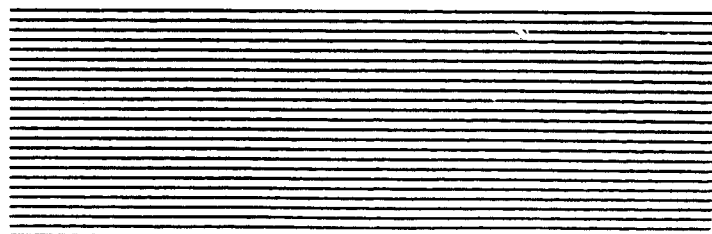
N 66 26245



FACILITY FORM 802

(ACCESSION NUMBER)	(THRU)
770	1
(PAGES)	(CODE)
CR 71926	09
(NASA CR OR TMX OR AD NUMBER)	(CATEGORY)

TEXAS INSTRUMENTS  
INCORPORATED



**STUDY OF SOLID-STATE INTEGRATED  
MICROWAVE CIRCUITS**

**Scientific Report No. 1**

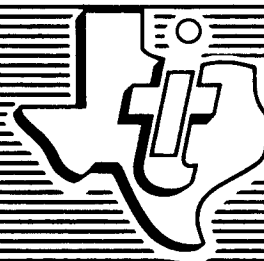
**U4-811500-4**

**31 December 1965**

Prepared for

**NATIONAL AERONAUTICS AND  
SPACE ADMINISTRATION  
Electronics Research Center  
Cambridge, Massachusetts**

Work Performed Under  
Contract No. NAS 12-75  
Control No. ERC/R&D 65-45



**TEXAS INSTRUMENTS  
INCORPORATED**

ABSTRACT

26245

A study of solid-state microwave devices, techniques, and components associated with the 1 - to 6-GHz frequency range is presented. The purpose is to determine the current state of the art of these active and passive devices when applied to integrated circuits.

Separate sections of the report present material on: transistors; striplines; thin-films; lumped-constant circuits; other semiconductor devices, including varactors, PIN diodes, and Schottky barrier diodes; high dielectric constant materials; ferrites; and filters. A summary of the findings is presented as Section II.

## PREFACE

A study of Solid-State Integrated Microwave Circuits, under the sponsorship of the Electronics Research Center of the National Aeronautics and Space Administration, is being performed by Texas Instruments Incorporated under Contract NAS 12-75. The objective of this contract is to perform the analytical study of solid-state integrated microwave circuits, techniques, and components necessary to accurately define the problem areas associated with integrated circuits when various combinations of active and passive circuit elements are required to perform a complete circuit function at microwave frequencies.

In pursuance of this objective, this report presents the results of work performed under the first of four items of the work statement. The period covered is 15 September 1965 through 14 December 1965. This first task is concerned with a study of solid-state microwave devices, techniques, and components associated with the 1- to 6-GHz frequency range. The purpose is to determine the current state of the art (as well as a reasonable projection thereof) of these active and passive devices when applied to integrated circuits. Under subsequent items of the work statement, this information will be used in the design of a simple hypothetical microwave subsystem, specifically, an FM telemetry transmitter.

Separate sections of the report present discussions of each of the major areas of devices, techniques, and components, that is, transistors, striplines, thin-films, etc. In each of these sections, an attempt has been made to present fundamental material that is sufficient for establishing the desired characteristics or parameters of the device, technique, or component discussed. This general information is then followed, wherever possible, with the results of experimental investigation. Most of these results are of very recent origin, and because new information becomes available almost daily, what appears to be a problem today might not be six months from now. Nevertheless, an attempt has been made in the Summary, Section II, to draw conclusions and to outline the problem areas.

Throughout the first phase of the study program, extensive use has been made of the results of company-sponsored programs and, in particular, the work done on the Molecular Electronics for Radar Applications (MERA) program under Contract AF 33(615)-1993 with the Air Force Systems Command, Systems Engineering Group (RTD), Wright-Patterson Air Force Base. The cooperation of MERA program personnel is gratefully acknowledged.

## TABLE OF CONTENTS

Section	Title	Page
I	INTRODUCTION. . . . .	1
II	SUMMARY . . . . .	3
III	TRANSISTORS . . . . .	13
	A. General . . . . .	13
	B. Basic Considerations . . . . .	14
	C. Advances in Microwave Transistors . . . . .	21
	D. Transistor Amplifiers. . . . .	27
IV	STRIPLINES . . . . .	37
	A. General . . . . .	37
	B. Characteristics of Striplines . . . . .	37
	C. Applications of Striplines. . . . .	45
	D. Advances in Integrated Circuit Striplines . . . . .	49
	E. Application Information. . . . .	52
V	THIN-FILMS . . . . .	67
	A. General . . . . .	67
	B. Resistors . . . . .	68
	C. Capacitors . . . . .	77
VI	LUMPED-CONSTANT CIRCUITS. . . . .	85
	A. General . . . . .	85
	B. Design Considerations. . . . .	85
	C. Flat Square Spirals at 500 MHz . . . . .	92
	D. Work In Progress . . . . .	94
VII	OTHER SEMICONDUCTOR DEVICES . . . . .	97
	A. Varactors . . . . .	97
	B. PIN Diodes . . . . .	102
	C. Schottky Barrier Diodes . . . . .	112
	D. Gunn Effect . . . . .	120
VIII	HIGH DIELECTRIC CONSTANT MATERIALS . . . . .	123
	A. General . . . . .	123
	B. Low-loss High Dielectric Constant Resonators . . . . .	123

TABLE OF CONTENTS (Continued)

Section	Title	Page
IX	FERRITES . . . . .	129
	A. General . . . . .	129
	B. Microwave Properties of Ferrites. . . . .	129
X	FILTERS . . . . .	133
XI	PROGRAM PERSONNEL . . . . .	145
XII	CONCLUSION . . . . .	147
	BIBLIOGRAPHY . . . . .	149
	LIST OF SYMBOLS. . . . .	155

LIST OF ILLUSTRATIONS

Figure	Title	Page
1	Approximate High-frequency Equivalent Circuit for a Transistor . . . . .	15
2	Coaxial Test Arrangement for Large-signal Characterization of a Transistor, Schematic Diagram. . . . .	17
3	FEB Configuration . . . . .	18
4	$f_{max}$ as a Function of Transistor Geometry . . . . .	19
5	Power Versus Frequency for Silicon Transistors. . . . .	20
6	Photograph of TI3016A Silicon Planar Transistor Geometry . . . . .	22
7	8306 Geometry. . . . .	26
8	8307 Geometry. . . . .	27
9	Power Gain and Efficiency Versus Peak Pulse Power Output, MERA Device A55D No. 4, 8307 Geometry . . . . .	28
10	Lead Pattern and Geometry for L-146 . . . . .	29
11	Three-stage Power Amplifier Breadboard on Ceramic Substrate . . . . .	30
12	Single-stage, 500-MHz IF Preamplifier . . . . .	31
13	Single-stage, 500-MHz IF Preamplifier, Schematic Diagram. . . . .	32
14	Two-stage, 500-MHz IF Preamplifier . . . . .	33
15	Two-stage, 500-MHz IF Preamplifier, Schematic Diagram. . . . .	34
16	Typical Cross Section of 500-MHz IF Preamplifier . . . . .	35

LIST OF ILLUSTRATIONS (Continued)

Figure	Title	Page
17	Two-stage Monolithic Amplifier . . . . .	36
18	Flat-pack Triplate . . . . .	39
19	$Z_0$ Versus $cn^2a$ . . . . .	41
20	$t/D$ Versus $W/D$ With $\sqrt{\epsilon_r}Z_0$ Ohms as Parameter . . . . .	42
21	Microwave Striplines . . . . .	44
22	Hybrid Ring . . . . .	47
23	Directional Coupler . . . . .	47
24	Branch Line Coupler . . . . .	48
25	Power Dividers . . . . .	50
26	Microstrip Transmission Lines . . . . .	51
27	Microstrip Lines on a Semiconductor Slice . . . . .	53
28	Line Loss as a Function of Top Conductor Thickness for Aluminum, Gold, and Silver Microstrip Lines . . . . .	54
29	Line Loss as a Function of Quartz Dielectric Thickness . . . . .	55
30	Meander Line . . . . .	56
31	Attenuation of Various Stripline Materials Versus Frequency. . . . .	64
32	Equivalent Circuits and Geometries for Diffused and Thin-film Resistors . . . . .	69
33	Variation in Junction Capacitance as a Function of the Ratio of the Total Voltage Across the Junction to the Net Impurity Concentration on the Lightly Doped Side of the Junction. . . . .	71
34	Practical High-frequency Operating Limit for Diffused Resistors . . . . .	72
35	Sheet-resistivity Ranges for Diffused and Thin-film Resistors . . . . .	74
36	Resistance Versus Frequency for a Ta-Ta <sub>2</sub> O <sub>5</sub> Resistor . . . . .	76
37	Equivalent Circuits and Geometries for Diffused, MOS, and Thin-film Capacitors . . . . .	78
38	Dissipation Factor Versus Frequency for Diffused and MOS Capacitors . . . . .	80
39	Capacitance per Unit Area Versus Applied Junction Voltage for the Single-sided Diffused Capacitor . . . . .	81
40	Integrated Circuit Inductors . . . . .	86
41	Characteristics of Loosely Coupled TEM Lines . . . . .	87
42	Inductance of the Flat, Square Spiral as a Function of the Length on a Side D with the Width of the Conductor and the Number of Turns as Parameters . . . . .	88
43	Self-resonant Frequency of the Flat, Square Spiral as a Function of the Length on a Side D with the Width of the Conductor and the Number of Turns as Parameters . . . . .	90

LIST OF ILLUSTRATIONS (Continued)

Figure	Title	Page
44	Coil Q at $f_0/4$ as a Function of the Conductor Thickness $t$ with the Number of Turns as a Parameter . . . . .	91
45	Approximate Q Versus Resistivity . . . . .	94
46	Q Versus Frequency for Four Coils . . . . .	95
47	Q Versus Temperature . . . . .	96
48	Normalized Junction Capacitance of a Typical Varactor . . .	98
49	Measured Capacitance Versus Voltage for Surface-oriented Varactor Diode . . . . .	101
50	PIN Diode Configuration . . . . .	102
51	Diode Equivalent Circuit . . . . .	103
52	Forward Mode Switching Circuits . . . . .	104
53	Reverse Mode Switching Circuits . . . . .	106
54	Surface-oriented Diode Versus Conventional Planar Diode Structure . . . . .	107
55	Surface-oriented PIN Switching Diode and Equivalent Circuits . . . . .	108
56	Surface-oriented PIN Switching Diode in Microstrip Transmission Line at 500 MHz . . . . .	110
57	Power Input Versus Isolation of Surface-oriented PIN Switching Diode in Microstrip Transmission Line at 500 MHz . . . . .	111
58	Typical Construction for a Schottky Barrier Diode . . . . .	113
59	Cutoff Frequency Versus Noise Figure . . . . .	114
60	Experimental One-sided Schottky Diode . . . . .	115
61	Harmonic Generator Diode Structure . . . . .	116
62	Mixer Diode Comparison . . . . .	118
63	Burnout Test, X-band Mixer Diodes . . . . .	119
64	Theoretical Isolation for Microstrip Coupler . . . . .	121
65	Dependence of Dielectric Constant on Temperature for Titanium Dioxide . . . . .	124
66	Geometry and Axis Orientation of Resonator . . . . .	125
67	Mode-frequency Chart for Resonator . . . . .	125
68	Coupled Dielectric Resonators Inside a Cutoff Rectangular Waveguide . . . . .	126
69	Insertion Loss Response Curves for Bandpass Filters Shown ( $f_0 = 3.01$ GHz) . . . . .	126
70	Ferrite Permeability for Circularly Polarized Waves as a Function of Internal Magnetic Field . . . . .	130
71	Parallel Stripline Filter . . . . .	134
72	Parallel Stripline Resonator Filter, Supported Short Circuit Blocks . . . . .	135
73	Interdigital Stripline Filter . . . . .	135
74	Ideal Bandpass Response, $\omega_0 = (1/2)(\omega_1 + \omega_2)$ . . . . .	136



## LIST OF ILLUSTRATIONS (Continued)

Figure	Title	Page
75	Bandpass Response of Filter Using Stripline Elements . . . .	136
76	Parallel Resonator Stripline Filter . . . . .	138
77	Passband Response of a Well-matched Stripline Filter . . . .	139
78	Third Harmonic Response of a Well-matched Stripline Filter. . . . .	141
79	Interdigital Filter. . . . .	142
80	Wideband Response of an Experimental Parallel-coupled Half-wave Resonator Stripline Bandpass Filter . . . . .	143
81	Wideband Response of an Experimental Interdigital Stripline Bandpass Filter. . . . .	144

## LIST OF TABLES

Table	Title	Page
I	Characteristics of 2N3570 and TI3016A . . . . .	23
II	Characteristics of L-146 . . . . .	27
III	Present Versus Desired Performance of the L-146 Device .	29
IV	Merits of Striplines . . . . .	46
V	Types of Power Dividers . . . . .	57
VI	Tolerance Analysis of Stripline Design and Manufacture . . .	65
VII	Temperature Coefficients of Resistance . . . . .	75
VIII	Effect of Substrate and Conductor Thickness on Coil Q . . . .	93
IX	Characteristics of Surface-oriented Varactor Diodes . . . . .	100
X	Electrical Properties of Ferrites and Garnets . . . . .	132

## SECTION I

### INTRODUCTION

One of the major breakthroughs in solid-state electronics was the development of integrated circuits. These circuits have led to significant advances in the reduction of size and weight in electronic equipment, with accompanying orders of magnitude improvement in reliability. In the past, the bulk of the work has been limited to digital circuits, dc amplifiers, and low-frequency amplifiers. The frequency response of linear integrated circuits has been steadily increased, and recently introduced video differential amplifiers can provide 20-dB gain over a bandwidth of 100 MHz. This rapid progress has brought integrated circuit technology to the point where consideration of its application to the microwave frequency spectrum is now feasible.

It is, of course, a big step from 100 MHz to 1 GHz and above. First thoughts usually center around the capabilities of active devices in this frequency range, especially transistors. Improvements in high-resolution photography and in the control of shallow diffusions along with multiple base and emitter contacts have made possible laboratory transistors with CW power outputs of approximately 1 watt at frequencies above 2 GHz, and there is no particular reason to believe that a limit has been reached. Another important consideration involves interconnections. Although the small size of the circuits suggests the possibility of simple overlay lead patterns (because the lead lengths will in many instances be a small fraction of a wavelength), the associated series inductance and parasitic capacitance will generally preclude this simple solution. Sections of transmission line will overcome this problem. Specifically, the microstrip form of stripline is geometrically adaptable to integrated circuits, and laboratory investigations have verified that this is indeed a suitable interconnection technique.

Although many areas still require investigation and significant problems and detailed engineering work remain, it is clear that many of the standard microwave circuit functions can be performed in integrated circuitry. In this report, we have endeavored only to establish the current capabilities and limitations of the devices, components, and techniques required in the 1- to 6-GHz frequency range as applied to integrated circuitry.

## SECTION II

### SUMMARY

#### A. TRANSISTORS

High-frequency transistors require narrow base width, low base resistance, and low collector capacitance. The very small dimensions are made possible by advanced photomasking techniques, while improved control of shallow diffusions has allowed narrow base widths on the order of 0.01 mil. Narrow emitters and close spacing between emitter and base contacts are necessary for low base resistance. This resistance is also decreased by the use of a shallow diffusion, high concentration of impurities in the base region, and the paralleling of many paths. Capacitances are minimized by keeping junction areas small, and collector capacitance is lowered when collector resistivity is raised. The design of a transistor is, of course, a compromise and care must be exercised; otherwise, one parameter may be improved at the unwanted expense of another.

For high-frequency operation with a high power output, an interdigitated geometry with multiple emitter and base contacts is utilized. In general, power output capability is increased as the number of these contacts is increased. Examples are the TI3016A with 4 base and 3 emitter contacts and the experimental 8307 geometry with 65 fingers, 33 base and 32 emitter contacts. The latter device will deliver about 1 watt CW at 2 GHz with 3 dB power gain. The base and emitter contacts in the 8307 device are 0.2 mil wide and 3 mils long. The design of the device allows five emitter bonds and five base bonds, which reduces lead inductance below the level of previously constructed similar devices. At this writing, a new geometry having 85 interdigitated fingers which are narrower and shorter than those of the 8307 is in process. Improved performance including better thermal characteristics is expected.

Work on low-level, low-noise devices for integrated circuits is also progressing. Transistors being designed for use in a 500-MHz preamplifier for the MERA program now employ five interdigitated base emitter contacts. Measured noise figures fall between 3 and 4 dB, with most of the units measuring around 3.5 dB. Earlier devices, with measured noise figures ranging from 4 to 7 dB, used two base contacts and one emitter contact.

This study has shown that transistors are being designed specifically for application to microwave integrated circuits and that significant accomplishments have been made in recent months. The FM transmitter to be designed as a part of this study is required to have 1 to 5 watts output at 1 to 2 GHz. Laboratory devices currently under evaluation are capable of the lower power limit, 1 watt, at 2 GHz. Higher powers may be achieved by multiple device circuitry, although the impedance matching problems are tedious.

Device improvements and circuitry techniques for using the devices are progressing at such a rate that the situation may be considerably different five to six months from now. (This is also true of devices needed for circuits other than the power amplifier). At that time, the final design of the transmitter will be under way and we will be again evaluating device performance.

## B. STRIPLINES

Connections between devices in low-frequency and digital integrated circuits are usually made by simple overlay lead patterns. In microwave integrated circuits the reactance of this type of connection would be high because of the series inductance and parasitic capacitance of the lead. Furthermore, resonance and antenna effects would be prevalent at high frequencies, particularly when the length of the connections approach the wavelength. For these reasons, sections of transmission lines must be used for interconnections at high frequencies.

Investigations have shown that the microstrip configuration of stripline, consisting of a ground plane and a narrow strip conductor separated by a dielectric, can be applied to microwave integrated circuits. Its planar structure makes it generally applicable to integrated circuit processes. In principle, only three levels of material are required for microstrip, whereas five are required for triplate construction.

The characteristic impedance of microstrip is primarily influenced by the dielectric constant and the ratio of the width of the top conductor to the thickness of the dielectric. For this reason, scaling can be applied in the design of these lines to reduce their size to dimensions compatible with integrated circuit dimensions. For integrated circuit application it is desirable to use silicon as the dielectric. When this is done, the resistivity must be high (1500 ohm-cm or greater) if line losses are to be held low (below 1.0 dB/cm).

Measurements have been made recently on microstrip transmission lines deposited on slices of high resistivity P-type silicon which was used as the dielectric. The experiment included measurements on lines having different top conductor widths. For a dielectric thickness of 10 mils, it was found that the microstrip line having a top conductor width of 6 mils most nearly matched the 50-ohm test system (VSWR < 1.10). Measurements were also made on the effect of top conductor thickness on line loss for three different materials: aluminum, gold, and silver. The skin depth for these three materials varies between 27 and 35 microinches. For conductor thickness greater than about twice the skin depth, the loss essentially reaches its minimum value. These values were shown to be 0.55 dB/cm for aluminum, 0.40 dB/cm for gold, and 0.30 dB/cm for silver.

Thick-film evaporation techniques have been used to deposit aluminum and silver top conductors. Since silver does not adhere well to silicon, a

very thin film of vanadium is evaporated on the silicon first and the silver evaporated on the vanadium. A thick gold film is developed by plating over a thin evaporated gold film. Although these processes are being continually improved, the application of current process steps yields excellent microstrip components. However, when striplines are combined on the same substrate with active devices, which require high-temperature diffusions, the bulk resistivity of the silicon dielectric in the microstrip is sometimes reduced drastically. Although this problem is not completely solved, careful control of process steps minimizes its occurrence, and investigations aimed at its complete solution are being conducted.

Standard microwave components such as couplers, transforming sections, and a class of filters can be built using this stripline technique. For example, a balanced mixer consisting of a hybrid, the diodes, and an output filter has been constructed using microstrip techniques on a 160-by 260-mil chip.

### C. THIN-FILMS

Thin-film passive components such as capacitors and resistors offer several advantages over their diffused counterparts. Broadly speaking, there are two reasons for using thin-film passive components: First, it may be impossible to achieve the desired characteristics using diffused components, whereas these characteristics are possible with thin-films. Second, although it might be possible to achieve the desired characteristics using diffused components, the diffusion process would have been optimized for the passive components with the result of degrading the parameters of the active devices made on the same substrate.

Thin-film components have been used in two ways. The multichip approach, wherein the passive components are deposited on separate substrates from the active components, is the most versatile and the older of the two. In the second approach, all components are fabricated on the same substrate; this is the true hybrid thin-film/monolithic circuit and the approach of principal interest.

Tantalum and nickel-chromium metal films have been widely used to fabricate thin-film resistors. Such resistors offer improved performance over diffused resistors in their temperature coefficient of resistance, reduced distributed capacity, wider range of sheet resistance, higher voltage breakdown, lower tolerance, and much higher operating frequency limit. The improved high-frequency performance is due to the greatly reduced parasitic capacitance. These films can be used effectively when the passive components are deposited on a substrate separate from the active components. However, they are easily damaged by the high temperatures encountered in the integrated circuit final assembly operations, ball bonding and bar mounting.

Cermet (Ta-Ta<sub>2</sub>O<sub>5</sub>) resistors have much greater stability (they are an order of magnitude thicker than the metal films used) and compatibility with the high-temperature assembly operations mentioned. For this reason, Cermet is the material of chief interest for use with thin-film/monolithic circuits.

Cermet resistors can be fabricated with sheet resistivities over a wide range (1 to 5000 ohms per square), thus affording good control of parasitic capacity to substrate. Since this capacity is proportional to the area covered by the resistor pattern, the high-frequency performance is improved by keeping this area small. The temperature coefficient of resistance will, depending upon a number of factors, lie between the limits of -20 and -1000 ppm/°C.

Cermet resistors are stabilized by baking at 350°C prior to the ball-bonding and bar-mounting operations which are performed at 300°C; they readily withstand these temperatures. These resistors are suitable for use at high frequencies. Their performance is a function of value and physical size because of the influence of these two parameters on the effect of and the value of parasitic capacity. Furthermore, the silicon substrate resistivity influences the high-frequency characteristics and should be kept high. Circuits using these resistors have shown excellent performance at frequencies as high as 500 MHz, which is the limit of current application requirements and not a fundamental performance limit.

As the dielectric material SiO<sub>2</sub> and Ta<sub>2</sub>O<sub>5</sub> have been used extensively in the fabrication of thin-film capacitors, Ta<sub>2</sub>O<sub>5</sub> has been used at frequencies up to about 10 MHz, above which its dielectric properties are degraded. This material is usually used at the lower frequencies, where the need for larger values of capacitance is more readily satisfied by its dielectric constant (which is higher than the dielectric constant of SiO<sub>2</sub>). Since the basic dielectric properties of SiO<sub>2</sub> are good out to about 25 GHz, it is the material of interest in this study.

An important benefit derived from the use of thin-film capacitors is the much reduced parasitic capacity to substrate as compared to that encountered when diffused capacitors are used. The ratio of desired to parasitic capacity for diffused capacitors can be as low as 2 to 1, whereas this ratio can easily be made greater than 10 to 1 when thin-film capacitors are used. A capacity per unit area as high as 0.6 pF/mil<sup>2</sup> can be achieved with SiO<sub>2</sub> as the dielectric. For high-frequency applications, thick capacitor plates are needed if reasonable values of Q are to be achieved. When thick plates are required, thicker dielectrics are also required. This limits the attainable capacities per unit area to 0.1 to 0.2 pF/mil<sup>2</sup> for capacitors to be used at high frequencies. SiO<sub>2</sub> capacitors have temperature coefficients ranging from 6 to 30 ppm/°C, a marked improvement over the 700 ppm/°C typical for diffused units.

Both aluminum and molybdenum-gold plates have been used successfully. Both are compatible with the 300°C final assembly integrated circuit

operations of ball bonding and bar mounting. The development of pinholes in the dielectric is still a problem which lowers yields, in spite of improved processing which has alleviated the problem somewhat. This is the reason thick dielectrics are used when thick plates are used. SiO<sub>2</sub> capacitors have been fabricated with values ranging from 5 to 10 pF for signal-path applications and values between 125 and 300 pF for bypass applications. Measurements have shown that no appreciable increase in Q is obtained for plates thicker than about two times the skin depth. As a typical example, the Q of a 15-pF capacitor was measured to be 200 at 1 KHz and 47 at 500 MHz. Tests at higher frequencies have not been made because of the lack of an application, but as in the case to thin-film resistors, good performance at higher frequencies is expected.

#### D. LUMPED-CONSTANT CIRCUITS

Interest in lumped-constant circuits in integrated microwave circuits stems from the possibility of realizing circuit elements of small size. While there is no sharp line defining the boundary between which lumped-constant and distributed constant circuits can be used, the most fundamental consideration is the size of the lumped-constant circuit element relative to the operating wavelength. In general, the largest dimension of the element should be no more than 1 percent of the wavelength. At 1 GHz the wavelength is 30 cm, which would indicate that circuit element dimensions on the order of 0.3 cm (118 mils) could be used. Fortunately, this dimension is compatible with the values of inductance and capacity which might be useful in this frequency range. Thin-film capacitors having a capacity per unit area of 0.1 pF/mil<sup>2</sup> can be reliably fabricated. Assuming that the geometry for the capacitor is square and the values needed are in the range of 5 to 75 pF, the dimensions will range between 7 and 27 mils on a side. Similarly, inductors can be made by using thick-film deposition processes. Assuming that the "coil" is square and that values in the range of 0.5 to 10 nH will be required, the geometry can be less than 50 by 50 mils. In both cases the physical size is compatible with the 1 percent of wavelength criterion.

Unfortunately, this basic size consideration is only part of the problem, the other part being with parasitic effects. Integrated circuit inductors have undesired parasitic capacity to a lossy substrate and from turn to turn; resistors also have parasitic capacity to the lossy substrate; and capacitors have series resistance and inductance as well as parasitic capacity to the substrate. These undesired "circuit elements" limit the usefulness of these so-called lumped-constant circuits.

Resistors, capacitors, and inductors are needed for lumped-constant circuits. The performance of resistors and capacitors suitable for application to integrated circuits has been discussed in the preceding subsection. For integrated circuits, inductors in the form of flat, square spirals may be used. Experimental work has been at 500 MHz, the application being an IF preamplifier.

Measurements have shown that the inductance of a flat, square, spiral inductor operating at 500 MHz can be calculated within  $\pm 10$  percent, based on the geometry of the coil, using low frequency inductance formulas. Similarly, self-resonant frequencies can be approximated based on the geometry. However, an analytical approach to determining the  $Q$  of the inductor is not yet available. A simple approach based on determining the effective plate resistance yields an upper bound on the  $Q$ . Realized  $Q$ 's are less than this value by a factor of about 3. The major factor contributing to this reduction is the resistivity of the substrate. Using P-type silicon substrates with an 8000 Å insulating layer of SiO<sub>2</sub> and an aluminum-deposited conductor, measurements show a factor of 3 increase in  $Q$  as the substrate resistivity is increased from 1000 to 4000 ohm-cm. The  $Q$  increases with increased conductor thickness up to the point where the thickness is twice the skin depth of the material; beyond this thickness, the increase of  $Q$  is negligible. A specific example indicates the present status of the experimental work. A 4-turn coil with a 4-mil-wide conductor and 4-mil turn separation deposited on 5000 ohm-cm P-type material has a 29-nH inductance at 500 MHz. With a conductor thickness of 300 microinches, the  $Q$  is 25. Such inductors will be suitable for many applications and the thick-film deposition processes are compatible with other integrated circuitry processes.

#### E. OTHER SEMICONDUCTOR DEVICES (VARACTORS, PIN DIODES, SCHOTTKY BARRIER DIODES)

The nonlinear capacitance of a varactor is useful in many ways. Generally speaking, these involve conversion of power at one RF frequency to another. Two, three, four or more frequencies may interact in the varactor, and of those some may be useful inputs or outputs, while others are idlers that are not part of any input or output although they may be necessary to the operation of the device.

The chief requirement is for high-frequency varactor diodes to be capable of use in frequency multiplier circuits as well as being structurally compatible with integrated circuit design techniques. For use in a frequency multiplier chain, a surface-oriented diode has been developed. For this variable reactance device, maximum possible  $Q$  is essential. The surface-oriented varactor diode structure has several unique advantages. The extensions of the heavily doped N<sup>+</sup> and P<sup>+</sup> material into the high resistivity substrate allows all of the effective diode area to be confined to the low resistivity epitaxial layer. This results in maximum possible varactor  $Q$  attainable from the device.

Surface-oriented varactor diodes have been fabricated, and extremely high leakage currents were observed. This may be explained by the external high surface concentrations. The leakage currents were reduced by the introduction of a three-hour 900°C oxygen step following the boron diffusion.



The diodes have been evaluated in the  $\mu$  mesa\* package using the third terminal as a ground terminal for capacitance measurements. The metal case was also connected to the ground terminal to minimize the package capacitance. This was found to be an extremely beneficial step since it reduced the package capacitance from 0.30 pF to 0.04 pF. The results of experimental work has verified the analytical procedures used. Fabrication of surface-oriented varactor diodes has been compatible with stripline interconnection techniques. The results so far are quite promising.

Pin diodes are ideal for switching applications, and the surface-oriented PIN switching diode has been developed for compatible interconnection with microstrip transmission lines. At microwave frequencies, stray capacitance must be reduced to a minimum to avoid loss of component function. The use of a surface-oriented diode structure allows the reduction of stray capacitance resulting from contacts expanded over oxide-protected active substrates. These diodes have a geometry in which the anode and cathode areas are adjacent at the surface of a silicon chip and have a carrier flow under bias which is approximately parallel to the surface. The requirement is for low resistance on forward bias to provide low insertion loss and low capacitance on reverse bias so as to obtain high isolation.

For the conventional planar diode, the contacts to the other elements of the integrated circuit are made by means of metal stripes of the required width, separated from a ground plane by high resistivity silicon, forming a microstrip transmission line. The diode design must be compromised to conform to the required geometry. Large capacitance results from design requirements for other diode parameters. In order to reduce the diode resistance on forward bias, a large anode area is needed; this will result in increased capacitance upon reverse bias. The metal contacts are expanded over oxide-protected active substrates, thereby further increasing the capacitance.

In the surface-oriented diodes, we have typically anode and cathode diffusions into the high resistivity silicon and metallic contacts in opposite directions to form the microstrip transmission line. On forward bias, carriers are injected into the I region all along the PN junction, reducing the series resistance by means of conductivity modulation. On reverse bias, there exists a number of parallel capacitors with the maximum capacitance occurring at the closest spacing. The reverse bias capacitance is therefore largely determined by the depth of diffusion. To achieve low resistance on forward bias, the spacing between anode and cathode is made very small, causing the diodes to punch through on reverse bias; but the larger capacitance of a punch-through condition is offset by the ability to control capacitance by the diffusion depth. The surface-oriented diode conforms readily to microwave stripline geometry, and effects of expanded contacts are minimized.

When the equivalent circuit for a PIN diode is considered as an RX meter parallel circuit, the MOS and barrier capacitance are combined into

---

\*Trademark of Texas Instruments Incorporated.

one measurable value. A large value of MOS capacitance could reduce the effectiveness of the small reverse bias capacitance and make the diode switch useless at high frequencies. To evaluate this possibility, data were taken for typical values of elements for two different substrate resistances. The results showed that the MOS capacitance essentially disappears above 10 MHz and that only the barrier capacitance is effective.

Schottky barrier diodes are well suited for use in integrated circuits in the microwave frequency region. A planar structure which utilizes the properties of a metal-semiconductor junction, the Schottky barrier exhibits the properties of an abrupt junction rather than the graded junction characteristics of the diffused junction devices. The use of thin epitaxial layers in conjunction with planar Schottky barrier junctions has produced very high Q microwave devices.

An important area of application for Schottky barrier diodes is in microwave mixers. A single-sided silicon microwave mixer diode has been fabricated; it is suitable for integration with a microstrip hybrid formed directly on high-resistivity silicon. The diodes are formed on epitaxial material that has been grown in vapor etched pockets in high-resistivity P-type silicon substrate material. These holes are selectively placed on the substrate, their positions being determined by windows in the oxide layer, which acts as a barrier to the etch where no windows exist. The holes, which are about 0.1 mil deep, are then refilled with N-type epitaxy of about 0.05 ohm-cm resistivity. Portions of the epitaxial region which are to act as ohmic contacts are then given a heavy N<sup>+</sup> deposition and molybdenum gold is evaporated to form a metal-semiconductor contact. Diodes fabricated in this way have been subjected to extensive testing and the results are quite promising.

#### F. HIGH DIELECTRIC CONSTANT MATERIALS

High dielectric constant materials have been used at microwave frequencies in essentially two ways. First, they have been used to reduce the size of microwave components such as cavities. The size reduction is proportional to the square root of the dielectric constant. This is due to the fact that the wavelength in the material is reduced by this same factor. Thus, for a dielectric-filled cavity where the dielectric constant is 100, the volume of the cavity would be reduced by a factor of 1000 compared to an air-filled cavity. The materials have been used to build tunable cavities having high Q's and broad tuning ranges. In the second type of application, the characteristic of the material exhibits resonances in various modes when operated with free space boundaries. Microwave filters utilizing coupled dielectric resonators have recently been constructed and tested. Three-dB bandwidths of less than 20 MHz have been realized at 3 GHz.

The most general material considered for use is TiO<sub>2</sub>. Its dielectric constant is around 100 at 25°C. The main problem with this and other

materials is the strong dependence of the dielectric constant on temperature. Materials such as  $\text{BaTiO}_2$  and  $\text{SrTiO}_2$  have higher dielectric constants and even greater dependence on temperature.

Although the characteristics of these materials can be utilized to reduce the size of standard microwave components and to provide small high Q filters, it is not yet evident how they may be used in microwave integrated circuits.

## G. FERRITES

Magnetic oxides have become particularly important because in addition to their magnetic properties they possess very high electrical resistivities ( $\rho > 10^6$  ohm-cm). Hence, they can be used at very high frequencies. On the other hand, magnetic metals, with their relatively low resistivities, exhibit such severe skin effect at high frequencies that magnetic fields do not penetrate into the bulk of the metal and their inherent magnetic properties cannot be exploited. In engineering practice almost all magnetic oxides are called ferrites, regardless of whether they contain iron.

The property of extremely high resistivity makes it possible to use ferrites as microwave circuit elements, whereas with iron a microwave signal sees an effective reflector. In the case of ferrite the wave can enter and pass through substantial amounts of the material without excessive reflection or attenuation, and in the process the wave has an opportunity for strong interaction with the spinning electrons. As a result of this interaction, nonreciprocal phase shift and attenuation as well as nonlinear effects can, under certain suitable conditions, be manifested.

Presently, the state of the art in ferrite devices is quite limited with regard to integrated circuits. This limitation is due to the difficulty of achieving small dimensions compatible with integrated circuits while providing the external field required. To avoid this problem, several of the circuit functions customarily assigned to ferrite devices will be performed with surface-oriented diodes, for example, switches, modulators, and phase shifters. Other circuit functions can be performed with ferrite devices having small dimensions compatible with integrated circuits as an external circuit element, for example filters, isolators and circulators.

## H. FILTERS

Transmission line structures compatible with integrated circuitry can be accomplished in microstrip form. Since this is the case, an important class of filters can be fabricated in integrated circuits.

An example of this class of filters is a bandpass filter consisting of parallel half-wavelength stripline resonators. The resonators are positioned

adjacently but offset by half of their length; the coupling of these resonators is a function of the spacing between them. This filter allows the use of open-circuit resonators, which eliminates a major grounding problem. This construction is particularly convenient for printed-circuit filters. The filter has a second passband at the third harmonic and, if not precisely tuned, will exhibit a narrow spurious passband near the second harmonic. Such filters built in conventional printed-circuit form have a VSWR less than 1.15 and an insertion loss of 0.3 dB or less at a center frequency of 3 GHz.

The interdigital filter has an improved response characteristic, but unlike the preceding example, requires short-circuited resonators. This matter of providing an RF short circuit is, in practice, very difficult to achieve in conventional printed-circuitry and there is no reason to believe that it would be any easier in integrated circuits. Though experimental work has not been done in this area, there is sufficient reason to believe that many of the standard stripline filters can be realized in integrated circuits. One of the problems will be minimizing the loss-per-unit length of the integrated circuit microstrip line to avoid compromising the fundamental filter design.

## SECTION III

### TRANSISTORS

#### A. GENERAL

Germanium and silicon transistors with maximum operating frequencies  $f_{\max}$  in the range of 6 GHz have recently become available. This advance is due primarily to basic improvements in the technologies of diffusion and high-resolution photography. These improvements have made possible the realization of transistor amplifiers at correspondingly high frequencies and with higher gain-bandwidth products at lower frequencies.

The three materials generally considered for application to conventional transistor structures are germanium, silicon and gallium arsenide. The general status and capability of each of these materials are reviewed in the following paragraphs. In addition, the metal base transistor is discussed.

##### 1. Germanium

Germanium transistors with a maximum frequency of oscillation  $f_{\max}$  in excess of 10 GHz are presently being made in the laboratories. These are a result of investigations into the planarization of germanium, and further improvement in performance is expected. Germanium is the best currently available basic material for achieving the highest  $f_{\max}$ . Unfortunately, it is the poorest material from the standpoint of operating temperature. For a given frequency capability (i. e.,  $f_{\max}$ ), germanium will have the lowest power output, since its lower permissible junction temperature will limit power input.

##### 2. Silicon

Silicon transistors are at present in the best position to supply microwave power. The most serious limitation to silicon transistor performance is the relatively poor majority carrier mobility in the base, which results in a base resistance higher than that of germanium. However, this disadvantage has been almost completely overcome by the photomasking techniques now being used with silicon. With emitter stripe widths of 0.1 mil, it has been possible to reduce  $r_b$  to values comparable to that achieved in germanium. During the next two years, continuing improvements in photomasking techniques plus better control of shallow diffusions will result in raising the  $f_{\max}$  of silicon transistors to somewhere in the 9-GHz region.

##### 3. Gallium Arsenide

Gallium arsenide transistors have a typical temperature range from  $-200^{\circ}\text{C}$  to  $+300^{\circ}\text{C}$  and should yield transistors capable of operating at high frequencies. Devices with an  $h_{fe}$  of 40 to 50 at  $300^{\circ}\text{C}$  have been

obtained by Texas Instruments in the laboratory. The leakage current is better than that of silicon devices by an order of magnitude. In the current state of the art, gallium arsenide has several disadvantages: a high noise figure, a decreasing  $h_{fe}$  with increasing temperature, and a high emitter resistance. At the present time, efforts are being made to alleviate these problem areas so that a useful transistor can be built in the future.

Gallium arsenide transistors are not yet available for high-frequency power applications. Some relatively high-current gain cutoff frequencies have been realized, but not in conjunction with other desirable parameters. Although gallium arsenide and related III-V ternary materials are expected to provide a family of high-frequency devices in the 1- to 10-GHz region, it is unlikely that these will be fully developed in the next two years.

#### 4. Metal Base Transistor

A further consideration of transistors is the metal base transistor. Theoretical calculations on the metal base transistor indicate higher frequencies of operation and the possibility of achieving higher power levels. For investigation purpose at Texas Instruments, the Au/GaAs system has been chosen. Gold layers have been deposited on GaAs surfaces by various methods and examined under a variety of conditions. Little difficulty has been experienced with this technique in the formation of thin, ordered gold films. The further operation of producing a single-crystal GaAs film on the gold layer does present a problem, which has not yet been solved. Devices of this sort, while not presently available, must be considered in future applications because of their potential impact.

For the purpose of the present study, only the germanium and silicon technologies are sufficiently advanced. Of these two, silicon offers more in the combinational requirements of high ambient temperature, high-frequency operation and high power output.

### B. BASIC CONSIDERATIONS

High-frequency transistors require low base resistance  $r_b'$  and collector capacitance  $C_c$ . A useful equivalent circuit applicable for small-signal consideration is shown in Figure 1. Typical values of the parameters for a commercially available silicon NPN microwave transistor, the TI3016A, are:

$$r_b' = \text{base spreading resistance} \approx 10 \text{ to } 20 \text{ ohms}$$

$$C_c = \text{collector to base capacitance} \approx 0.5 \text{ pF}$$

$$r_e = \text{emitter resistance} \approx 26/I_E(\text{mA}) \text{ ohms} \approx 1.3 \text{ ohms at } 20 \text{ mA}$$

$$C_e = \text{emitter storage capacitance} \approx 1/2 \pi f_T r_e \approx 60 \text{ pF typical,}$$

where  $f_T$  is the frequency at which the common emitter current gain is unity, 1.8 GHz typical for this device.

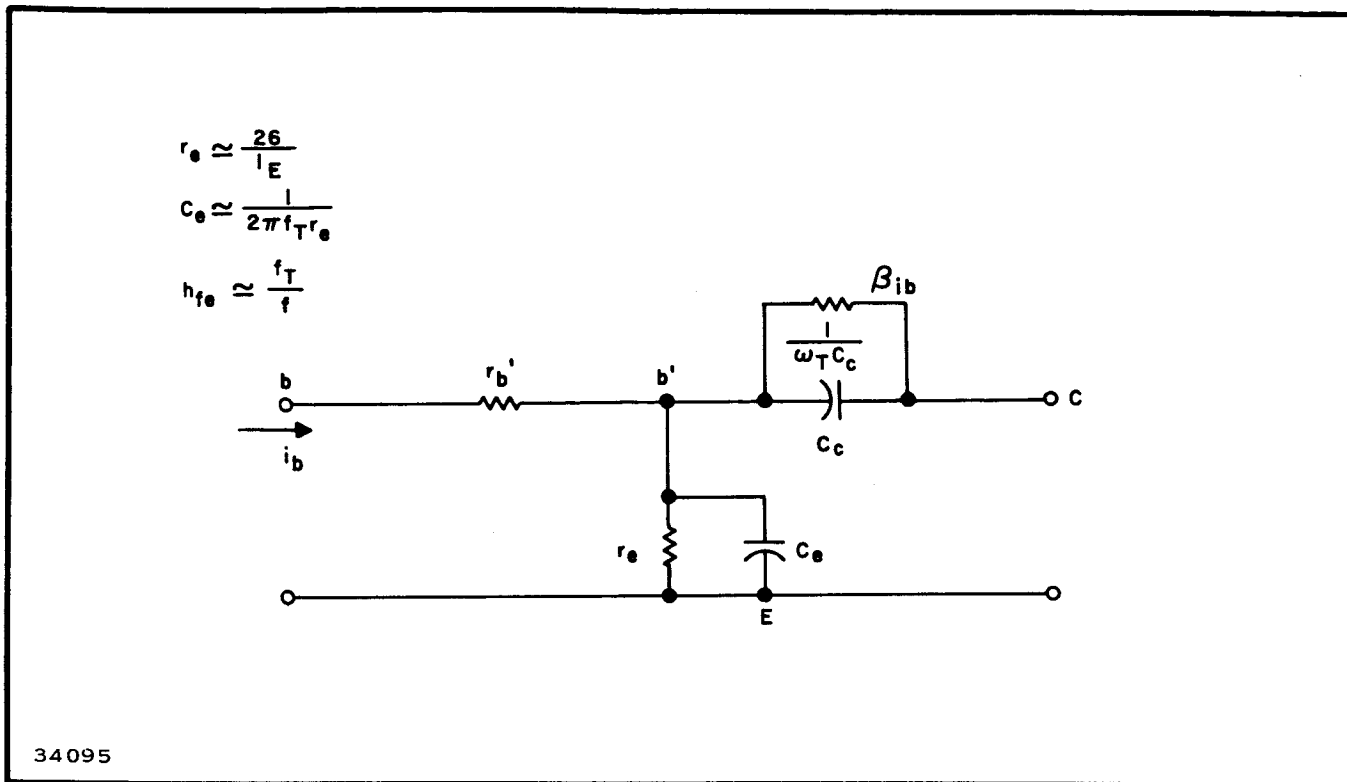


Figure 1. Approximate High-frequency Equivalent Circuit for a Transistor

Performance factors of high frequency transistors have been summarized by Cooke<sup>1</sup>, and only the pertinent relationships are repeated here.

Power gain of a transistor is given by

$$PG \approx \left( \frac{f_{\max}}{f} \right)^2 \quad (1)$$

where

$f_{\max}$  = maximum frequency of oscillation

$f$  = operating frequency

$f_{\max}$  can be determined by

$$f_{\max} = 200 \sqrt{\frac{\alpha_0 f_T}{r_{b'} C_c}} \quad (2)$$

where

$\alpha_0$  = low frequency alpha of the transistor

$f_T$  = frequency in MHz, where the common emitter current gain is unity

$r_{b'}$  = base spreading resistance in ohms

$C_c$  = collector to base capacitance in pF.

Combining Equations (1) and (2), we obtain

$$PG = \frac{4 \times 10^4 \alpha_o f_T}{f^2 r_b' C_c} \quad (3)$$

The 6-dB-per-octave gain rolloff implied by the square term in the denominator applies, of course, only in the high-frequency region.

Another important characteristic of transistors in their noise figure, which depends on much the same parameters as gain and is given by<sup>2, 3</sup>

$$F = 1 + \frac{r_b'}{R_g} + \frac{r_e}{2R_g} + \frac{(r_b' + r_e + R_g)^2}{2\alpha_o R_g r_e} \left[ \frac{1}{h_{fe}} + \left(\frac{f}{f_\alpha}\right)^2 \frac{I_{CO}}{I_E} \right] \quad (4)$$

For transistors operating under small-signal conditions, conventional characterization in terms of Y or other parameters may be used for circuit design. Accurate measurement of the parameters is somewhat more difficult than at lower frequencies; nevertheless, in principle and practice, the same techniques employed at lower frequencies to measure transistor parameters can also be applied in the microwave region.

Transistors designed with higher current and power dissipation ratings, while maintaining performance capabilities well into the microwave region, are becoming increasingly available. Single transistors capable of delivering a 2-watt output above 2 GHz are now available in the laboratory. It is desirable to utilize such transistors as oscillators and amplifiers where power output and efficiency are of prime importance. The maximum power output and efficiency from a given transistor is obtained under Class C operations (i.e., collector current flowing appreciably less than one-half cycle), and in general the parameters of the transistor under such large-signal operation vary considerably from small-signal values. This variance of parameters is not necessarily objectionable when it is possible to incorporate tuning adjustments in the amplifier or oscillator circuit. However, it is often undesirable, from either a fabrication or a design philosophy viewpoint, to employ tuning adjustments in integrated circuit applications. Under such conditions it is necessary to obtain a knowledge of the transistor characteristics at various "levels" of large-signal operation.

One method of obtaining the information desired in a form directly applicable to amplifier circuit design<sup>7</sup> is shown in Figure 2. This figure represents a single-stage test amplifier with the networks  $N_i$  and  $N_o$  being adjustable and capable of presenting a wide range of impedance variation to the transistor. The transistor under measurement is operated in the test amplifier at various output powers and at the desired frequencies. The source and load admittances (or impedance) can then be determined either directly from the tuning stub positions or by VSWR measurements made looking back toward the source (or load) and referenced to the



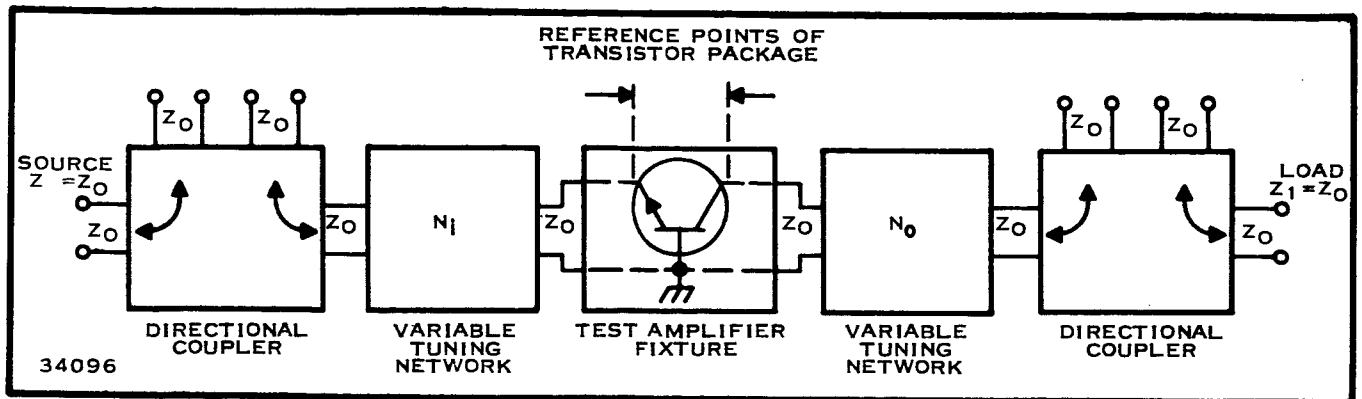


Figure 2. Coaxial Test Arrangement for Large-signal Characterization of a Transistor, Schematic Diagram<sup>7</sup>

transistor terminals. The important point is simply that the small-signal equivalent circuit is no longer applicable for large-signal operation.

The choice of whether the basic circuit configuration should be common emitter or common base or, in some cases, common collector, depends upon a detailed analysis of a number of factors such as the operating frequency, circuit function to be realized, transistor parameters, and impedance levels. However, the following general comments can be made.

The common base (CB) configuration is characterized by a relatively low input and high output impedance and a positive internal feedback. The feedback is due to the collector capacitance  $C_C$ , which makes circuit instabilities possible if the input and output loading is not correct. As the current gain  $\alpha$  is less than unity, the power gain is obtained purely by impedance transformation.

The common emitter (CE) configuration has a somewhat higher input impedance and a lower output impedance than the common base. The internal feedback due to  $C_C$  is negative, which tends to reduce the gain below the maximum power gain unless  $C_C$  is neutralized. When the transistor has an  $f_T$  suitably higher than the operating frequency (on the order of two times or more), it is generally preferable to operate in the CE configuration because of the inherent stability of this mode of operation.

At the higher frequencies ( $f > f_T/2$  typically) the CB configuration becomes more attractive. The common collector circuit has a number of limitations and is not generally the best choice for high-frequency amplifier circuits.

In general, semiconductor networks are fabricated around an NPN structure for transistor fabrication and the third PN junction for isolation as shown in Figure 3. This is the simple triple diffused structure. There are several types of integrated device structures in use ranging from this relatively simple structure to the complex epitaxial structures. Resistors, capacitors, and diodes are fabricated at the same time as the transistor

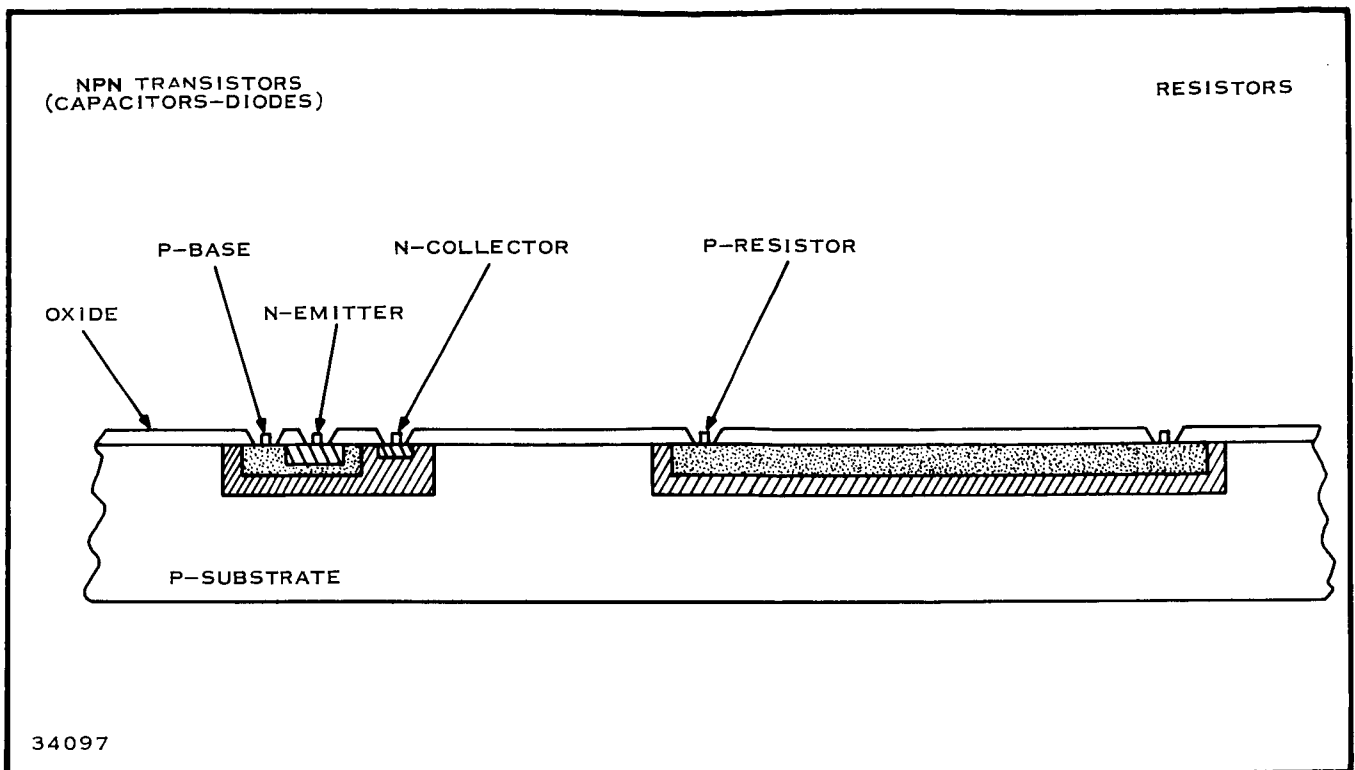


Figure 3. FEB Configuration

structure. In the diagram, only a transistor and resistor are shown, but the same general rules apply to the regions from which the other components are fabricated.

As the operational frequency of a device is increased, its active dimensions must decrease. This appears to be fundamental, independent of the type of device. Figure 4 demonstrates this for some discrete silicon devices of both experimental and production types. Since the frequency of operation of some devices being considered in this study is 1 to 6 GHz, devices with emitter dimensions of about 0.1 mil will be required.

There are two basic groups of transistor power amplifiers—the linear Class A amplifiers and the nonlinear Class C amplifier. Just which type of amplifier is best depends on what is wanted, the big difference being efficiency and gain. In both types of amplifiers the requirement is to produce as much power output as possible at frequencies over the range 0.30 to 3GHz, and then by the use of frequency multipliers, extend to the higher microwave frequencies.

The power generation sources currently available are limited to somewhere in the region of 3 GHz. Above this frequency, combinations of transistor and varactor will be used. Here is the point at which power generated by the basic amplifier multiplied by the frequency conversion factor

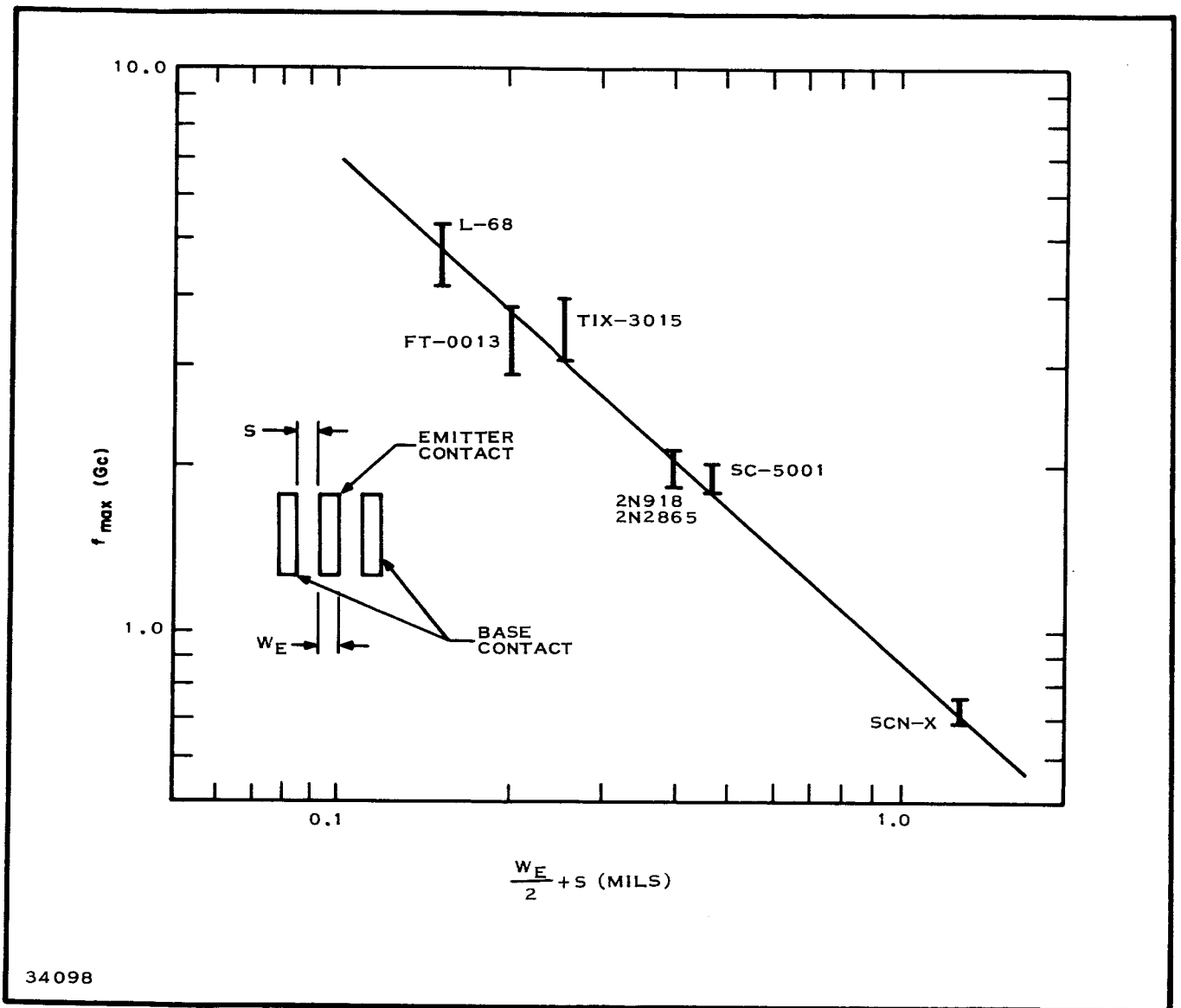


Figure 4.  $f_{max}$  as a Function of Transistor Geometry

and the attenuation of the varactor will result in a figure of merit for the combination which could be optimized for each particular solution depending on the final RF frequency and the output power required.

Almost all of the performance measurements made on power amplifiers to date have been made for pulse operation of the device. For CW operation approximately one-half this pulse power output can be realized. It is not possible to realize an increase in peak power output, over CW output, commensurate with duty cycle (as is the general case with vacuum tubes) because the power output of the semiconductor device is limited by the breakdown voltage and the maximum current the device can withstand. In addition, the structures required for power amplification need to have

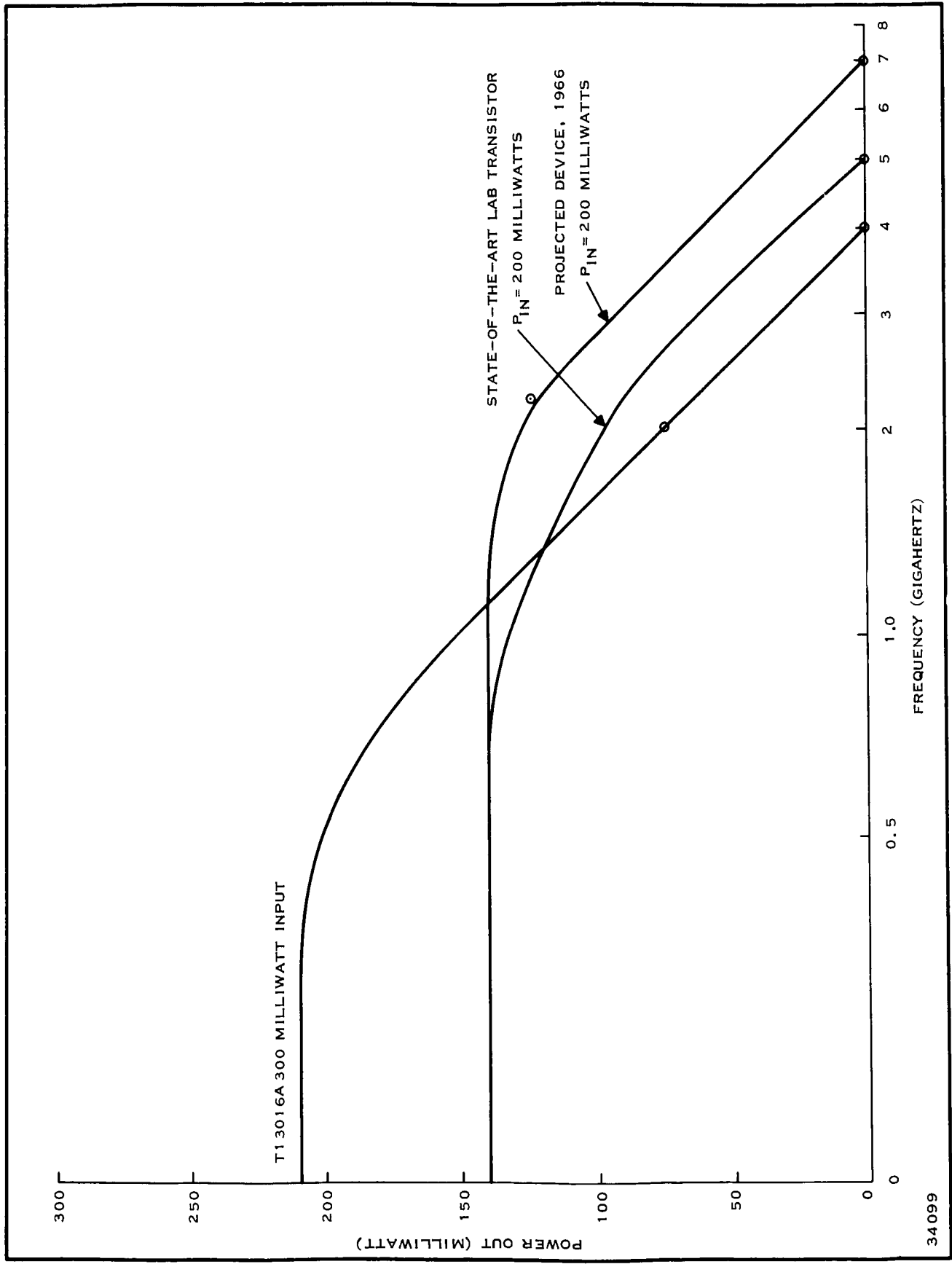


Figure 5. Power Versus Frequency for Silicon Transistors

good thermal characteristics to ensure that the junction temperature is kept as low as possible.

As the frequency capabilities of the transistors are extended, the devices necessarily become smaller and thus the power input must be less. This effect is illustrated in Figure 5. State-of-the-art devices one-third the size of the TI3016A show much improved efficiency at 3 GHz but with a more limited lower-frequency power-handling capability.

The problem of limited dissipation in small geometry transistors can be overcome to some extent by paralleling several devices dispersed about a chip. This approach is moderately effective below about 1 GHz. Above 1 GHz the effect of the parasitic capacitance introduced by the evaporated contacts becomes increasingly important and narrower; thicker contacts may be used to improve this situation. Recent investigations have shown that wires bonded individually to dispersed chips does not degrade performance as much as expected.

The most efficient solution to this high-frequency problem has been to enlarge the transistor area, keeping in mind that the thermal and electrical characteristics must be maintained. This has been accomplished by using multiple base and emitter contacts in an interdigitated configuration. This method has proved to be very effective and is the approach currently used to achieve high-power, high-frequency operation. The latest geometries have used a total of 65 base and emitter contacts.

### C. ADVANCES IN MICROWAVE TRANSISTORS

For the past several years, Texas Instruments has worked toward extending the frequency response and power handling capability of transistors. This has led to the development of transistors which represent a new generation of UHF silicon devices, for example, the TI3016A.

#### 1. TI3016A Transistor

The TI3016A and 2N3570 are electrically identical, but are supplied in different packages (TI-line\* and TO-18, respectively). These devices are planar-epitaxial silicon transistors that feature very small dimensions made possible by advanced photomasking techniques. Interdigitated base and emitter contacts result in very low base resistance. Figure 6 is a photograph of the completed silicon chip. Four base fingers and three emitter fingers are clearly seen, as well as the expanded areas for making external contacts. The total area of the base diffusion window is 7.2 sq mils.

---

\*Trademark of Texas Instruments Incorporated.

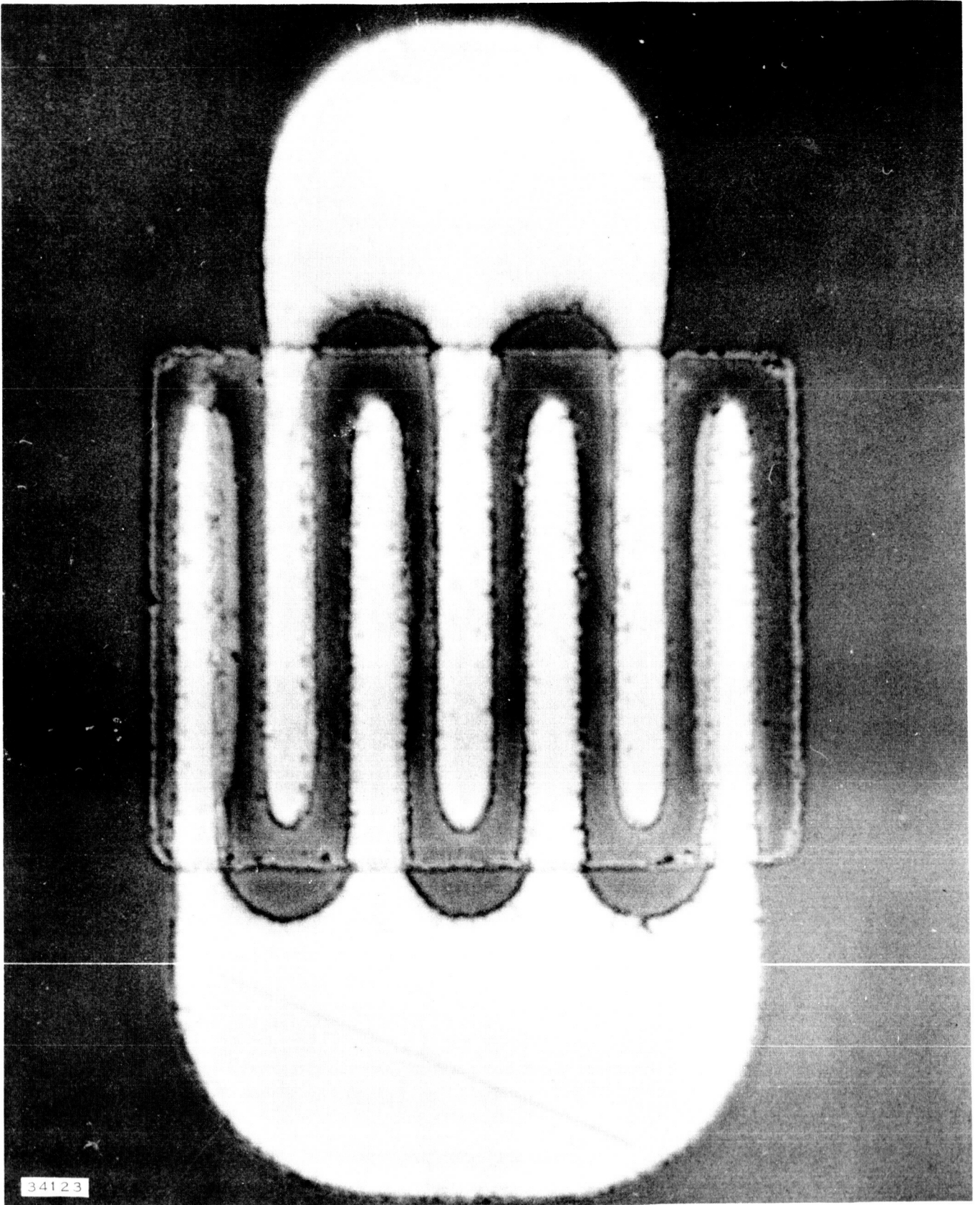


Figure 6. Photograph of TI3016A Silicon Planar Transistor Geometry

The outstanding performance of this unit results from the following high frequency parameters:

- Very-high cutoff frequency:  $f_T \approx 1.7$  GHz  
 Very-low base resistance:  $r_b^i \approx 10$  to 20 ohms  
 Low capacitance:  $C_c \approx 0.5$  pF.

These parameters are the result of a very narrow base (base width is in the order of 0.01 mil) and the other very small dimensions. The electrical characteristics of these units are summarized in Table I.

Table I. Characteristics of 2N3570 and TI3016A

Characteristic	2N3570*			TI3016A		
	Min	Typical	Max	Min	Typical	Max
$BV_{cbo}$	30 V (10 $\mu$ A)			30 V (10 $\mu$ A)		
$h_{fe}$ (6 V, 5 mA)	20		200	20		200
$r_b^i C_c$ (6 V, 5 mA)		5 ps	8 ps		5 ps	
$f_T$ (6 V, 5 mA)	1.56 GHz	1.7 GHz			1.7 GHz	
NF (1 GHz, 6 V, 5 mA)		7.0 dB			6.0 dB	
$f_{max}$		4 GHz			4 GHz	
$P_o$ (1 GHz, 20 V, 15 mA)		60 mW		30 mW ( 2 GHz)		

\* (Useful to 1.5 GHz and then) package limited.

During the design of these transistors, certain limitations presented themselves which are considered important.

**High Frequency Cutoff**—Several structure-determined time constants are involved in cutoff frequency. The most important of these is the base width. An important phase of the development of the TI3016A transistor was the development of suitable base and emitter diffusions so that a base width of about 0.01 mil could be consistently realized.

**Low Base Resistance**—For convenience the base resistance may be separated into two components: that part underneath the emitter and that part between the emitter

and base contacts. The first part may be minimized by using very narrow emitters. The emitter width is about 0.1 mil in the TI3016A. The second part is minimized by close spacing between emitter and base contacts and by paralleling many paths. The spacing between emitter and base contacts is 0.2 mil in these units, and the interdigitated geometry provides six parallel paths.

Base resistance may also be lowered by a proper diffusion profile, although other factors must be considered. The TI3016A has a very heavy concentration of impurities in the base and a very shallow diffusion front. These lower the resistivity of the base, particularly under the emitter where an appreciable portion of the base resistance usually exists. The combining of an optimum diffusion profile and an interdigitated geometry has resulted in a small-signal silicon transistor with  $r_b'$  in the order of 15 ohms.

**Low Capacitance**—Low capacitance is a desirable feature in any high-frequency device. The most effective way to reduce capacitance is to reduce the junction areas. The junctions of the TI3016A and 2N3570 are quite small, the actual areas being 7.2 sq mils for the collector-base junction and 0.9 sq mil for the emitter-base junction. It is possible to reduce collector capacitance by raising collector resistivity or by increasing the collector-base voltage. There are practical limits to these changes, however, and other factors must be considered. Among these factors are collector series resistance and behavior of the device at various voltages and currents (which is influenced by the width resistivity of the collector epitaxial region).

Measurements of a single-stage doubler have been made using the L-49 geometry with special diffusion schedules designed to increase the high frequency response and the power handling capability. (The geometry of the L-49 is the same as that used for the TI3016A.) Typical results for several devices tested showed that the doubler developed a 30-mW output at 4.5 GHz with a 10-mW input at 2.25 GHz.<sup>4</sup> These measurements were made under pulsed conditions. With the same devices operated under the same power levels, the output power at the fundamental, 2.25 GHz, would be approximately 60 mW.

It is believed that a better understanding of the mechanisms involved in frequency multiplication is desirable and that this mode of operation may



provide a simpler means of obtaining power at a higher frequency. It appears, however, that this method of conversion and amplification may not produce an efficiency as high as that obtained by a straight-through amplifier driving an optimized diode frequency multiplier.

## 2. 8307 Geometry

A number of transistors with a variety of basically different geometries were tested in a continuing effort to improve high-frequency, high-power performance. An example is the dual 35-contact geometry (Figure 7) designated the "8306 geometry." The fundamental problem with devices using this geometry is a relatively low efficiency. The 8307 geometry (Figure 8) was designed to improve the efficiency. The 8307 consists of sixty-five 0.2 mil by 3 mil interdigitated fingers in a single-device structure.<sup>4</sup> Because it allows for five emitter bonds and five base bonds, the inductance is somewhat lower than that of previous devices. The overall substrate size is 30 mils by 40 mils in the evaluation configuration. The final size will be considerably smaller.

Many devices with 65-stripe geometry have been tested as 2-watt amplifiers. All devices with good breakdown voltages met the 2-watt output and the 3-dB power gain criteria. Typical device performance<sup>4</sup> is shown in Figure 9.

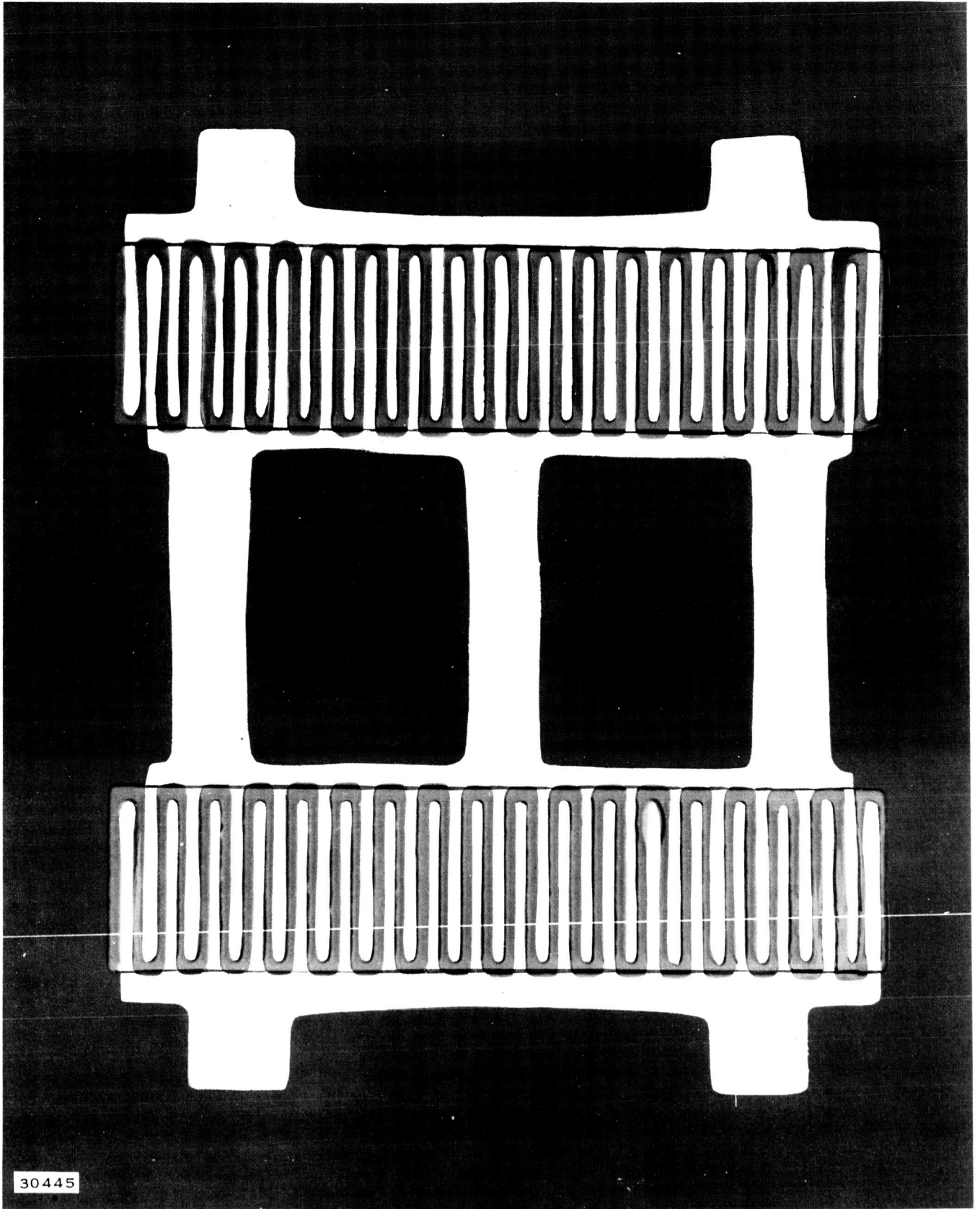
Additional 65-stripe geometry devices with a new ceramic carrier package have been fabricated and tested. Devices from run A-68 operated similarly to the A-63 device and gave good performance at 30 to 35 volts bias. Run A-69 was fabricated on thick epitaxial material, and consequently the device had reduced output capacitance (3 pF at 10 volts). However, these devices required greater than 50 volts bias to achieve good performance at the 2-watt level.

It appears that run A-63 is close to the optimum for good performance with 28 to 30 volts bias. Additional runs are in progress. The goal is to reduce the emitter transition capacitance and possibly improve the device performance as a Class C amplifier.

## 3. L-146 Device

An example<sup>5</sup> of a basic geometry considered for small-signal, high-frequency application is shown in Figure 10. This three-finger device has been considered for use in the MERA IF preamplifier which operates at center frequency of 500 MHz. This device is one version of the L-146 structure (the designation "L-146" is reserved for the device ultimately used in the preamplifier). The important characteristics of the device are given in Table II; the desired noise figure is 2.5 to 3.0 dB, and measured noise figures have run 1 to 3 dB higher than desired.

A device now under development appears to be the best geometry for the low-noise 500-MHz transistor. It is a five-finger transistor which is the equivalent of two-thirds of the L-49 in area, and the finger



30445

Figure 7. 8306 Geometry

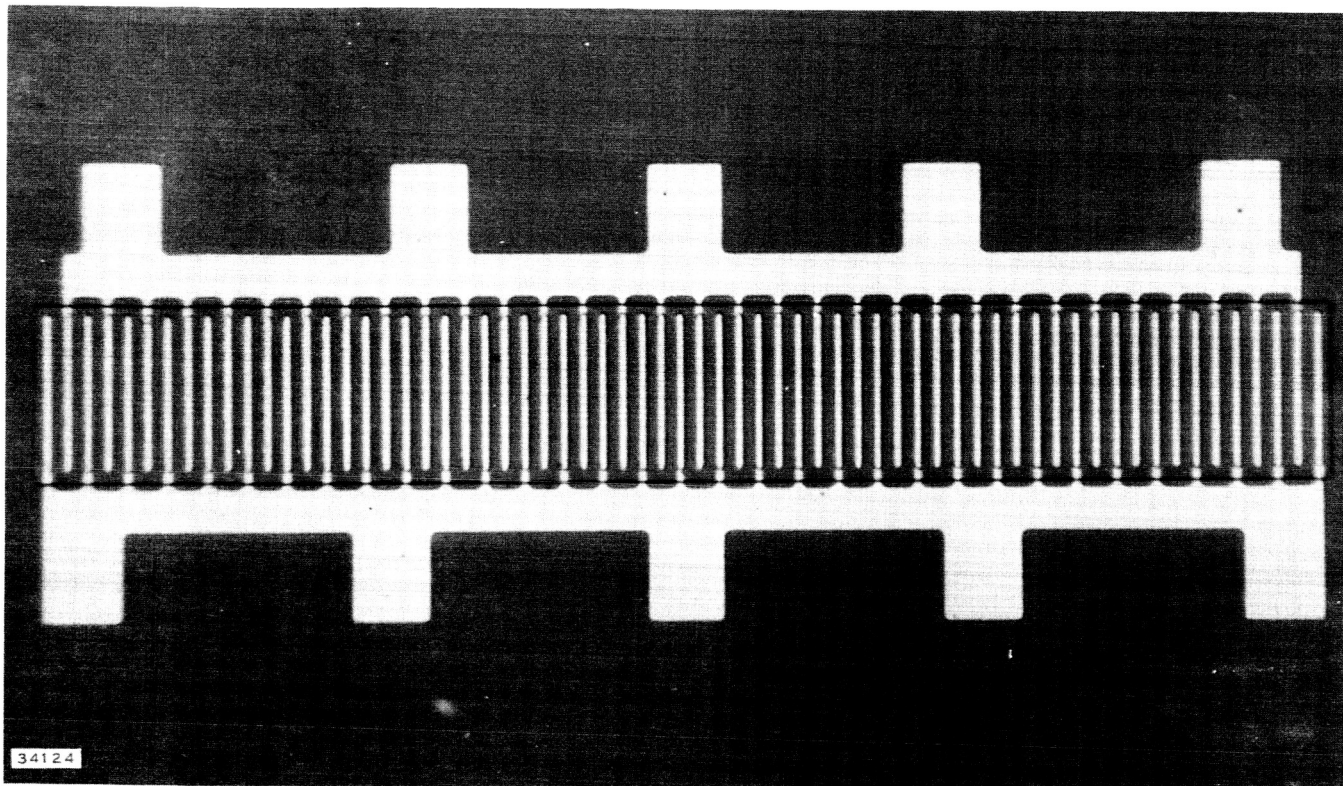


Figure 8. 8307 Geometry

Table II. Characteristics of L-146

Characteristic	Typical (MTEW Slice 18)	Desired
$f_t$ (6 V, 2 mA)	1.25 GHz	1.5 to 2.0 GHz
$r_b'$ (6 V, 2 mA)	30 to 40 ohms	30 to 40 ohms
$C_c$ (6 V)	0.33 pF	0.1 pF

width and spacing is 0.2 mil. The product  $r_b' C_c$  is on the order of 3 ps, at 6 volts and 2 mA, one-third the value achieved with the device described above. Noise figures are consistently lower, ranging between 3 and 4 dB. Such a device as this will be important for low-noise, small-signal, high-frequency application.

#### D. TRANSISTOR AMPLIFIERS

Experiments with power amplifiers conducted under the MERA program have been directed toward achieving gains of 33 dB, power output of 2 watts peak, and the capability of operating at duty cycles of at least 10 percent.

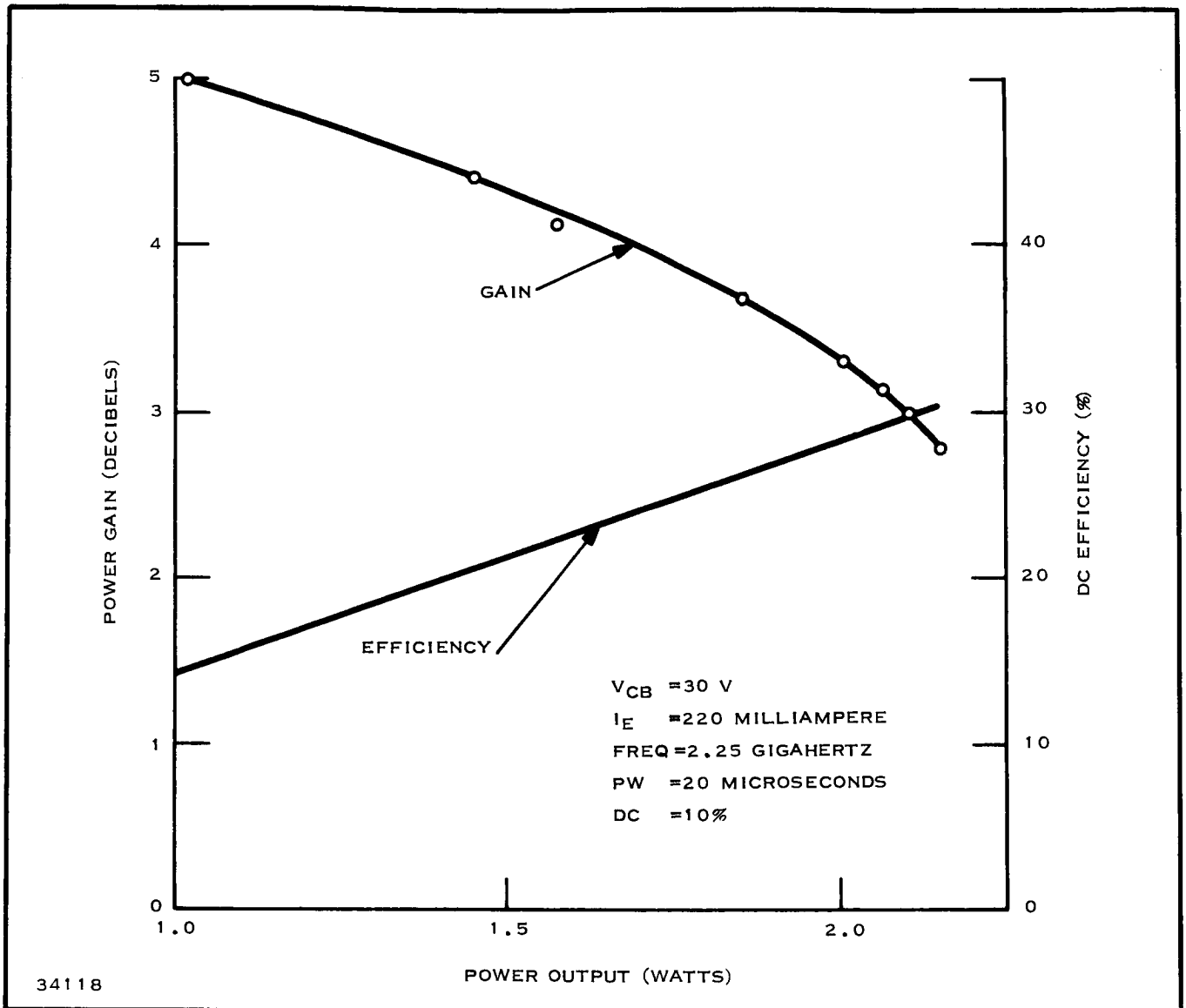


Figure 9. Power Gain and Efficiency Versus Peak Pulse Power Output, MERA Device A55D No. 4, 8307 Geometry

A number of breadboards of a three-stage amplifier employing L-49 devices were constructed (Figure 11) and the units evaluated.<sup>4</sup> A gain of 25 dB at 1.5 GHz was obtained. Difficulties in realizing the circuit were encountered, which did not allow operation at 2.25 GHz. Present work is directed toward single-stage circuit testing using the 8307 geometry device in a package. An extensive program in device characterization is under way.

A single-stage IF preamplifier has been constructed on a printed circuit board measuring 0.75 by 0.75 inch. Used between silicon substrates were 1-mil gold wire interconnections. The L-146 transistor was mounted on a metal tab with input/output/power connections made through subminiature

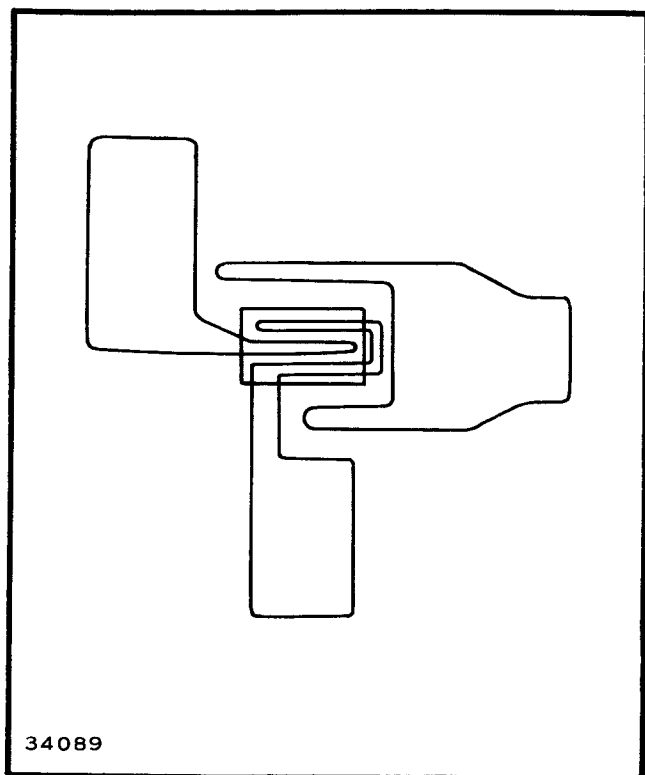


Figure 10. Lead Pattern and Geometry<sup>5</sup> for L-146

connectors mounted on the reverse side of the board. Figure 12 is a photograph<sup>4</sup> of the amplifier, Figure 13 a schematic diagram. Performance of the amplifier was:

$f_o$	480 MHz
BW (-3 dB)	200 MHz
Power gain	7 dB.

Following the construction of the single-stage amplifier, a two-stage amplifier using two L-146 transistors was built on a printed circuit board 0.75 by 1.0 inch. The only difference between the construction techniques was in the two-stage amplifier, where all passive components were located on top of the ground plane to simulate the ground plane under the silicon substrate when the circuit is reduced to monolithic form. A photograph<sup>4</sup> and schematic diagram<sup>4</sup> are shown in Figures 14 and 15 respectively.

A comparison of the present and desired performance is presented in Table III.

Table III. Present Versus Desired Performance of the L-146 Device

	Present	Desired
$f_o$	505 MHz	500 MHz
BW (-3 dB)	100 MHz	$\geq 80$ MHz
$P_g$	14 dB	$\geq 15$ dB
NF	7 dB	3 dB
Dynamic range	-103 dBm to -14 dBm [BW (-3dB) = 4 MHz]	-106 dBm to -32 dBm
Size	$< 0.18$ in. <sup>3</sup>	$< 0.03$ in. <sup>3</sup>
Power supply	24 V at 18 mA	12 V at 8 to 10 mA

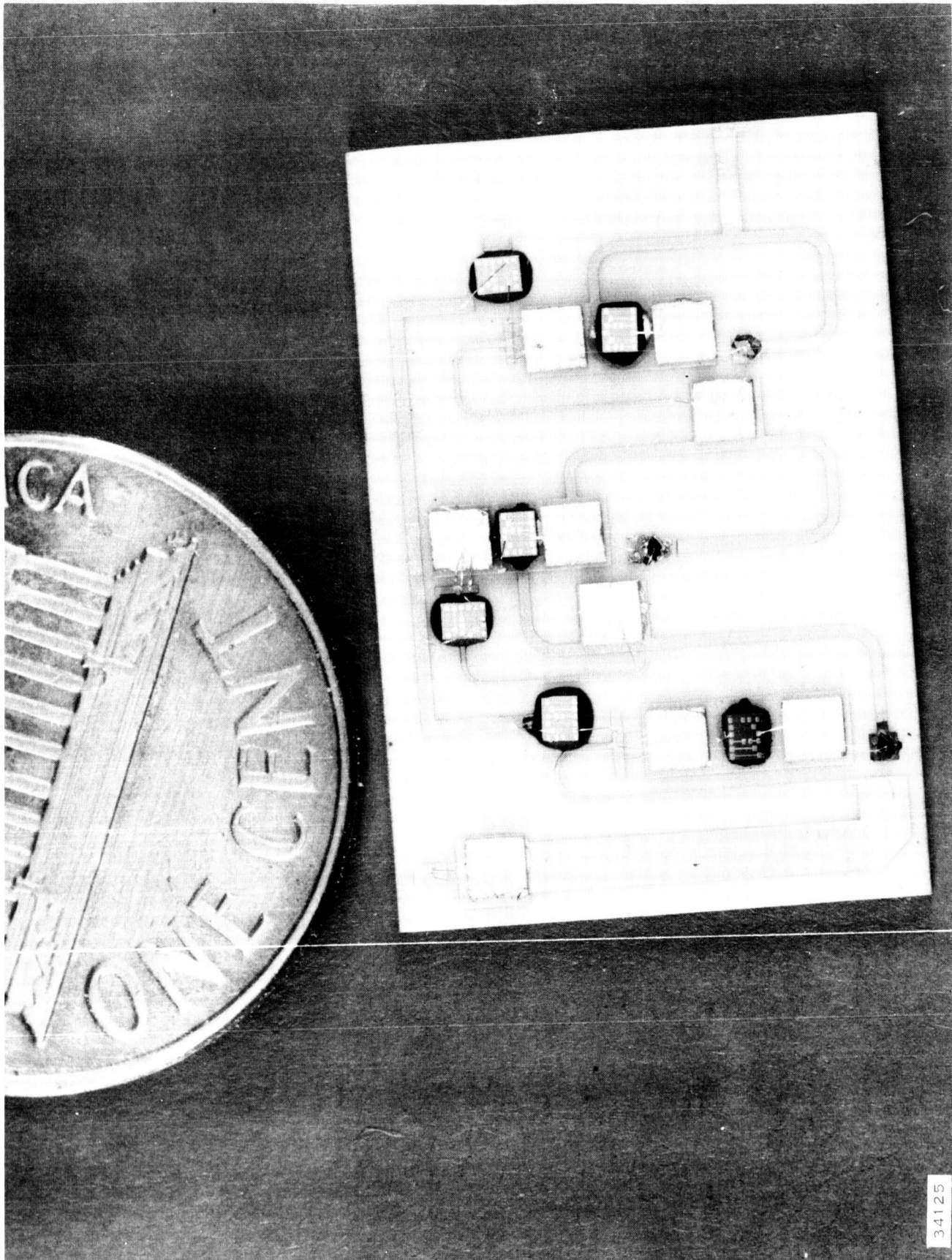
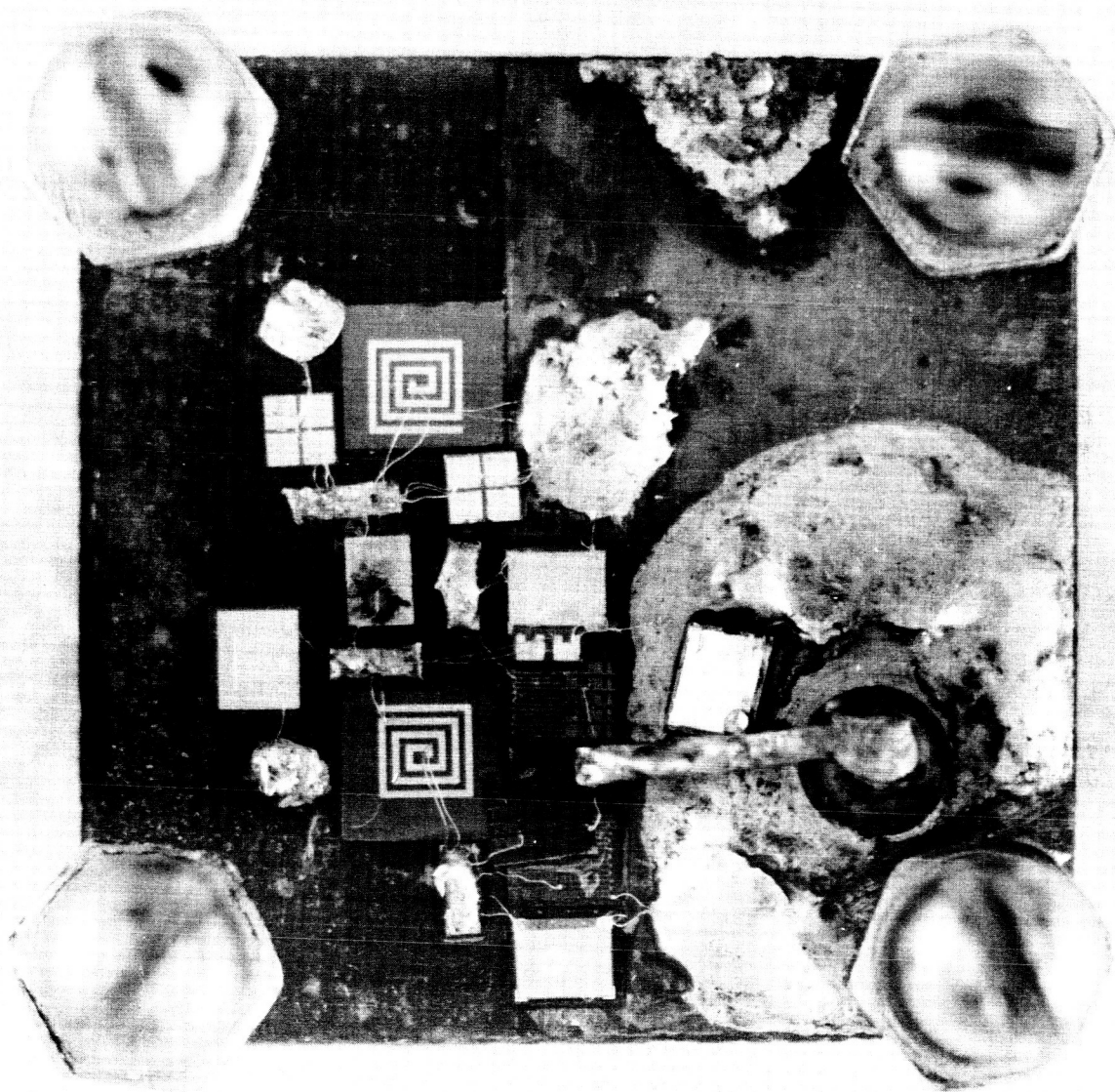


Figure 11. Three-stage Power Amplifier Breadboard on Ceramic Substrate<sup>4</sup>

34125



34122

Figure 12. Single-stage, 500-MHz IF Preamplifier<sup>4</sup>

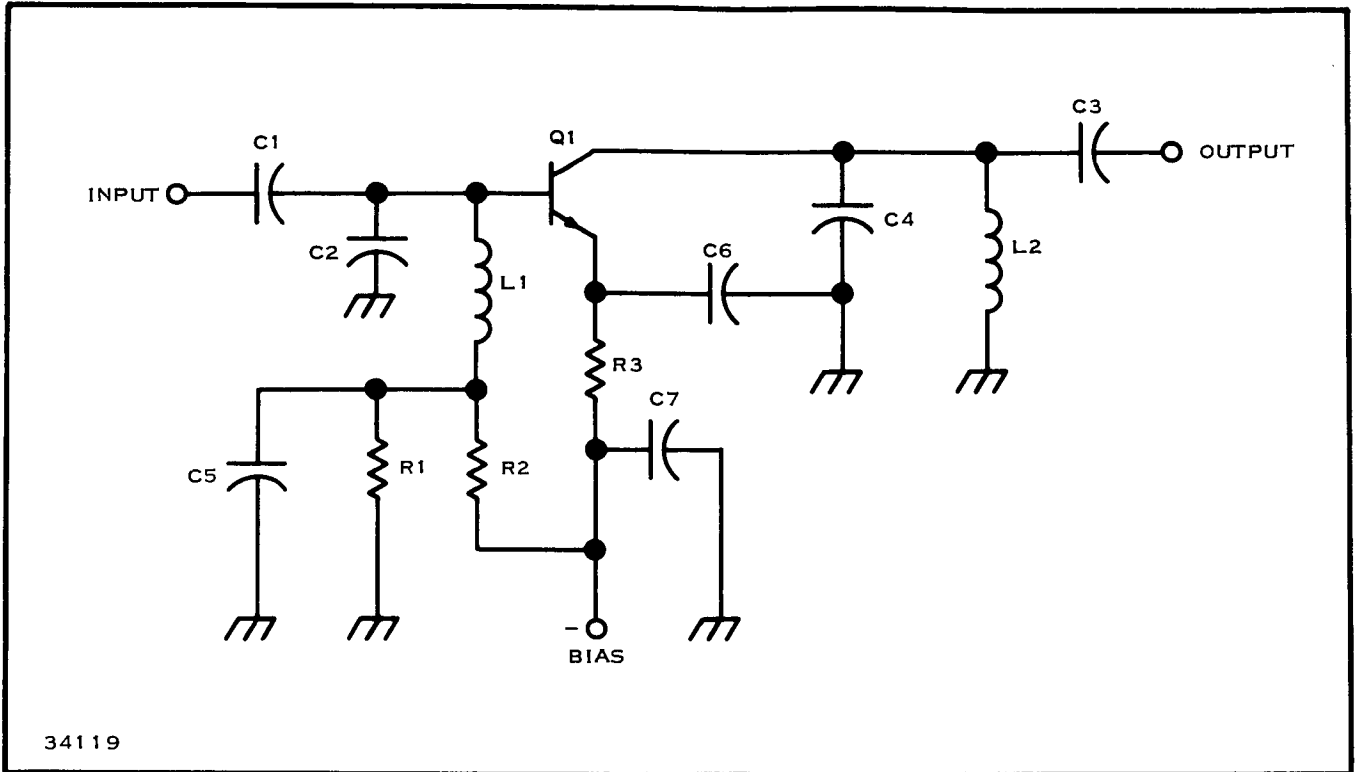
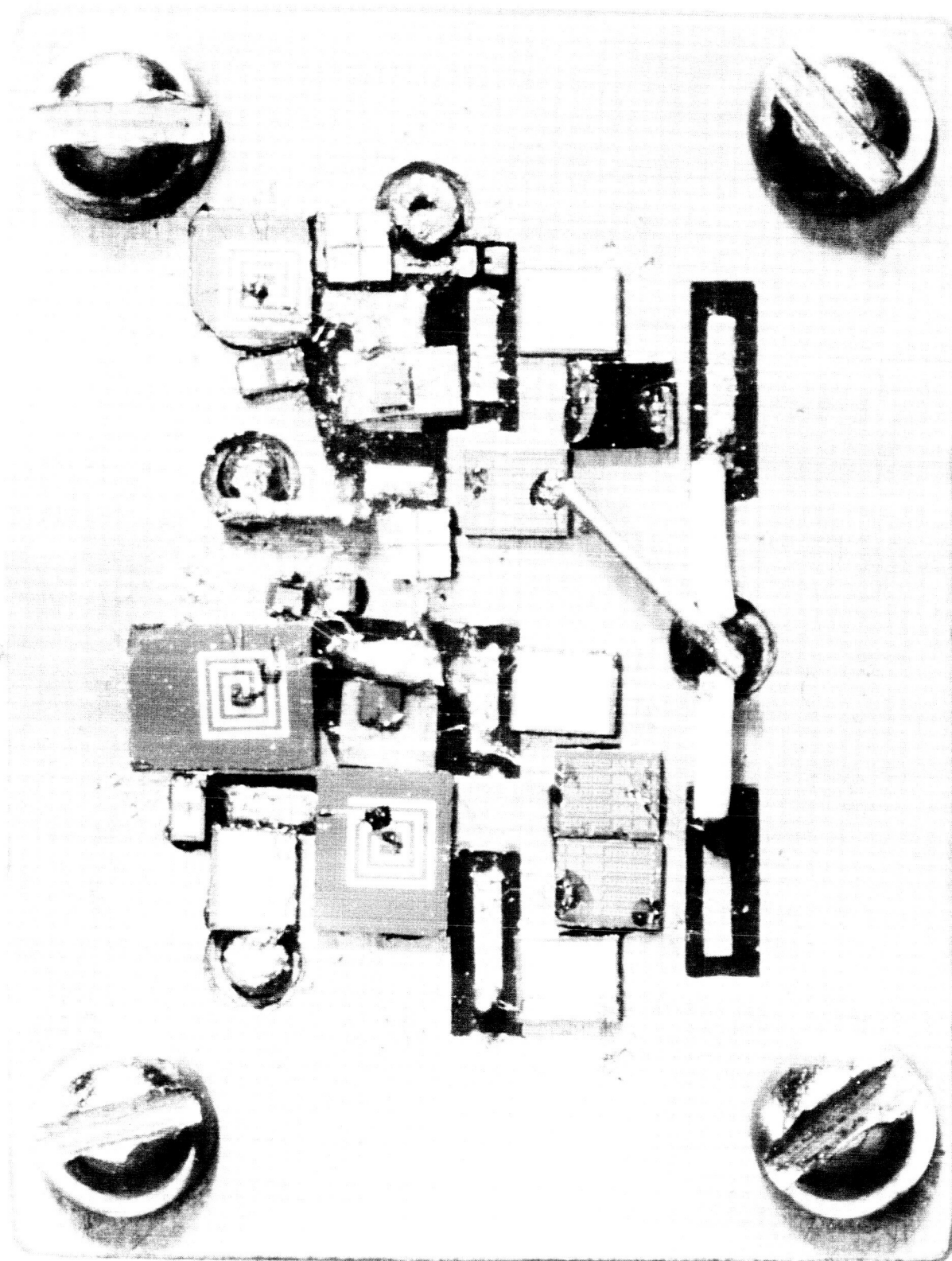


Figure 13. Single-stage, 500-MHz IF Pre-amplifier, Schematic Diagram<sup>4</sup>

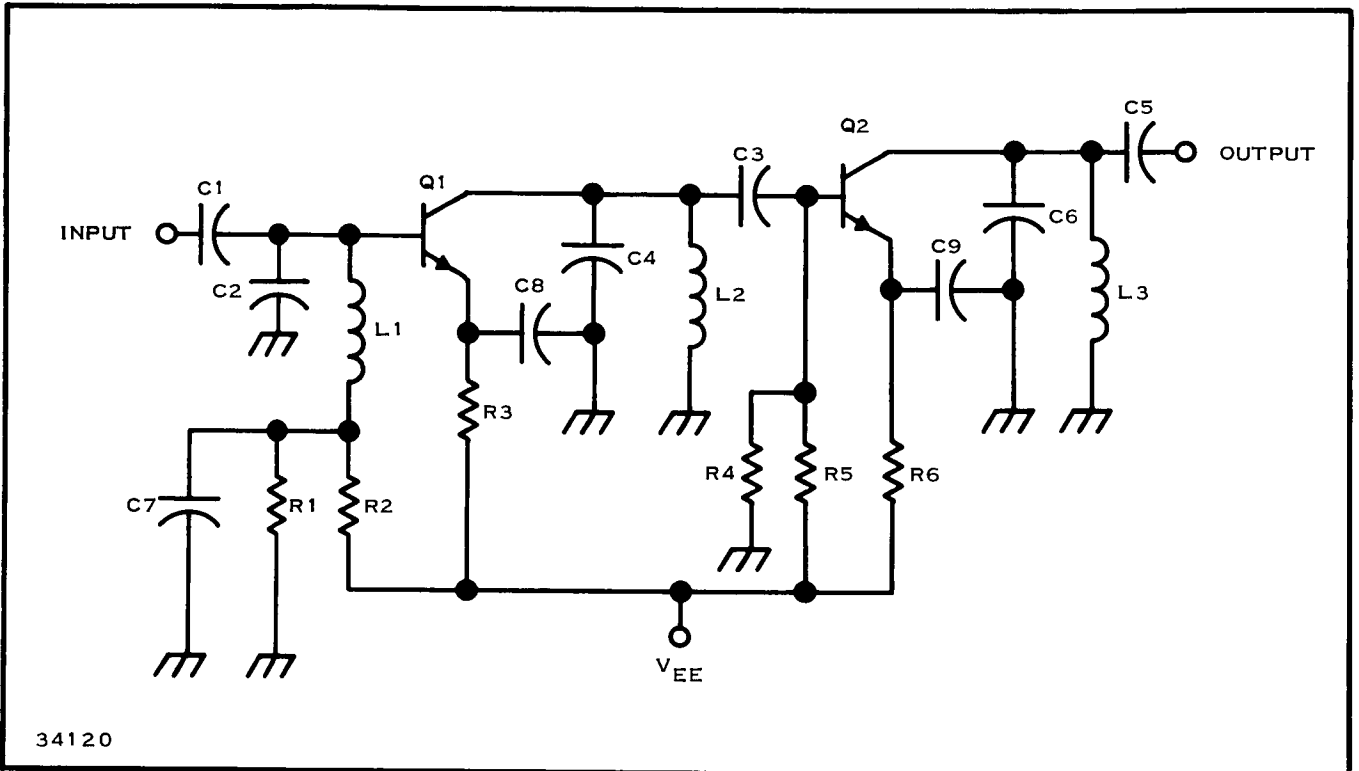
A monolithic version of the two-stage amplifier of Figure 15 is shown in a cross-sectional view in Figure 16. The appearance of the amplifier in monolithic form is shown in Figure 17. This design along with the results of breadboard tests indicate that the final form of the amplifier will meet design requirements. The complete circuit will be on a single silicon substrate, with all components (transistors, capacitors, resistors, and inductors) fabricated by selective epitaxial deposition.





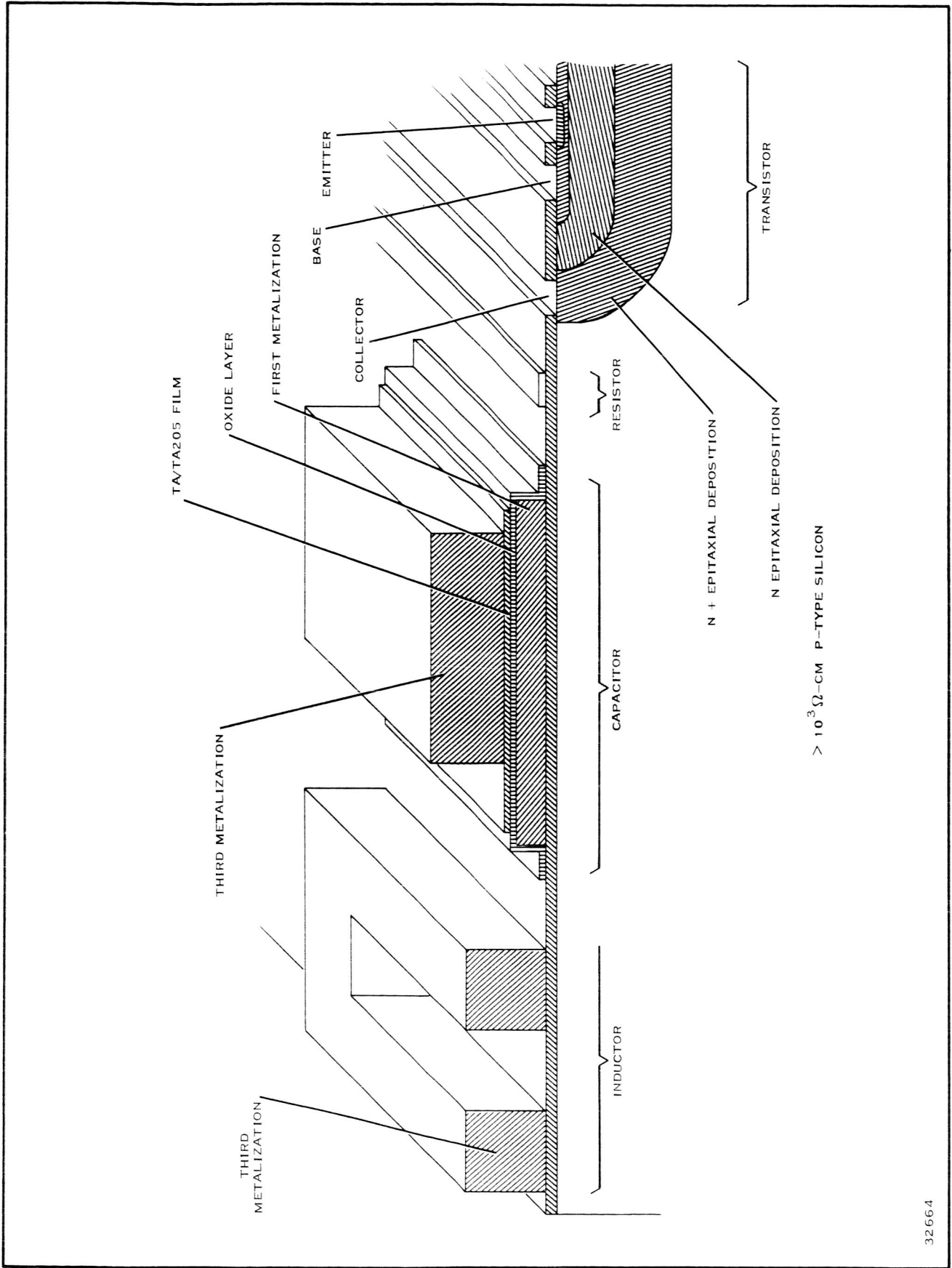
34121

Figure 14. Two-stage, 500-MHz IF Preamplifier<sup>4</sup>



34120

Figure 15. Two-stage, 500-MHz IF Preamplifier, Schematic Diagram<sup>4</sup>



32664

Figure 16. Typical Cross Section of 500-MHz IF Preamplifier

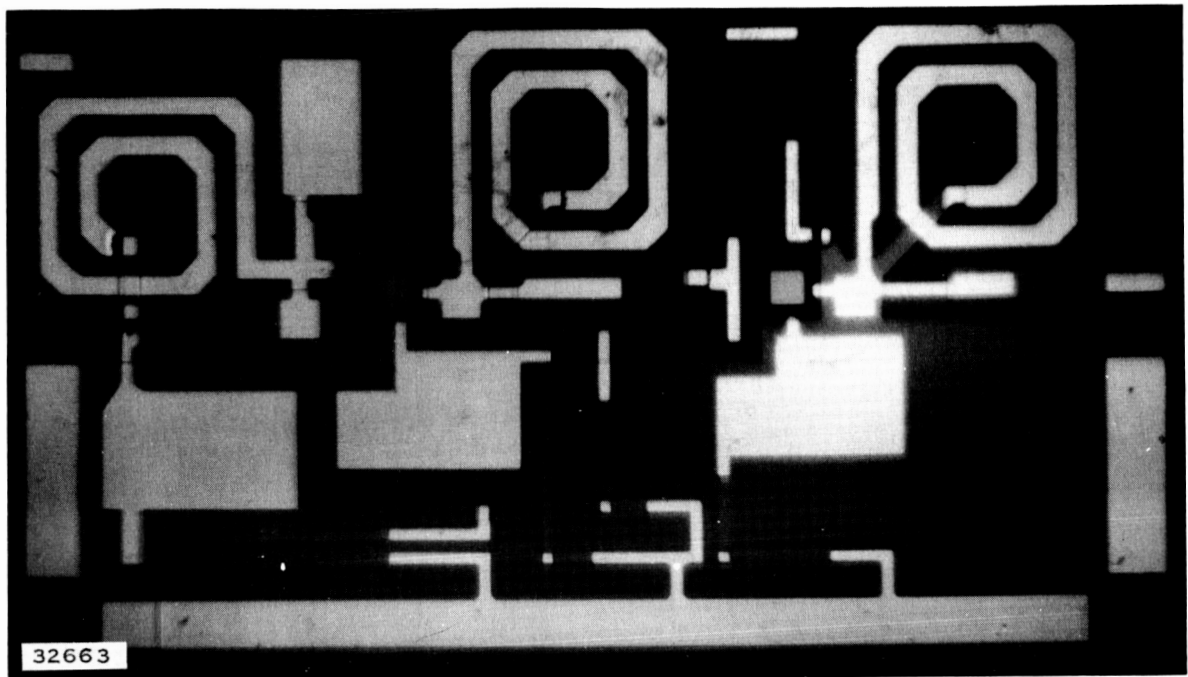


Figure 17. Two-stage Monolithic Amplifier

## SECTION IV

### STRIPLINES

#### A. GENERAL

Recent advances in high-frequency transistor techniques indicate that integrated circuits using transistors with a maximum frequency in the region of 0.5 to 5 GHz will be fabricated in the near future. In this frequency range stripline connections will be required with characteristic impedances between 50 and 200 ohms. The dimensions of striplines with these characteristics—considering frequencies in the lower gigahertz range—are entirely compatible with integrated circuit dimensions.

In addition to the standard circuit elements for integrated circuits, there must be available transmission line components such as couplers, transforming sections and filters. With processes and materials compatible with other circuitry components, these components must be fabricated from transmission line sections having low loss and well defined characteristic impedance properties.

#### B. CHARACTERISTICS OF STRIPLINES

##### 1. Characteristic Impedance

The flat-strip transmission system, upon which the microwave printed circuit technique is based, evolves fundamentally from the coaxial transmission system. A cursory examination of the flat-strip line would lead one to believe that the capacity of the line, which determines its characteristic impedance, could be readily calculated from the parallel-plate capacitance formula. For wide, low-impedance strips this is true, but for strips which have characteristic impedance in the order of 50 ohms, the capacity due to fringing effects at the edge of the center conductor is an appreciable portion of the total capacity and produces a noticeable effect. As the strip is narrowed, for even higher impedance, another effect becomes apparent, namely, interaction between the fringing fields at the two edges of the center conductor. This effect, which becomes appreciable for very narrow strips, must be taken into account in the analysis of high-impedance transmission lines.

The flat-strip line,<sup>12</sup> like the coaxial line, operates in the TEM mode. For engineering applications the most important characteristics of any transmission system operating in this mode are the velocity of propagation  $V_p$  and the characteristic impedance of  $Z_0$ , which can be calculated from the known relation

$$Z_0 = \sqrt{L/C} . \quad (1)$$

The velocity of propagation of the principal mode in such a transmission system is given by the relation

$$V_p = \frac{1}{\sqrt{LC}} \quad (2)$$

Combining Equations (1) and (2), we obtain

$$Z_o = \frac{1}{V_p C} \quad (3)$$

The velocity of propagation is also given by

$$V_p = \frac{V_o}{\sqrt{\mu\epsilon}} \quad (4)$$

Substituting Equation (4) into Equation (3), we obtain

$$Z_o = \frac{\sqrt{\mu\epsilon}}{CV_o} = \frac{\epsilon}{CV_o} \sqrt{\frac{\mu}{\epsilon}} \quad (5)$$

In the MKS units these equations are:

$$V_p = \frac{3 \times 10^8}{\sqrt{\mu\epsilon}} \text{ m/s} \quad (4a)$$

$$Z_o = \frac{\sqrt{\mu\epsilon}}{3C \times 10^8} \text{ ohms} \quad (5a)$$

where

L = inductance per unit length

C = capacitance per unit length

$Z_o$  = characteristic impedance

$\mu$  = relative permeability (equal to 1 for free space and most dielectrics)

$\epsilon$  = dielectric constant (equal to 1 for free space)

$V_p$  = velocity of propagation in material with properties  $\mu$  and  $\epsilon$ .

An approximate calculation based upon the well known parallel-plate capacitance formular is instructive and gives some insight into the operation of this type of transmission system. The use of this formula to compute the

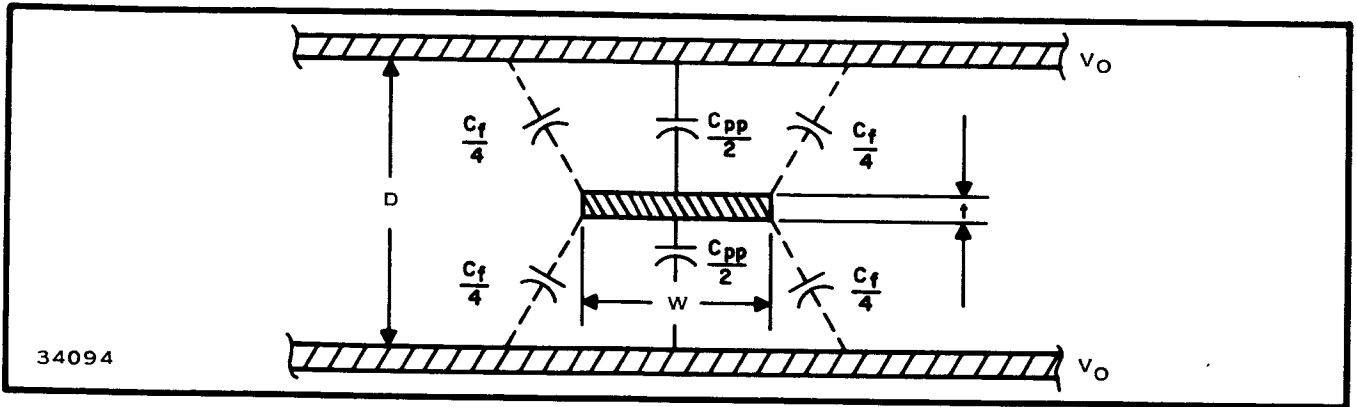


Figure 18. Flat-pack Triplate

characteristic impedance is permissible for an impedance below 25 ohms. The fringing field capacitance becomes an appreciable portion of the total capacitance for impedance greater than this and must be utilized in the calculations. Under these conditions the total capacitance  $C$  would be

$$C = C_{pp} + C_f \quad (6)$$

where

$C_f = f(W, t/D)$  fringing field capacitance per unit length in pF/m

$C$  = capacitance per unit length of line in pF/m

$C_{pp}$  = parallel plate capacitance in pF/m.

When this capacitance is combined into the equation for the capacitance<sup>1</sup> of three parallel planes, which is

$$C_{pp} = 35.4 \left( \frac{\frac{W}{D}}{1 - \frac{t}{D}} \right) \epsilon \text{ pF/m} , \quad (7)$$

we obtain

$$C = \epsilon \left( 35.4 \frac{\frac{W}{D}}{1 - \frac{t}{D}} + C_f \right) , \quad (8)$$

and the impedance obtained from Equations (8) and (5a), Figure 18, is

$$Z_o = \frac{\sqrt{\mu\epsilon} \left( 1 - \frac{t}{D} \right)}{3 \times 10^8 \left[ 35.4 \frac{W}{D} + \left( 1 - \frac{t}{D} \right) C_f \right] \epsilon} \quad (9)$$

where

W = center conductor strip width in cm

D = plate spacing in cm

t = plate thickness in cm.

If we let  $C_f$  equal a constant, which is determined experimentally, the formula for the characteristic impedance will hold up to 100 ohms, at which point the interaction between the fringing fields becomes important; it is then a function of  $W/D$  and  $t/D$ .

Equation (9) will yield good results for small values of  $t/D$ . It appears, however, that the exact equations found by Bates<sup>13</sup> are needed for calculating  $\sqrt{\epsilon_r} Z_0$  for values of  $t/D$  greater than about 0.25 and for values of  $W/D$  less than about 1.0.

The exact expressions found by Bates are:

$$\frac{W}{D} = \frac{2K}{\pi} \left[ \frac{k^2 \operatorname{sn}(a) \operatorname{cn}(a)}{\operatorname{dn}(a)} - Z(a) \right]$$

$$\frac{t}{D} = \frac{a}{K} - \frac{2K'}{\pi} \left[ \frac{k^2 \operatorname{sn}(a) \operatorname{cn}(a)}{\operatorname{dn}(a)} - Z(a) \right]$$

where

$\operatorname{sn}(z)$ ,  $\operatorname{cn}(z)$ ,  $\operatorname{dn}(z)$  = Jacobian elliptic functions

$K$  = real quarter period of  $\operatorname{sn}(z)$

$jK'$  = imaginary half period of  $\operatorname{sn}(z)$

$Z(z)$  = Jacobian Zeta function

$k$  = modulus of the elliptic functions.

The most convenient way of evaluating these formulas was found to be the following:

Assume a value of  $Z_0$

From Figure 19 find the corresponding value of  $\operatorname{cn}(a)$

Substitute this value of  $\operatorname{cn}(a)$  into the two equations and calculate  $W/D$  and  $t/D$  for several values of  $k$ .

Bates calculated a few of these values and Figure 20, a plot of the results, shows values of  $t/D$  versus  $W/D$  with  $\sqrt{\epsilon_r} Z_0$  as the parameter.

## 2. Physical Limitations

Since all microwave lines and components have practical limitations on their physical size, it is expected that striplines would also.



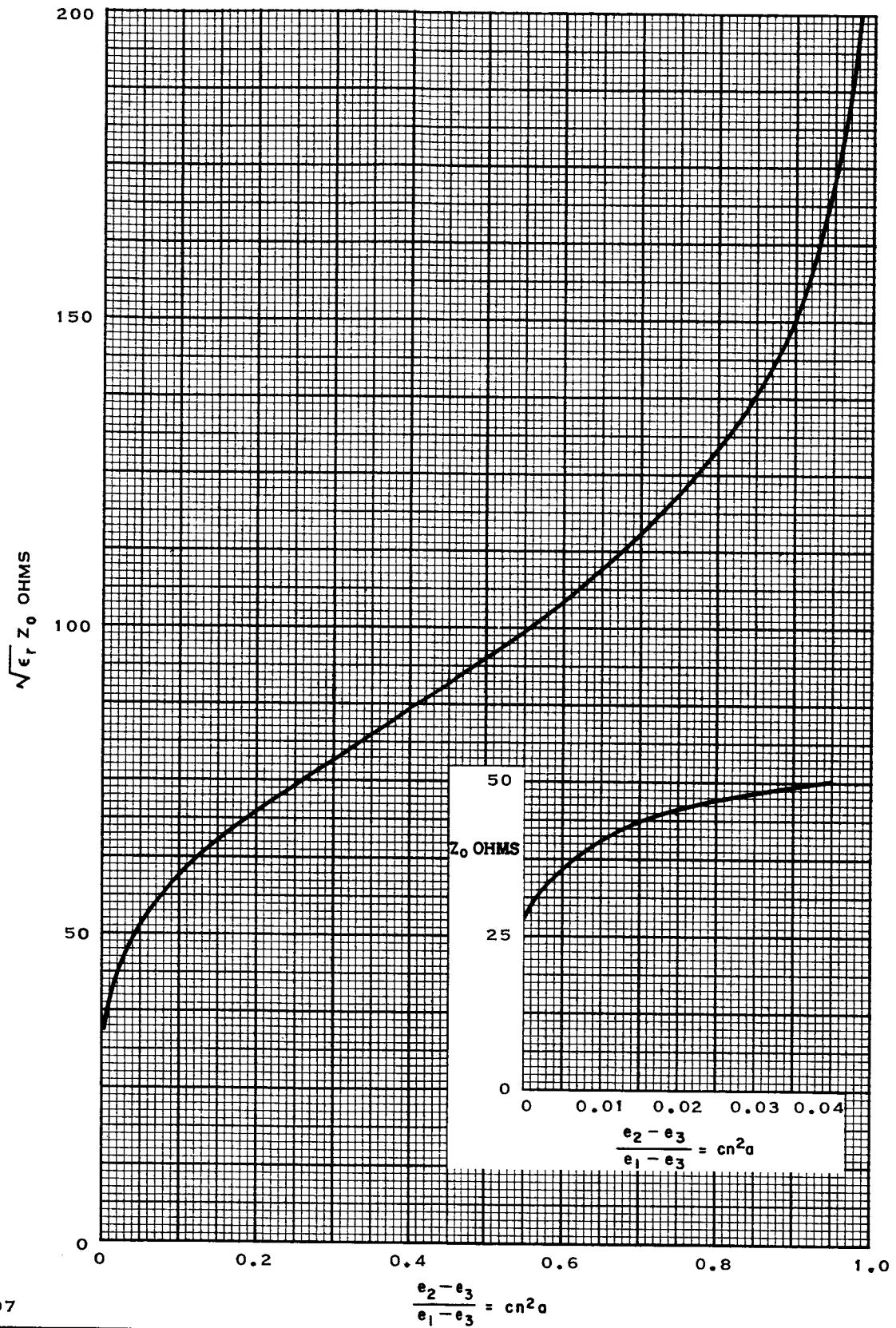
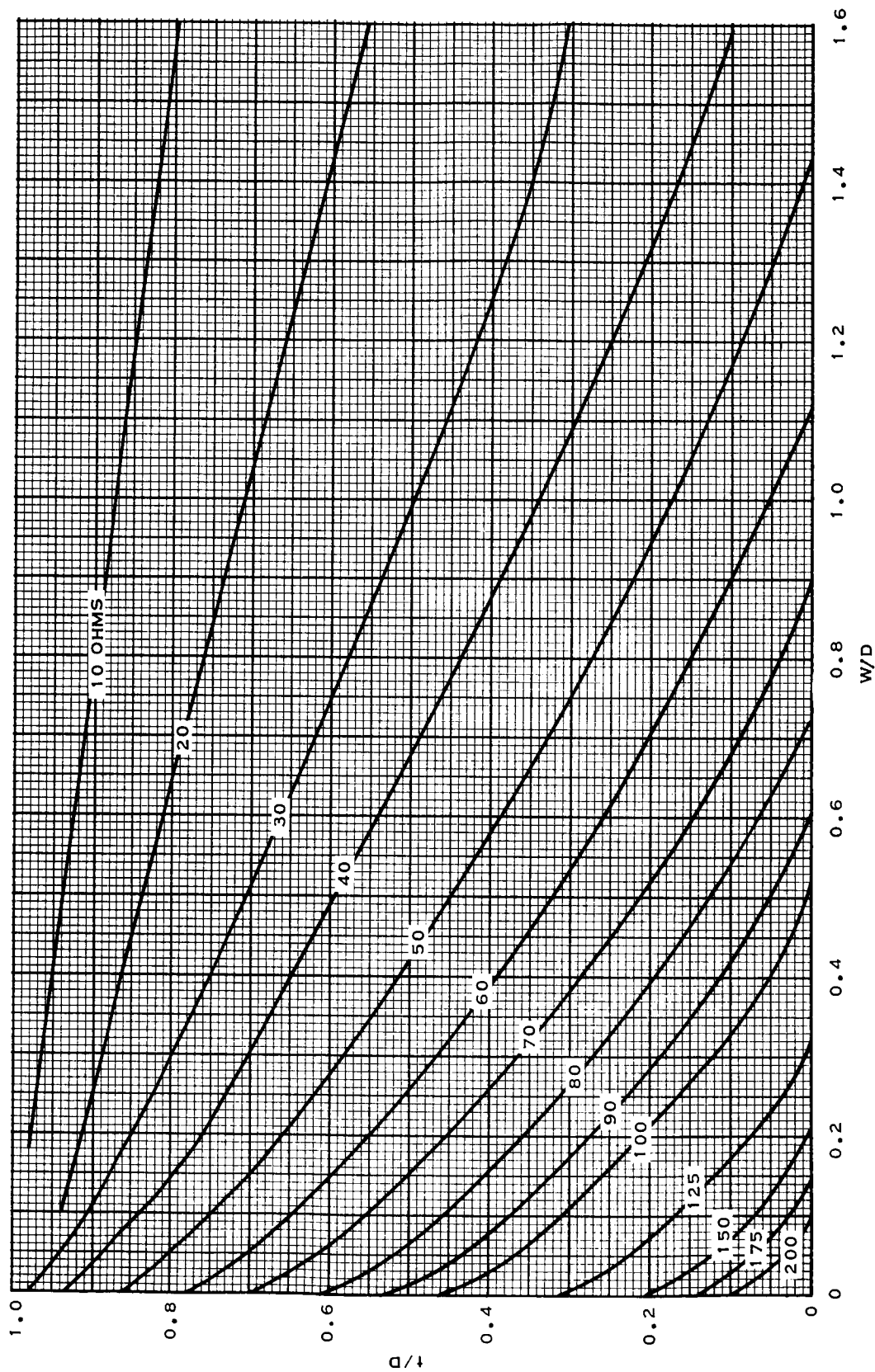
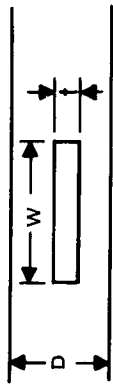


Figure 19.  $Z_0$  Versus  $cn^2 a$



34106

Figure 20.  $t/D$  Versus  $W/D$  With  $\sqrt{\epsilon_r} Z_0$  Ohms as Parameter

For the dominant mode (TEM) to exist, certain conditions must be met; these apply both to certain dimensions and to the symmetry of the structure:

(1) ground plane spacing must be less than half a wavelength, (2) equivalent electrical width of the strip conductor must be less than half a wavelength, and (3) the center strip conductor must be approximately centered between the ground planes and must be approximately parallel to them. This parallelism is important for high  $Q$  applications, such as resonators, where an extremely small radiation loss in the parallel plate TEM mode or TE mode can have significant effect on the  $Q$ .

When the ground plane spacing equals or exceeds half a wavelength, higher order modes can propagate and radiate to free space or couple to other circuits. This must be avoided.

If the electrical width of the strip exceeds half a wavelength, higher order modes with circumferential variations can exist on the strip in a manner similar to that of a large coaxial line. The electrical width is greater than the physical width of the strip because of fringing effects at the edges.

Tolerances on centering a strip conductor between ground planes may be quite loose without harmful effects. On the other hand, the tilt of the center conductor is very critical in high  $Q$  applications. To alleviate the tolerances on tilt, metal posts or barriers can be used to prevent propagation between ground planes of high-order TE and parallel-plane TEM modes. This is usually unnecessary in low  $Q$  or matched applications.

### 3. Types of Striplines

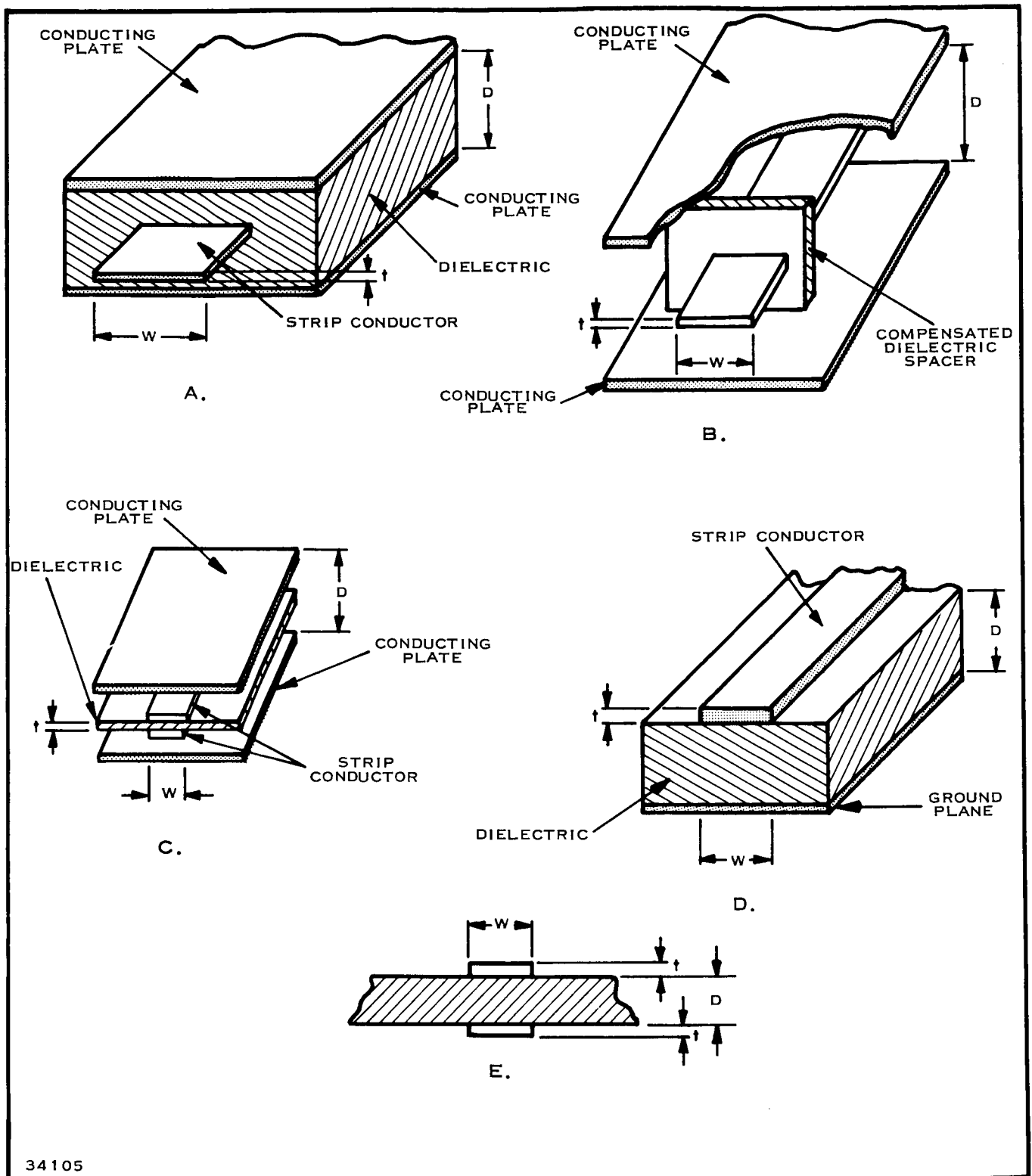
Although striplines have been called by many different names, they always refer to the same type of geometry. Figure 21 shows some of the geometry and names of the most commonly used striplines, which will be investigated in the following subsections. Merits of the principal forms of striplines are summarized in Table IV.<sup>14</sup>

#### a. Sandwich Line

When the center conductor of the sandwich line is limited to a very thin center conductor, such as metal foil or a printed conductor, it has the same characteristics as the flat-pack triplate mentioned previously. This system is ideally suited for the printed circuit technique and has been widely used by the Air Force Cambridge Research Center.

#### b. Sheet-supported or Compensated Stub-supported Transmission Line

These lines are of value when the losses due to a continuous dielectric sheet cannot be tolerated, when the weight of the structure is of prime importance, when the center strip is to be thick, or when high power is to be carried by the system.



34105

Figure 21. Microwave Striplines: A. Sandwich line, dielectric sandwich transmission line; B. Sheet-supported or compensated stub-supported transmission line; C. Dielectric sheet-supported transmission line, stripline, double metal-clad line, high Q triplate; D. Microstrip, half section; E. Balanced line.

c. Dielectric Sheet-supported Transmission Line or Stripline

This type of arrangement offers very low losses, because if the two strips are connected in parallel at the input and output of the circuit, the electric field from each strip conductor is to its corresponding ground plane and only fringing fields exist in the dielectric sheet. However, in a resonant structure strong fields exist at voltage maxima, especially in coupling regions, and it is the practice of some manufacturers to remove the dielectric from these regions. This type of structure offers high Q's because the conductor losses are the only important ones; therefore this type of line permits the design of high Q components such as microwave filters.

d. Microstrip or Half Section

Microstrip is a wideband transmission system developed as a substitute for waveguide or coaxial lines, especially for the development of microwave components and microwave circuitry. Microstrip also offers low Q's and allows the manufacture of microwave plumbing to be reduced to a printed circuit technique capable of great accuracy, adaptable to mass production, and resulting in a great saving of cost, space, and weight.

## C. APPLICATIONS OF STRIPLINES

### 1. Hybrid Ring

A hybrid ring may be formed (Figure 22) if four striplines at quarter-wavelength intervals are joined onto a ring having an impedance times that of the lines and a mean circumference of one and one-half  $\sqrt{2}$  wavelengths. A signal originating at arm A of Figure 22 will split its power into two paths traveling around the ring, combining at B and D in phase and out of phase at C. Similarly, a signal starting at arm C divides and arrives in phase at B and D and out of phase at A; hence, the hybrid ring may be used as a balanced mixer by feeding in a signal and local oscillator in arms A and C and placing crystal holders at B and D. If the hybrid is used as a mixer, it should be noted—when a signal is injected in arm A of some power K—that the power out of arms B and D will be down slightly and equal, but at arm C the power will be down considerably (20 to 30 dB or even greater). The VSWR looking into arm A, with the others terminated in a matched load, will be low.

### 2. Directional Couplers

A typical directional coupler is shown in Figure 23 and has been found to be quite satisfactory. The parameters which affect the coupling are the separation X of the two lines, the length L over which the separation is maintained, and the angle  $\theta$  between the arms. A signal entering arm A will travel to arm B, and a predetermined portion of this signal will appear at arm C. There will be zero output at arm D. If the main signal travels in

Table IV. Merits of Striplines

	Balanced Strip	Microstrip	Triplate	High Q Triplate
<b>ORDER OF MERIT</b>				
Ease of fabrication	2	1	3	4
Bulk and weight	1	1	2	3
Ease of testing	2	1	4	3
Ease of analysis	3	3	1	2
Dissipative losses	2	2	3	1
Radiation losses	2	2	1	1
<b>GENERAL</b>				
Topological limitations	Difficult to feed from unbalanced transmission line.	Phase reversals not possible, but ground plane easily tapered away to give balanced line.	E-plane series junction difficult. Phase reversals impossible. Discontinuities must in principle be symmetrical.	
Appropriate field of application	Broadband hybrid junctions involving phase reversals and/or series junctions.	Broadband low Q Components.	Broadband components and medium Q filters	Broadband and narrowband components. Filters generally including high Q resonators.
Use to date	Considerable	Extensive	Considerable	Extensive

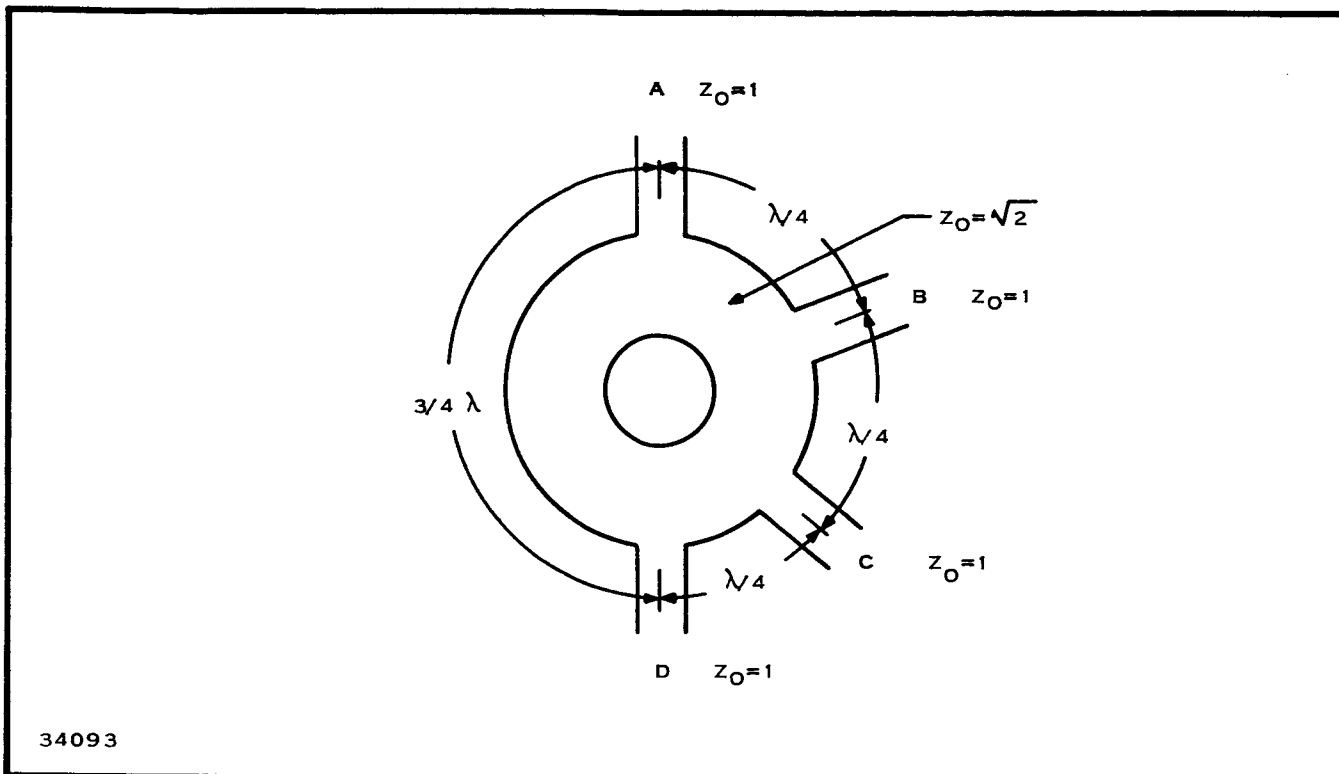


Figure 22. Hybrid Ring

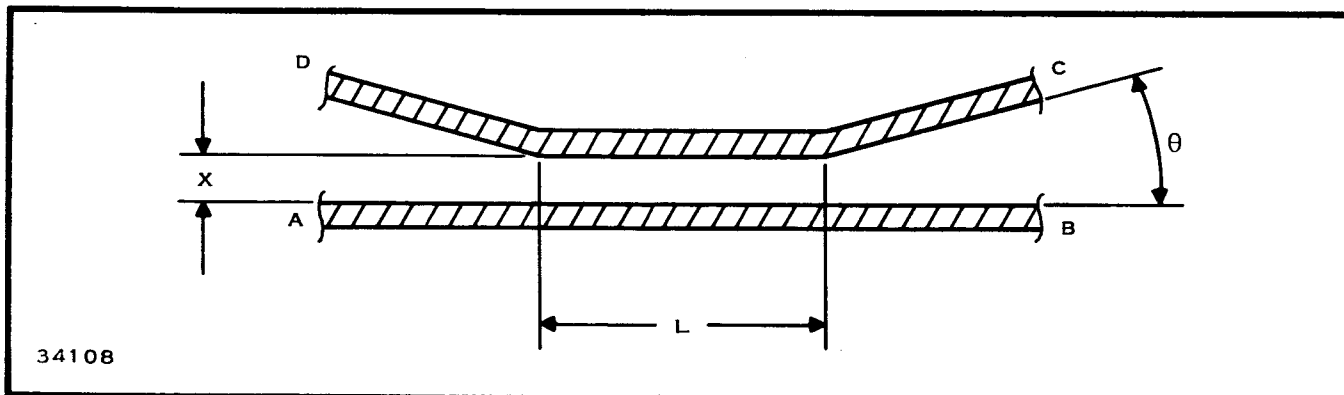


Figure 23. Directional Coupler

the reverse direction, from arm B to arm A, the small coupled signal will appear at the arm which was isolated in the first case.

The coupling of a directional coupler is the ratio of the input power to the coupled output power expressed in decibels. Thus, if the power output of arm C is 1/100 of the power into arm A, the component is a 20-dB coupler. It should be noted that the power output of arm B must be

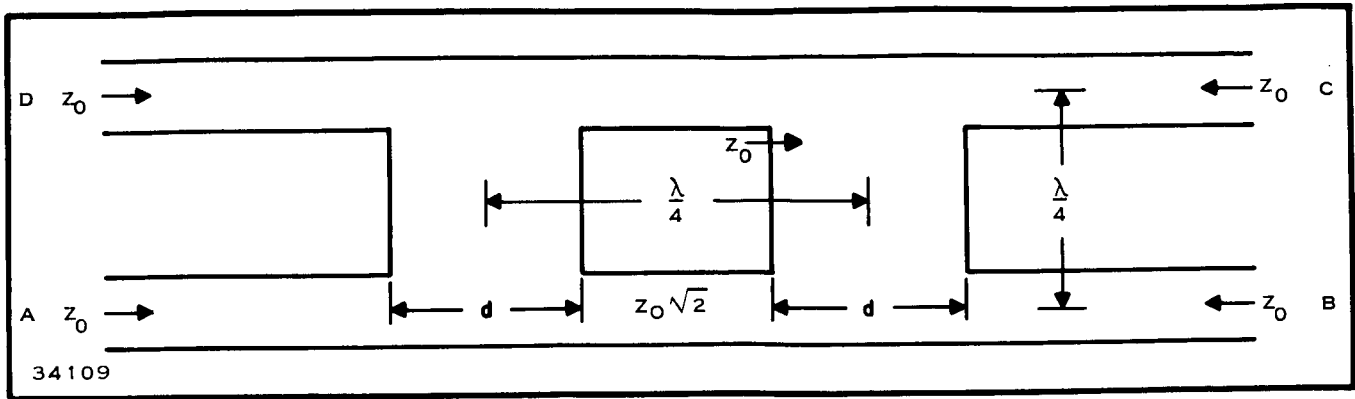


Figure 24. Branch Line Coupler

reduced by the amount coupled out of arm C. The directivity, as measured by the difference in power levels in arms C and D, is dependent upon the angle  $\theta$ : the smaller the angle, the greater the directivity and vice versa (up to 90 degrees).

Another type of coupler, shown in Figure 24, is commonly called a "branch line coupler." Ports A and D are isolated. The coupling and the matching of this device are determined by the characteristic impedance of the branches. Increasing the number of branches increases the bandwidth and the directivity. The outputs are in quadrature here as they were in the parallel type of coupler.

### 3. Filters

There is no basic difference in techniques between stripline and other types of transmission-line filters. However, if the fullest possible advantage is to be taken of printed-circuit techniques, all the elements should be in planar form. In itself this is not a serious restriction, for there exists an adequate range of such elements. On the other hand, since the designer has only two dimensional freedom, he is frequently restricted in regard to the range of electrical values possible. This can, of course, be overcome by a local reduction of the ground plane spacing, but mechanical complications of this kind are undesirable.

Another important consideration is the  $Q$  factor of the elements, and in this respect a high  $Q$  triplate line has a definite superiority. In the first place the dissipative losses are a good deal lower, and second, it is easier to limit the loss by radiation or mode conversion. This does not, however, exclude the possibility of satisfactory filters in microstrip. In the case of low-pass filters it is not essential for the elements to have a very high  $Q$  factor; it is sufficient that the elements have no marked tendency to radiate. In the case of band-stop filters, it has been found that the problem may be circumvented quite successfully by fabricating the critical elements as enclosed cavities which are coupled to the microstrip line by suitable means.



#### 4. Power Dividers

The use of the microwave printed circuit naturally lends itself to the problem of power distribution and division. Usually these networks are built in the form of a tree; Figure 25 shows some typical forms of power dividers. In the first two dividers, matching is achieved by the use of quarter-wave transformers, whereas in the third a gradual taper is used.

#### 5. Attenuators or Matched Loads

Attenuators and matched loads are obtainable in striplines by printing a resistive paint on the dielectric sheets prior to printing the conductors. Other ways of obtaining attenuators and loads are by attaching a tapered piece of carbon-backed card of prescribed shape to the strip conductor. If the position of the card can be adjusted so as to alter the amount of energy intercepted, a variable attenuator is obtained. This is accomplished by sliding the card laterally across the line. A hinged-flap arrangement may be used if lateral space is at a premium.

Carbon-backed cards are satisfactory for loads, but they are not the best material for attenuators. The properties of carbon-backed cards vary with temperature and humidity, and they are not very rigid unless supported. Another material being used is metallized-glass in different arrangements.

In general, attenuators and loads involving insertion of lossy material between strip conductor and ground plane will work satisfactorily only if the material is homogeneous and extends the full distance between ground plane and strip conductor.

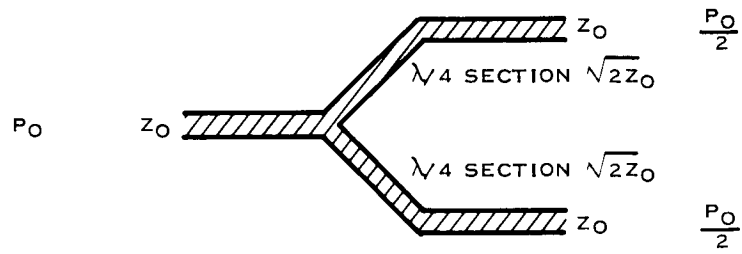
Since all of the attenuators mentioned present slight difficulties, it is believed where accurate and reproducible results are required, a precise attenuator as developed by Dukes<sup>14</sup> (microstrip short-circuit piston) would prove the most satisfactory.

### D. ADVANCES IN INTEGRATED CIRCUIT STRIPLINES

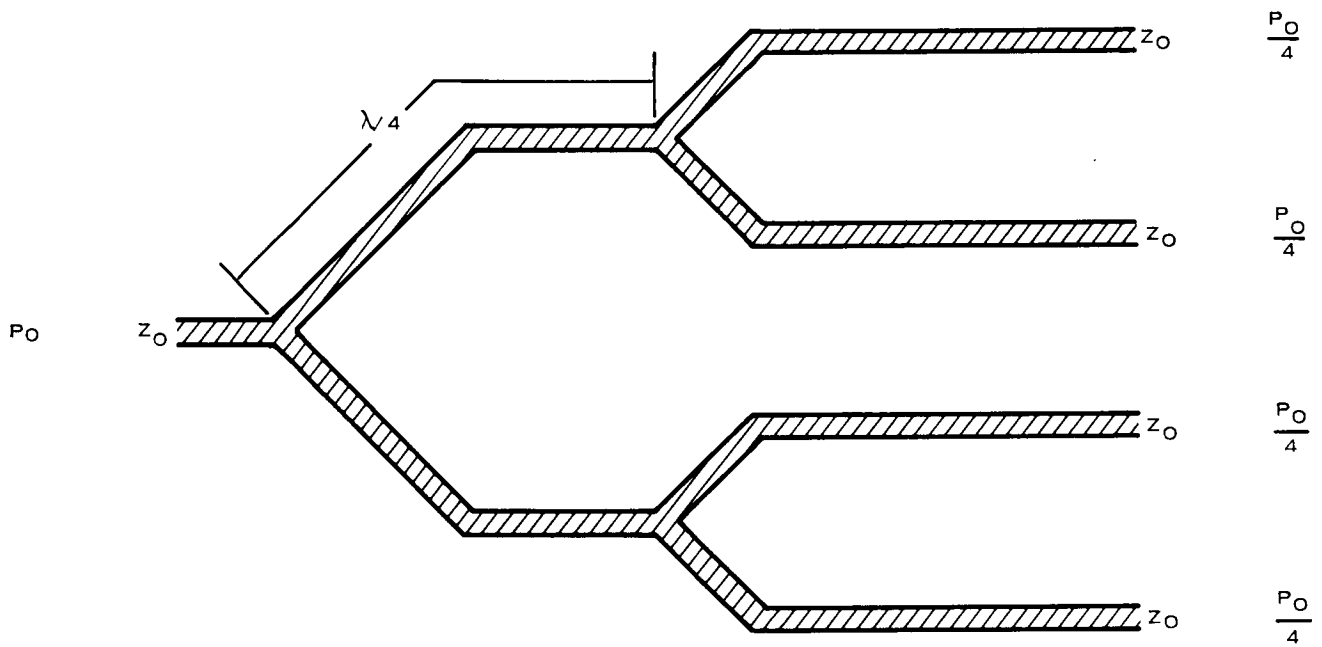
Microstrip<sup>15, 16, 17</sup> has been developed as a substitute for waveguides or coaxial lines, especially for the development of microwave components and microwave circuitry.<sup>25</sup> As indicated in Table IV, microstrip is used extensively throughout industry.

At the present time Texas Instruments is investigating integrated-circuit striplines, some of the findings of which are presented in the following paragraphs.

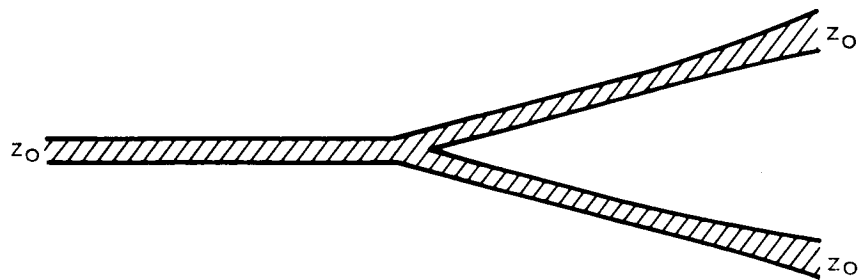
In a recently completed investigation, "Fabrication of Microstrip Interconnections for Microwave Hybrid/Monolithic Circuits,"<sup>18</sup> two configurations of the microstrip line were considered (Figure 26). The first type (A of the figure) was fabricated from a semiconductor slice, with the



QUARTER-WAVE TRANSFORMER



QUARTER-WAVE TRANSFORMER



TAPERED

34104

Figure 25. Power Dividers

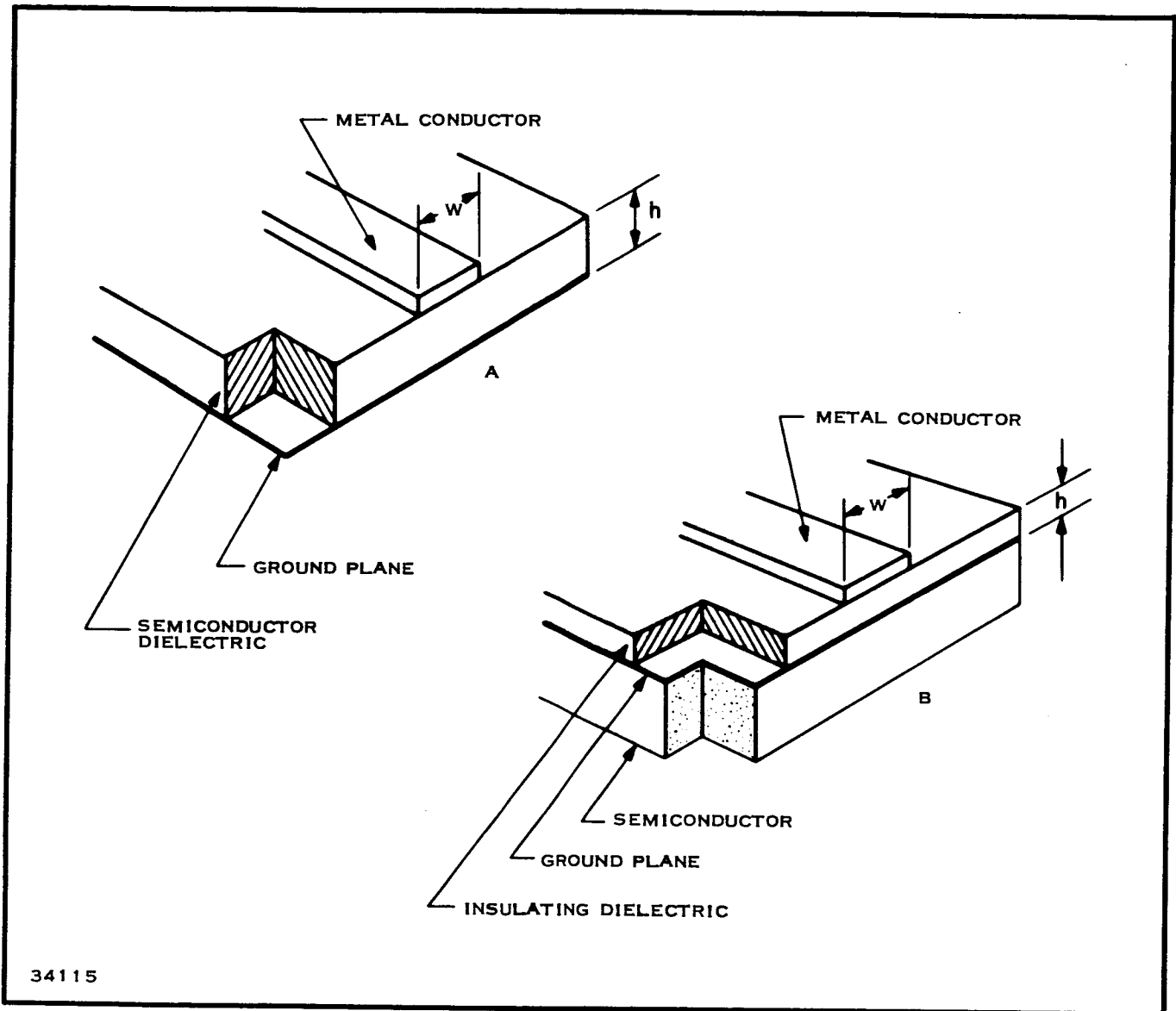


Figure 26. Microstrip Transmission Lines<sup>18</sup>

ground plane and top conductor deposited on each side of the slice. The semiconductor slice serves as the dielectric for the transmission line. This structure is easily applied to integrated circuits since the top conductor is coplanar with the contact surface of the active devices on the silicon surface.

The second configuration (B of the figure) was considered in order to eliminate the semiconductor material from the transmission line. The ground plane for the transmission line is deposited on the surface of the semiconductor material containing the active elements. An insulator is deposited above the ground, and finally the top conductor is deposited. Since the semiconductor surface is coplanar with the ground plane instead of the top conductor, provisions must be made for connecting the top conductor to the active devices.

These devices (Figure 26) were fabricated with three different materials: aluminum, molybdenum-gold, and vanadium-silver. The Figure 26B stripline was fabricated with a quartz dielectric and aluminum conductor.

The microstrip lines were evaluated by measuring the power dissipated by a section of transmission line. Slices with each conductor in various thicknesses were prepared with top conductor line widths of 1, 2, 4, 6, 8 and 10 mils for each slice. Coupling between adjacent lines was prevented by keeping the lines sufficiently separated. Figure 27 shows a typical slice prepared for measurement.

Power measurements at 9 GHz were made on each slice using standard insertion loss techniques.<sup>19</sup> Pressure contact was made by a pin protruding from each side of a test fixture.<sup>22</sup> Ground connection was made by the body of the fixture which is grounded to the outer connector of the input and output lines.

The loss at 9 GHz for various thicknesses of vanadium-silver, molybdenum-gold, and aluminum lines is shown in Figure 28. The loss is proportional to the bulk resistivity of the materials involved and increases rapidly for film thickness less than 50 microinches. Since the skin depth for these materials at 9 GHz is between 27 and 35 microinches, the minimum loss for each conductor system is approached when the thickness of the film is approximately two times the skin depth at the operating frequency.

Figure 29 shows the loss for quartz dielectric microstrip lines. For thin dielectric layers the loss is very high, but decreases to acceptable values for films approximately 2 mils thick. Loss in the conductors is included in the values given.

The measurements cited were taken in a 50-ohm test system with a microstrip line that had a 6-mil-wide conductor. For this case the VSWR was less than 1.10 at the input.

From the foregoing findings, it is evident that low-loss interconnections for microwave integrated circuits can be constructed as sections of microstrip transmission lines. All the types of material used are suitable for fabricating microstrip lines, with the loss in each case being proportional to the bulk resistivity of the principal metal.

## E. APPLICATION INFORMATION

Recent investigation of striplines applications by Texas Instruments have made information available on several different types of stripline devices.

### 1. Power Dividers

Some types of power dividers take on different forms for use at different frequencies. This is shown by the N-way power divider which was built in both lumped-constant and distributed transmission-line form.

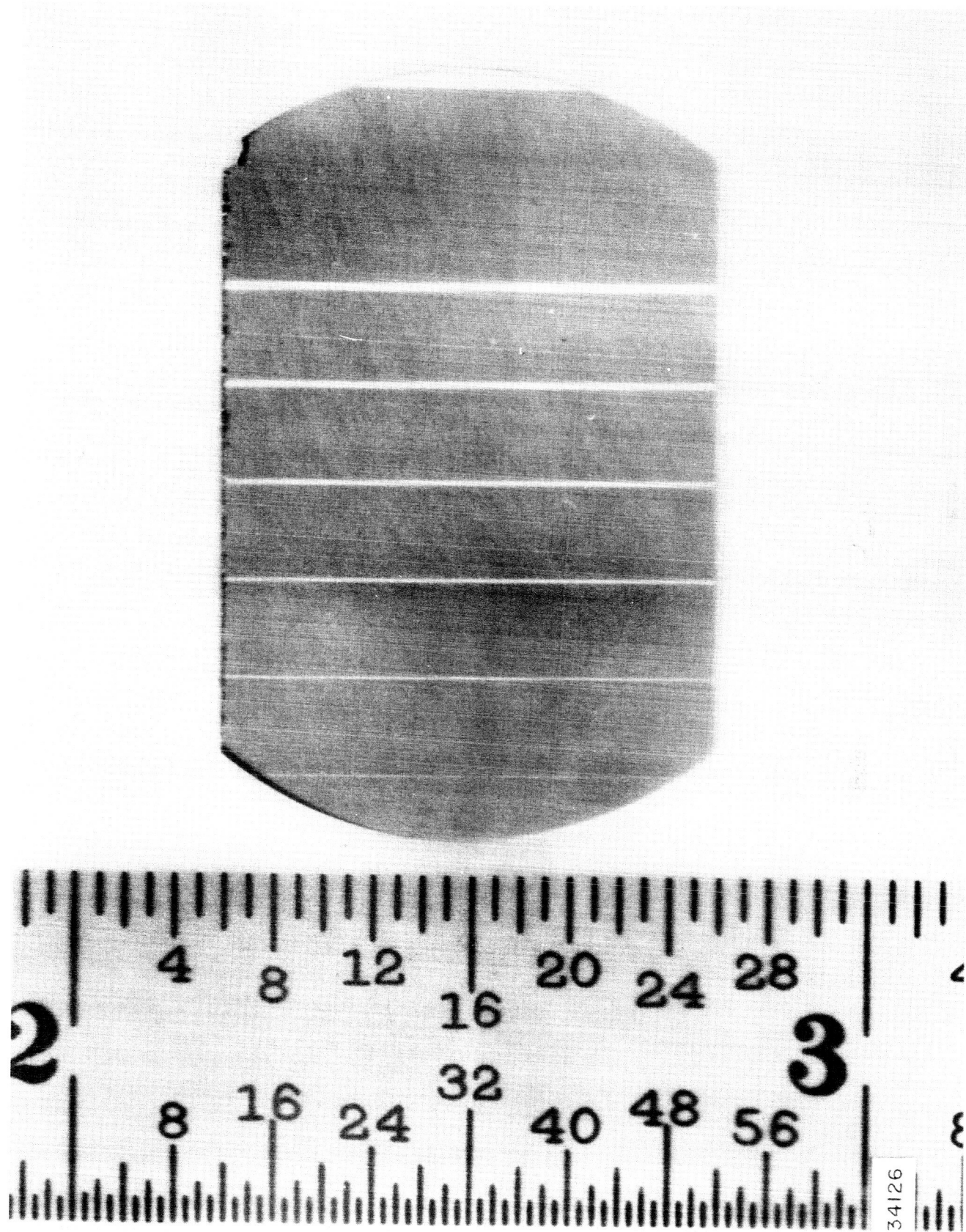


Figure 27. Microstrip Lines on a Semiconductor Slice<sup>18</sup>

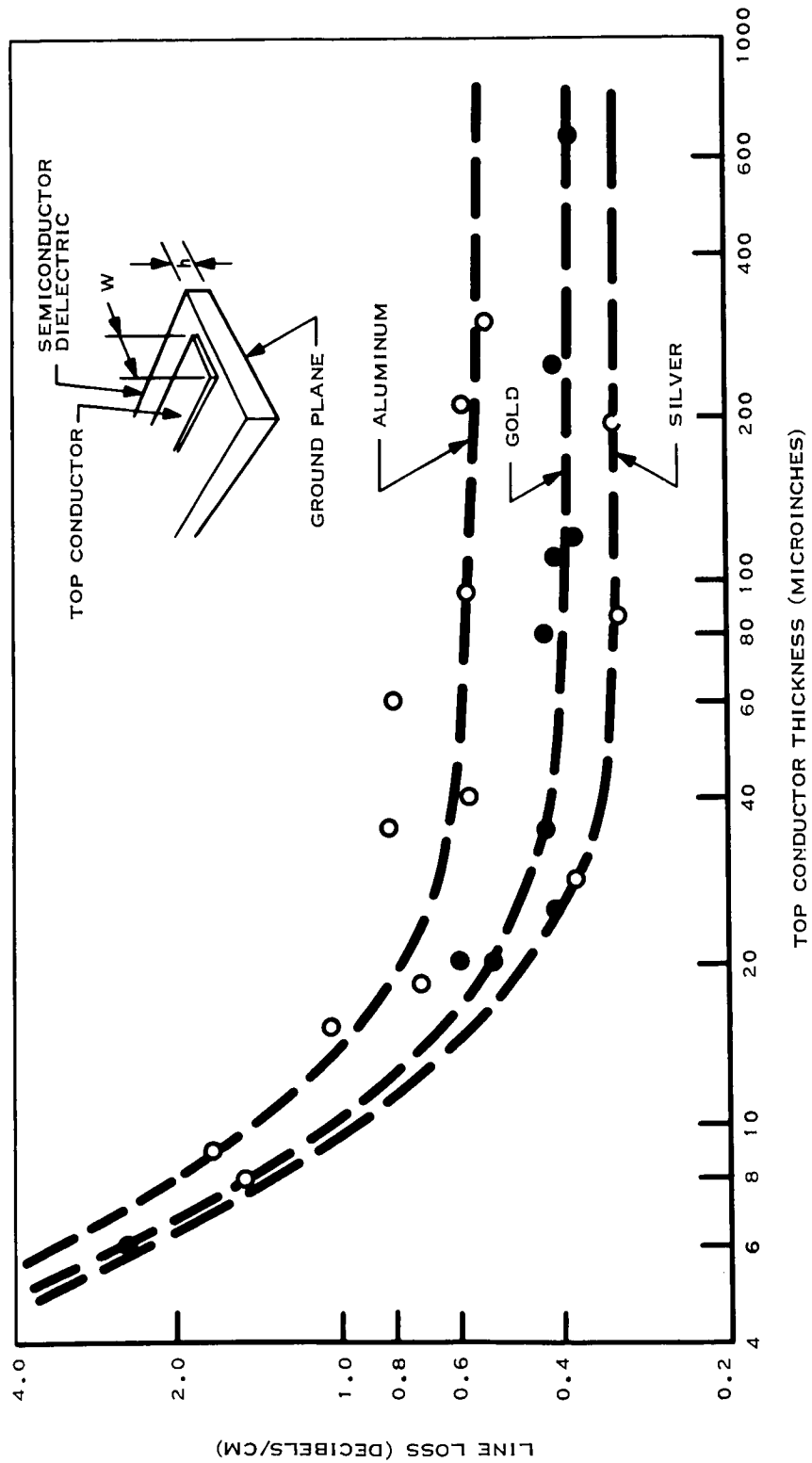
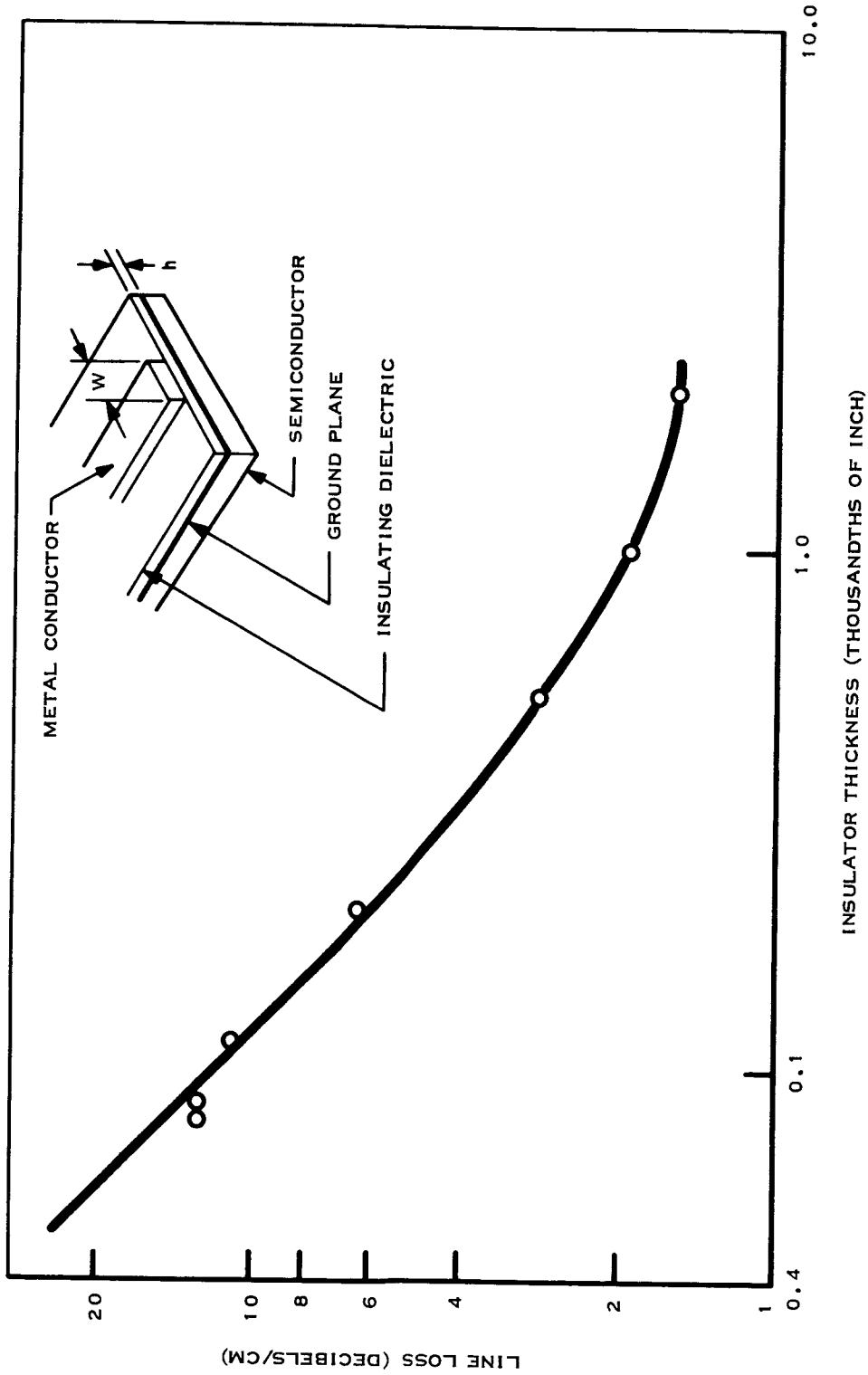


Figure 28. Line Loss as a Function of Top Conductor Thickness for Aluminum, Gold, and Silver Microstrip Lines<sup>18</sup>

34116



34117

Figure 29. Line Loss as a Function of Quartz Dielectric Thickness 18

The types considered are referred to as resistive, reactive, toroid, N-way, branch line, coupled line, and hybrid power dividers. The results of the findings from a MERA investigation on these power dividers are presented in Table V.<sup>20</sup>

## 2. Stripline Terminations

In the design of power dividers with isolation, dissipative terminations or resistors are needed. In order to ensure terminations of low VSWR, several test pieces were built for measuring film resistors fabricated especially for stripline. Two types of termination were considered, one with the lines behind the resistor shorted directly to ground as close to the resistor as possible and the other, a quarter-wave open-circuited stub behind the resistor. Both approaches provided VSWR's of less than 1.1 at all frequencies up to 2.125 GHz (typical values being 1.05), with the quarter-wave stubs being slightly better. At 8.5 GHz only the quarter-wave stub was satisfactory (1.04 VSWR), the shorted line giving 1.7 VSWR. Both wide and narrow versions of Filmohm resistors were used. Generally, it was found that use of transmission lines and resistors of approximately the same width resulted in better VSWR's.

In addition, some EMC pill-type terminations were tested. These were satisfactory up to 500 MHz with less than 1.08 VSWR, but the VSWR become 1.3 and greater at 2.215 GHz and above.

## 3. Meander Lines

A meander line is a transmission line which has been folded or compressed in order to conserve space or to achieve a desired phase shift in a relatively small space. Such a device may be desirable in a system, especially at 125 and 500 MHz where a quarter-wavelength of line is prohibitively long.

In stripline, the meander line may be in the form shown in Figure 30. It is evident from the figure that various degrees of coupling may exist between the elements of the meander line, depending upon the

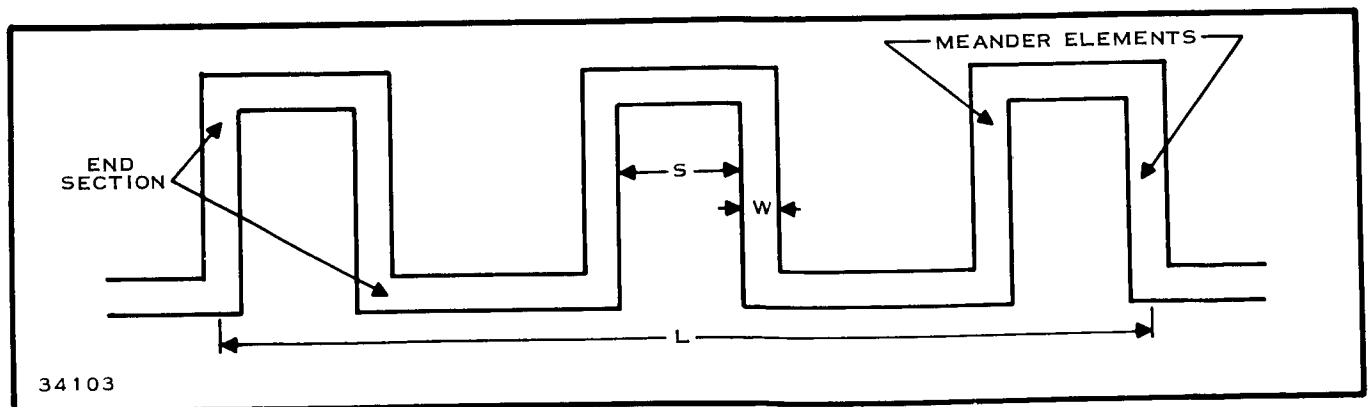
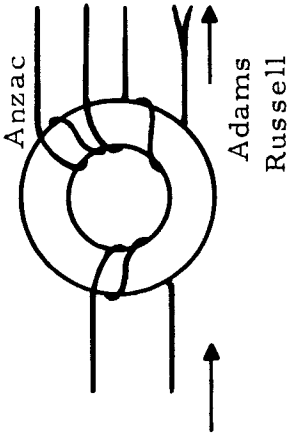
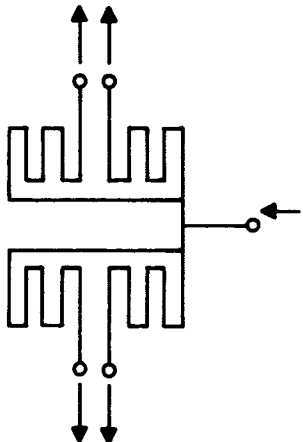


Figure 30. Meander Line



Table V. Types of Power Dividers

Design	Theory	Performance	Comments
125-MHz toroid		<p>VSWR 1.08</p> <p>Amplitude unbalance 0</p> <p>Isolation 35 dB</p> <p>Volume 0.06 in.<sup>3</sup></p> <p>VSWR 1.05</p> <p>Amplitude unbalance 0</p> <p>Phase unbalance 4 deg</p> <p>Isolation 37 dB</p> <p>Volume 0.12 in.<sup>3</sup></p>	<p>Accuracies at 125 MHz</p> <p>Amplitude &lt; 0.2</p> <p>Phase accuracy &lt; 1 deg</p> <p>High cost</p>
125-MHz, 4-way power divider		<p>VSWR 1.07</p> <p>Insertion loss (dissipated) 0.1 dB</p> <p>Amplitude unbalance 0</p> <p>Isolation 36 dB</p> <p>Volume 1/32-inch board</p> <p>1/16-inch board</p>	<p>Centered at 150 MHz</p> <p>0.2 dB at 175 MHz</p>

Resistors between outputs

Table V. Types of Power Dividers (Continued)

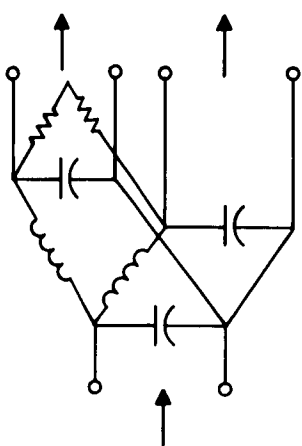
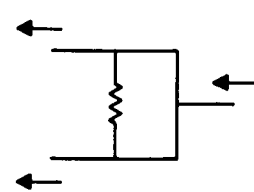
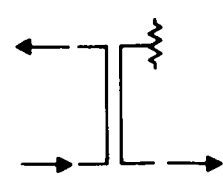
Design	Theory	Performance	Comments
<p>125 - MHz lumped-constant</p> 		<p>Mismatch</p> <p>Amplitude unbalance</p> <p>Phase unbalance</p> <p>Isolation</p> <p>Volume</p> <p>1/32-inch board</p> <p>1/16-inch board</p>	<p>55 ohms or</p> <p>1.1 VSWR</p> <p>0.2 dB</p> <p>1 deg</p> <p>46 dB</p> <p>0.46 in.<sup>3</sup></p> <p>0.105 in.<sup>3</sup></p> <p>4-way</p> <p>(0.034 coax)</p>
<p>500 - MHz, 2-way unbalance</p> 	<p>Unbalance on outputs of</p> <p>2.3 dB</p>	<p>VSWR</p> <p>Amplitude unbalance</p> <p>Phase unbalance</p> <p>Isolation</p> <p>Volume, 1/16-inch board</p>	<p>500 MHz</p> <p>Phase accuracy &lt; 2 deg</p> <p>Amplitude &lt; 0.2 deg</p> <p>1.03</p> <p>2.2 dB</p> <p>0.35 deg</p> <p>26 dB</p> <p>2 in.<sup>3</sup></p>
<p>500 - MHz coupled line</p> 	<p>Unbalance of input to output</p> <p>15 dB</p> <p>Phase unbalance</p> <p>90 deg</p>	<p>VSWR</p> <p>Input-output unbalance</p> <p>Isolation</p> <p>Phase unbalance</p> <p>Volume, 1/16-inch board</p>	<p>90 deg at 420 MHz</p> <p>1.04</p> <p>15.3 dB</p> <p>43 dB</p> <p>103 deg<sub>3</sub></p> <p>0.8 in.<sub>3</sub></p>

Table V. Types of Power Dividers (Continued)

Design	Theory	Performance	Comments
500 - MHz branch line	Coupling 3 dB Phase unbalance 90 deg	VSWR Amplitude unbalance Phase unbalance Isolation Volume, 1/16 -inch board	1.08 0.6 dB 93 deg 21 dB 3.15 in. <sup>3</sup> 25 dB at 530 MHz
500 - MHz branch line	Phase unbalance 90 deg	VSWR Amplitude unbalance Phase unbalance Isolation Volume, 1/16 -inch board	1.03 0 92.2 deg 27 dB 4.7 in. <sup>3</sup>
500 - MHz, unbalanced 3-way		VSWR Amplitude unbalance Phase unbalance Isolation Volume, 1/16 -inch board	1.02 all within 0.2 dB of calculated 2.5 deg 16.2, 21.8, 21.8 dB 2 in. <sup>3</sup> Excluding resistors

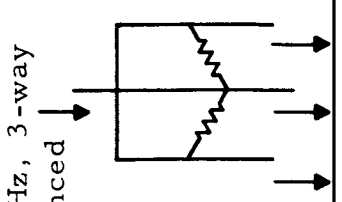
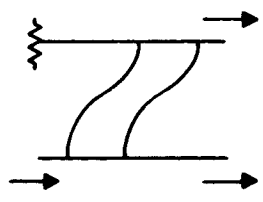
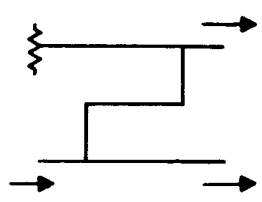


Table V. Types of Power Dividers (Continued)

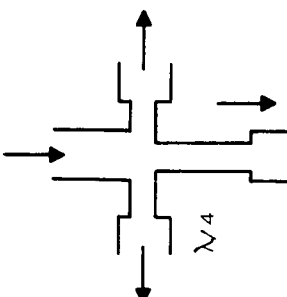
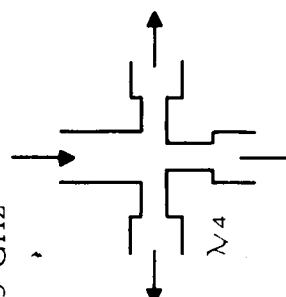
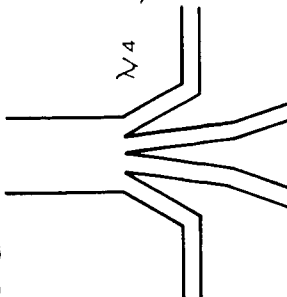
Design	Theory	Performance	Comments
500-MHz reactive unbalance 	VSWR Amplitude unbalance  Phase unbalance  Volume, 1/16-inch board (rerouted)	1.06 Within 0.3 dB of calculated values 1.8 deg  5.3 deg at 550 MHz and increases rapidly  0.80 in. <sup>3</sup>	-3, -5, 7, -7.6
2.125 GHz 	VSWR Output unbalance Phase unbalance Volume, 1/16-inch board (rerouted)	1.09 0.3 dB 2.5 deg 0.18 in. <sup>3</sup>	Error < 0.2 dB Error < 2 deg
2.125 GHz reactive 	VSWR Output unbalance Phase unbalance in pairs Volume, 1/16-inch board	1.15 0.1 dB  0.4 deg, 2.7 deg 0.252 in. <sup>3</sup>	

Table V. Types of Power Dividers (Continued)

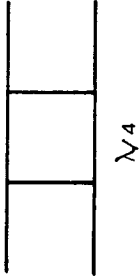
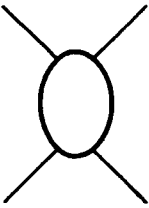
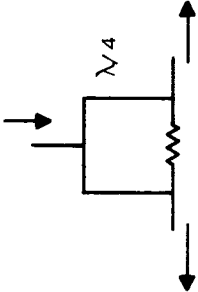
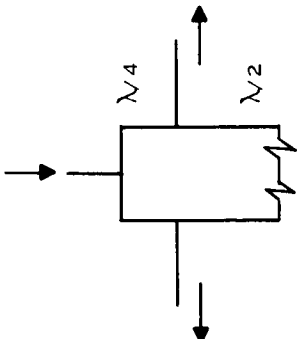
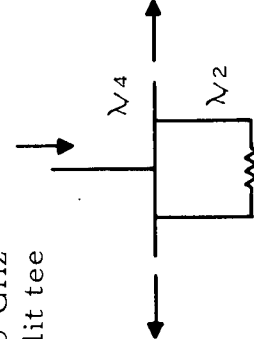
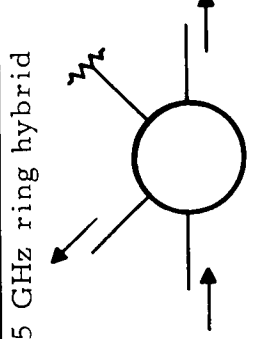
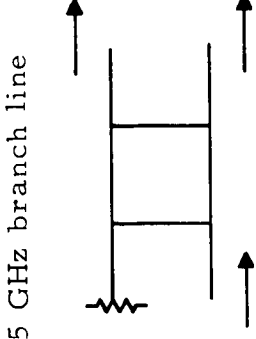

Design	Theory	Performance	Comments
2.125 GHz branch line	Phase unbalance 90 deg	VSWR Output unbalance Phase unbalance Volume, 1/16-inch board	1.04 0.45 dB 85.1 deg 0.49 in. <sup>3</sup>
			
2.125 GHz coupled line cascade coupler	Output balance ≈ 0.5 dB	VSWR Output unbalance Phase unbalance Isolation Volume, 1/16-inch board	1.04 0.5 dB 97.5 deg 24.5 dB 0.71 in. <sup>3</sup>
			
2.125 GHz split tee		VSWR Output unbalance Isolation Volume, 1/16-inch board	1.35 0.1 dB 14 dB (BAD) 0.21 in. <sup>3</sup>
			

Table V. Types of Power Dividers (Continued)

Design	Theory	Performance	Comments
Split tee 2.125 GHz 	Two 50-ohm Filmohm resistors	VSWR Output unbalance Phase unbalance Isolation	1.07 0.1 dB 13.5 deg 39 dB
8.5 GHz split tee 	One 100-ohm composition resistor	VSWR Output unbalance Phase unbalance Isolation Volume, 1/16-inch board	1.08 0.1 dB 0.1 deg 29 dB 0.35 in. <sup>3</sup>
8.5 GHz split tee 		VSWR Amplitude unbalance Phase unbalance Isolation Volume, 1/16-inch board	1.25 1.14 0.1 dB 1.5 deg ±3.0 deg 22 dB 0.113 in. <sup>3</sup>
8.5 GHz ring hybrid 	Phase 180 deg	VSWR Amplitude unbalance Phase unbalance Isolation Volume, 1/16-inch board	1.07 0.1 dB 179.3 deg 33.2 dB 0.16 in. <sup>3</sup>
8.5 GHz branch line 	Phase 90 deg	VSWR Amplitude unbalance Phase unbalance Isolation Volume, 1/16-inch board	1.5 5.6 dB 115 deg 12 dB 0.14 in. <sup>3</sup>

spacing between elements; this coupling has the effect of reducing the effective phase shift across the meander line and also of lowering the impedance of the line. Equations have been derived which relate the effective phase across the meander line to the physical length of a meander element; another equation relates image impedance of the meander line to physical length of one meander element.

It is relatively simple to determine the characteristics for a given design. Many lines will have electrical lengths from 10 to 90 degrees and characteristic impedances from 15 to 115 ohms. Only a small number of designs are required, and accordingly, the design procedure employed uses a trial-and-error selection in conjunction with a limited computer program. This procedure will normally enable the synthesis of a meander line of specified electrical length  $a$  and specified image impedance  $Z_i$  in 20 to 30 minutes. Test sections have been built and tested at 125 MHz. The results verified the analytical procedure.

#### 4. Material Considerations

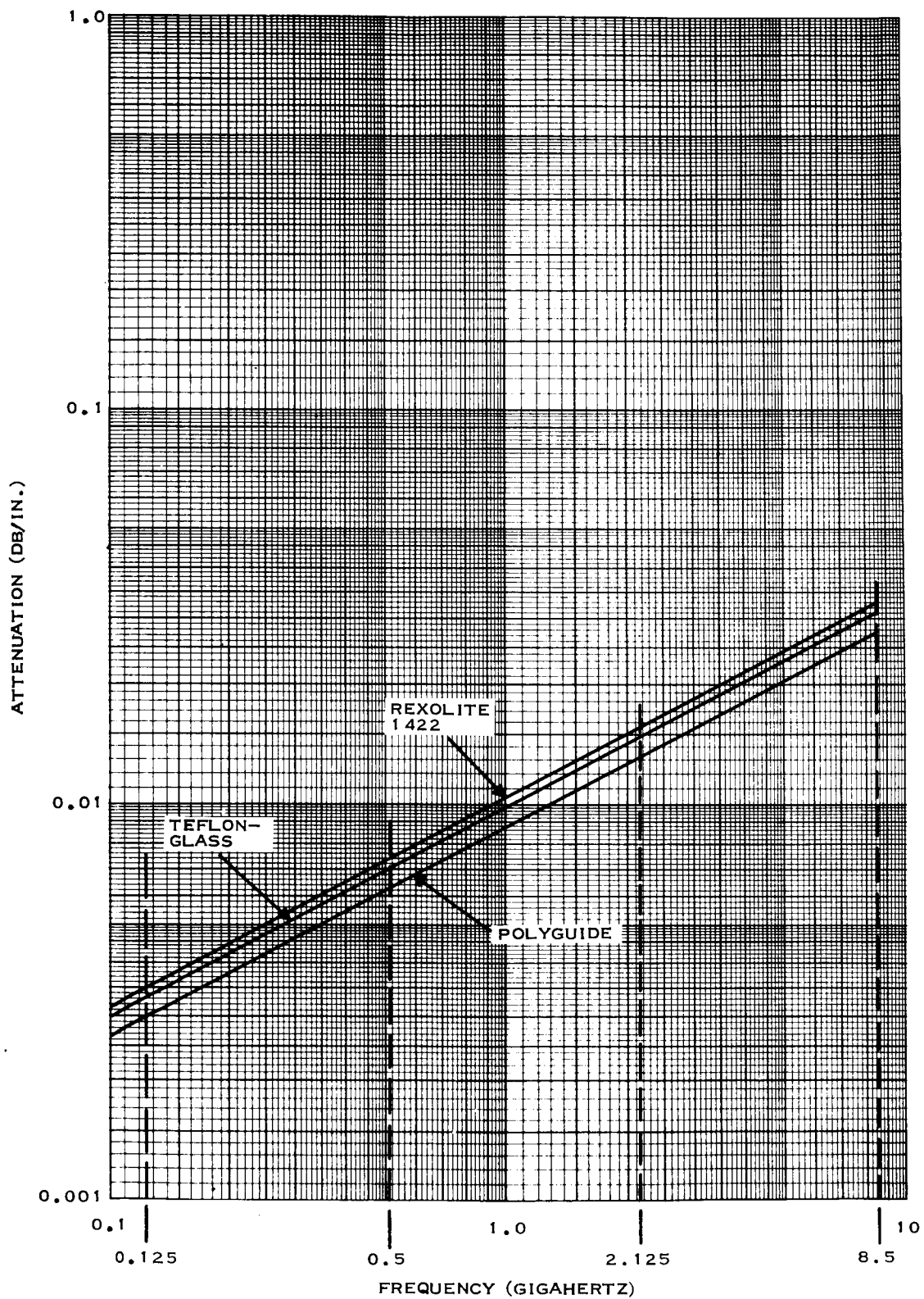
After a preliminary evaluation of the various stripline materials available, three materials were selected for detailed evaluation.

These are glass-Teflon, Rexolite and Polyguide. The relative attenuation values of these materials over the frequency range of interest are shown in Figure 31.<sup>20</sup> It can be seen that Polyguide is the most desirable material to use from the standpoint of loss. Table VI summarizes the characteristics<sup>20</sup> of the materials and notes the impedance and phase variations due to the allowable tolerances.

Where possible, single registration should be used to eliminate the problem of obtaining close alignment of the image circuits required in double registration. The only problem noted in using single registration is that no air gap can be allowed between the circuit board and its ground plane board. One-ounce copper-clad was selected because of the undercutting problems encountered in the etch process on boards with two-ounce clad or greater. Etching problems are due to the etching tolerance required and the severe warpage which occurs in Polyguide and Rexolite.

Stripline resistors are required in the hybrid power dividers to obtain isolation between outputs. So far only two vendors have been found to manufacture these resistors, Filmohm and EMC. The standard Filmohm resistors are too wide for high-frequency, low-VSWR use. The standard EMC resistors are 0.012 to 0.040 inch thick, requiring the stripline material to be milled out to accept them.

Some effort was applied to the use of 0.1-watt composition resistors, and it seems likely that these inexpensive resistors can be used at the lower frequencies at least.



34102

Figure 31. Attenuation of Various Stripline Materials Versus Frequency<sup>20</sup>



Table VI. Tolerance Analysis of Stripline Design and Manufacture

	Tolerance			
	Teflon-Glass 1/16 in., 1 oz, e = 2.6	Rexolite 1422 1/16 in., 1 oz, e = 2.53	Polyguide 1/16 in. or 1/32 in. 1 oz, e = 2.33	
Board thickness (1 board)	±0.002 in.	±0.002 in.	±0.001 in.	
Dielectric constant	±0.05 in.	±0.001 in.	±0.005 in.	
Drawing	±0.001 in.	—	—	
Etching	±0.0014 in.	—	—	
Increase $Z_0$ by increasing board thickness or by decreasing strip width or dielectric constant				
Impedance variation (nominal 50-ohm line)	Teflon-Glass 1/16 in., 1 oz	Rexolite 1422 1/16 in., 1 oz	Polyguide	
			1/16 in., 1 oz	1/32 in., 1 oz
	47.7 to 51.5 ohms	48.2 to 52.2 ohms	49.8 ohms to 52.8 ohms	48.25 ohms to 51.5 ohms
	-2.945 to +3.44 deg	-0.048 to +0.723 deg	-0.2325 to +0.464 deg	
Attenuation Comparison (See Figure 31)				
Method of Calculation	Teflon-Glass	Rexolite 1422	Polyguide	
	tan $\delta$ given on data sheet for 0.001 GHz, and it is about five times tan $\delta$ for Rexolite at 0.001 GHz; tan $\delta$ assumed to be five times that of Rexolite at 1 GHz.	Calculated from known values of tan $\delta$ given on Rexolite data sheet from 0.1 to 10 GHz.	Attenuation given on data sheet for 1.3 GHz; straight line drawn through this point with same slope as Rexolite curve.	

## SECTION V

### THIN-FILMS

#### A. GENERAL

In a number of areas thin-film passive components such as resistors and capacitors offer distinct advantages over their diffused counterparts. Circuit requirements in many instances cannot be met with diffused resistors and capacitors, and in these instances, the advantages of thin-film components can be exploited. There are essentially two reasons for using thin-films.

First, it may not be possible to achieve the desired characteristics for the diffused resistor or capacitor whereas the characteristics can be achieved in thin-films. Thin-film capacitors provide improved characteristics in the areas of improved temperature coefficient, reduced dissipation factor, reduced parasitic capacitance, higher breakdown voltage levels with greater consistency, reduced sensitivity of capacitance to voltage level, lower series resistance, and higher frequency of operation. Similarly, thin-film resistors offer wider range of sheet resistance, reduced distributed capacity, improved temperature coefficient, higher voltage breakdown, and a much greater high-frequency operating limit.

Second, though it might be possible to achieve the desired characteristics with diffused components, the required diffusion would seriously degrade the transistor parameters. In effect, this limits the flexibility of the diffusion process for optimizing transistor parameters; for instance, if a transistor with a high  $h_{fe}$  is required, a narrow base width is necessary. A diffused capacitor on the same substrate would thus have a thin diffused region over the large surface required to achieve the desired capacitance. Low yields would result because of the difficulty in maintaining the thin-diffused region over a large area. In another case, where a good low-level transistor is required, a low-concentration base diffusion is necessary. A resistor formed with this low-concentration diffusion would have a high temperature coefficient that would be unacceptable in many applications. In both cases, the use of thin-film passive components would allow the diffusion process to be tailored to the best transistor design.

Two approaches are used to apply thin-film resistors and capacitors to thin-film/monolithic circuits. In one approach, the resistors and capacitors are deposited on one or more silicon substrates, with the active devices contained on other substrates. This multichip approach is the older and more versatile of the two. In the second approach, the thin-film passive components are deposited with the active devices on the same substrate. This approach represents the ultimate integration of thin-film/monolithic circuits, but requires modified assembly processes to prevent damage to the films due to conventional high-temperature assembly processes.

In the following subsections, the characteristics of thin-film resistors and capacitors suitable for use in the microwave region are presented and compared with their diffused counterparts.

## B. RESISTORS

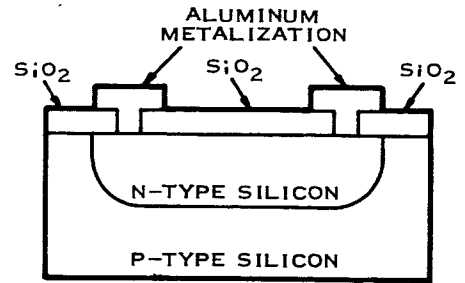
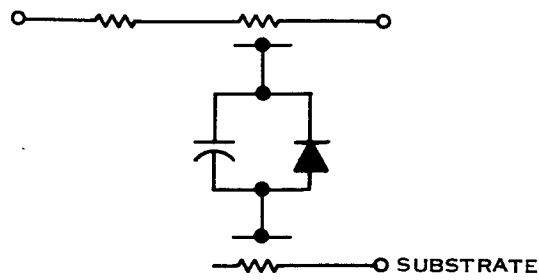
Typical equivalent circuits and geometries for the thin-film and diffused resistors are shown in Figure 32. The diffused resistor can be used as an integral part of the monolithic circuit or on a separate substrate for incorporation into hybrid circuits; both uses are shown in Figure 32.

The equivalent circuit for the diffused resistor for use in hybrid circuits consists of a small series lead and contact resistance plus the main diffused resistance. Associated with this main resistance is a distributed capacity and diode to the substrate. Most of the problems with this resistor are due to the high parasitic capacitance, which results from the reverse-biased junction used to obtain isolation for the resistor from other components on the same substrate. This parasitic junction capacitance is on the order of 0.1 to 0.2 pF/mil<sup>2</sup> and is the main reason for the limited application of diffused resistors at high frequencies.

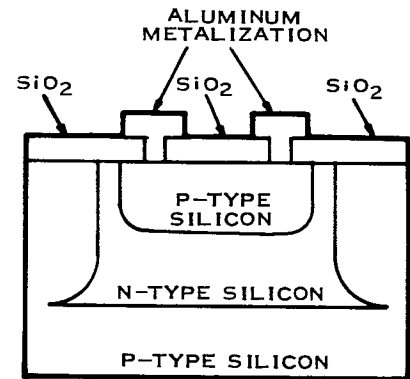
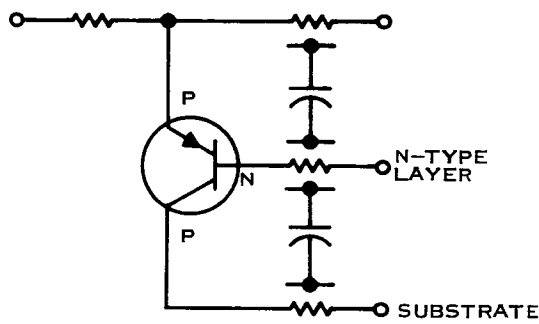
When diffused resistors are incorporated into monolithic circuits, the equivalent circuit is more complex, as shown at B of Figure 32. In this case a distributed transistor becomes a part of the circuit. As shown in the typical geometry, the N-type region becomes the base of this distributed transistor, which has a relatively low  $h_{fe}$  due to the thickness of the N-type diffusion—on the order of 1. The base-emitter junction must be kept reverse biased to avoid the possibility of forward biasing resulting from leakage. If this is not done, shunt leakage between the resistor and the substrate will occur.

The equivalent circuit for the thin-film resistor, C of Figure 32, is much simpler (only the distributed capacity to the substrate is shown). This capacity is much lower than that associated with the diffused resistor—at least an order of magnitude. Because the films can be made with higher sheet resistivity than that obtained with the diffused resistor, the area covered can be smaller and the distributed capacity can be reduced to a very low value.

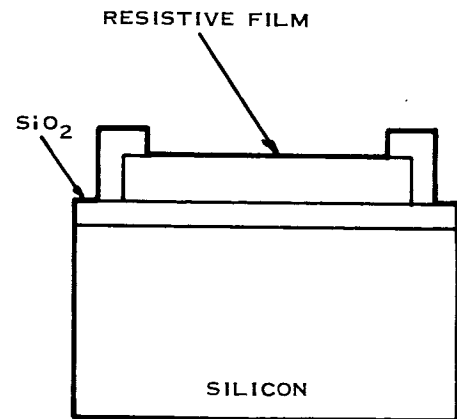
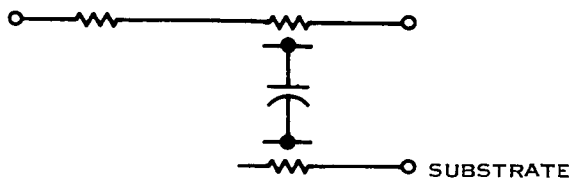
A large number of materials have been used in the fabrication of thin-film resistors, notably, metal films, nickel-chromium and tantalum, and the cermet material, tantalum-tantalum pentoxide. The chief advantages of cermet are its higher sheet resistivity, greater stability, and compatibility with the high-temperature integrated circuit processes of bar mounting and ball bonding. Because of the small size of resistors normally required in microwave circuitry, the higher sheet resistivities are not essential; where the higher sheet resistivity can be used, however, the distributed-capacity effects will be less because of the smaller area. A disadvantage of cermet



A. DIFFUSED RESISTOR FOR HYBRID CIRCUITS



B. DIFFUSED RESISTOR FOR MONOLITHIC CIRCUITS



C. THIN-FILM RESISTOR

34101

Figure 32. Equivalent Circuits and Geometries for Diffused and Thin-film Resistors

is its relatively high temperature coefficient of resistance (-20 to -1000 ppm/°C) as compared, for example, to that of Nichrome (0 to +100 ppm/°C). An advantage of tantalum film resistors is that the resistance value can be trimmed by anodizing the film. With the other two materials, scratch patterns must be used to trim the value of resistance if precise tolerance is required. All three materials have been used at Texas Instruments with good results. For the most part, the metal film resistors have been used on substrates separate from the active components where the resistors were not later subjected to the high temperature processes mentioned.

### 1. Characteristics

The high-frequency performance of the diffused resistor is limited primarily by the distributed capacity associated with the reverse-biased junction previously discussed. The amount of capacity per unit area is a function of the voltage across the junction and the doping level on the lightly doped side of the junction. An approximate expression for this capacitance per unit area, assuming a step junction, is given by

$$C_t = \sqrt{\frac{qk\epsilon_0 N}{2V_t}} \quad (1)$$

where

$q$  is the charge on the electron

$k$  is the dielectric constant

$\epsilon_0$  is the permittivity of free space

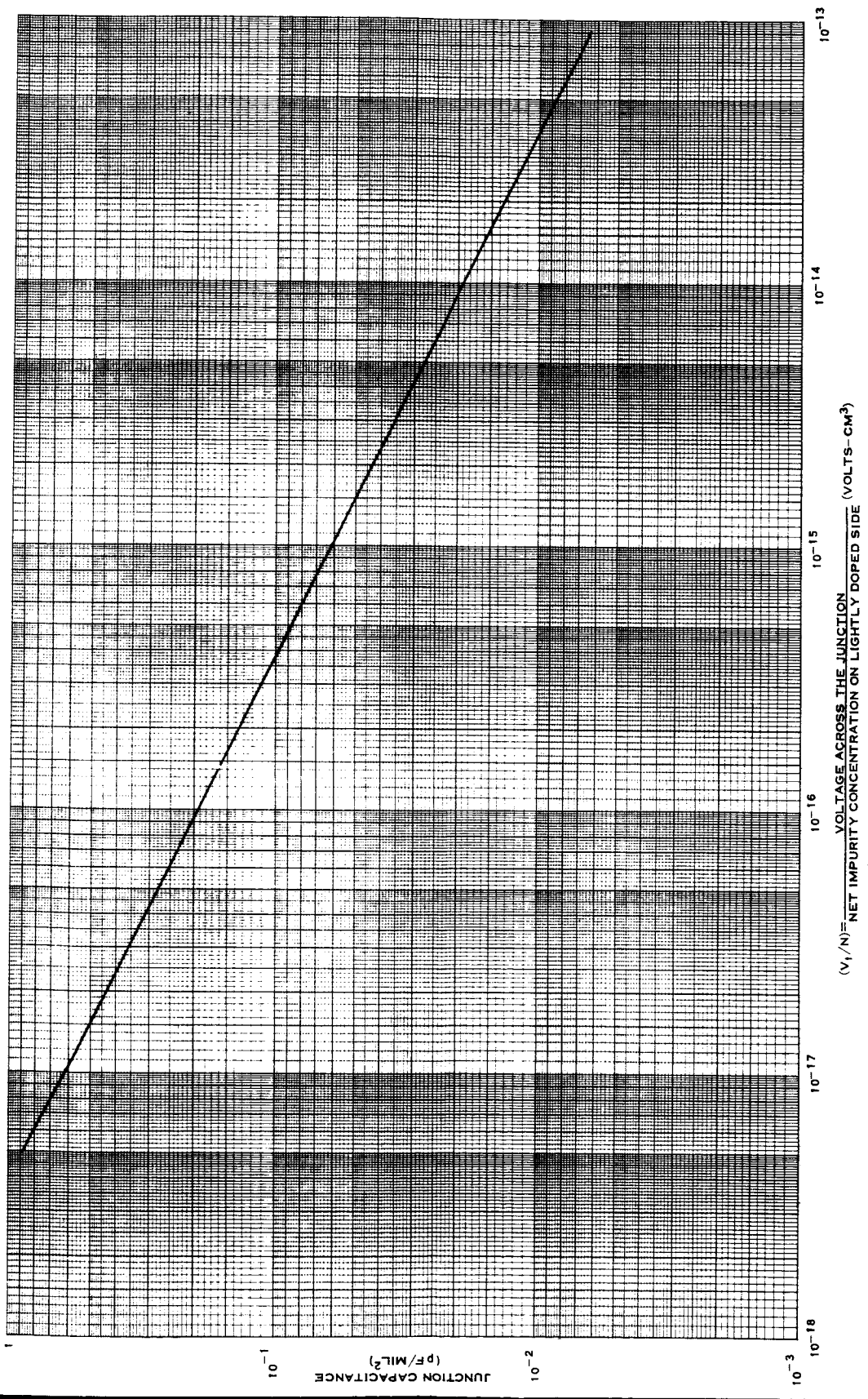
$N$  is the net impurity concentration on the lightly doped side of the junction

$V_t$  is the total voltage across the junction.

A plot of Equation (1) is shown in Figure 33 for typical values of the ratio  $V_t/N$ . Figure 33 shows further that the capacitance per square mil will normally lie in the range between 0.05 to 0.5 pF/mil<sup>2</sup> for the doping levels normally used.

In general, we may define the practical high-frequency operating limit for resistors to be that frequency where the reactance of the distributed capacity equals the dc resistance. When this is done and consideration is given to the sheet resistivities available as well as to the values of resistors normally encountered in high-frequency circuitry, diffused resistors may be used at fairly high frequencies. The important point is that no simple statement can be made about the upper frequency limit of diffused resistors.

Figure 34 shows the practical high-frequency limit as a function of the resistor value and geometry. The capacitance per unit area used is the



34100

Figure 33. Variation in Junction Capacitance as a Function of the Ratio of the Total Voltage Across the Junction to the Net Impurity Concentration on the Lightly Doped Side of the Junction

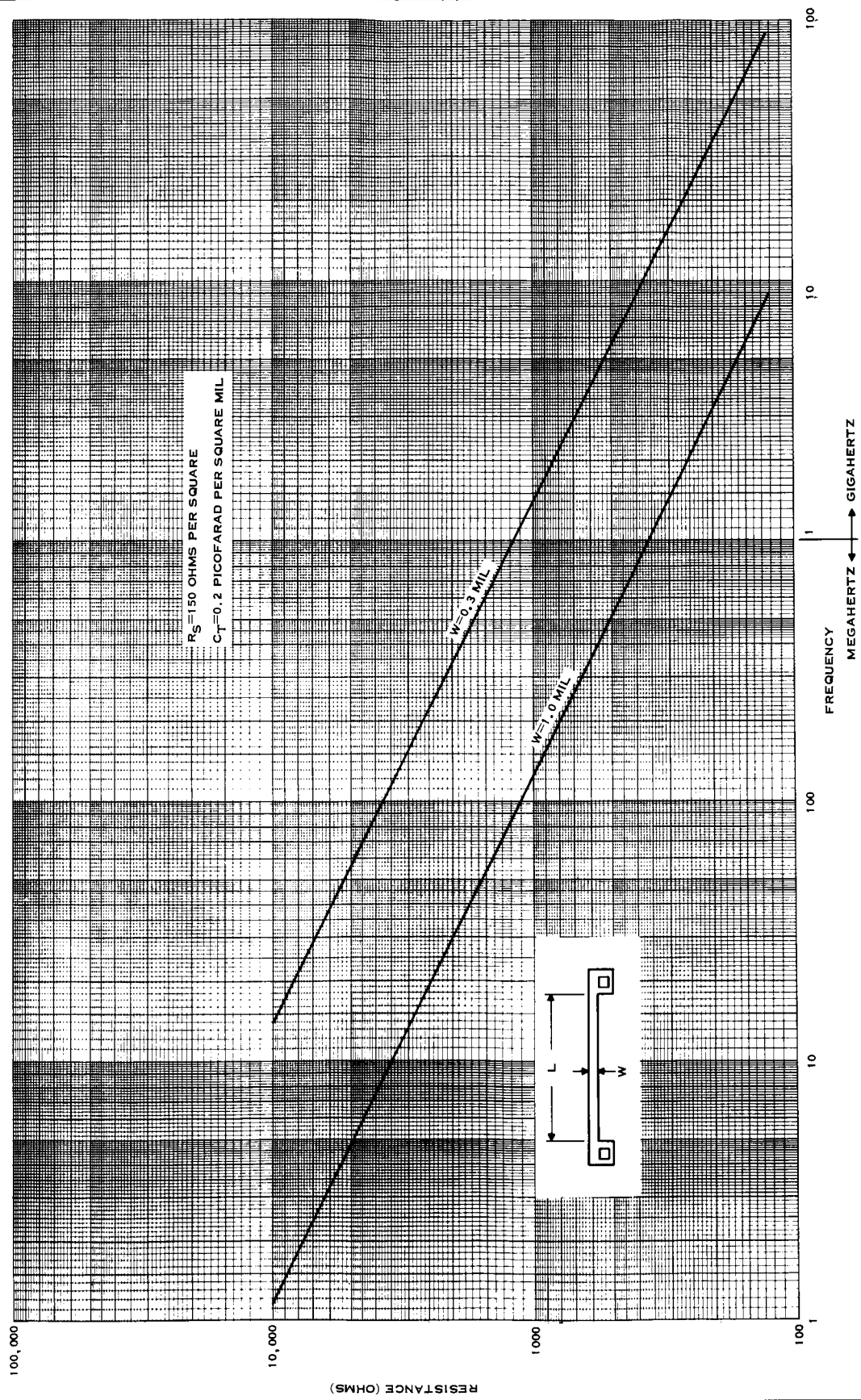


Figure 34. Practical High-frequency Operating Limit for Diffused Resistors

nominal value of 0.2 pF/mil.<sup>2</sup> The sheet resistivity used is 150 ohms/square and is typical for diffused resistors. The geometry using a 0.3-mil-wide resistor naturally has a greater high-frequency operating limit because of its smaller area. This width is the smallest that should be considered at this time. Measurements (based on the definition in the preceding paragraph) made on 0.5-mil resistors having values in the 3000- to 5000-ohm range show high-frequency limits of 10 MHz to 20 MHz. These measurements agree with the values that would be obtained from Figure 34. For small values of resistance, with narrow line widths, operation up to a few hundred megahertz should be quite feasible. Indeed, this is currently being demonstrated in integrated circuit operational amplifiers.

In contrast, thin-film resistors have a distributed capacity that is at least an order of magnitude lower than diffused resistors.<sup>28</sup> In addition, the higher sheet resistivities available allow this parasitic capacity to be held low even when large values of resistance are required. This basically lower capacity combined with the increased flexibility in design due to the greater range of sheet resistivity extends the useful operating frequency range for resistors well into the gigahertz range.

In most cases, the range of sheet resistivity for diffused resistors is governed by the base diffusion for transistors and falls between 80 and 200 ohms/square. Resistors made at the same level as the collector or emitter are not normally used. The collector diffusion is a relatively deep diffusion with a higher sheet resistivity, the value of which is difficult to control. Furthermore, the temperature coefficient of resistance is poor. The emitter diffusion has a high impurity concentration with the result that the temperature coefficient of resistance is low but the sheet resistivity is also low. Thus, the emitter diffusion is useful only for making resistors of very low value. Although the sheet resistivity can be extended beyond the range noted (by adjusting the diffusion parameters), this is not normally done since it compromises the parameters of the transistors on the same substrate.

Greater latitude in the choice of sheet resistivity is found when thin-film resistors are used. Nichrome thin-films can be made with sheet resistivities ranging from very low values (around 1 ohm/square) up to 300 ohms/square. Tantalum films are limited to about 150 ohms/square. The cermet material (tantalum-tantalum pentoxide) is available with resistivities up to 5000 ohms/square; this material is also more stable than the metal films, in part due to its greater thickness. It is usually an order of magnitude thicker than the metal films. Figure 35 shows the range of resistivities for the diffused resistors and the three metal films.

A comparison of the temperature coefficient of resistance (TCR) for the different resistors is shown in Table VII. For diffused resistors using the P-type base diffusion, the TCR ranges from 1000 ppm/°C to 2500 ppm/°C for the range of resistivities normally encountered. On the other hand, a



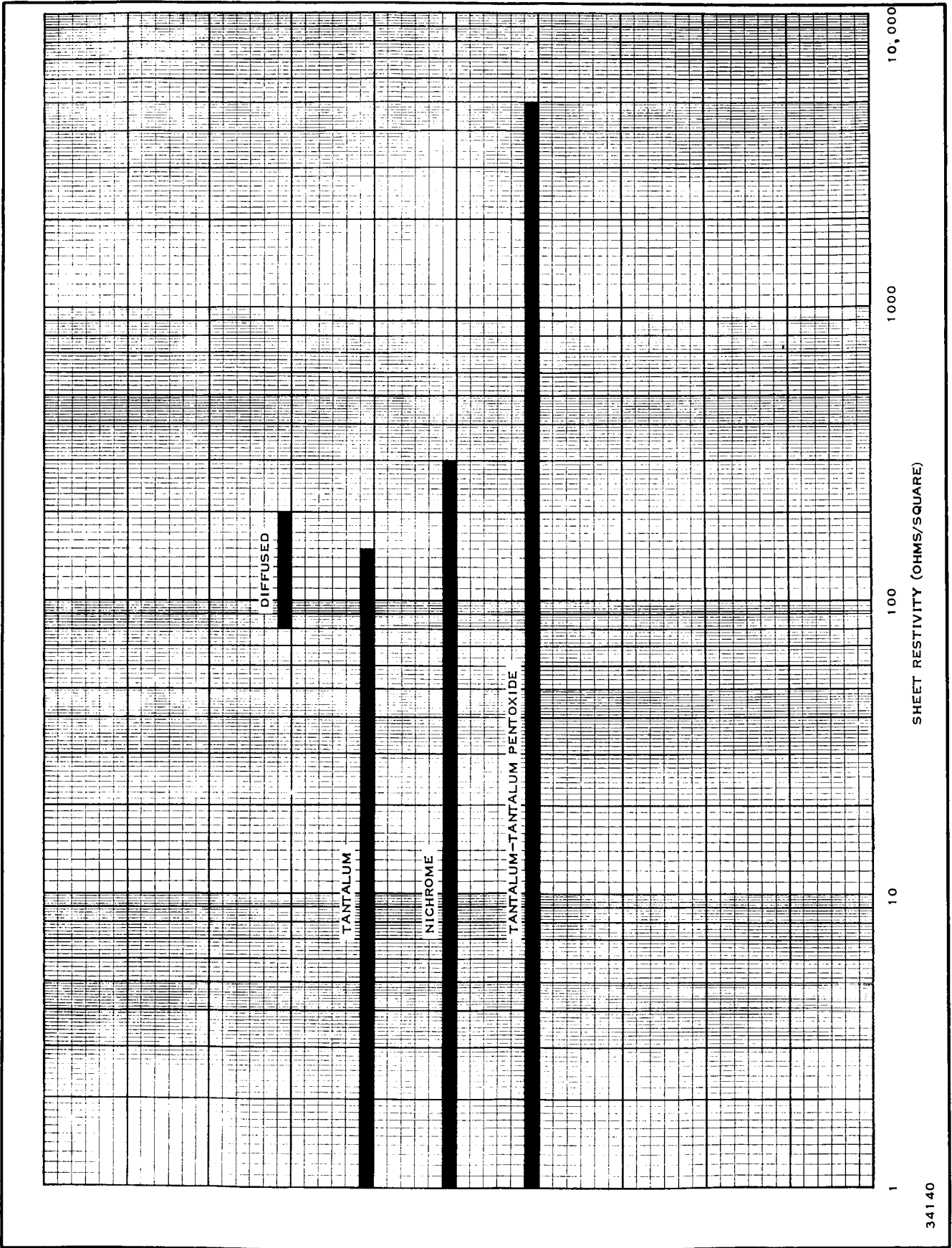


Figure 35. Sheet-resistivity Ranges for Diffused and Thin-film Resistors

34140

Table VII. Temperature Coefficients of Resistance

Resistor	ppm/°C
Diffused (P-type base diffusion)	1000 to 2500
Nichrome	0 to 50
Ta-Ta <sub>2</sub> O <sub>5</sub>	-20 to -1000

200-ohm/square Nichrome film, has a TCR between 0 and 50 ppm/°C. If required, the evaporation process can be controlled such that the TCR can be maintained consistently within 25 ppm/°C. The cermet materials have a relatively high TCR, -20 to -1000 ppm/°C.

Another disadvantage of diffused resistors is the often excessively low breakdown voltage between the resistor and the substrate. This is generally attributed to junction imperfections and is a yield problem that increases with the area of the diffused junction and the operating voltage. The use of thin-film resistors on top of the oxidized silicon substrate eliminates the problem, since the breakdown of the silicon dioxide layer ranges from 200 to 1000 volts.

The minimum width for the thin-film resistors should be not less than 1 mil because of the difficulty in maintaining control over the line width and preventing undercutting. As the width of the line is reduced, the resistor tolerance increases as a result of this process control problem. Initial tolerance ranges between 5 and 10 percent for a 1-mil thin-film resistor. The tolerance can be reduced either by using a scratch pattern or, in the case of tantalum, by oxidizing the film. For comparison, diffused resistors offer a tolerance of about 20 percent.

## 2. Process Compatibility

Problems have been encountered when thin-film resistors are deposited on the same substrate with active devices. The major problem arises from the high temperatures used in the subsequent assembly operations. The bar-mounting operation normally used takes place at 375° to 475°C under oxidizing conditions. This environment is much too severe for metal films and high sheet-resistance films. The film may be damaged or the surface of the film will likely oxidize, and the resulting reduction in thickness of the film will increase the sheet resistance. This situation is improved by using gold-germanium preforms for mounting. The temperature required is about 375°C, and the atmosphere is an inert gas.

At Texas Instruments this high-temperature problem has been solved by using the more stable Ta-Ta<sub>2</sub>O<sub>5</sub> film for compatible thin-film/

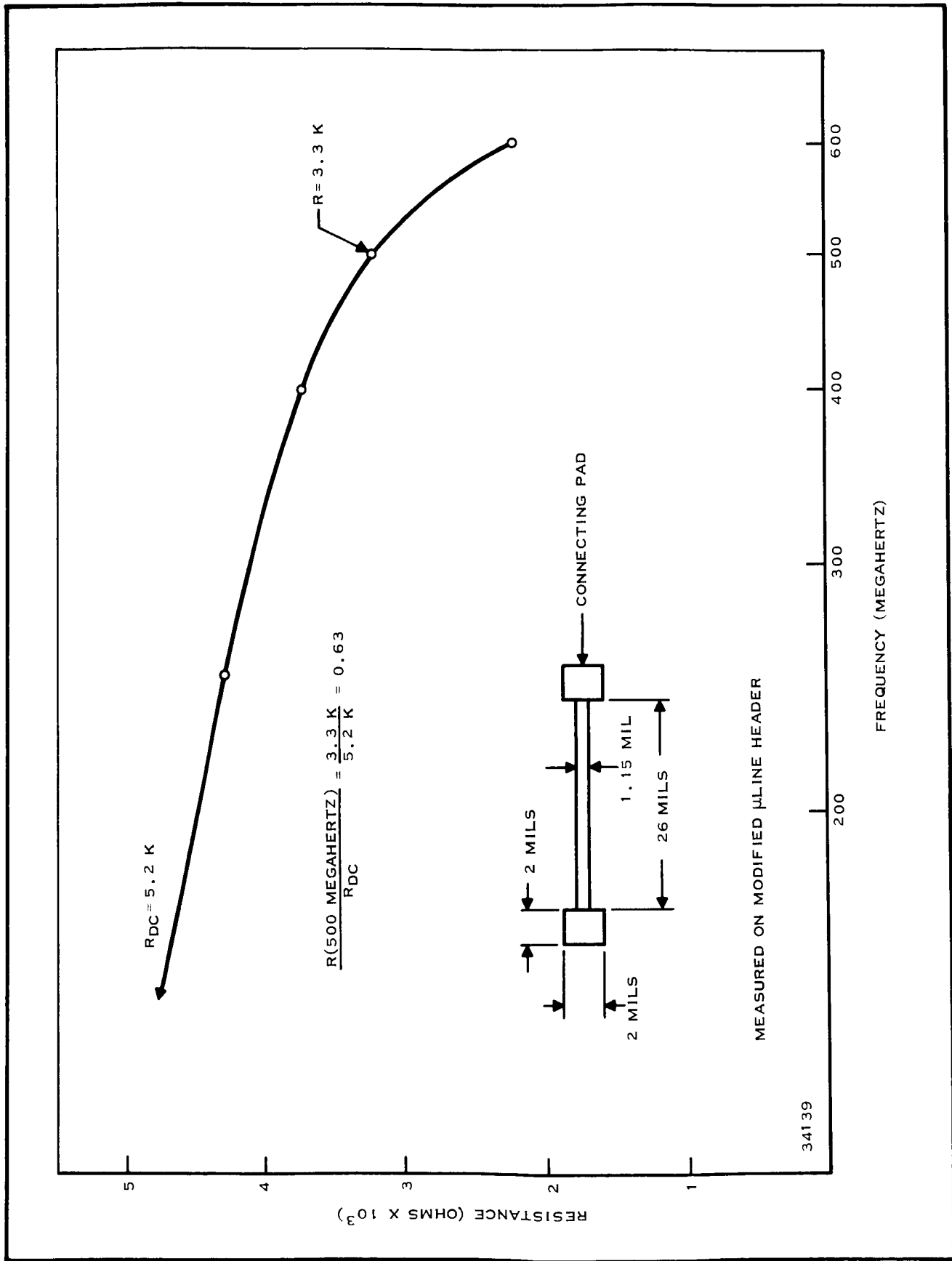


Figure 36. Resistance Versus Frequency for a Ta-Ta<sub>2</sub>O<sub>5</sub> Resistor<sup>5</sup>

monolithic circuits in conjunction with reduced temperatures for the final assembly operations. The bar-mounting operation, performed at 300°C, uses an epoxy to mount the bar in the header. In addition, a technique for ball bonding at 300°C is used; the Ta-Ta<sub>2</sub>O<sub>5</sub> is stabilized by baking at 350°C for one hour prior to the ball-bonding and bar-mounting operations.

### 3. Recent Performance Measurements

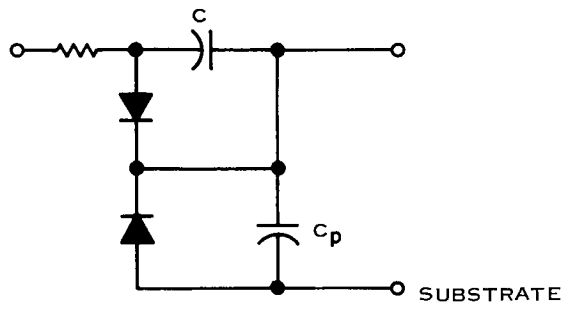
Recently, reactively sputtered Ta-Ta<sub>2</sub>O<sub>5</sub> resistors have been made for a breadboard of a 500-MHz IF preamplifier for the MERA program. These resistors were made on a relatively low resistivity silicon substrate, 50 ohm-cm, which limits their high-frequency performance. Figure 36 is a plot of the resistance versus frequency for one of these resistors,<sup>5</sup> and also shows the resistor geometry. The resistance decreased to 63 percent of its dc value at 500 MHz. The curve provides strong evidence that thin-film resistors built on high-resistivity substrates should work well at much higher frequencies.

Attempts to compare these measurements with calculations based on the simple model used to obtain Figure 34 will show that the resistor is performing satisfactorily at a frequency one order of magnitude higher than would be predicted by simply determining the frequency for which the lumped capacitive reactance equals the resistance. The general reason for this is that the simple model does not take into account the resistivity of the substrate and its influence on the operating frequency. Another reason, in the specific case of the results of Figure 36, is that the substrate was not grounded when the measurements were made. It will be possible in many instances to use a ground plane but leave the resistors floating, which minimizes the capacitive effects. Thus, the frequencies determined from Figure 34 are representative of a worst case situation. Distributed line equivalent circuits have been used to analyze the performance of resistors, but the real difficulty comes in determining the effect of the lossy substrate. Until this analytical approach is further developed and corroborated with experimental results, computations based on the simple model (series resistance and shunt capacitance) may be used to establish a lower boundary on the high-frequency limit.

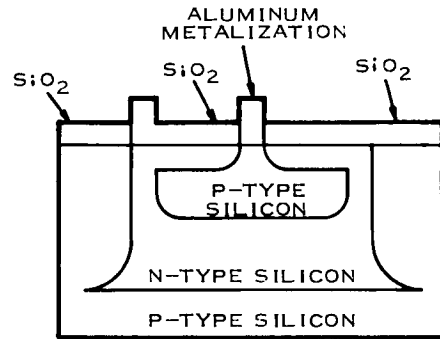
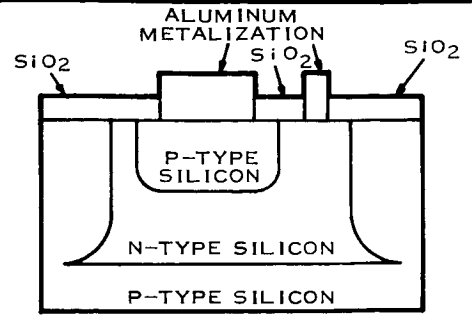
### C. CAPACITORS

Typical simplified equivalent circuits and geometries for diffused, MOS, and thin-film capacitors are shown in Figure 37. The diffused capacitor is often made in the double sided form shown in Figure 37B. In this case, the collector and emitter regions are shorted and the connection to the N-type region is made at the point of high impurity concentration (N<sup>+</sup> area), since this is the area of lowest resistivity. This N<sup>+</sup> area comes about because of the N (emitter) diffusion into an existing N (collector) region.

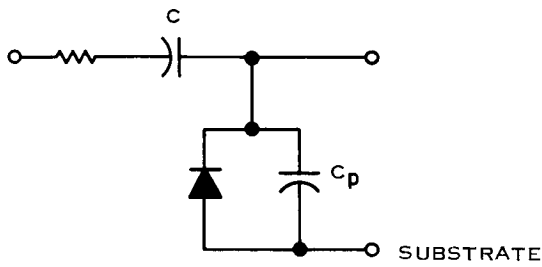
One of the major problems with the diffused capacitor is the large parasitic capacity C<sub>p</sub> associated with the isolating N-P junction; this



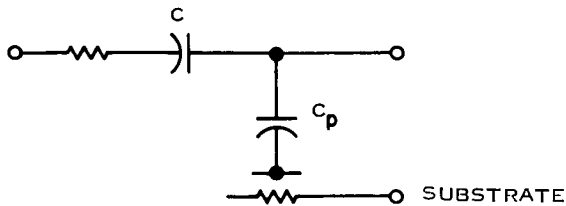
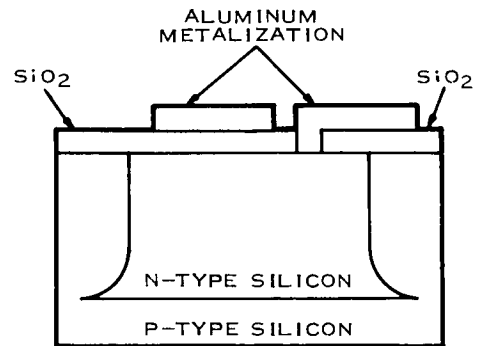
A. DIFFUSED SINGLE-SIDED CAPACITOR FOR MONOLITHIC CIRCUITS



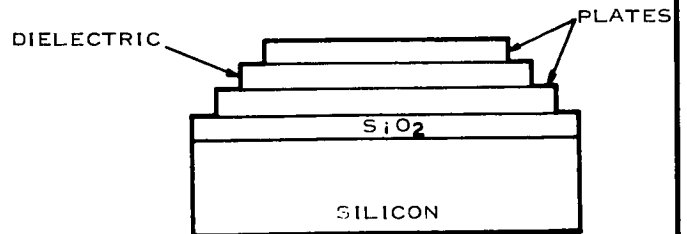
B. DIFFUSED DOUBLE-SIDED CAPACITOR FOR MONOLITHIC CIRCUITS



C. METAL OXIDE SEMICONDUCTOR CAPACITOR



D. THIN-FILM CAPACITOR



34138

Figure 37. Equivalent Circuits and Geometries for Diffused, MOS, and Thin-film Capacitors

capacitance can be as much as one-half the desired series capacitance, depending on the relative biases across the diodes. This capacitance is an order of magnitude greater than the parasitic capacitance of an equivalent thin-film capacitor.

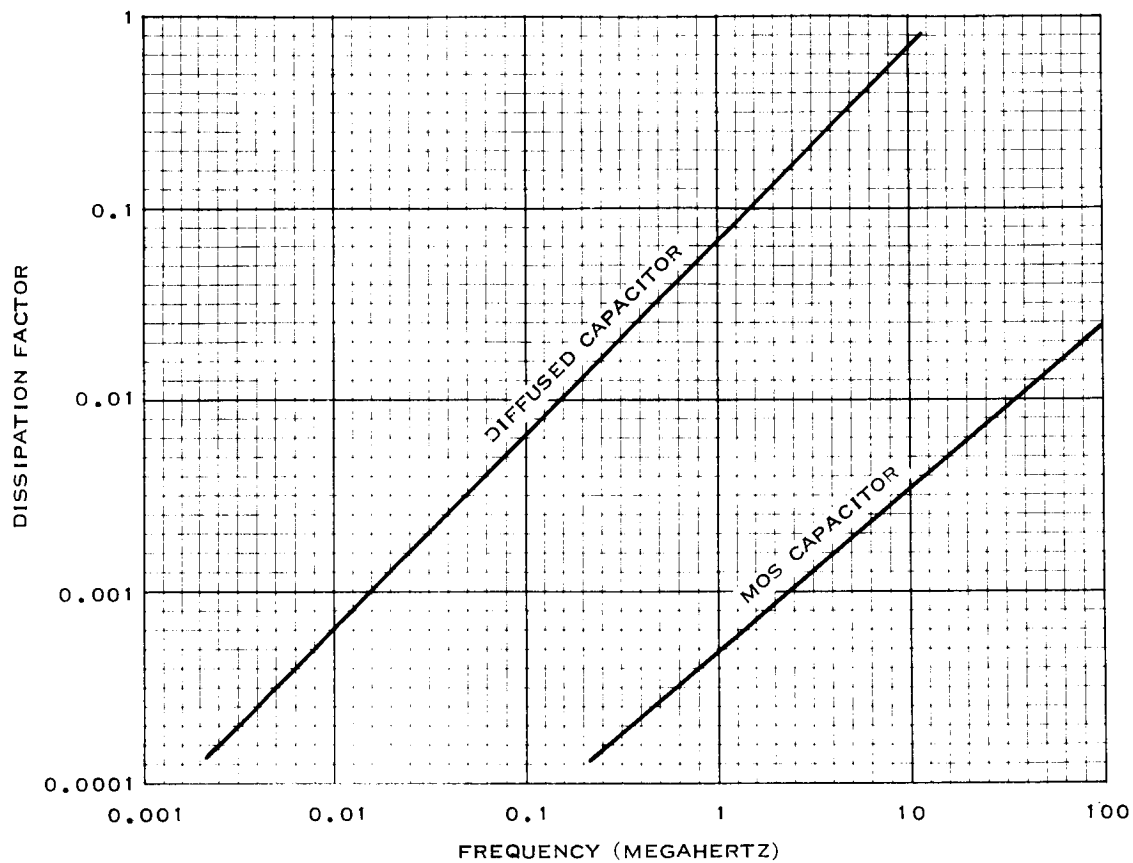
The metal oxide semiconductor (MOS) capacitor has the same sort of parasitic capacitance found in the diffused capacitor. Its desired series capacitance is made up of a conventional capacitor provided by the two plates separated by the dielectric. In addition, depletion layer effects account for an additional voltage-variable capacity.

The thin-film capacitor, Figure 37D, is free of the diode effects associated with the diffused and MOS capacitors, but has, of course, a small parasitic capacity to the substrate. This capacitor is much more useful at high frequencies because of not only its lower parasitic capacity but also its much reduced plate resistance. The series resistance of this capacitor is about two orders of magnitude lower than that of the diffused-capacitor series resistance. The reduction results from the use of metal plates rather than plates composed of semiconductor material. The thin-film capacitor is nonpolar, since no diode junctions are involved. Furthermore, its capacitance is constant with applied voltage, again due to the absence of diode junctions. These characteristics make it a more useful capacitor in many circuit applications.

Most thin-film capacitors have used silicon dioxide or tantalum pentoxide ( $Ta_2O_5$ ) as the dielectric material. Both materials have been widely used at Texas Instruments; however, high-frequency capacitors usually have been made with  $SiO_2$  dielectric.  $Ta_2O_5$  has been used at lower frequencies, where the need for larger values of capacitance can be more readily satisfied with its higher dielectric constant. In addition, the basic dielectric properties of  $SiO_2$  hold up to about 25 GHz, while the properties of  $Ta_2O_5$  are degraded considerably below this frequency. Several workers have investigated the properties of titanium dioxide as a capacitor dielectric. The characteristics of  $TiO_2$  are good at frequencies as high as 100 GHz and at temperatures as high as 300°C. The dielectric constant is high—30 to 170. Work with this material as a thin-film capacitor dielectric is still experimental. It is not evident that processing techniques have been developed for controlling the value of the dielectric constant or the loss tangent, or that the processing steps are compatible with other process steps in the manufacture of monolithic circuits.

### 1. Characteristics

The high-frequency performance of capacitors is limited by the dissipation factor and lead inductance. The dissipation factor for diffused capacitors is determined primarily by the large series resistance of the high-resistivity material used for the plates. There is little that can be done about this problem in monolithic circuits, since the resistivity required



34111

Figure 38. Dissipation Factor Versus Frequency for Diffused and MOS Capacitors

is determined by transistor parameters. The dissipation factor of the MOS capacitor is more than an order of magnitude lower than that of the diffused capacitor because its only semiconductor plate has an order of magnitude lower resistivity than the highest resistivity plate of the diffused capacitor. The dissipation factors of these two capacitors as a function of frequency is shown in Figure 38. The dissipation factor for the diffused capacitor reaches 0.1 at about 1 MHz. Though the performance of the MOS capacitor is better, neither capacitor is useful in the gigahertz region. In contrast, the dissipation factor of the  $\text{SiO}_2$  capacitor can be held relatively low, since thick, low-resistivity metal plates can be used. Even so, the ohmic lead and plate inductances limit the useful frequency range to below 5 GHz in spite of the fact that the characteristics of  $\text{SiO}_2$  are useful to 25 GHz.

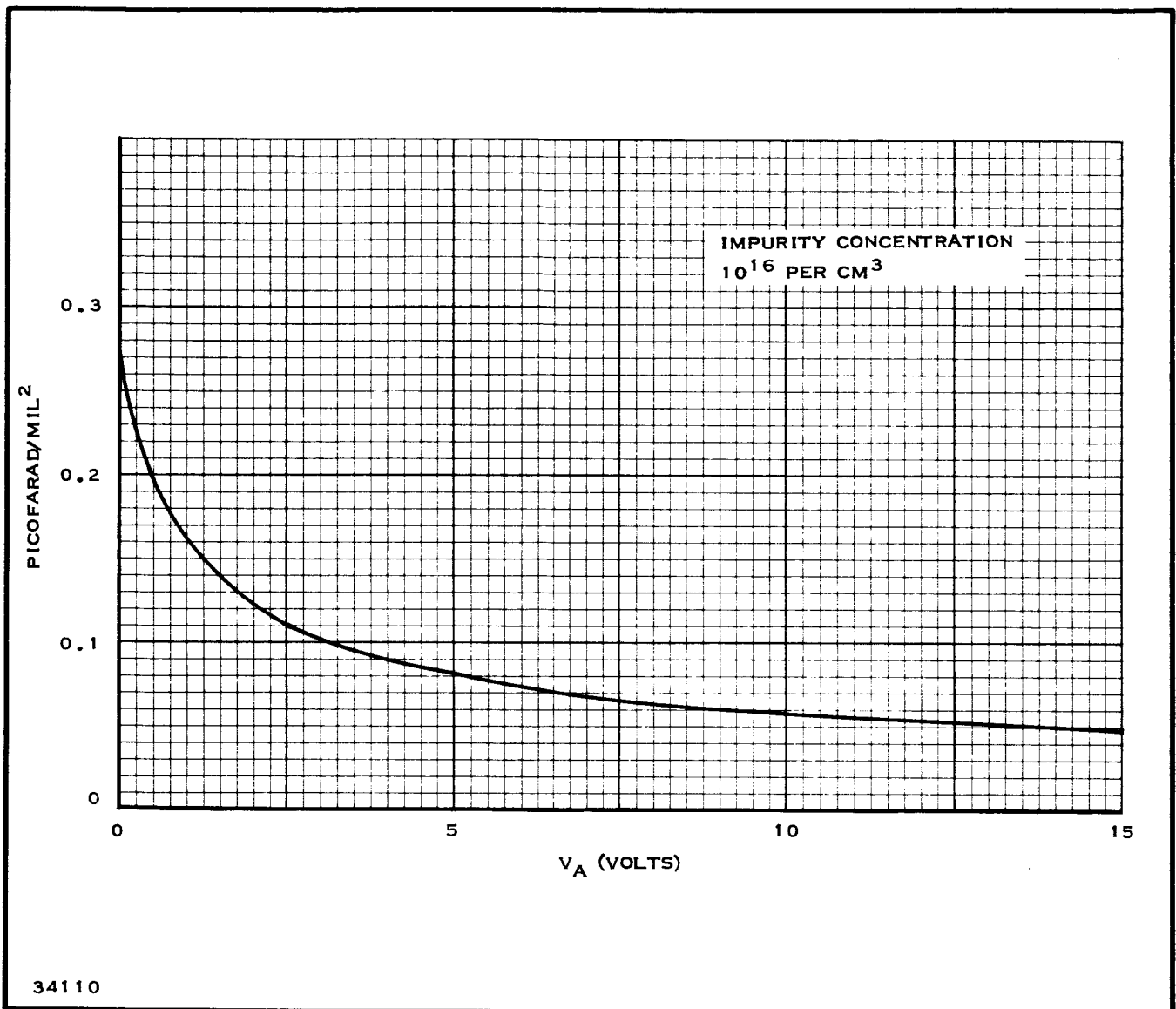


Figure 39. Capacitance per Unit Area Versus Applied Junction Voltage for the Single-sided Diffused Capacitor

The capacitance per unit area of diffused capacitors using the single-sided structure of Figure 37A is 0.1 to 0.2 pF/mil<sup>2</sup>. For the double-sided structure of Figure 37B, the capacitance per unit area is approximately 80 percent higher. These values only indicate the order of magnitude, since the capacitance is a function of the total voltage across the junction and the net impurity concentration on the lightly doped side of the junction. Using Figure 33, which is based on Equation (1), and assuming an impurity concentration of 10<sup>16</sup> per cm<sup>3</sup> (N-type 0.5 ohm-cm material), one may obtain the variation of capacitance per unit area as a function of voltage across the junction (Figure 39). Although diffused capacitors have been fabricated with capacities per area as high as 0.8 pF/mil<sup>2</sup>, the typical



upper bound is more on the order of  $0.5 \text{ pF/mil}^2$ . When consideration is given to other requirements, such as transistor parameters, this value drops even more.

Thin-film capacitors using silicon dioxide as the dielectric can be fabricated with capacities as high as  $0.6 \text{ pF/mil}^2$ . When  $\text{Ta}_2\text{O}_5$  is used, the capacity can be up to  $2.5 \text{ pF/mil}^2$ . A high-frequency thin-film capacitor requires thick metalization for the plates if reasonable values of  $Q$  are to be obtained. With thicker plates, the problem of pinholes becomes more severe and thicker dielectrics are required. For this reason, the practical limit for capacity per unit area is in the range of  $0.1$  to  $0.2 \text{ pF/mil}^2$  for high-frequency silicon dioxide capacitors.

As shown in the equivalent circuit of Figure 37A, the parasitic capacitor acts in conjunction with the desired series capacitor to form a capacitive divider. This parasitic capacitance is also a voltage variable capacity, and thus the ratio of the desired to parasitic capacitance is a function of impurity concentrations and junction voltages. With normal concentrations, this ratio is rarely less than 1.5 or greater than 5, depending on the relative junction voltages. For capacitors used in the signal line, this high parasitic capacitance may be a real problem. However, if the application is as a bypass capacitor, the parasitic is no problem.

The thin-film capacitor also has a parasitic capacitance to substrate. This is the same capacitance discussed in connection with thin-film resistors. For an isolating silicon dioxide layer  $10,000 \text{ \AA}$  thick between the bottom plate and the silicon, the parasitic capacity is  $0.02 \text{ pF/mil}^2$ . Should this capacity be a problem in monolithic circuits, the thin-film capacitors can be made on separate substrates where the resistivity can be high and the effect of the parasitic capacitor to substrate minimized.

The temperature coefficient of capacitance for diffused capacitors is high, approximately  $800 \text{ ppm/}^\circ\text{C}$ . MOS capacitors are slightly better,  $500 \text{ ppm/}^\circ\text{C}$ . Silicon dioxide dielectric capacitors have temperature coefficients ranging from  $6$  to  $30 \text{ ppm/}^\circ\text{C}$ , a marked improvement over the diffused units.

## 2. Process Compatibility

Thin-film silicon dioxide capacitors have been fabricated with aluminum plates and molybdenum-gold plates. Aluminum reacts strongly with the silicon dioxide under high temperature conditions. This reaction was a major problem when thin-film capacitors were made on monolithic circuits and the subsequent high temperature operations of bar mounting and ball bonding were performed. An initial solution was obtained by isolating the silicon dioxide from the aluminum with a thin tantalum film.<sup>29</sup> This prevented the aluminum silicon dioxide reaction. Later, as lower temperature processes were developed for the bar mounting and ball bonding,

the tantalum depositions were eliminated. This could be done, since the reaction is strongly dependent on temperature and is negligible at the reduced process temperatures.

One of the problems with thin-film capacitors is a yield problem caused by pinholes in the dielectric. The problem is intensified when thick plates are required to maintain reasonable values of  $Q$  at high frequencies. Substrate surface variations should be reduced as much as possible before evaporating the bottom capacitor plate. Both chemical polishing and mechanical polishing have been used, with the latter producing the better result. The chief problem seems to be that during deposition the metal tends to "grow" along preferred crystalline directions, resulting in surface irregularities on the dielectric side of the bottom plate. The problem is compounded by the need for thick plates for high-frequency capacitors. Depending on the thickness of the dielectric subsequently sputtered onto the bottom plate, pin-holes may develop. This is the reason thick dielectrics are used for high-frequency capacitors. Process improvements have reduced the pinhole problem and investigations in this area continue. Though the problem of pinholes is not major, it currently limits the maximum capacity per unit area available in thin-film capacitors.

### 3. Recent Performance Measurements

A number of thin-film silicon dioxide capacitors have been made recently for a 500-MHz IF preamplifier. Although the preamplifier is currently only a breadboard and as such uses the multichip approach, it will ultimately be made on a single substrate and will be a hybrid thin-film/monolithic circuit. The values range from 5 to 10 pF for signal path capacitors and from 125 to 300 pF for bypass capacitors. The capacity per unit area used is  $0.1 \text{ pF/mil}^2$ . The plates are aluminum. Measurements show no appreciable increase in  $Q$  for thicknesses greater than 300 micro-inches. Skin depth of aluminum at 500 MHz is 150 microinches. The  $Q$  of a 15-pF capacitor at 1 KHz is 200 and drops to 47 at 500 MHz.

## SECTION VI

### LUMPED-CONSTANT CIRCUITS

#### A. GENERAL

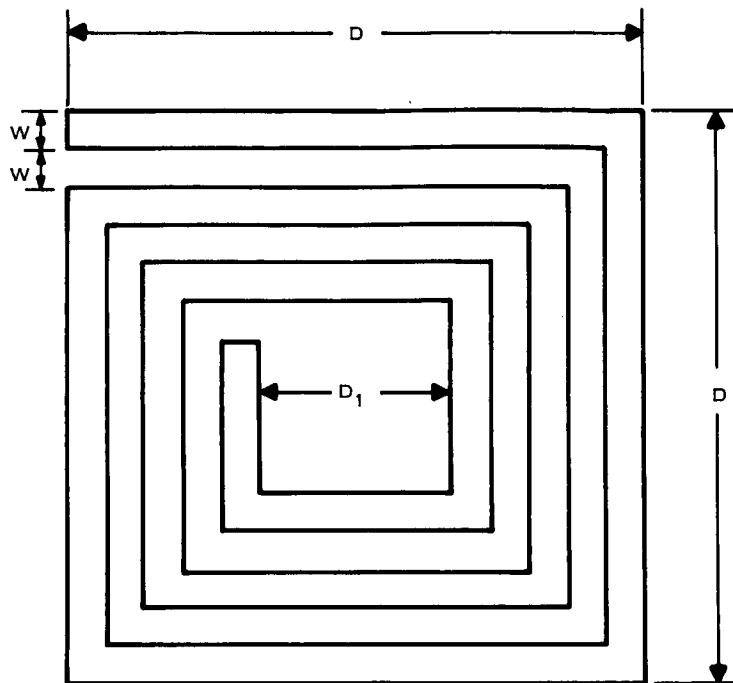
In the past, microwave circuits have employed the distributed-constant or transmission line approach exclusively because of the size of lumped-constant elements relative to the wavelength involved. There is, of course, no sharp line defining the boundary between which lumped-constant and distributed-constant circuits can be used. The most fundamental consideration is the size of the lumped constant element relative to the wavelength. In general, the largest dimension of the element should be no more than 1 percent of the wavelength. At 1 GHz the wavelength is 30 cm, which would indicate that element dimensions on the order of 0.3 cm (118 mils) could be used. This dimension is compatible with the size of lumped-constant circuit elements that might be useful in this frequency range. For instance, thin-film capacitors having a capacity per unit area of  $0.1 \text{ pF/mil}^2$  can be reliably fabricated. Assuming a square format for the capacitor and the needed values to be in the range of 5 to 75 pF, we find the dimensions ranging between 7 and 27 mils on a side. Similarly, inductors can be made using thick-film deposition processes. Assuming a square "coil" and the required values to be in the range of 0.5 to 10 nH, we find that the geometry can be less than 50 by 50 mils, compatible with the 1 percent of wavelength criterion.

This basic size consideration is only part of the problem; the other part is concerned with parasitic effects. For instance, inductors have parasitic capacities to a lossy substrate and from turn to turn; resistors also have parasitic capacities to substrate; and capacitors have series resistance and inductance as well as parasitic capacity to substrate. These undesired "circuit elements" limit the usefulness of the so-called lumped-constant elements. The capabilities of diffused and thin-film resistors and capacitors are discussed in Section V of this report. Here we will review our experience with lumped-circuit inductors.

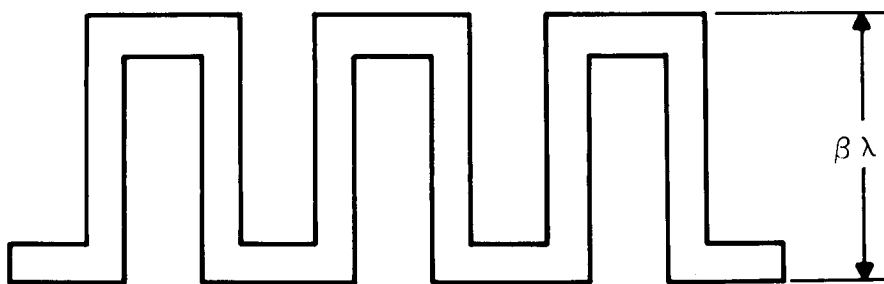
#### B. DESIGN CONSIDERATIONS

Small inductances can be realized with flat coils such as the flat, square spiral shown in Figure 40A. For maximum Q the ratio of D to  $D_1$  is 5. A considerable amount of work has been done with this geometry at Texas Instruments, where the application is to a 500-MHz IF preamplifier to be fabricated with integrated circuits.

The problem with this configuration is the need for a tunnel to make connection to the inside terminal of the coil. The meander line configuration of Figure 40B, which is also useful for small values of inductance, offers one way to avoid the connection problem. If the spacing between the turns is



A. FLAT, SQUARE, SPIRAL INDUCTOR



B. MEANDERLINE INDUCTOR

34114

Figure 40. Integrated Circuit Inductors

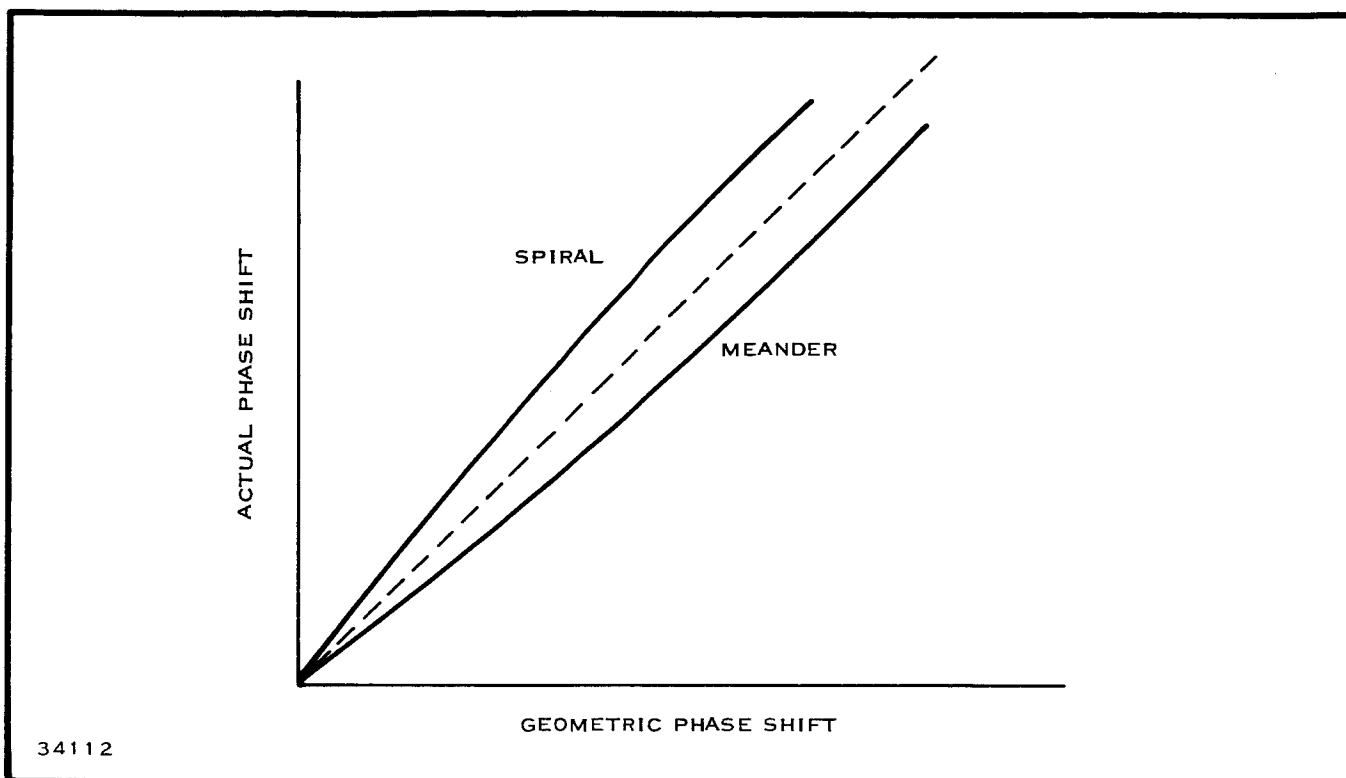


Figure 41. Characteristics of Loosely Coupled TEM Lines

comparable to the spacing between the coil and the ground plane, the coupling between adjacent sections of the meander line is on the order of 0.1. For this case, the actual phase shift is less than the geometric phase shift (Figure 41). For comparison, the actual phase shift of the spiral as a function of the geometric phase shift is shown in the same figure. The figure shows that the meander line would have to be slightly longer than the spiral for equal electrical phase shifts, but the problem of making connection to the inside terminal of the spiral is eliminated.

It is, of course, possible to realize the required value of inductance with a short-circuited transmission line. This line is made less than a one-quarter wavelength long, the actual length being chosen to provide the required inductive reactance. The inductance is given by

$$L = \frac{Z_0}{2\pi f} \tan \left( 2\pi \frac{l}{\lambda} \right) \quad (1)$$

where

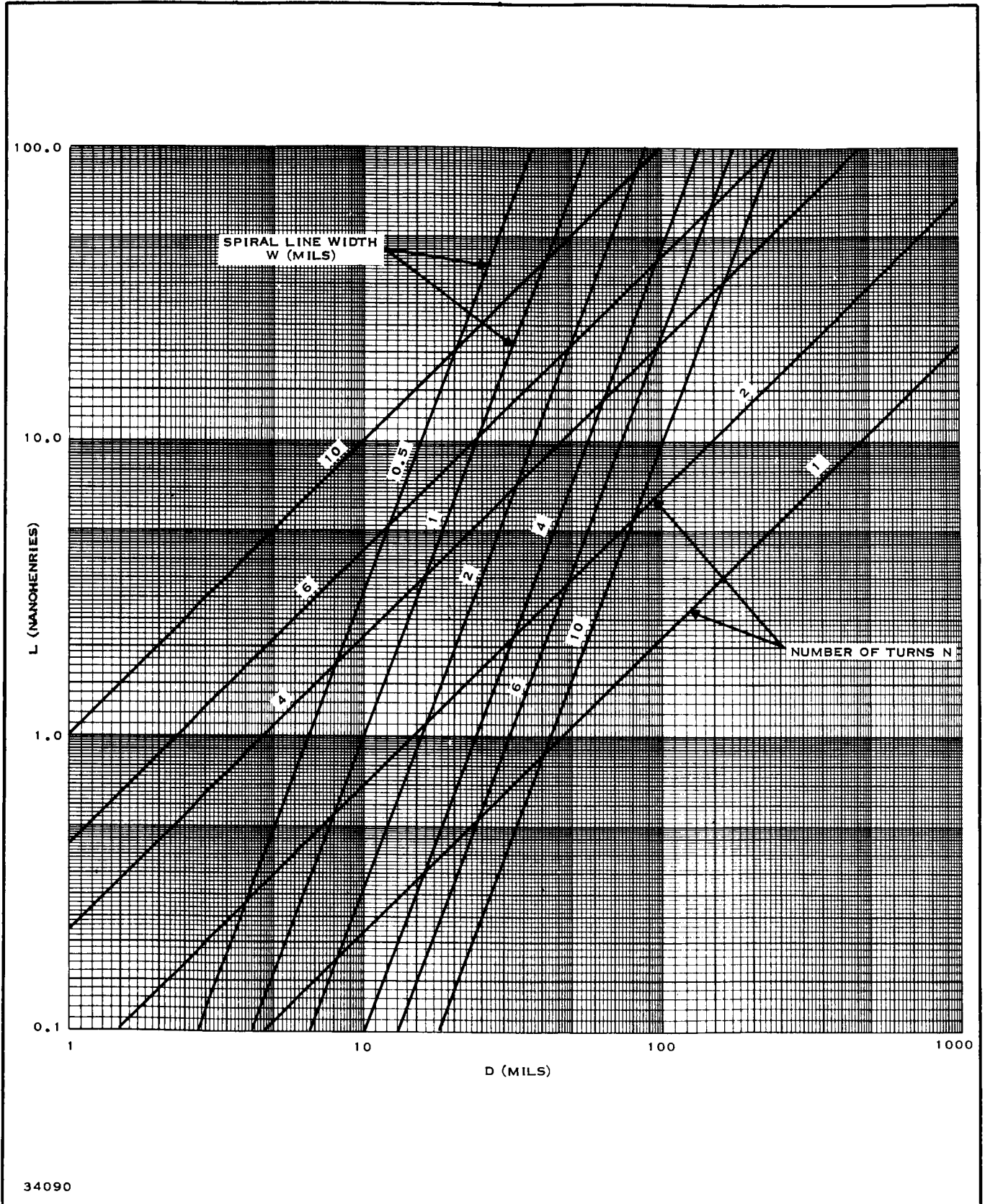
$L$  is the inductance

$Z_0$  is the characteristic impedance of the line

$f$  is the frequency of operation

$l$  is the length of the line

$\lambda$  is the wavelength.



34090

Figure 42. Inductance of the Flat, Square Spiral as a Function of the Length on a Side  $D$  with the Width of the Conductor and the Number of Turns as Parameters

If the line is meandered to conserve space on the substrate, then its length will have to be slightly longer than if it were laid out straight on the substrate. This is indicated in Figure 41.

The information presented in Figures 42, 43, and 44 may be used as a guide in determining the geometry of the coil (area covered, conductor width, and thickness of conductor) required to realize a particular value of inductance while maintaining a suitably high self-resonant frequency and an acceptable level of  $Q$ . These curves are based on established design formulas<sup>33</sup> and involve certain simplifications; nevertheless, they can be used to roughly approximate the required geometry before proceeding with more exact calculations.

The curves shown in these figures are based on the geometry of Figure 40A and assume a square coil with spacing between the edges of adjacent conductors equal to the width of the conductor and with dimension  $D_1$  equal to zero. Under these conditions the inductance is given by

$$L = 2.16 \times 10^{-2} DN^{5/3} \text{ nH} \quad (2)$$

where  $D$  is the length of a side in mils and  $N$  is the number of turns.

Figure 42 is a plot of Equation (2) for values of  $N$  ranging from 1 to 10 (larger values of  $N$  are not useful in the frequency range of interest here). Also shown in Figure 42 is the relationship of spiral line width to the number of turns and the dimension of a side. This relationship is based on the simple geometry of Figure 40A and is given by

$$w = \frac{D}{4N} \text{ mils.} \quad (3)$$

The self-resonant frequency of the spiral is another parameter of interest. It is given in Figure 43 as a function of the dimension on a side of a coil for the same range of  $N$  and  $w$  used in Figure 42. This self-resonant frequency is derived by determining the frequency for which the spiral, considered to be a transmission line, is one-quarter wavelength long. The dielectric constant of the substrate is assumed to be 4. On this basis, the self-resonant frequency is given by

$$f_0 = \frac{7.38 \times 10^2}{DN} \text{ GHz.} \quad (4)$$

An upper bound of the  $Q$  on the inductor may be determined by computing the series resistance of the coil based on the resistivity of the material used for the conductor and its cross-sectional area. This is shown in Figure 44 as a function of the thickness of the conductor, assumed to be aluminum, for values of  $N$  from 1 to 10. The inductive reactance used is the value corresponding to a frequency one-fourth the self-resonant frequency. The frequency

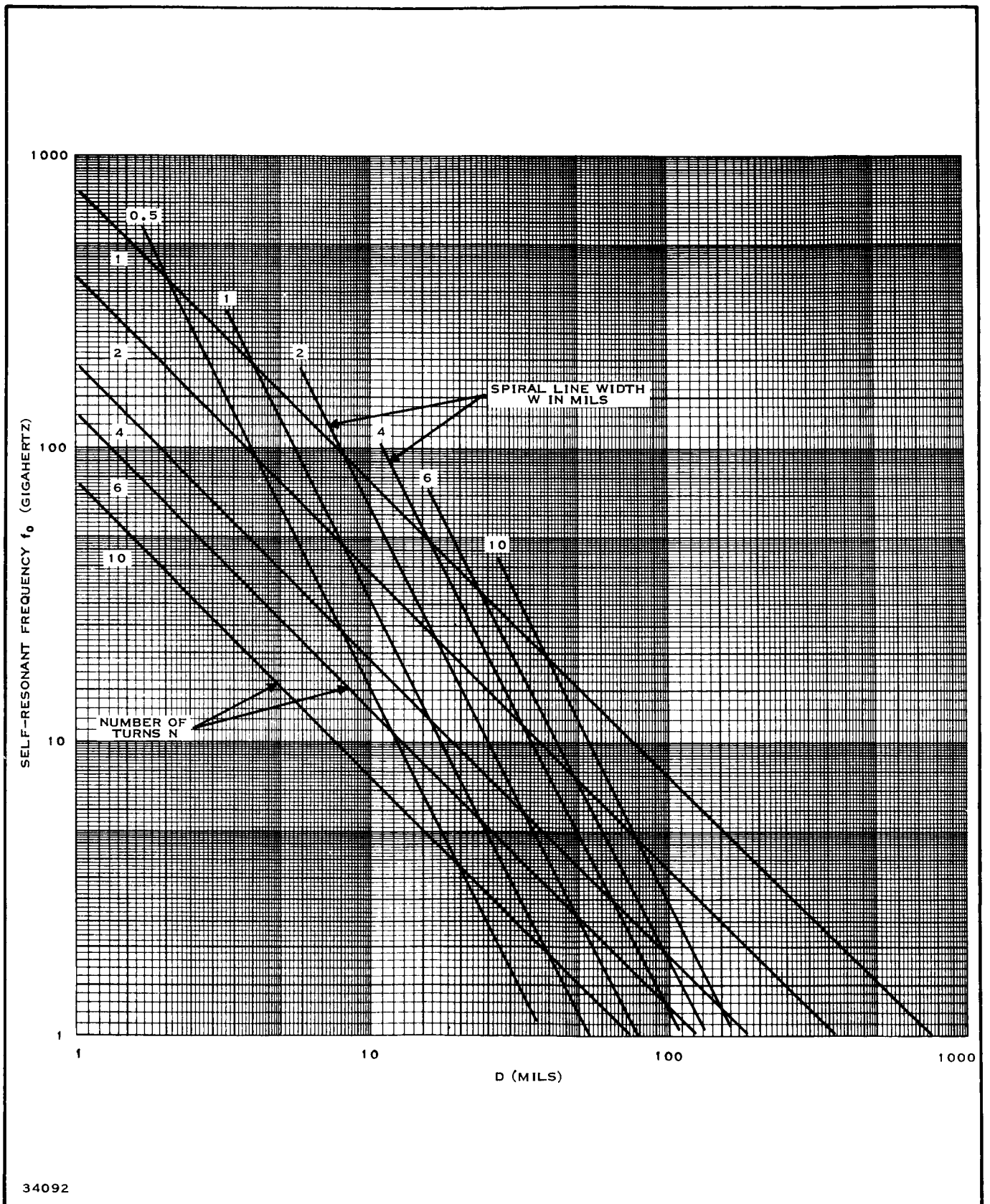


Figure 43. Self-resonant Frequency of the Flat, Square Spiral as a Function of the Length on a Side D with the Width of the Conductor and the Number of Turns as Parameters



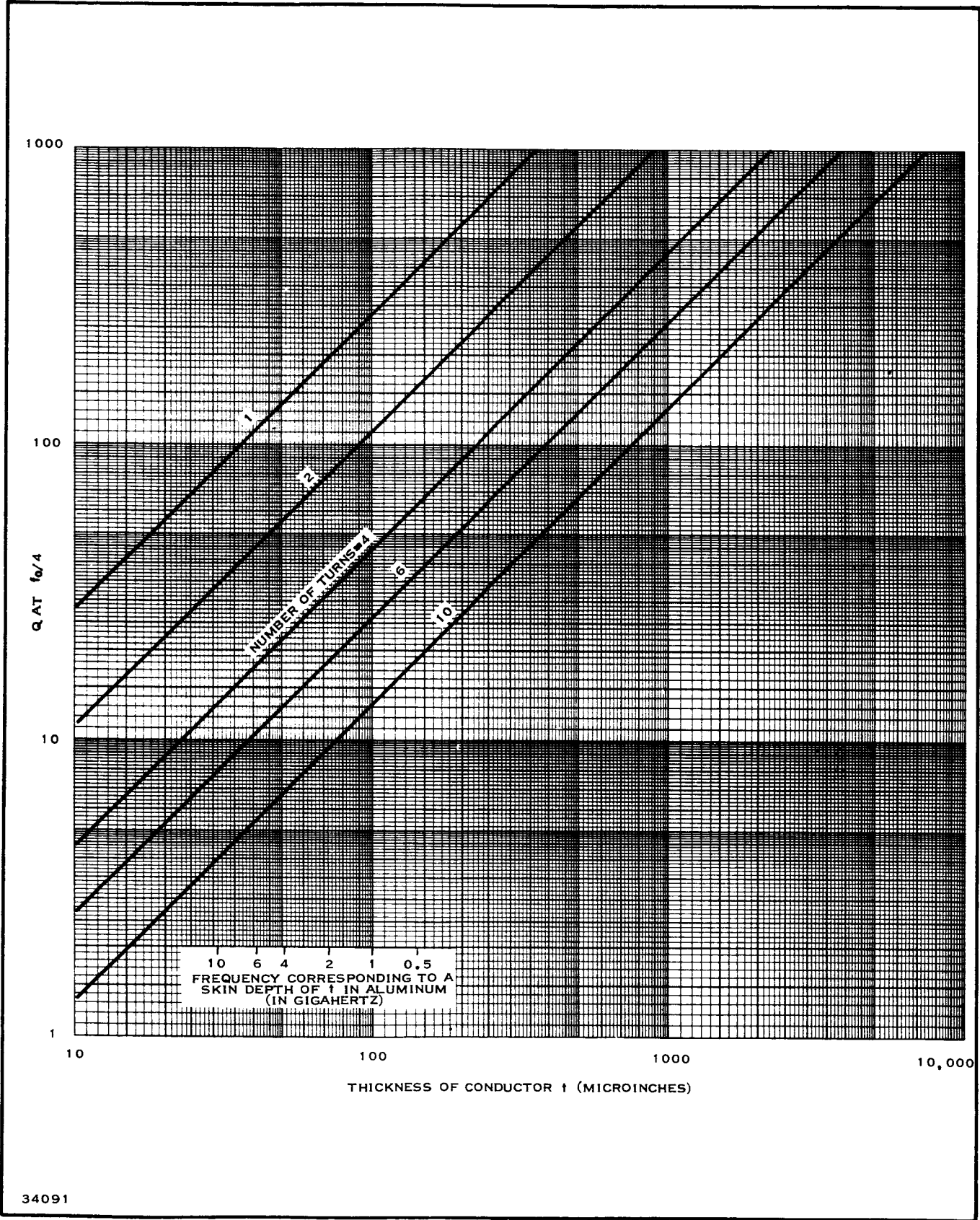


Figure 44. Coil Q at  $f_0/4$  as a Function of the Conductor Thickness  $t$  with the Number of Turns as a Parameter

corresponding to the skin-depth thickness is also shown on the abscissa of Figure 44. For this special case  $Q$  is given by

$$Q = 2.82 tN^{-4/3} \quad (5)$$

where  $t$  is the thickness of the aluminum conductor in microinches.

### C. FLAT, SQUARE SPIRALS AT 500 MHz

In recent months, considerable work has been directed toward the design and fabrication of flat, square spiral coils for use in a 500-MHz IF preamplifier. The results obtained at this frequency give some indication of the performance that can be obtained at higher frequencies.

Equation (2) and Figure 42 may be used to determine the geometry of the spiral required for a specific value of inductance, but a more accurate computation<sup>34</sup> of the low-frequency inductance may be made using

$$L_o = 0.02032 N^2 S \left( 2.303 \log_{10} \frac{S}{Nw} + 0.2235 \frac{Nw}{S} + 0.726 \right) - 0.02032 NS(A+B) \quad (6)$$

where

$L_o$  is the low frequency inductance in  $\mu H$

$N$  is the number of turns

$w$  is the distance between turns in inches

$S$  is the average length of a side in inches

$A$  is a constant determined from the ratio of the conductor diameter to the distance between turns

$B$  is a constant determined from the number of turns in the coil.

Coil designs based on this formula have measured inductances falling within  $\pm 10$  percent of the calculated value.<sup>35</sup> The values of inductance required are readily obtained with the single-layer coils.

Here, the major problem is one of fabricating a coil with an acceptable level of  $Q$ . Measured coil  $Q$ 's are below calculated values for the reason that the simple formulas available do not take into account the resistivity of the substrate. Losses, of course, increase with decreasing substrate resistivity. Measurements were made on a flat, square spiral coil of 4 turns. An evaporated aluminum conductor having a width and conductor spacing of 4 mils was used. The inductance of this coil is about 30 nH. Table VIII shows the results of the measurements made at 500 MHz. The conductor thickness was chosen to provide approximately the same  $Q$  for the three different substrates. For the silicon substrate a silicon dioxide layer approximately 8000 Å thick isolated the coil from the substrate.

Table VIII. Effect of Substrate and Conductor Thickness on Coil Q

Material	Conductor Thickness (Microinches)	Q
Ceramic	200	23.7
Glass	200	22.2
5000 ohm-cm P-type silicon	300	25.0

The same coil geometry was used on several different samples of P-type silicon having resistivities ranging between 500 ohm-cm and 5000 ohm-cm. With a conductor thickness of 300 microinches, the coil Q as a function of substrate resistivity was determined and is shown in Figure 45. This figure clearly shows the importance of a high-resistivity substrate.

Measurements were made of coil Q as a function of frequency<sup>35</sup> over the range of 300 MHz to 1 GHz. The substrate was 5000-ohm-cm material and the silicon dioxide layer was 8000 Å. The measurements were made on four coils, which had conductor widths of 2, 3, 4, and 5 mils; as before, conductor width was made equal to conductor spacing. The results are shown in Figure 46. These coils had self-resonant frequencies above 4 GHz.

The effect of temperature on coil Q was also determined. This variation is shown in Figure 47 for the 4-mil 4-turn coil with two different conductor thicknesses. No appreciable increase in Q has been obtained for a conductor thickness greater than two times the skin depth. Since the skin depth in aluminum at 500 MHz is 148 microinches, the 300-microinch conductor satisfies the requirement.

Significant experimental work with inductors in the 1- to 6-GHz region is yet to be done, and techniques of applying thin and thick ferrite films to increase the coil Q are in the early stages of investigation.

Thus, it is too early to state generally the ultimate outcome of this work. However, for the present low circuit Q will be the major drawback of the thick-film lumped-constant inductor. Whether this is truly a drawback depends on the circuit function. Many applications, such as broadband amplifiers, employ loaded-Q's that are relatively low, thus the values of unloaded Q currently available will be adequate.

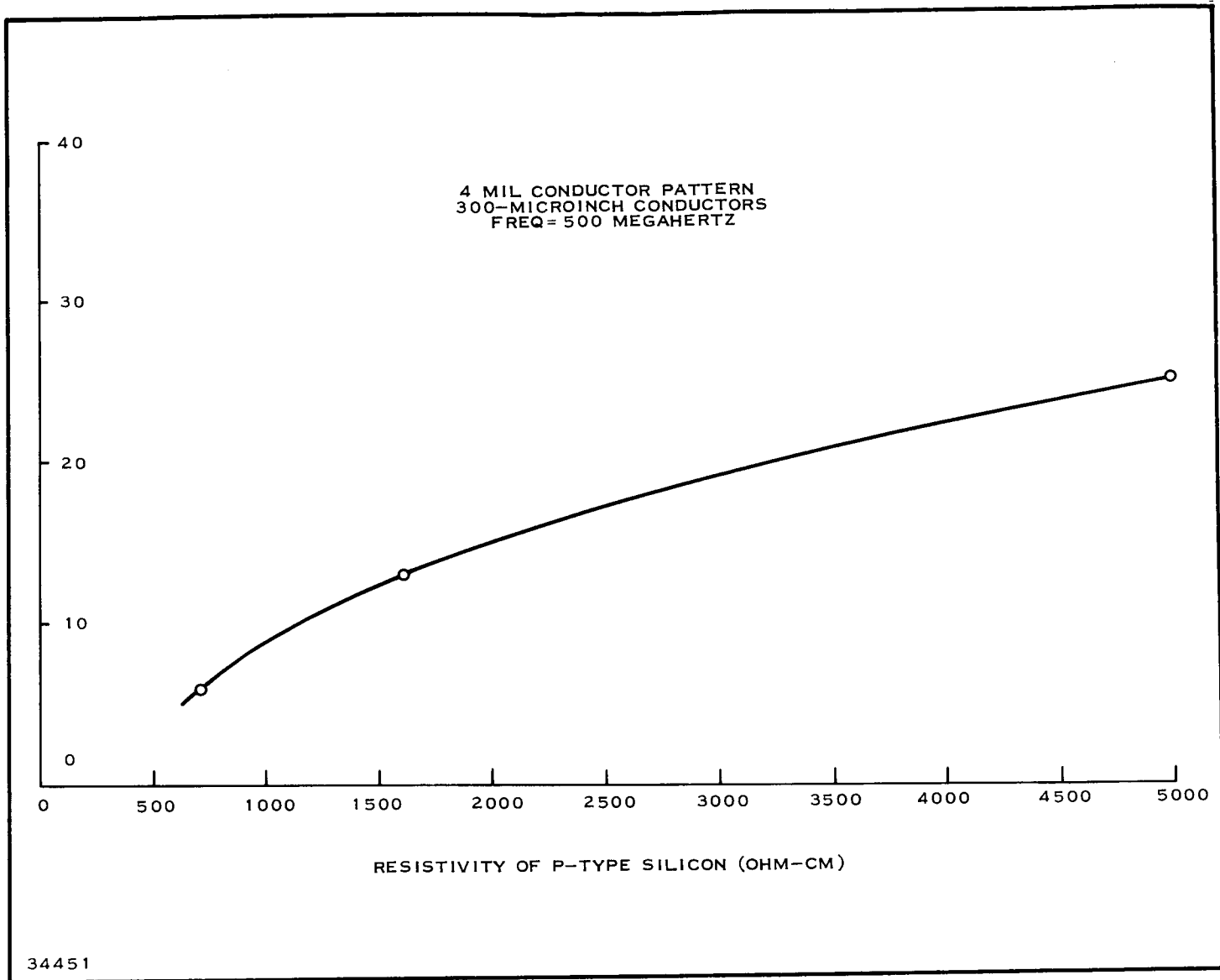
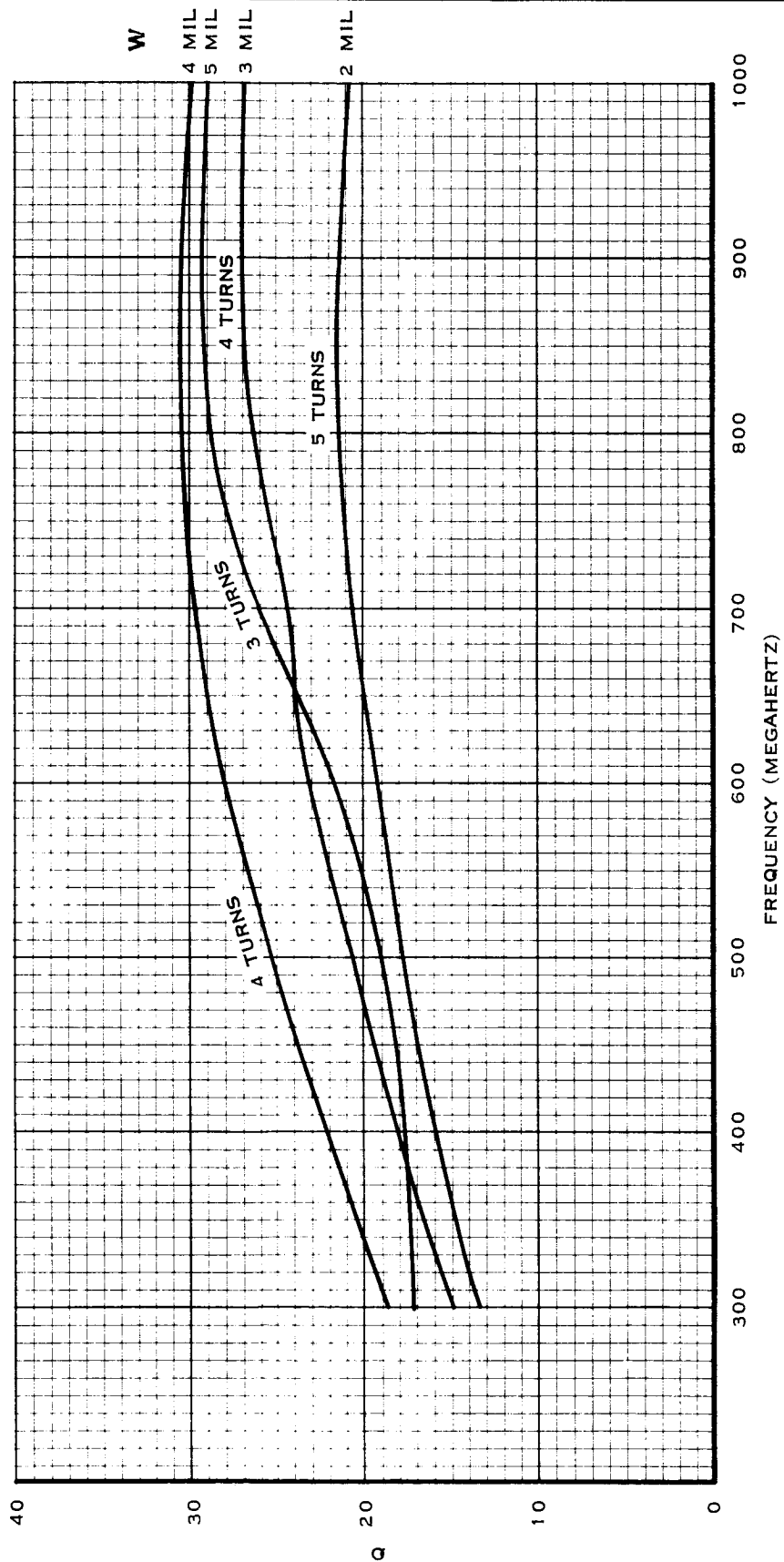
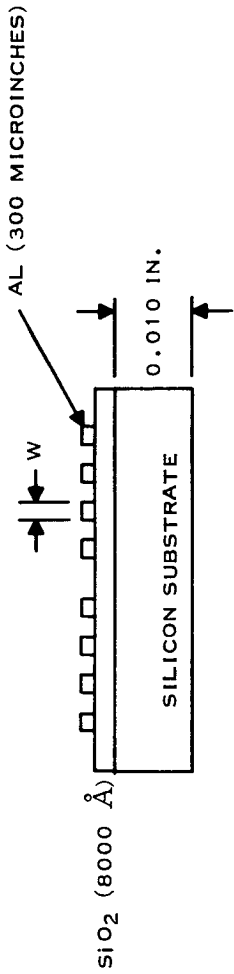


Figure 45. Approximate Q Versus Resistivity

#### D. WORK IN PROGRESS

Fabrication of coils using gold conductors is planned in an effort to achieve higher Q's. The difficulty arises here when the gold thickness exceeds the photoresist thickness that defines the coil geometry, and the gold bridges over the photoresist and appreciably widens the coil. Experiments using very viscous KTFR are being conducted to allow the formation of 1-mil KTFR plating masks.

Insulation layers of quartz, 1 mil thick, between the low resistivity substrates and the coil will help raise the value of Q; however, the fabrication of thick quartz films is at present a problem.



34452

Figure 46. Q Versus Frequency for Four Coils

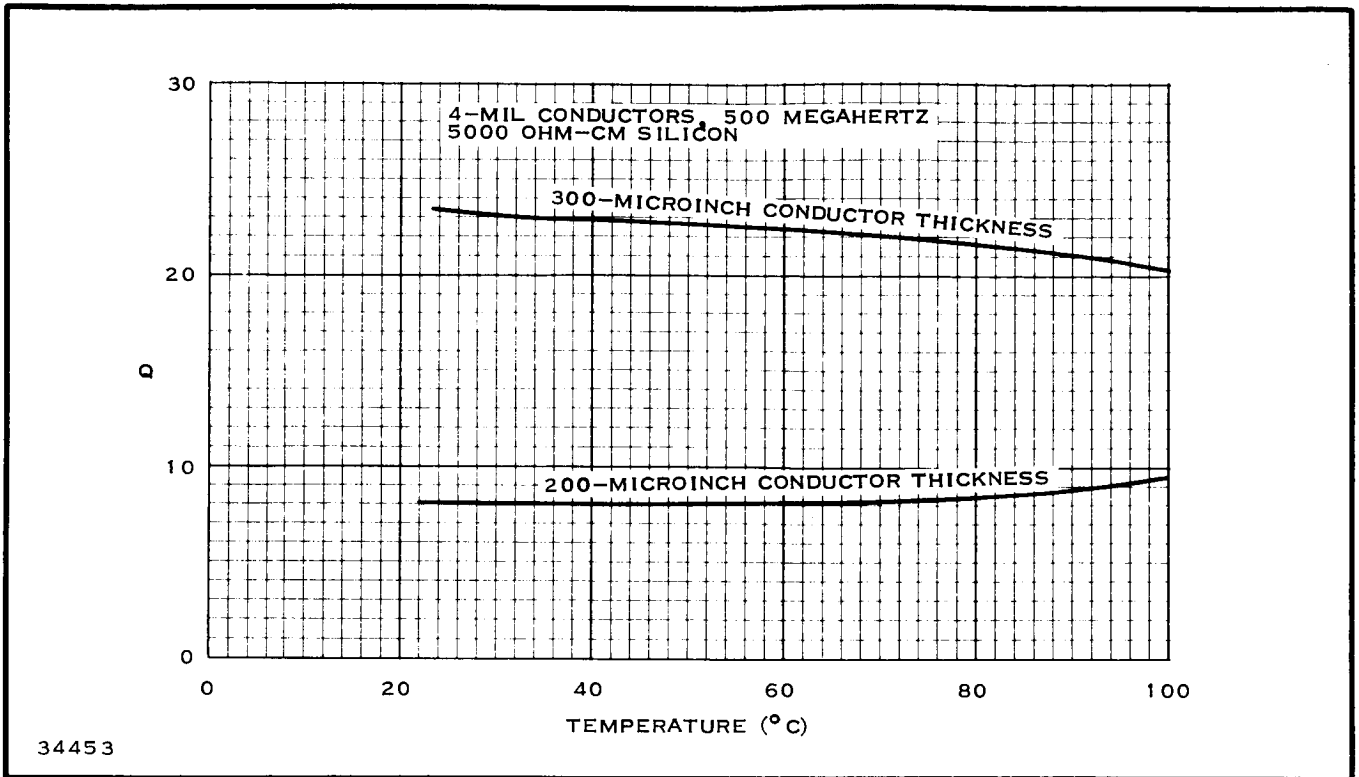


Figure 47. Q Versus Temperature

Ferrite films are being investigated to increase the reactance of the inductor and thereby increase the Q for a given value of inductance. A preliminary experiment consisted of depositing a magnetic alloy on a silicon substrate covered by a 10,000 Å quartz insulating film. An inductor was then deposited on the quartz. The film did not appreciably improve the Q. Further tests are planned using thick and thin films above and below the coil. Tests will also be made to determine the shielding qualities of YIG films.

## SECTION VII

### OTHER SEMICONDUCTOR DEVICES

#### A. VARACTORS

##### 1. General

Varactors are classified as semiconductor PN-junction or point-contact diodes which exhibit a voltage-dependent junction capacitance<sup>36, 37, 38</sup> when they are biased between the forward conduction region and reverse breakdown. The capacitance variation of the silicon diffused junction devices is described by

$$C_t = C_p + C_j = C_p + \frac{C_{j0}}{\left(1 + \frac{V_{\text{bias}}}{\phi}\right)^{1/3}} \quad (1)$$

where

$C_t$  = total capacitance measured at diode terminals

$C_p$  = package capacitance

$C_j$  = junction capacitance

$V_{\text{bias}}$  = dc bias voltage

$\phi$  = contact potential

$C_{j0}$  = junction capacitance at 0 volts.

The normalized junction capacitance of a typical diffused junction varactor versus reverse bias is shown in Figure 48.

The nonlinear capacitance of a varactor is useful in many ways. Generally these involve conversion from one RF frequency to another. Two, three, four or more frequencies may interact in the varactor, and some may be useful inputs or outputs, while others are idlers. These idlers may be necessary to the operation of the device, but are not part of any input or output.

Frequency multiplication is one of the most used applications of varactors. The varactor is excited at a frequency  $f_0$  and power is delivered to the load at a frequency  $Kf_0$  for some integer  $K$ . Typical solid-state sources deliver from a few milliwatts to a few watts of power at 1 GHz to 10 GHz or higher, the varactor stages themselves often having as high as 90 percent efficiency. The series resistance of a varactor limits the efficiency at high frequencies.

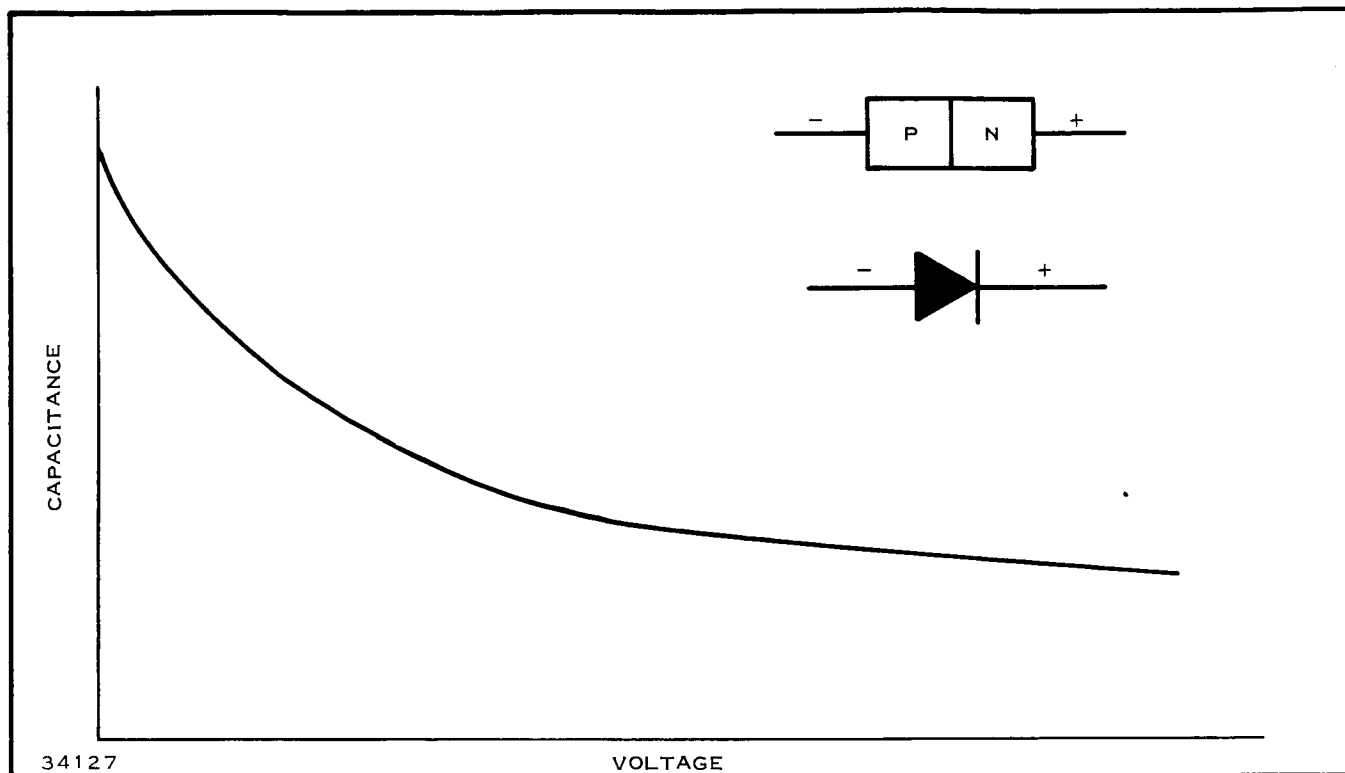


Figure 48. Normalized Junction Capacitance of a Typical Varactor

Another simple application is in frequency division. The varactor is excited at  $f_0$ , and the power delivered to a load is at  $f_0/K$  for some integer  $K$ . The series resistance limits the frequencies at which division can take place, the efficiency of power conversion, and the speed with which subharmonic oscillations can grow.

Some other varactor applications require three or more useful frequencies. If a large and a small current at frequency  $f_p$  and  $f_s$ , respectively, are put through a varactor, sidebands are generated with frequencies of the form  $nf_p + f_s$ , for  $n$  a positive or a negative integer. The circuit is called a frequency converter if power flows at one of these frequencies to a load. When the output frequency is larger than  $f_s$ , it is an up-converter, and when the output frequency is smaller than  $f_s$ , it is a down-converter. A small excitation at  $f_s$  and at the generated sidebands produces a linear conversion, which can be used for communication purposes. The frequencies at which this conversion can take place is limited by the series resistance, which also limits the gain and introduces noise at high frequencies.

The process of passing a large current at frequency  $f_p$  through the varactor is known as pumping, and the pumped varactor behaves like a time-varying capacitance, rather than a nonlinear one. The series resistance dissipates power because of the pumping current, and the allowable swing in capacitance is limited by the maximum elastance ( $1/C$ ) of the varactor.



There are other applications of varactors such as parametric amplifiers, solid-state sources of microwave power, parametrons, and rational fraction generators. These devices and a detailed analysis of the multiplier and divider previously mentioned are covered adequately in the literature.

## 2. Application to Integrated Circuits<sup>44</sup>

### a. Frequency Quadrupler

An effort has been initiated on the MERA program to develop an integrated frequency quadrupler capable of delivering 1.0 watt output power at 9.0 GHz with 2.0 watts input power. The 4.5- to 9.0-GHz doubler inherent in the eight-varactor quadrupler circuit has been built using independent-loop tuning. The circuit operated as a frequency multiplier, but with extremely low efficiency. Insufficient power output prevented checking the bandwidth of the circuit. Because of the small size of the circuit, it was impractical to try to increase the efficiency by making changes in the circuit, such as varying inductance or changing the varactors.

Unlike the eight-varactor quadrupler, a four-varactor quadrupler can be breadboarded in stripline form. Although this circuit requires a passive filter not required in the eight-varactor circuit, passive components are readily adaptable to stripline construction and to independent evaluation.

Two very simple doublers have been constructed using packaged silicon varactors with ceramic substrates and Teflon-fiber glass stripline board. The purpose of these two circuits will be to determine the bandwidth and operating properties of simple stripline circuits as well as to obtain experience in building circuits of this type.

Transmission line construction in which inductive and capacitive functions are performed by suitable lengths of striplines will be used to construct all circuits in the future. The principal disadvantage of stripline construction for breadboard circuits is the lack of adjustments that can be made after the circuit is constructed. In the case of the quadrupler circuit, a crossover of two transmission lines must be made; with presently available techniques, this is not practical in breadboard circuits. Because of this and because of the complexity of the eight-varactor quadrupler, two simpler approaches to the problem are being studied—a four-diode quadrupler (with no crossover) and two cascaded doublers.

### b. Varactor Design

The varactor diode effort requires design and development of a high-frequency diode that is capable of use in frequency doubler circuits and is structurally compatible with integrated circuit design techniques. For use in a frequency multiplier chain, a surface-oriented diode has been

developed by Texas Instruments on the MERA program. The surface-oriented varactor diode structure has several unique advantages. Among these is the extension of the heavily doped  $N^+$  and  $P^+$  material into the high resistivity substrate, thus allowing all of the effective diode area to be confined to the low resistivity epitaxial layer. This results in the maximum possible varactor  $Q$  attainable from the device.

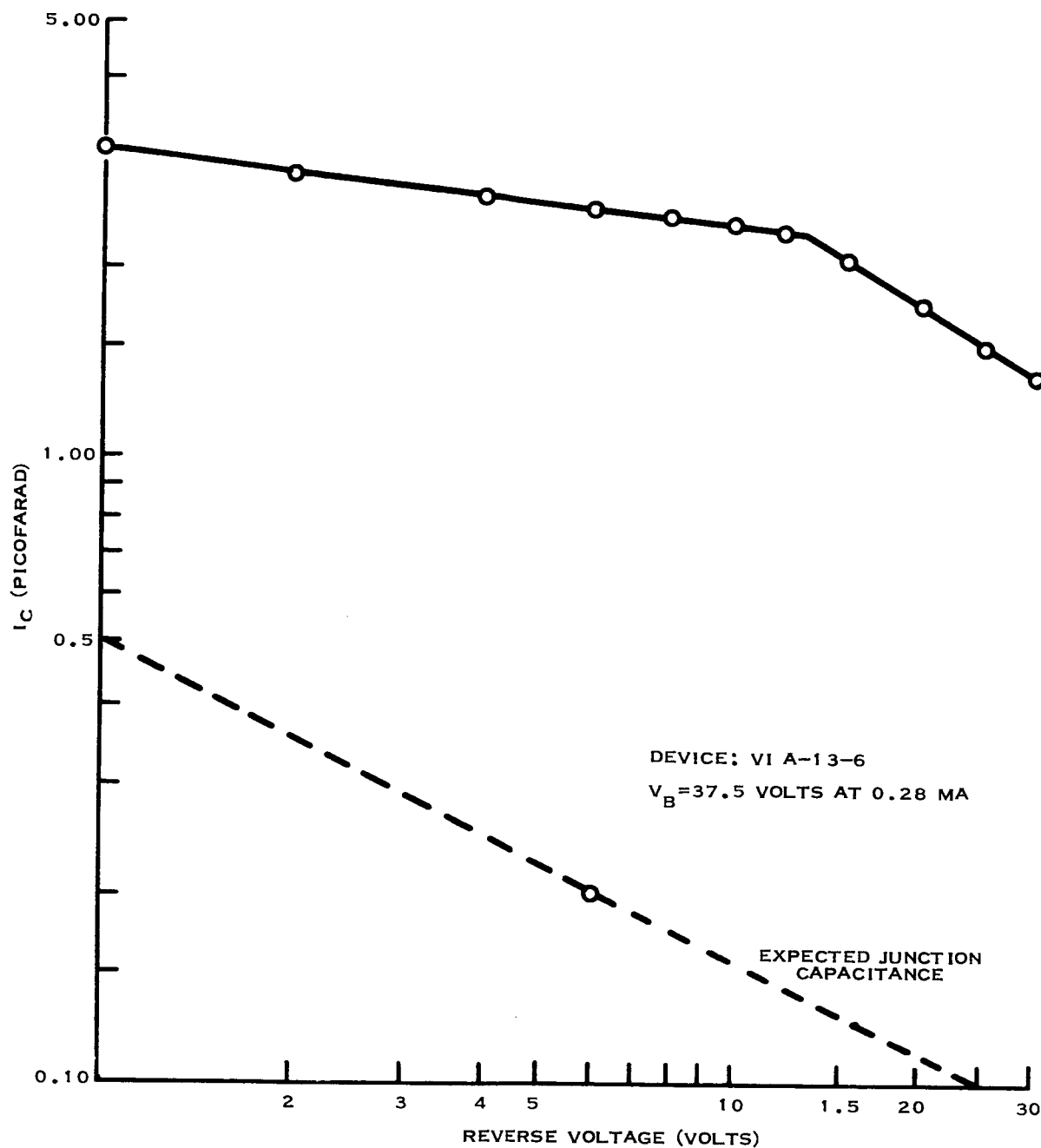
Surface-oriented varactor diodes have been fabricated from two diffusion runs. Extremely high leakage currents were observed: 0.25 mA to 10 mA at breakdown. This may be explained by the extremely high surface concentrations. By introducing a three-hour, 900°C dry-oxygen step following the boron diffusion, the leakage currents were reduced to 10  $\mu$ A, and devices were fabricated from this diffusion run. Although the first diodes were very leaky, measurements of capacitance versus voltage were taken at 1 MHz in the TI-line\* package. These diodes exhibited an MOS characteristic as expected. A typical plot<sup>44</sup> is given in Figure 49.

Following these earlier experiments, low-leakage surface-oriented varactor diodes were fabricated from two additional diffusion runs. These diodes were made from material with high resistivity P-type substrates (>1500 ohm-cm). The capacitance of these diodes agreed with the calculated value within the accuracy of measurement. The effects of MOS capacitance and low resistivity substrate material were evaluated. However, a true evaluation of the diode performance must be made in a stripline configuration at microwave frequencies. Typical data recorded from the two diffusion runs which produced the low leakage devices are given in Table IX.

Table IX. Characteristics of Surface-oriented Varactor Diodes

Characteristic	Run 3 Slice 12	Run 7 Slice 50
Junction area	$3.37 \times 10^{-5}$ cm	$2.52 \times 10^{-5}$ cm
Substrate resistivity	1500 ohm-cm, P-type	1900 ohm-cm, P-type (gold-doped)
Epitaxial resistivity	0.32 ohm-cm	0.39 ohm-cm
Voltage	40 V	70 to 90 V
Leakage at $V_B$	2 to 7 $\mu$ A	6 $\mu$ A
Junction capacity ( $V_B = -6$ )		
Calculated	0.372 pF	0.357 pF
Measured	0.58 pF	0.40 pF

\* Trademark of Texas Instruments Incorporated.



34455

Figure 49. Measured Capacitance Versus Voltage for Surface-oriented Varactor Diode<sup>44</sup>

The calculated junction capacity agrees reasonably well with the measured value. The measured junction capacity has been corrected for MOS and package capacitance.

Following the diffusion runs which produced the low leakage devices, surface-oriented varactor diodes were fabricated without the effects of a parallel MOS capacitance. This was accomplished by using a modified contact mask which confined the metal fingers to the diffused areas, thus eliminating the metal-over-oxide contacts. The diodes were evaluated in the  $\mu$ mesa\* package, the third terminal being used as a guard terminal for capacitance measurements. The metal case was also connected to the guard terminal in order to minimize the package capacitance. This was found to be an extremely beneficial step since it reduced the package capacitance from 0.30 pF to 0.04 pF.

## B. PIN DIODES

PIN diodes as shown in Figure 50 consist of a thin slice of high-resistivity (intrinsic) semiconductor material between heavily doped low-resistivity P and N regions. The intrinsic region behaves as a slightly lossy dielectric at microwave frequencies and the heavily doped regions act as good conductors.

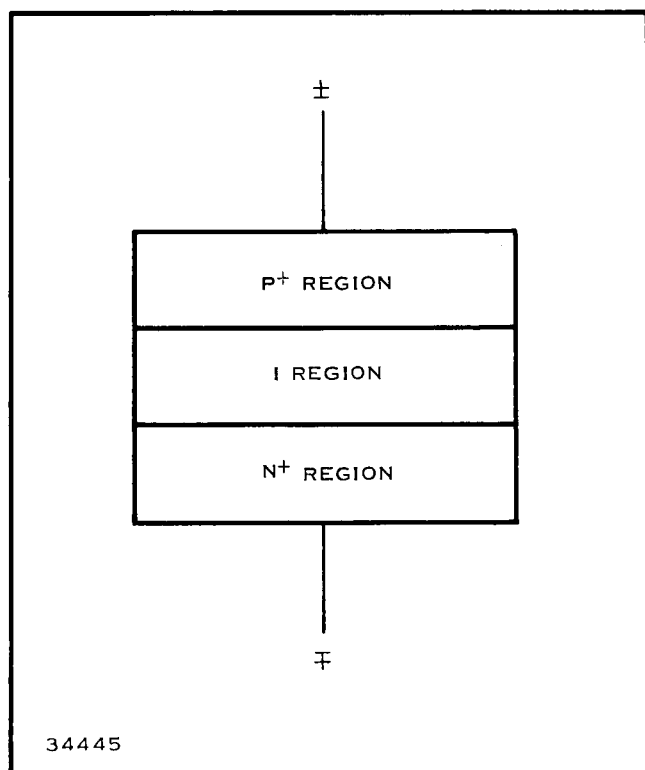


Figure 50. PIN Diode Configuration

The capacitance at microwave frequencies is determined by the area, thickness, and dielectric constant of the intrinsic region and is independent of the reverse bias voltage. The series resistance proves to increase with decreasing reverse bias and rises to a maximum value at about 0.5 volt forward bias, where forward conduction begins because of flooding of the intrinsic region with holes and electrons.

As the dc forward-condition current increases, the intrinsic region is changed from a slightly lossy dielectric to a fairly good conductor at microwaves. In forward bias, the capacitance component of the circuit disappears and the equivalent circuit becomes a small resistance whose value decreases with increasing forward dc current.

\*Trademark of Texas Instruments Incorporated.

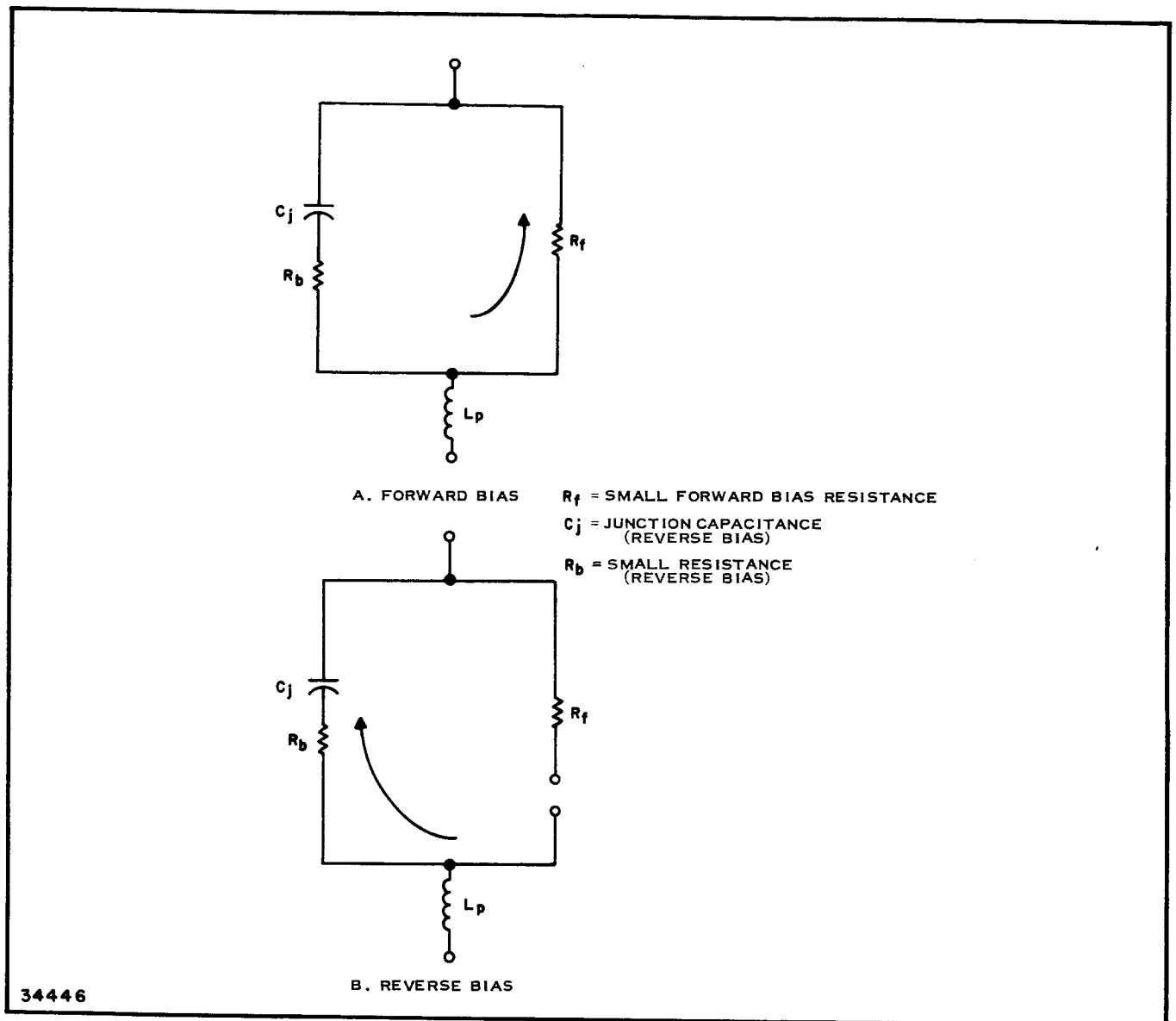
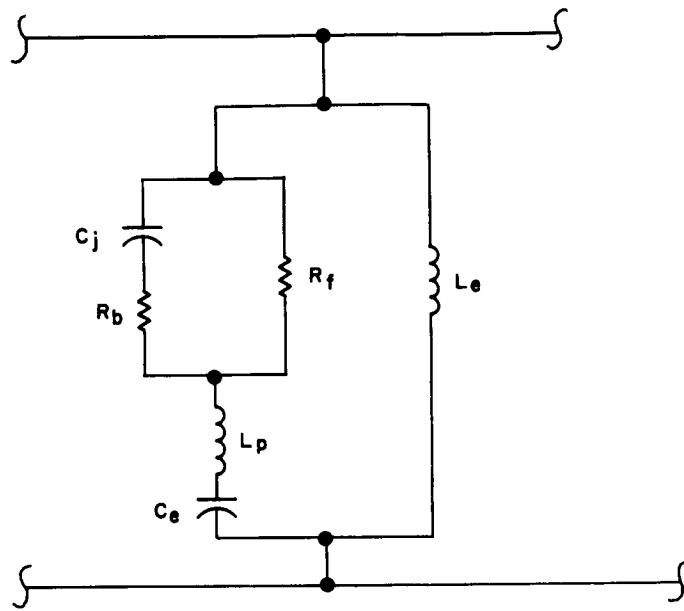


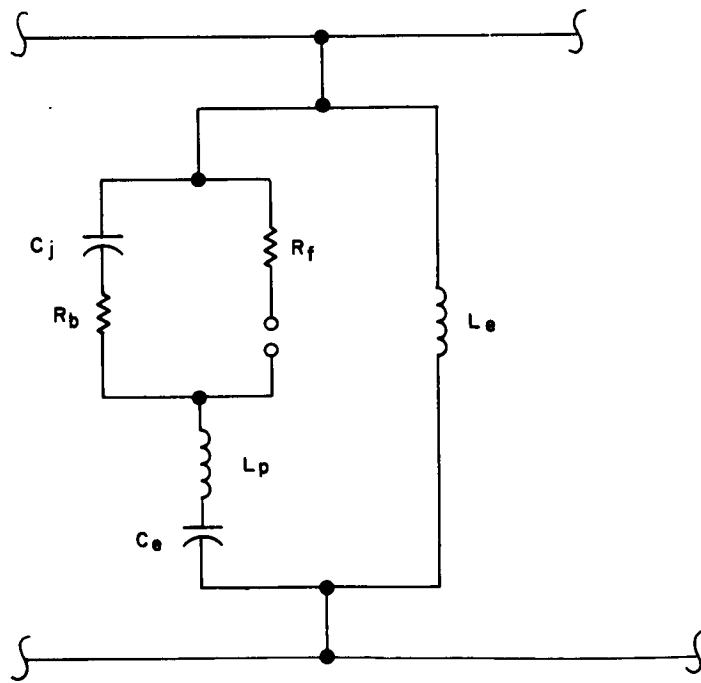
Figure 51. Diode Equivalent Circuit

The equivalent circuit of the PIN diode (or any diode) is shown in Figure 51. The values of the small forward bias resistance  $R_f$  and the small series resistance  $R_b$  in reverse bias depend on the bias values chosen. When an external tuning circuit is added, the diode will give switching action between forward and reverse bias states.

When the diode and external circuit are arranged as shown in Figure 52 a forward mode switching circuit is achieved, and when forward bias is applied (Figure 52A) an RF short circuit is obtained as a result of the external tuning capacitor  $C_e$ , which series resonates the diode lead inductance  $L_p$ . In the reverse bias configuration (Figure 52B) an open circuit is obtained by parallel resonance between the diode junction capacitance  $C_j$  and the external tuning inductor  $L_e$ .



A. FORWARD MODE SWITCH, FORWARD BIAS



B. FORWARD MODE SWITCH, REVERSE BIAS

34447

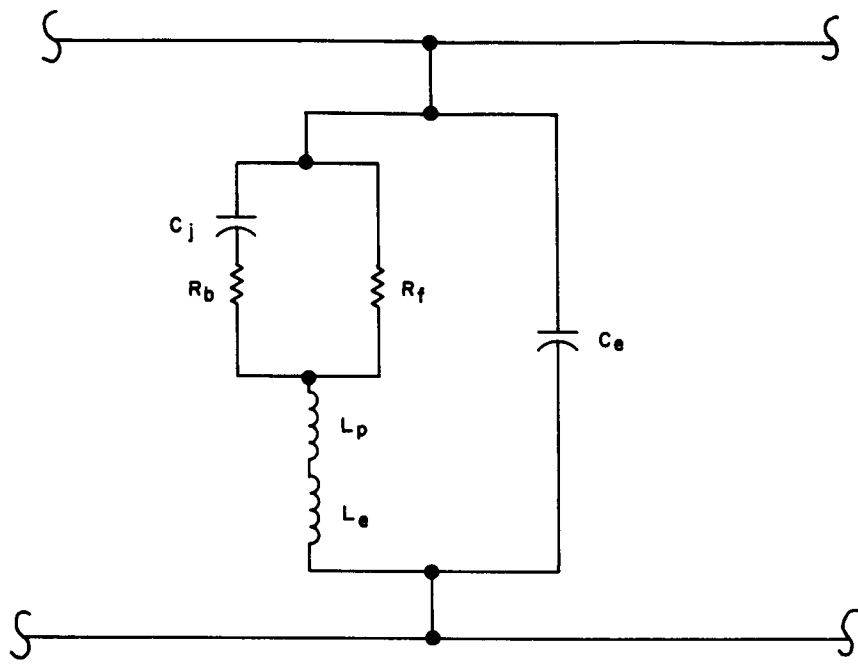
Figure 52. Forward Mode Switching Circuits

When the diode and external circuit are arranged as shown in Figure 53, a reverse mode switching circuit results. With forward bias (Figure 53A) an open circuit condition is achieved by parallel resonance between the two inductors  $L_p$  and  $L_e$  and the external capacitance  $C_e$ . When reverse bias is applied, series resonance is obtained and an RF short circuit exists.

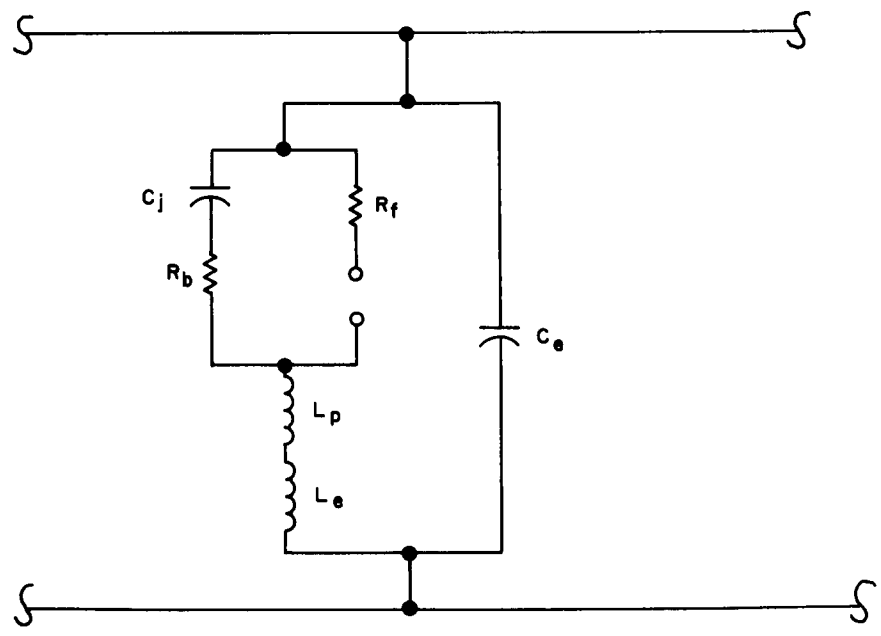
This type of device is presently being applied as a phase shifter in the MERA system. In this use, the diode will be subjected to high power in both forward and reverse bias states. In the forward bias state the PIN diode circuit will have the same small resistance for both high and low power levels. The RF current amplitude may be tens of amperes, whereas the dc bias current is measured in only tens of milliamperes without current switching into reverse bias. This is because the switching time necessary to remove the plasma is on the order of  $1 \mu s$ . The high power limit in forward bias is thus determined by the maximum permitted  $I^2R$  heating of the junction.

Surface-oriented PIN switching diodes<sup>50, 51</sup> have been designed to allow compatible interconnection with microstrip transmission lines on high-resistivity silicon for a monolithic, integrated phase-switching circuit. At microwave frequencies, stray capacitance must be reduced to a minimum to avoid loss of component function. The use of a surface-oriented diode structure allows the reduction of stray capacitance resulting from contacts expanded over oxide-protected active substrates. The geometry of these diodes provide adjacent placement of the anode and cathode areas at the surface of a silicon chip, and the diodes have a carrier flow under bias which is approximately parallel to the surface.

Figure 54 compares a surface-oriented microwave switching diode with a conventional planar diode structure. In this type of application a dead short on forward bias is needed to provide low insertion loss and low capacitance on reverse bias so as to obtain high isolation. For the conventional planar diode, the conduction system to make contact to the other elements of the integrated circuit is by means of metal stripes of the required width, separated from a ground plane by high resistivity silicon, forming a microstrip transmission line. The diode design must be compromised to conform to the required geometry. Large capacitance results from design requirements for other diode parameters; for example, in order to reduce the diode resistance on forward bias, a large enough anode area will result in increased capacitance upon reverse bias. The metal contacts are expanded over oxide protected-active substrates, thereby further increasing the capacitance. In the case of the surface-oriented diode, we have anode and cathode diffusions into the high-resistivity silicon and metallic contacts in opposite directions to form the microstrip transmission line. On forward bias, carriers are injected into the I region all along the PN junction, thus reducing the series resistance by means of conductivity modulation. On reverse bias, we have in effect a number of parallel capacitors with the maximum capacitance occurring at the closest spacing. The reverse bias capacitance is therefore largely determined by the depth of diffusion. In order to achieve low resistance on



A. REVERSE MODE, FORWARD BIAS

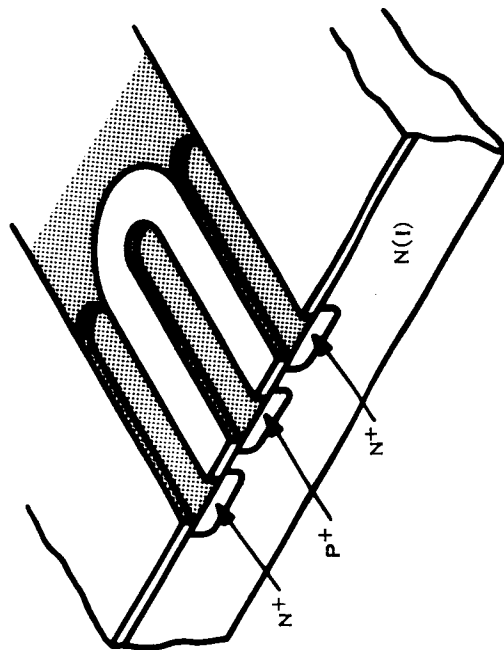


B. REVERSE MODE, REVERSE BIAS

34448

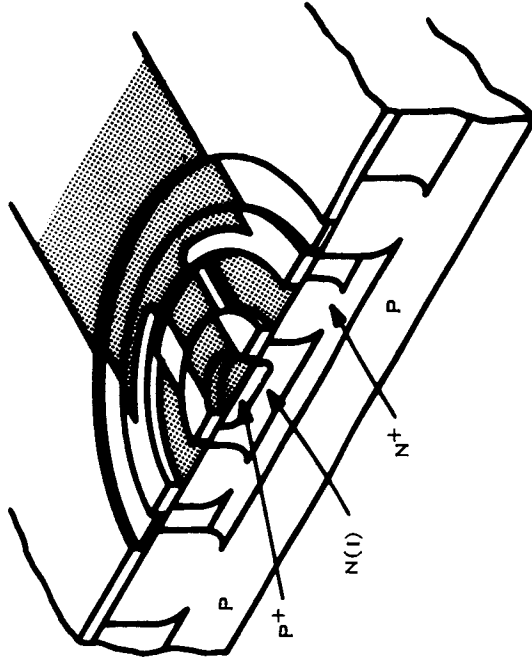
Figure 53. Reverse Mode Switching Circuits





**SURFACE-ORIENTED DIODE**

1. CONFORMS READILY TO MICROWAVE STRIPLINE GEOMETRY.
2. SMALLER CAPACITANCE POSSIBLE BECAUSE OF SMALLER PARALLEL PLATE AREA.
3. NO EXPANDED CONTACTS REQUIRED--- STRAY CAPACITANCE MINIMIZED.



**CONVENTIONAL PLANAR DIODE**

1. DESIGN MUST BE COMPROMISED TO CONFORM TO MICROWAVE STRIPLINE GEOMETRY.
2. LARGER CAPACITANCE RESULTS FROM DESIGN REQUIREMENTS FOR OTHER DIODE PARAMETERS.
3. MUCH STRAY CAPACITANCE.

Figure 54. Surface-oriented Diode Versus Conventional Planar Diode Structure

34449

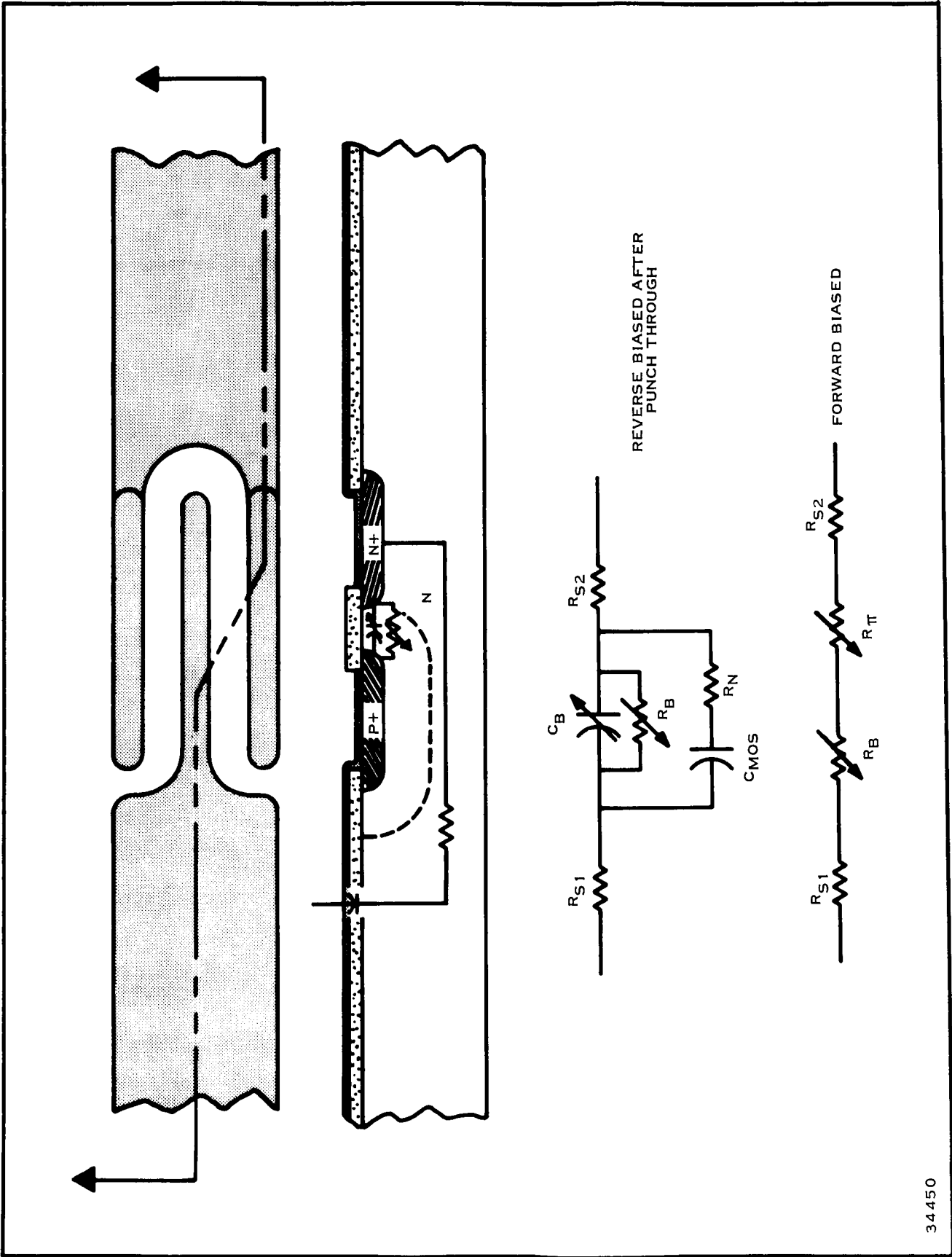


Figure 55. Surface-oriented PIN Switching Diode and Equivalent Circuits 50

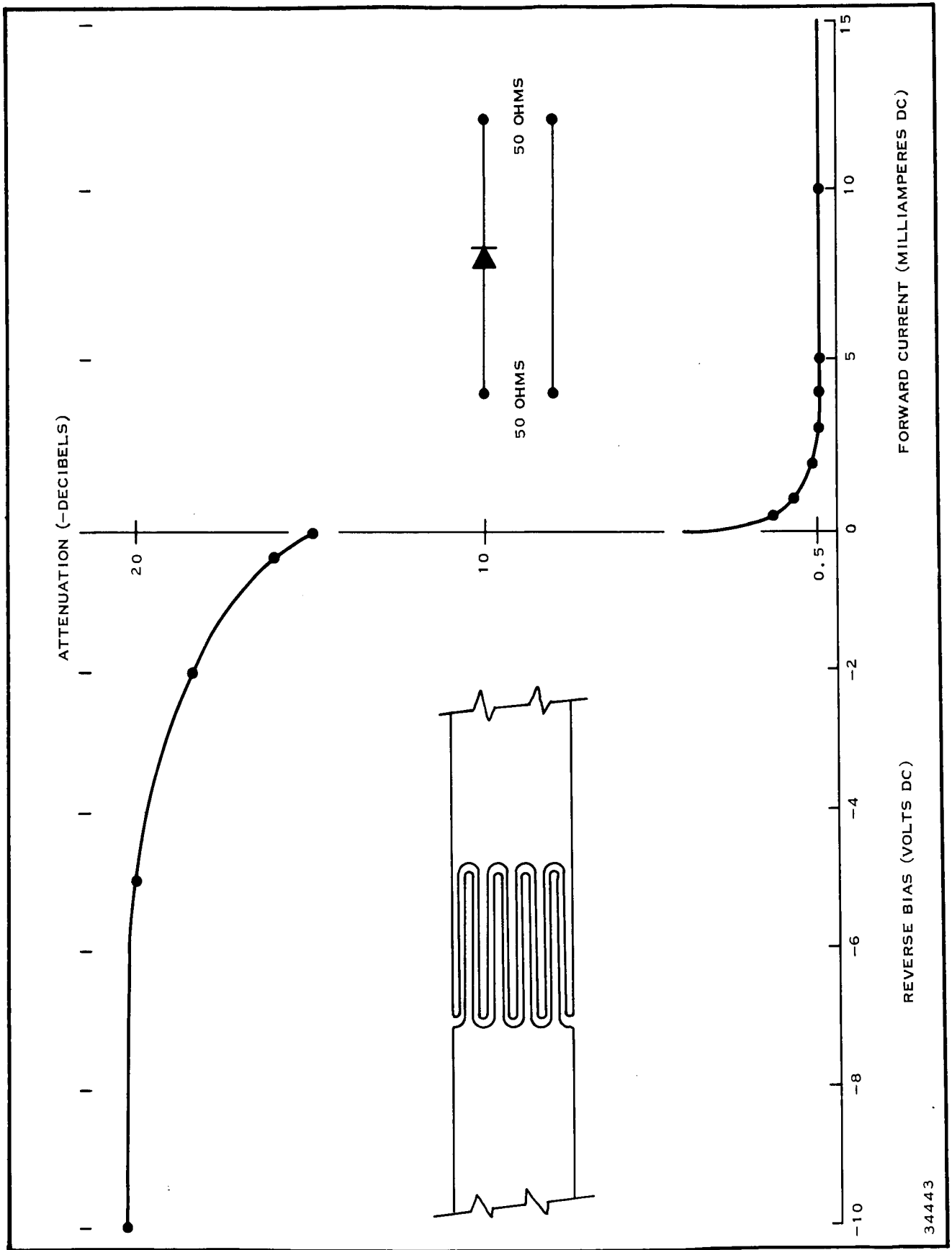
forward bias, the spacing between anode and cathode is made very small, causing the diodes to punch through on reverse bias; but the larger capacitance of a punch-through condition is offset by the ability to control capacitance by the diffusion depth. The surface-oriented diode conforms readily to microwave stripline geometry and the effects of expanded contacts are minimized.

The equivalent circuit<sup>50</sup> for a surface-oriented PIN switching diode is shown in Figure 55 and consists of a 6-mil stripline, 10-mil high-resistivity substrate, ground plane, and anode and cathode region. The diode may or may not be constructed in selective epitaxial pockets as shown. Some of our most successful devices were constructed directly in P-type silicon, with resistivity greater than 50 ohm-cm. In this case, the silicon substrate becomes the I region of the PIN diode. The equivalent circuit of the diode structure only, on forward bias, consists of the series resistance of the two metallic striplines, the conductivity-modulated junction resistance and the resistance of the I region, also conductivity modulated. All of these resistances are small. On reverse bias, the circuit shown consists of the series resistance of the metallic striplines, the voltage dependent barrier capacitance shunted by the barrier resistance, a lumped equivalent of the MOS capacitance produced by the metallic stripline, the oxide substrate, and the silicon substrate. This capacitance is in series with the resistance of the substrate material.

When this circuit is considered as an RX meter parallel circuit,<sup>51</sup> the MOS capacitance and the barrier capacitance are combined into one measurable value. One might think that a large value of MOS capacitance would completely obliterate the small reverse bias barrier capacitance and make the diode switch useless at high frequencies. To evaluate this possibility, typical values were used for  $C_B$ ,  $R_B$  and  $C_{MOS}$ ; two different values were used for  $R_N$ , representing the substrate resistance in series with the MOS capacitance. The results showed that the MOS capacitance essentially disappears above 10 MHz and that only the barrier capacitance is effective.

Figure 56 shows the insertion loss and the isolation to 500 MHz RF possible from a typical surface-oriented diode switch under conditions of forward and reverse dc bias.<sup>51</sup> The insertion loss is about 0.5 dB for all values of forward current above 2 mA, and the isolation is approximately 20 dB at -5 volts bias. The RF power incident on the diode was 1 mW. The measurements were made on a nine-finger diode.

A family of curves<sup>51</sup> for different bias levels is shown in Figure 57. The isolation is constant until the diode self-rectification of the incident RF voltage produces a peak large enough to overcome the negative dc bias. At 2 watts into a 50-ohm load, the peak power is 14 volts. For 5 and 10 volts negative bias, essentially constant isolation was obtained out to approximately 100 mW, and at 20 volts negative dc bias constant isolation was found to approximately 1 watt of RF power. These diodes are 6 mils wide and approximately 7.5 mils long.



34443

Figure 56. Surface-oriented PIN Switching Diode in Microstrip Transmission Line at 500 MHz<sup>51</sup>

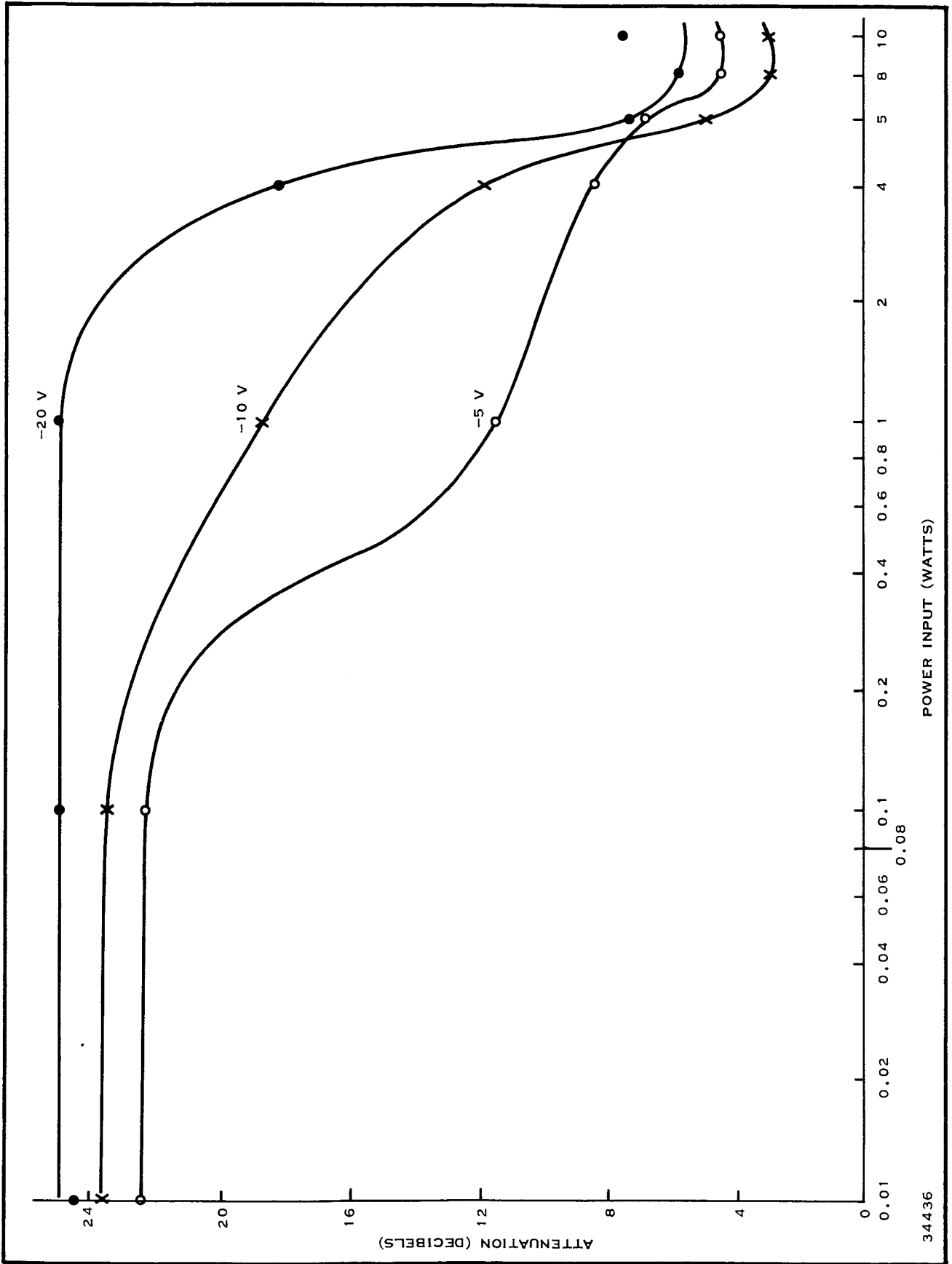


Figure 57. Power Input Versus Isolation of Surface-oriented PIN Switching Diode in Microstrip Transmission Line at 500 MHz<sup>51</sup>

### C. SCHOTTKY BARRIER DIODES

Schottky barrier varactor and mixer diodes are well suited for use in integrated circuits in the microwave region. As a planar structure using the properties of a metal semiconductor junction, the Schottky barrier exhibits the properties of an abrupt junction rather than the graded-junction characteristics of the diffused junction devices. The capacitance variation of the abrupt junction is

$$C_t = C_p + C_j = C_p + \frac{C_{j0}}{\left(1 + \frac{V_{\text{bias}}}{\phi}\right)^{1/2}} \quad (2)$$

where

$C_t$  = total capacitance measured at the diode terminals

$C_p$  = package capacitance

$C_j$  = junction capacitance

$V_{\text{bias}}$  = dc bias voltage

$\phi$  = contact potential

$C_{j0}$  = junction capacitance at 0 volts.

The use of thin epitaxial layers in conjunction with planar Schottky barrier junctions has produced very high Q microwave devices. With the barrier metal extended over a silicon dioxide insulating layer, this "expanded" contact is wirebonded to eliminate the metal springs that are found in the very small mesa structures on point contact diodes of conventional construction. The structure of the diode is shown in Figure 58.

The relative quality Q of a varactor is defined in terms of its cutoff frequency:

$$Q = \frac{f_{\text{co}}}{f_0} \quad (3)$$

where

$$f_{\text{co}} = \frac{1}{2\pi R_s C_j}$$

$f_0$  = frequency of operation.

To be of high quality, a varactor must have a high cutoff frequency; therefore for a fixed capacitance, it must have a low resistance. The Schottky barrier device can be made from several different semiconductor materials, such as GaAs, Ge, and Si. Because of the difference in electron mobility, there are differences in the total resistances of the devices. The GaAs Schottky barrier device has very high cutoff frequencies. These higher cutoff

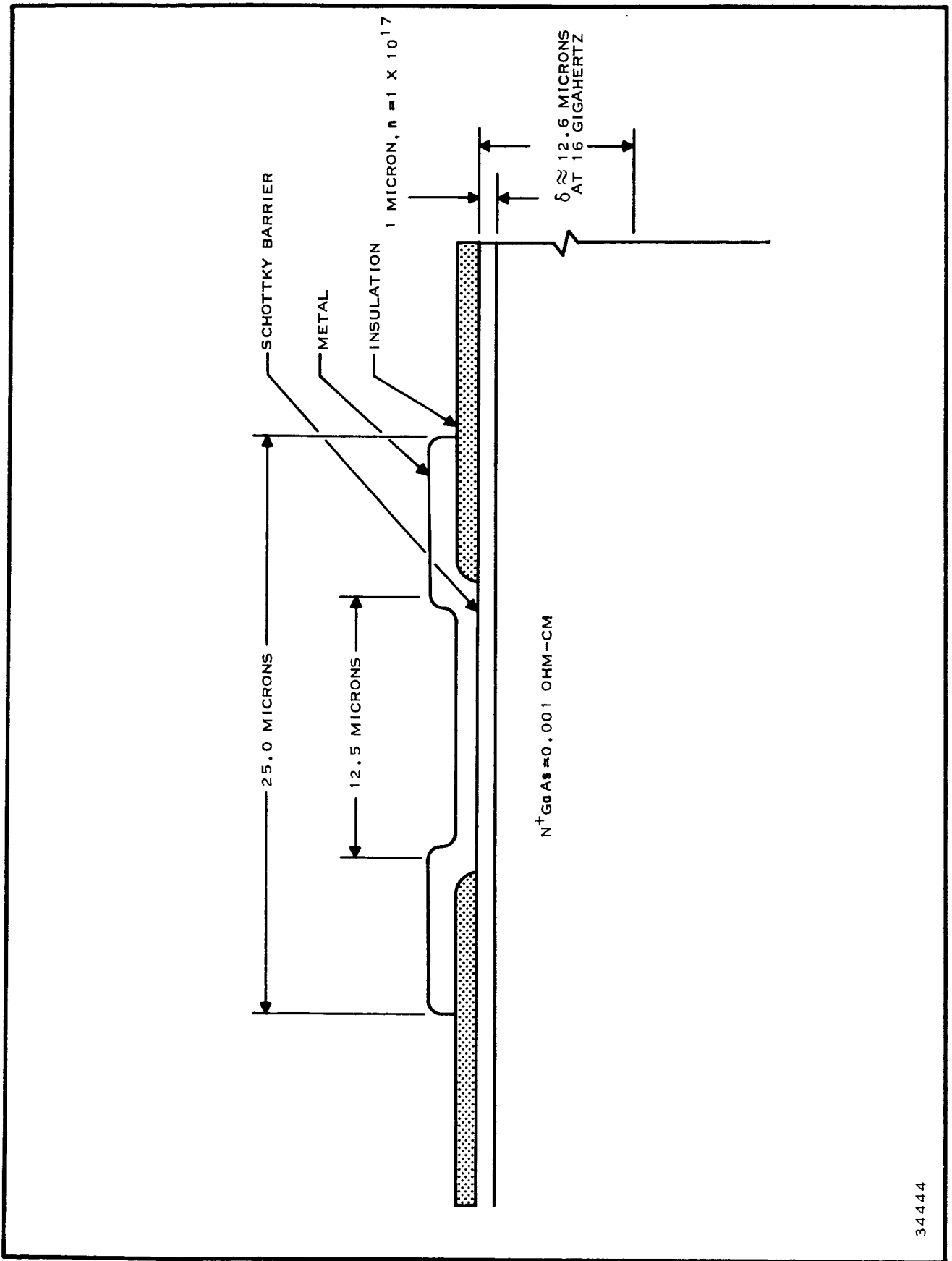


Figure 58. Typical Construction for a Schottky Barrier Diode

34444

frequencies seemed to be desirable for parametric amplifier work, so a GaAs Schottky barrier varactor was used as the active element in a  $K_u$ -band nondegenerate parametric amplifier; the results improved the state of the art.<sup>54</sup>

Because the Schottky barrier varactor appears to be an abrupt junction, the Fourier capacitance ratio  $\gamma$  should be higher than it is for the conventional GaAs varactor. This proved to be true. The minimum  $\gamma$  of 0.4 was calculated from the noise figure data and the cutoff frequency obtained from characterizations of the diode. Figure 59 is a plot of the minimum noise figure with the cutoff frequency as the variable; the following is the minimum noise figure equation<sup>52</sup> solved for  $\gamma$ :

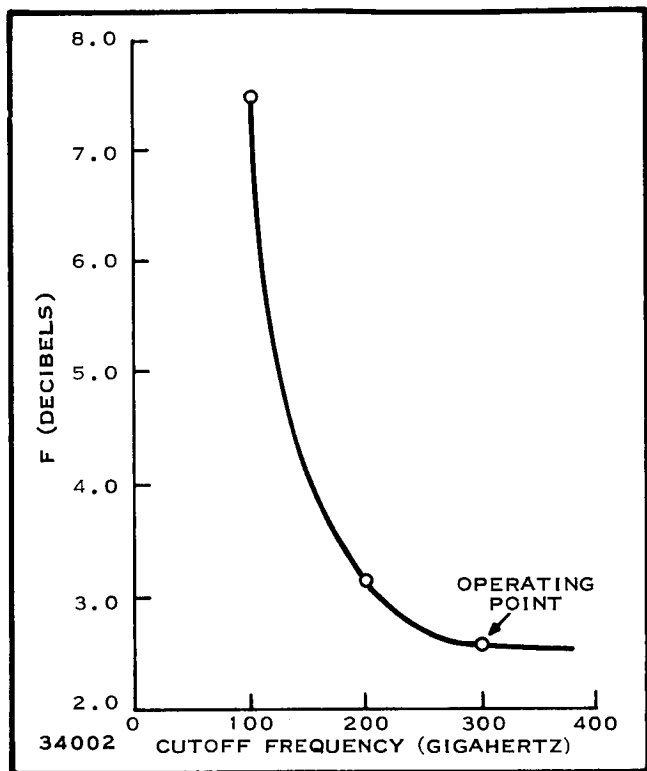


Figure 59. Cutoff Frequency Versus Noise Figure

$$\gamma_{\min} = \frac{\left(\frac{f_p}{f_s} - 1\right)^{1/2}}{Q \left(1 - \frac{f_s}{f_p} - \frac{1}{F}\right)^{1/2}} = \text{Fourier capacitance ratio} \quad (4)$$

where

$$\text{cutoff frequency} = f_{co} = \frac{1}{2\pi R_s C_j}$$

$$\text{quality of the varactor} = Q = \frac{f_{co}}{f_s(K)}$$

$$\frac{\text{pump frequency}}{\text{signal frequency}} = \frac{f_p}{f_s} = 2.5$$

$$\text{Fourier capacitance ratio} = \gamma = 0.4$$

$$\text{increase in capacitance of the varactor due to pumping} = K \approx 1.3.$$



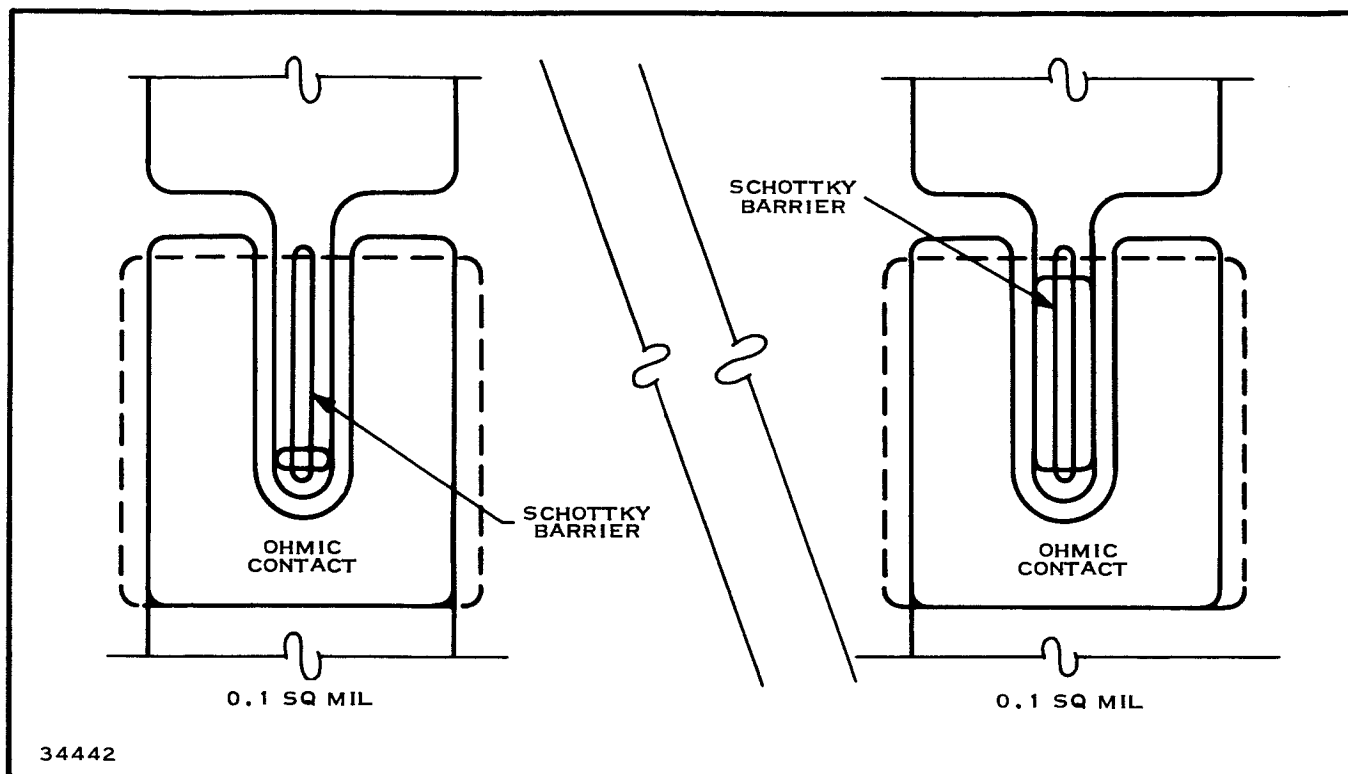
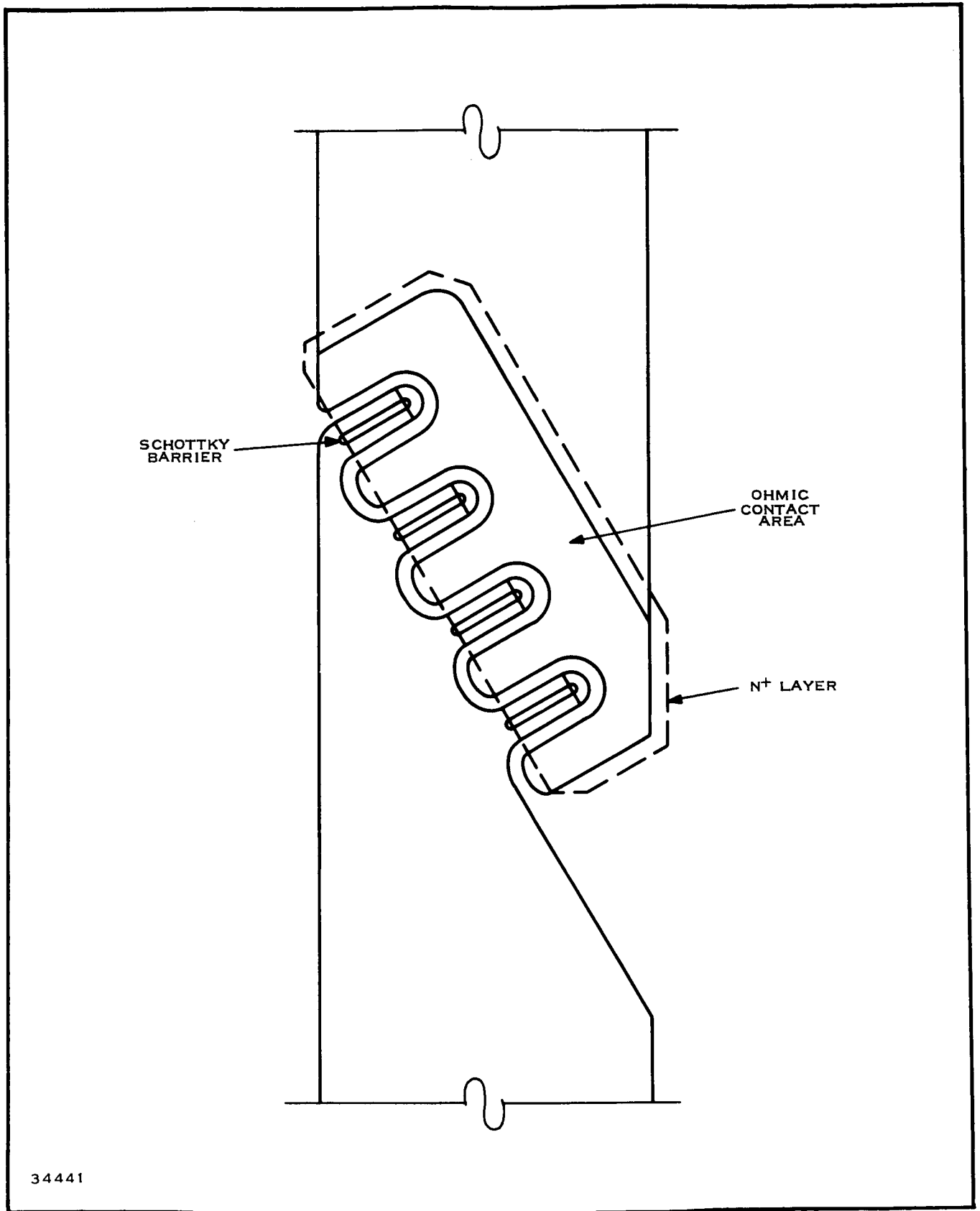


Figure 60. Experimental One-sided Schottky Diode

The Schottky barrier varactor should also be able to fulfill the multiplier functions described in Subsection A. High efficiencies can be obtained in this function because of the high  $Q$ 's and breakdown voltages obtainable in the Schottky barrier. Also, when the forward characteristics of the Schottky barrier are optimized, the device acts as an efficient, low-noise mixer diode.

Using these two functions of the Schottky barrier and the effects described by Gunn,<sup>55</sup> Texas Instruments has begun a program to develop a millimeter-wave receiver front end in a functional electronic block. This functional electronic block will consist of a Gunn-effect oscillator operating at 31 GHz and a Schottky barrier varactor tripler to provide a local-oscillator signal at 94 GHz. Also, a Schottky barrier balanced mixer will be constructed to provide the frequency conversion to an intermediate frequency. The entire electronic block will be built on semi-insulating GaAs, with deposits of epitaxial GaAs used for the Gunn-effect oscillator and the Schottky barrier varactors. All circuitry will be in microstrip transmission line.

The device configuration for the Schottky barrier is shown in Figures 60 and 61. The critical features in this structure, from the materials aspect, are (1) accurate doping control to produce a carrier concentration of approximately  $5 \times 10^{16} \text{ cm}^{-3}$  in the N-region while maintaining a high carrier mobility in the deposit and (2) achieving reproducible layer thicknesses of less than  $1 \text{ } \mu\text{m}$  (estimated thicknesses  $0.25 \text{ } \mu\text{m}$  and  $0.7 \text{ } \mu\text{m}$ ). It is proposed



34441

Figure 61. Harmonic Generator Diode Structure

that the deposition system used to prepare these deposits be the same as that used for commercial devices. This proven system should ensure production of the high-quality material that will be required. To achieve the desired deposit thickness, the operating conditions will be modified to slow down the deposition rate. With the current deposition rates (approximately  $15 \mu\text{m/hr}$ ) a deposition run of only one minute would be required. Slower growth rates (approximately  $1$  to  $3 \mu\text{m/hr}$ ) would be desirable for achieving better thickness control and minimizing startup deposition differences. This result can be readily achieved by reducing the rate of  $\text{AsCl}_3$  input into the reactor. A constant check of material quality will be made during this process modification. Selective depositions of epitaxial GaAs will be performed to provide the junctions. No difficulty is expected in attaining the desired geometrical definition.

Both GaAs and silicon have been used in building Schottky barrier mixer diodes. Figure 62 shows the noise figure performance of the GaAs Schottky barrier mixer diode (L-79) in a conventional X-band mixer. This data is compared to that of 1N23WE and 1N23G point-contact diodes.

These measurements were taken in the same test set, using appropriate mixer holders in each case and showing the best noise figure obtained for more than one diode of each type. The IF noise figure was corrected to the standard value of  $1.5 \text{ dB}$  at  $30 \text{ MHz}$  from calibration obtained with an input resistor equal in value to that of the diode under test and connected to the input terminals of the amplifier.

Resistance to burnout of both the 1N23WE silicon point-contact diodes and the GaAs Schottky barrier diodes was made. Two different diameters of metal-to-semiconductor contacts were tested by means of apparatus made according to military specification MIL-S-19500/233B. Results are shown in Figure 63, from which it may be noted that Type 1N23WE withstood the specified 2-erg level quite well and showed deterioration following pulse at the 3-erg level. The Schottky barrier diodes under test in the same apparatus showed resistance that was 3 to more than 10 times better in this comparison run; the larger diameter contact showed better resistance.

Satisfactory mixer operation was obtained over a wide range of local oscillator power. A change in input level from  $0 \text{ dBm}$  to  $-10 \text{ dBm}$  resulted in little change in either noise figure or in VSWR.

A single-sided silicon microwave mixer diode has been fabricated, and is suitable for integration with a microstrip-hybrid formed directly on high-resistivity silicon. The diodes are formed on epitaxial material that has been grown in vapor-etched pockets in high resistivity P-type silicon substrate material. These holes are placed selectively on the substrate; their positions are determined by windows in an oxide layer, which acts as a barrier to the etch where no windows exist. The holes, about  $0.1 \text{ mil}$  deep, are then refilled with N-type epitaxy of about  $0.05\text{-ohm-cm}$  resistivity. Portions of

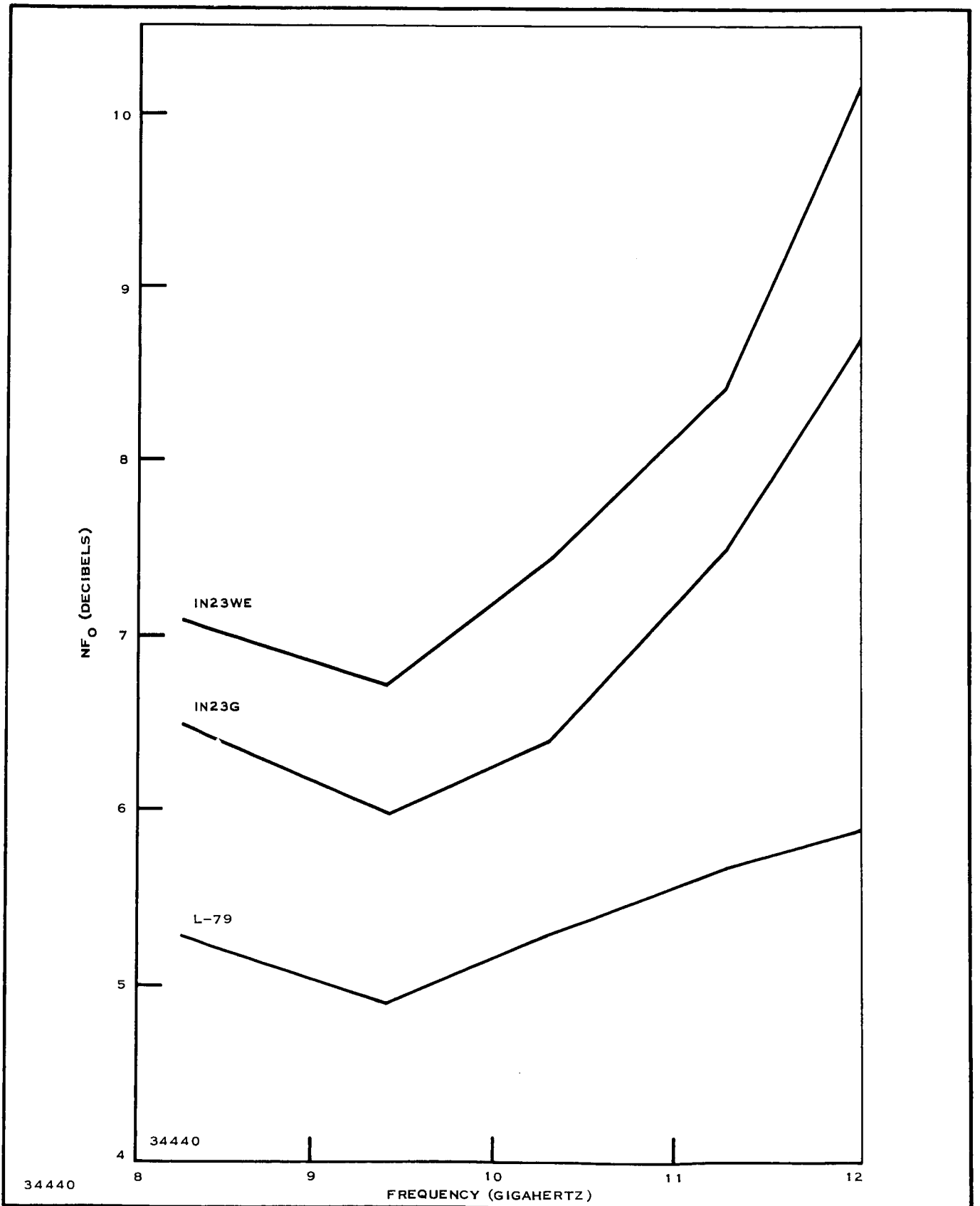


Figure 62. Mixer Diode Comparison

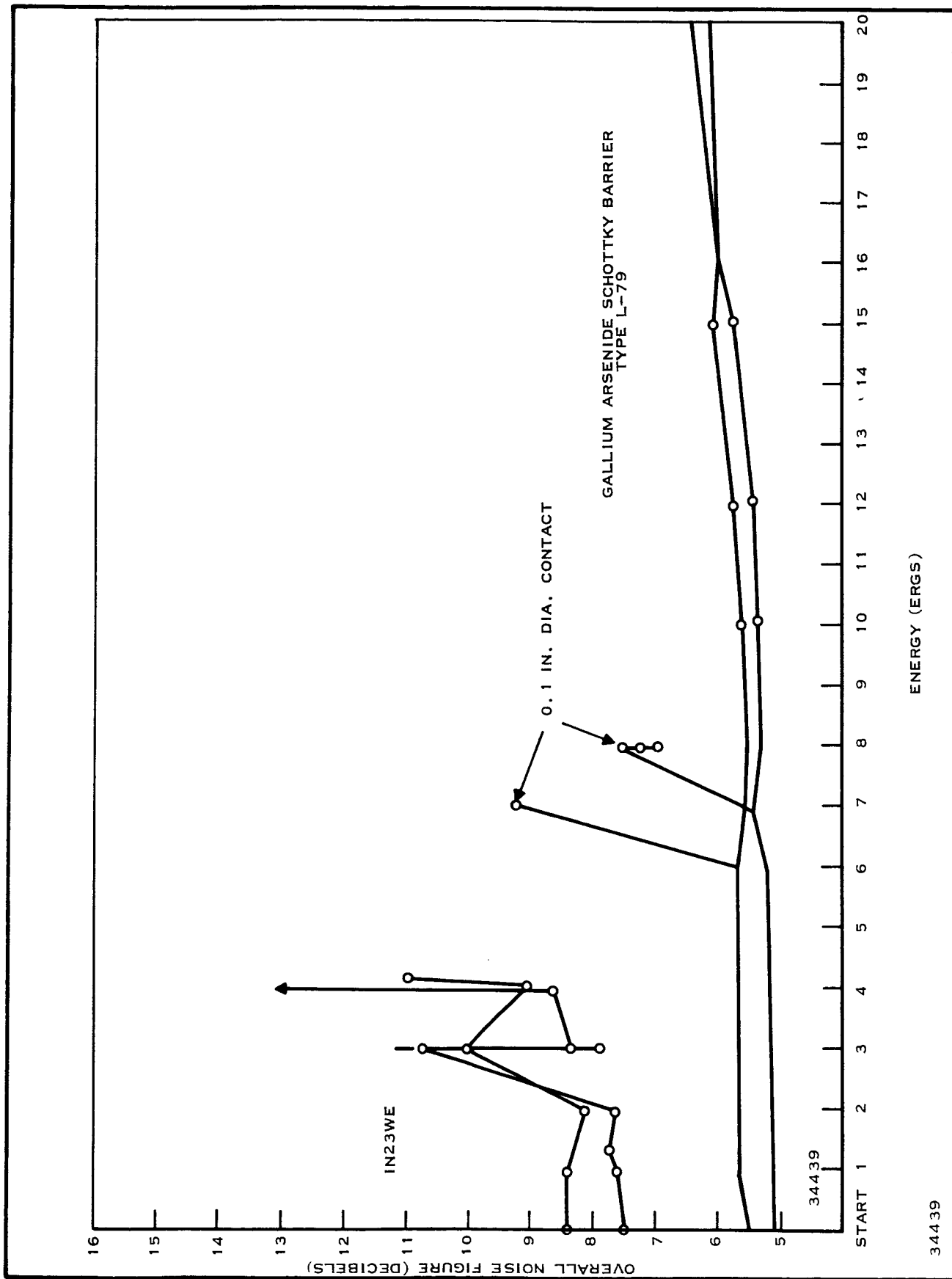


Figure 63. Burnout Test, X-band Mixer Diodes

the epitaxial region which are to act as ohmic contacts are given a heavy  $N^+$  deposition and then molybdenum-gold is evaporated to form a metal-semiconductor contact.

Measurements of the forward characteristics of these devices as a function of temperature indicate that they are true Schottky barrier diodes. Although the noise figures have been higher than those usually expected for a Schottky barrier device, the results are early and by no means represent expected figures of optimum value.

Performance of a balanced mixer function, in addition to the mixer diode, requires means for mixing the incoming signal with the local oscillator and for providing output filtering. The most satisfactory means for mixing the signal and local oscillator is provided by a hybrid structure, either phase reversal or quadrature. The use of a hybrid provides a mixer with natural separation of signals and rejection against noise generated in the local oscillator source.

The parallel-line directional coupler was investigated for X-band balanced mixer application because its required area is considerably less than that of the branch-line coupler. The inhomogeneous dielectric of the microstrip construction gives rise to forward coupling which limits the isolation available from a quarter wavelength parallel-line directional coupler. This effect is shown in Figure 64, with a theoretical output at the normally isolated port shown as a function of the ratio of the even- and odd-mode velocity. For the coupling structures studied, these velocities differed from 3 to 5 percent, yielding a limiting value of isolation slightly over 20 dB. An additional problem with the parallel-line coupler is in obtaining the necessary even- and odd-mode impedances for 3-dB coupling. The spacing required to obtain 3-dB coupling is at the limits of semiconductor processing techniques and building such structures reproducibly is still an unsolved problem.

The branch-line hybrid shown is being used for developmental work, although the parallel-line coupler is still being investigated. This hybrid structure has isolation of approximately 20 dB over the range of 8.5 to 9.6 GHz; the noise figure is essentially that of the mixer diode alone.

Present technological advances have made the Schottky barrier the best conventional varactor or mixer diode available. These devices have improved the state of the art in noise figure performance by at least 1 dB in both parametric amplifiers and mixers. Their use in integrated circuits has been successfully demonstrated by a silicon X-band balanced mixer constructed in microstrip transmission line, and in the near future the performance of integrated circuit devices should rival that of their conventional counterparts.

#### D. GUNN EFFECT

Gunn<sup>55</sup> has discovered a new kind of current oscillation at microwave frequencies, in N-type GaAs and in InP. When a uniform electric field applied to a bulk specimen of N-type GaAs is raised above a certain critical value, a

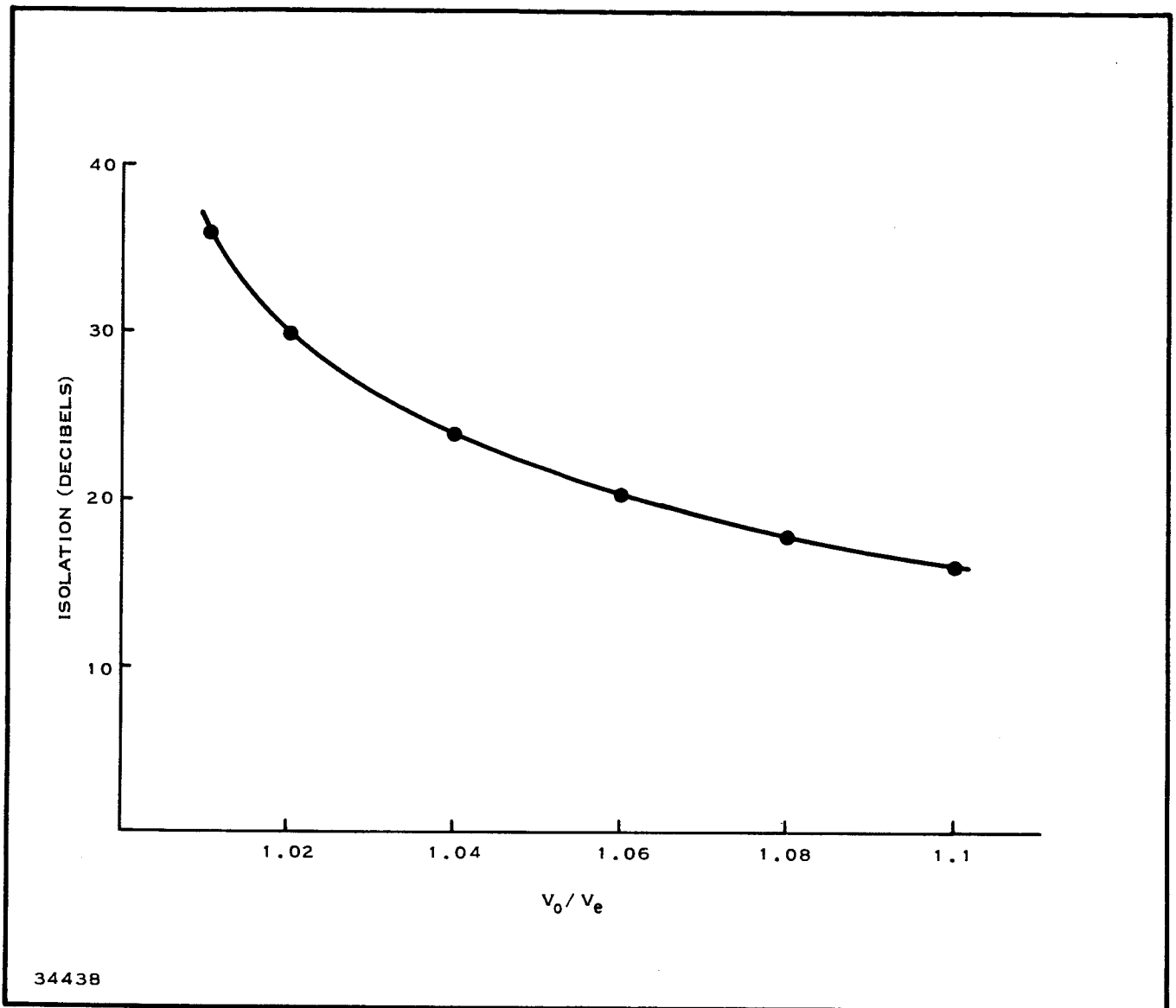


Figure 64. Theoretical Isolation for Microstrip Coupler

time-dependent decrease in the current is observed. In long specimens this decrease resembles random noise, but in short specimens it is found to be periodic and of extremely high frequency which is determined by the specimen length. Sufficient microwave power can be transferred to an external load to suggest that the effect may take on technological importance. Similar effects are found in N-type InP, but not in P-type GaAs.

Gunn observed that the period of the oscillation was related to the transit time of the electrons through the sample; for this reason high frequencies can only be obtained by using very thin samples. A typical value for the electron drift velocity is  $1.5 \times 10^7$  cm/s; hence, frequencies in the 1- to 2-GHz range would require a range of sample thickness from 42 to 85 microns. Epitaxial layers of GaAs provide the easiest means of obtaining these thin samples.

The application of the Gunn effect to microwave oscillators has been investigated by Texas Instruments<sup>56</sup> and Bell Telephone Laboratories<sup>57</sup> with good results. The work done at the former dealt with pulsed microwave oscillators in epitaxial layers of GaAs, whereas that at the latter dealt with CW microwave oscillators using GaAs.

The resulting devices that could be built would possess the advantages—common to solid-state devices—of compactness, ruggedness, and low operating voltage. They would also have a very wide modulation bandwidth, and their manufacture should be straightforward because of their structural simplicity and convenient dimensions.

At present the state of the art of the Gunn effect is limited due to difficulty in obtaining pure material. The application to oscillators seems possible with resulting peak power outputs of 0.5 to 1.5 watts at about 3 to 5 GHz. This will simplify transmitter design by eliminating multipliers and drivers. A significant point is that the stability of a device made by this process is probably better than that of the standard oscillator. It is believed that at 1 GHz a stability of better than 0.005 percent can be obtained.



## SECTION VIII

### HIGH DIELECTRIC CONSTANT MATERIALS

#### A. GENERAL

There are two principal applications of high dielectric constant materials in the microwave frequency range. In one of these the material has been used to reduce the size of microwave components such as cavities. The linear dimensions of the cavity are reduced by the square root of the dielectric constant of the material. This reduction is a result of the wavelength in the material being reduced by this same factor compared to the wavelength in free space. Thus, if the material has a dielectric constant of 100, the volume reduction of the dielectric filled cavity is 1000. Single-ended and double-ended tunable cavities have been recently analyzed using waveguide filled with a dielectric material for part of the length but with free-space boundaries adjacent to tunable shorting plungers.<sup>60</sup> High Q's can be maintained over large tuning ranges. In this instance, the size of the component is reduced and the flexibility of tuning is retained.

The second application of high dielectric constant materials is a result of its resonance properties. A material with a high dielectric constant will exhibit resonances in various modes when operated with free space boundaries. To be useful, the loss tangent of the material must be low in order to allow the realization of high circuit Q's. A variety of materials can be considered for this application; however, single and polycrystalline rutile (TiO<sub>2</sub>) is the material most generally considered. Its dielectric constant is on the order of 100 and its loss tangent is low. The main problem of application is the strong dependence of the dielectric constant and the loss tangent on operating temperature. Materials such as strontium titanate and barium titanate have much higher dielectric constants with even greater dependence on temperature. Our main interest in these resonance properties is in their application to filter design. The analytical expressions for the resonance properties have been presented elsewhere;<sup>61</sup> experimental results and design information have also been reported.<sup>62-66</sup>

#### B. LOW-LOSS HIGH DIELECTRIC CONSTANT RESONATORS

To minimize the size of the resonator, the dielectric constant of the material should be high, since

$$\lambda = \frac{\lambda_0}{\sqrt{\epsilon}} \quad (1)$$

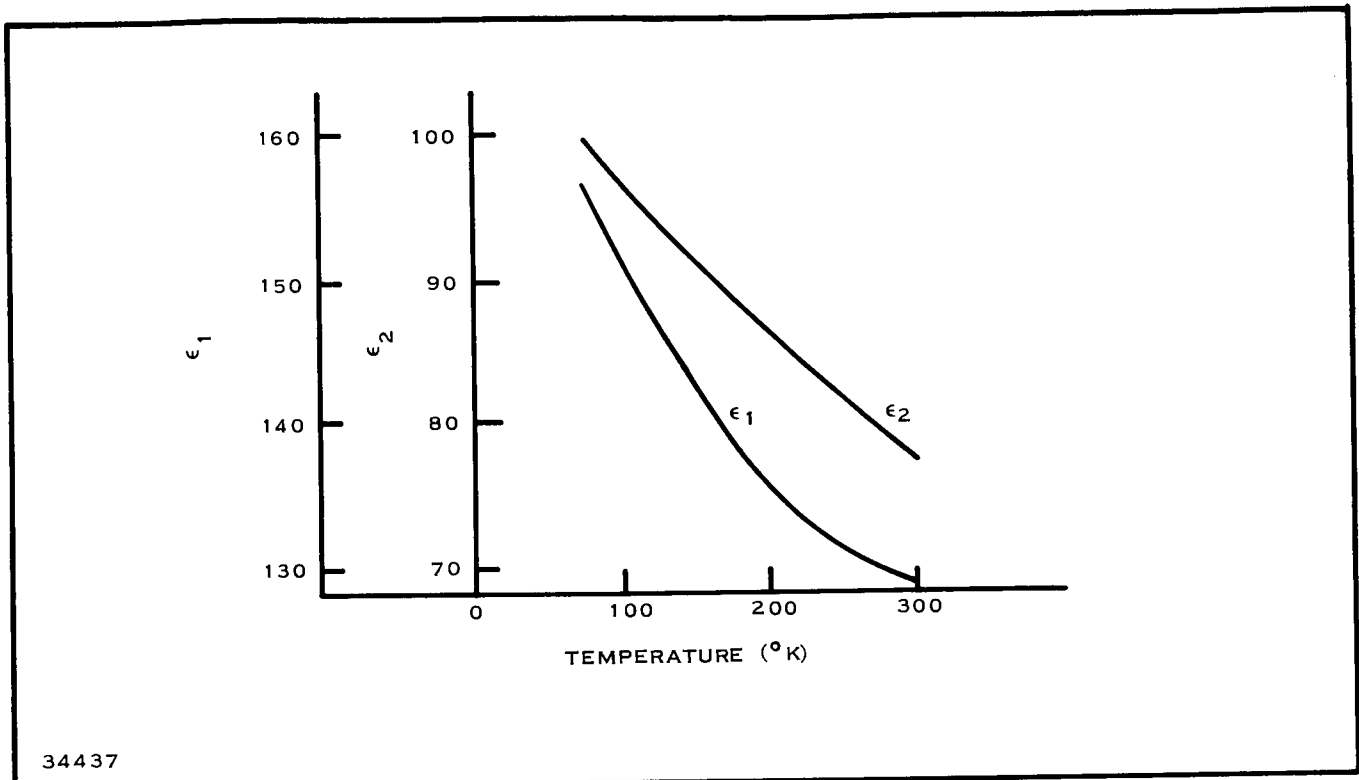


Figure 65. Dependence of Dielectric Constant on Temperature for Titanium Dioxide

where

$\lambda$  is the wavelength in the material

$\lambda_0$  is the wavelength in free space

$\epsilon$  is the dielectric constant.

In addition, with a high dielectric constant the fields external to the resonator attenuate rapidly with distance for any given mode. This means the radiation loss will be small and the unloaded  $Q$ ,  $Q_u$  will be determined by the coupling and dielectric losses. Thus, to a first approximation,

$$Q_u = \frac{\omega \epsilon}{\sigma} \quad (2)$$

where

$\sigma$  is the conductivity.

The strong dependence of the dielectric constant on temperature is shown in Figure 65 for  $TiO_2$ .<sup>61</sup> The dielectric constants parallel and perpendicular to the optic axis are  $\epsilon_1$  and  $\epsilon_2$ , respectively. Since the resonant frequency is proportional to the square root of the dielectric constant, lowering the temperature increases the frequency of operation. The variation of frequency with temperature is at least an order of magnitude greater than that for a brass-walled cavity.



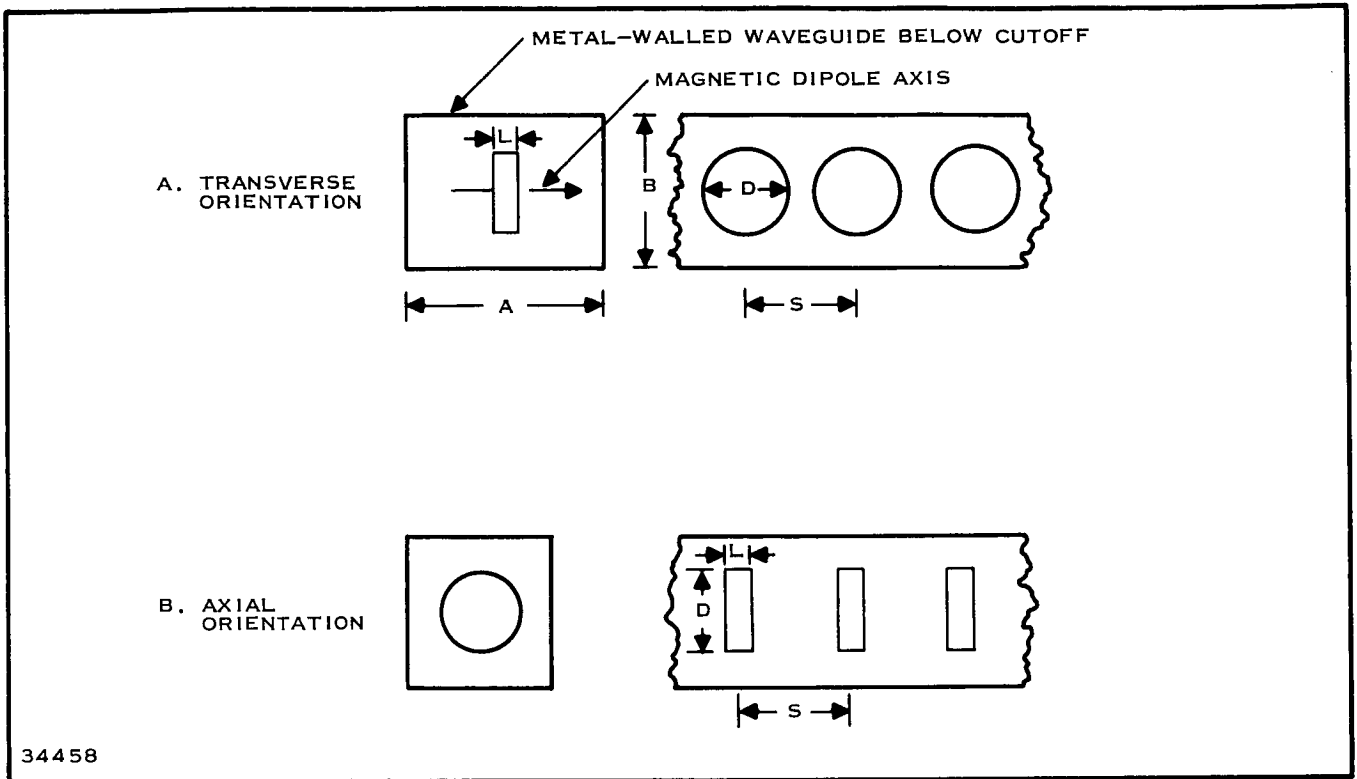


Figure 68. Coupled Dielectric Resonators Inside a Cutoff Rectangular Waveguide

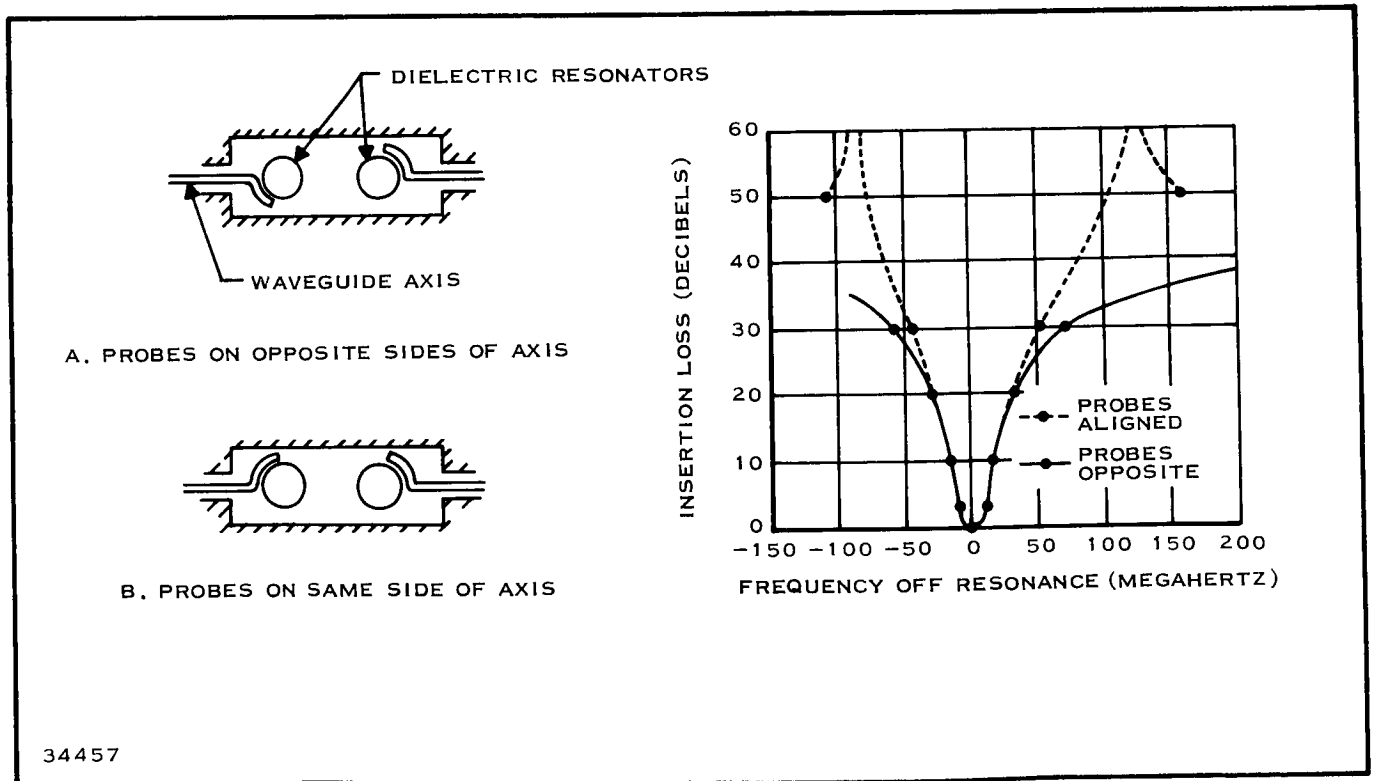


Figure 69. Insertion Loss Response Curves for Bandpass Filters Shown ( $f_0 = 3.01$  GHz)

in one case are evidently caused by the existence of parallel signal paths, one via the resonators and one between the probes.

Of considerable interest are the small size of these filters and the excellent response characteristics that can be realized due to the large  $Q$ 's. The diameters of the cylindrical resonators used to obtain the response of Figure 69 are 0.250 inch and 0.393 inch. Although this application of high dielectric constant materials is certainly not applicable to integrated circuit form, it is of interest as an external miniaturized circuit function.

## SECTION IX

### FERRITES

#### A. GENERAL

Magnetic oxides have become particularly important to the electronic engineer because, in addition to their useful magnetic properties, they possess very high electrical resistivities ( $\rho > 10^6$  ohm-cm). Hence, magnetic oxides can be used at very high frequencies, whereas magnetic metals with their relatively low resistivities exhibit such severe skin effect at high frequencies that magnetic fields do not penetrate into the bulk of the metal; thus their inherent magnetic properties cannot be exploited. In engineering practice, almost all magnetic oxides are called ferrites, whether or not they contain iron.

#### B. MICROWAVE PROPERTIES OF FERRITES

When subjected to a dc magnetic field, a ferrite sample exhibits less "magnetism" than does a similar-size sample of ferromagnetic material. The reasons for this phenomenon appears to be that alignment of the electron spins in ferromagnetic material is complete, whereas in the ferrimagnetic material there is only a net number of electron spins aligned in a given direction. Thus, more than half of the spins are aligned in a given direction within any domain.

For iron, a microwave signal "sees" an effective reflector; for ferrite, the wave can enter and pass through substantial amounts of the material without excessive reflection or attenuation. In the process the wave has an opportunity for strong interaction with the spinning electrons and as a result of this interaction, nonreciprocal phase shift and attenuation as well as nonlinear effects can, under suitable conditions, be manifested.

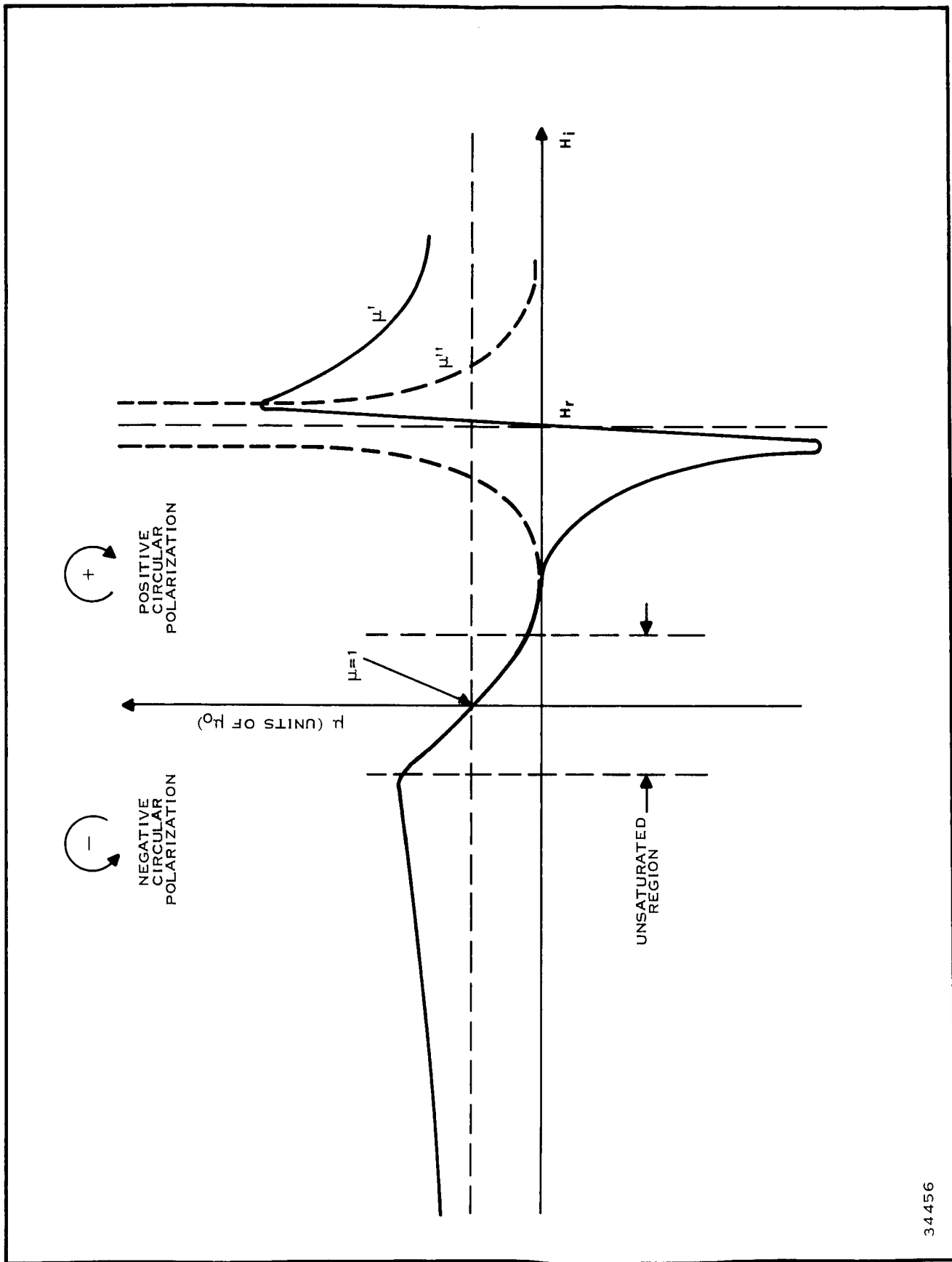
The vital property that makes ferrites so useful at microwave frequencies is the ability to vary their RF permeability. With circularly polarized waves, the permeability is scalar; its dependence upon a magnetic field  $H_i$  is shown in Figure 70. The  $\mu+$  (as seen by the positive circularly polarized wave) has been plotted to the right and the  $\mu-$  (as seen by the negative circularly polarized wave) has been plotted to the left of  $H_i = 0$  axis, with  $H_i$  increasing in both directions. The permeability is

$$\mu = \mu' \mu_0 \quad (1)$$

where

$\mu'$  = relative permeability

$\mu_0$  = permeability of free space;



34456

Figure 70. Ferrite Permeability for Circularly Polarized Waves as a Function of Internal Magnetic Field

the permeability may be considered to be complex because of residual losses, and  $\mu$  becomes

$$\mu^* = \mu_0 (\mu' - j\mu'') \quad (2)$$

where

$\mu^*$  = complex permeability including loss term

$\mu'$  = relative permeability

$\mu''$  = loss term.

The real part of the permeability  $\mu'$  has to do with phase shift, and  $\mu''$  the imaginary part is the loss component of the permeability. In a ferrite material saturated by a dc magnetic field, the magnetization vectors tend to be aligned parallel to the dc magnetic field. However, when a second magnetic field alternating at a microwave frequency is applied in a direction perpendicular to the dc magnetic field, the magnetization vector(s) precess about the direction of the dc magnetic field and in doing so couple energy out of the microwave field.

For resonance devices, it follows that operation would be desirable at a magnetic field value  $H_i$  at which  $\mu''$  is quite high. On the other hand, those devices in which the ferrite acts as a nonreciprocal phase shift element should be operated at values of  $H_i$ , for which  $\mu''$  is as low as possible consistent with the required value for  $\mu'$ .

Polycrystalline garnets—because of their narrower line widths, lower anisotropies and g-factors (spectroscopic splitting factor)—can be operated at substantially lower dc magnetic fields before these low field losses become troublesome.

Those electrical properties of greatest importance to the ferrite-device designer are saturation magnetization  $M$ , gyro-magnetic ratio  $\gamma$  (equal to  $0.0175 \times g$ -factor in the MKS system or  $1.4 \times g$ -factor in the CGS system), loss tangent  $\epsilon''/\epsilon'$ , linewidth  $\Delta H$ , curie temperature  $T_c$ , and anisotropy field  $H_a$ . Broad ranges of these quantities are commonly encountered in both ferrites and garnets; however, only the most usual ranges are shown in Table X.

The present state of the art in ferrite devices is limited in its application to integrated circuits. The limitation arises from the difficulty of achieving small dimensions compatible with integrated circuits while also providing the external field required. Surface-oriented diodes will be used to avoid this problem by performing several of the circuit functions customarily assigned to ferrite devices. Examples of such devices are switches, modulators, and phase shifters. Other circuit functions can be performed with ferrite devices having small dimensions and a compatibility with integrated circuits as an external circuit element, for example, filters, isolators, and circulators.



Table X. Electrical Properties of Ferrites and Garnets

Properties	Ferrites		Garnets	
	MKS	CGS	MKS	CGS
$M_s$	79,500 to 350,000	$\frac{1}{4\pi} \times$ (1000 to 4500)	4,000 to 155,000	$\frac{1}{4\pi} \times$ (500 to 1700)
g	2 to 4		2	
* $\epsilon''/\epsilon'$	0.0001 to 0.01		0.0005 to 0.05	
$\Delta H$	12,000 to 60,000	150 to 750	2,000 to 20,000	25 to 250
$T_c$	150 to 650		280	
** $H_a$	4,000 to 36,000	50 to 450	795 to 7950	10 to 100

\* at 20 MHz

\*\* Ferrites with a hexagonal crystal structure exhibit  $H_a$  typically in the range 640,000 to 950,000 At/m (8000 to 12,000 Oe) and linewidths  $\Delta H$  ground 160,000 At/m (2000 Oe).

## SECTION X

### FILTERS

Because transmission line structures compatible with integrated circuitry can be produced in microstrip form, an important class of filters can be fabricated in integrated circuits, namely, those using stripline techniques. Filters may be classified as low-pass, high-pass, band-pass, and band-stop filters; they may also be tunable or fixed tuned. Tunable filter structures, however, are not compatible with integrated circuit microstrip techniques. Furthermore, the problems associated with the design and fabrication of the different classes of filters are essentially the same. For these reasons, only the fixed-tuned, band-pass type of filter is considered here.

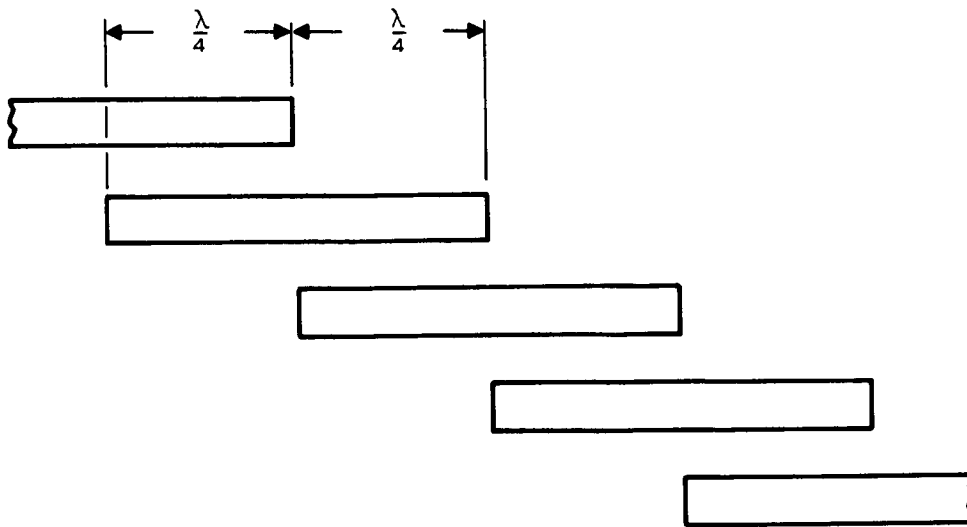
Part A of Figure 71 illustrates a band-pass filter consisting of parallel stripline resonators. These resonators are built of half-wavelength striplines and are positioned parallel to each other along half of their length. Placement of the resonators parallel to each other permits coupling to be varied proportional to the spacing between stripes. This construction is particularly convenient for printed-circuit techniques.

This type of filter yields a second pass-band at three times the center frequency and has first-order poles at zero and twice the center frequency. This structure lends itself well to printed-circuit fabrication. However, it is very sensitive to tuning; the slightest mistuning will yield a narrow spurious pass-band near the second harmonic. (For designs having a large value of fractional bandwidth or designs for high-pass application, Figure 72 is applicable.)

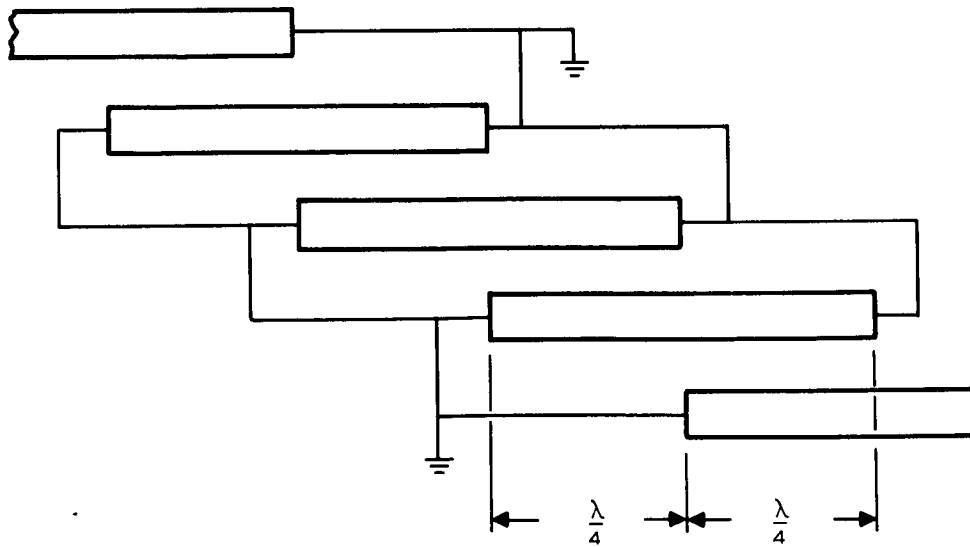
The dual of this filter, Figure 71A, may be achieved by placing short circuits at both ends of the resonators as shown in Figure 71B. Both types have the same transmission characteristics, the main difference being in their ease of fabrication.

Figure 72 shows another possible way of fabricating a parallel-coupled filter with  $\lambda/2$  resonators. This structure consists of rectangular bars which are supported by short circuit blocks at their ends. Such an arrangement eliminates dielectric losses since no dielectric support material is required. The rectangular bars afford a tighter coupling, thus yielding larger bandwidths. The filter characteristics are similar to the two previously mentioned. The short circuit blocks provide mechanical support for the resonators. Functional bandwidths of 0.01 to 0.70 can be achieved.

A more recently developed device uses a somewhat different method of construction to achieve better characteristics. This device, called an "interdigital filter," consists of stripline resonators between parallel ground planes (Figure 73). The resonators are a quarter-wavelength long and are



A. PARALLEL STRIPLINE RESONATOR FILTER, OPEN CIRCUIT ENDS



B. PARALLEL STRIPLINE RESONATOR FILTER, SHORT CIRCUIT ENDS

34462

Figure 71. Parallel Stripline Filter

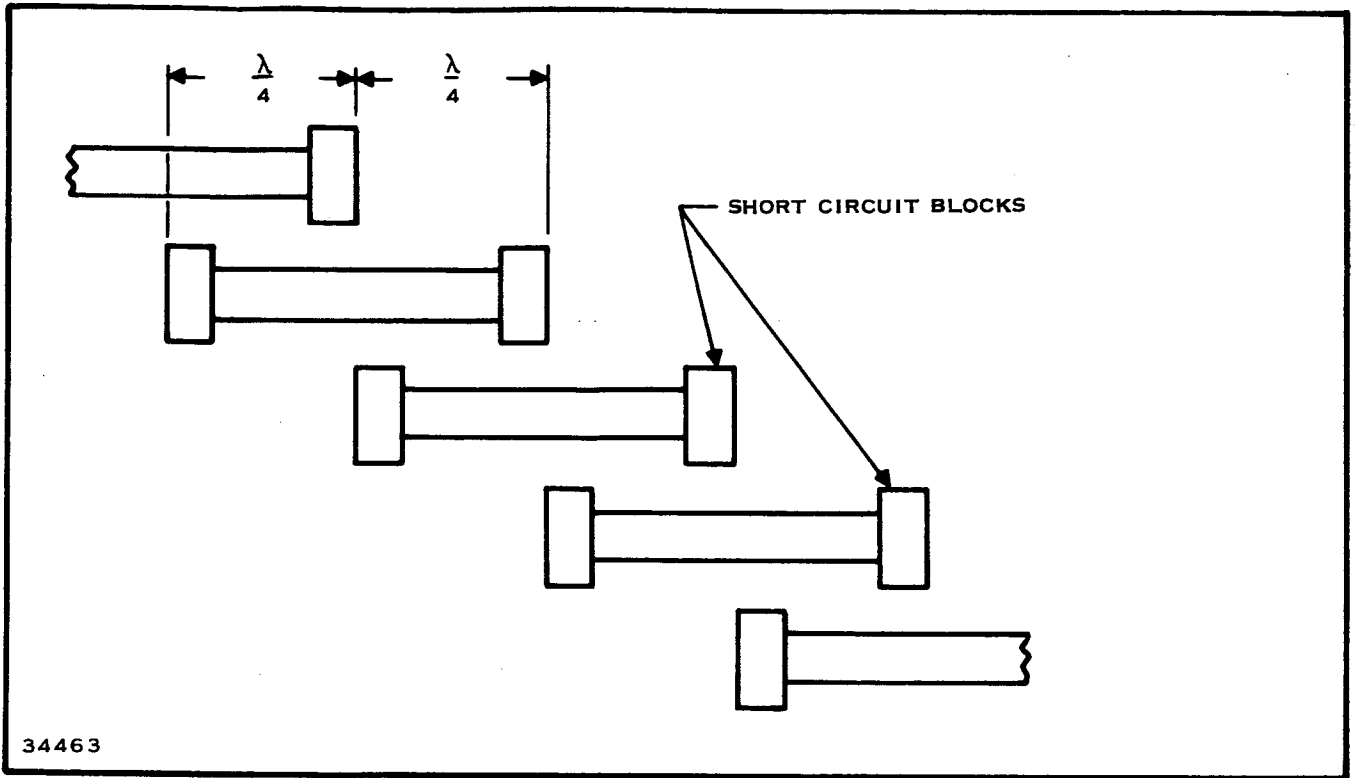


Figure 72. Parallel Stripline Resonator Filter, Supported Short Circuit Blocks

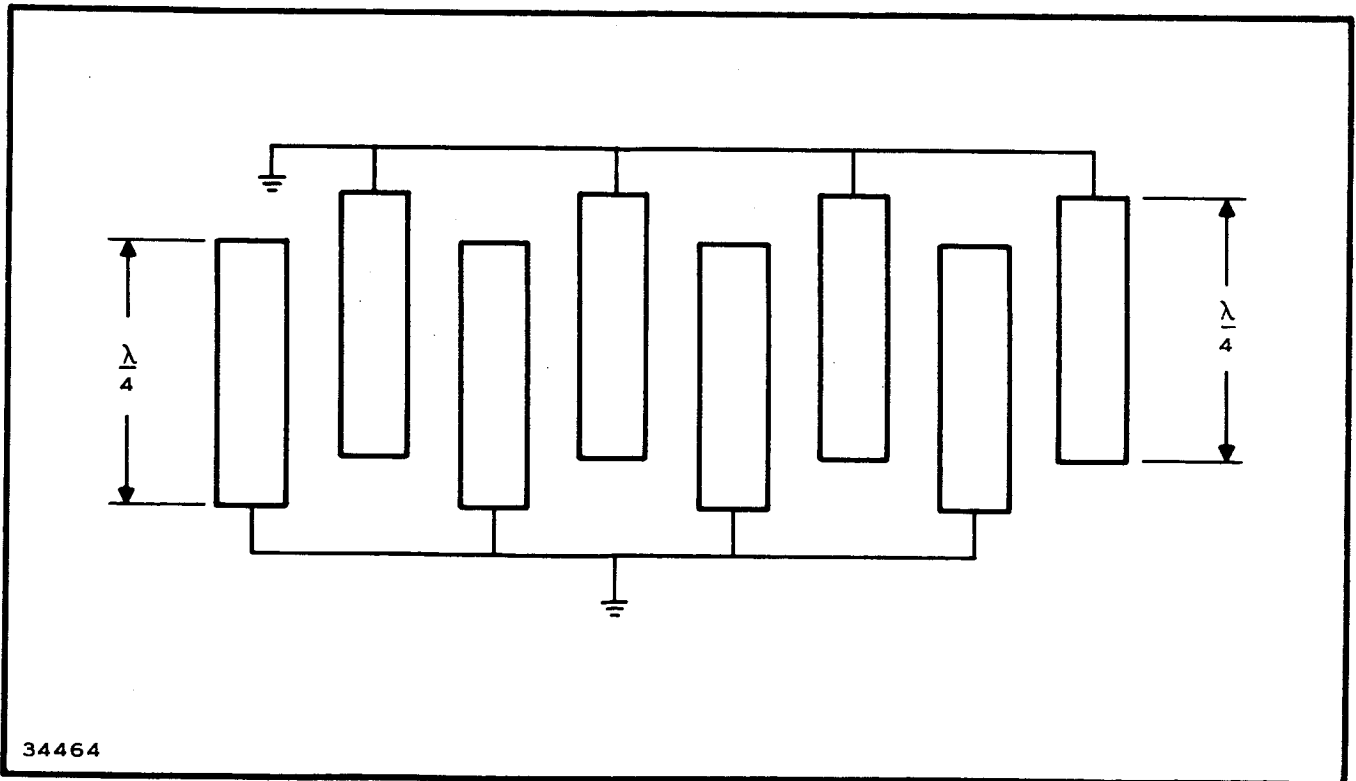


Figure 73. Interdigital Stripline Filter

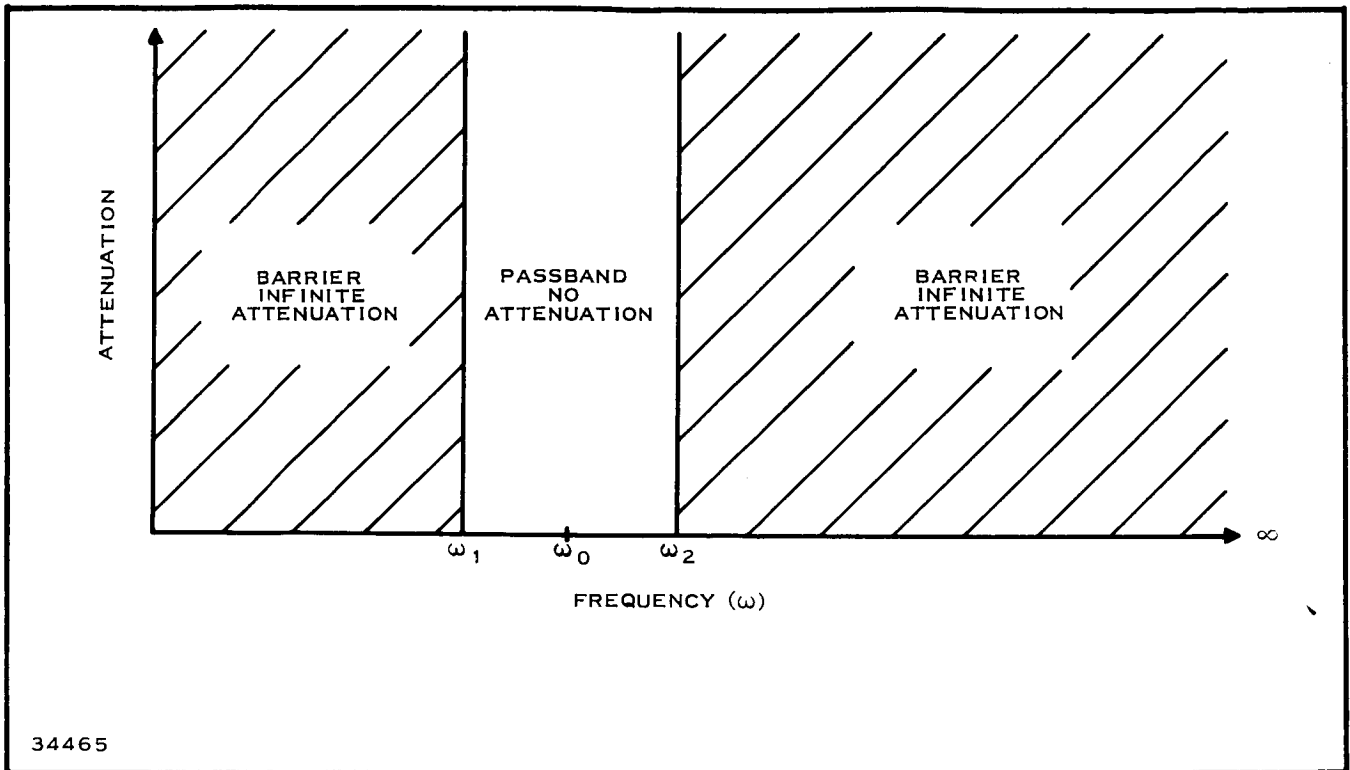


Figure 74. Ideal Bandpass Response,  $\omega_0 = (1/2)(\omega_1 + \omega_2)$

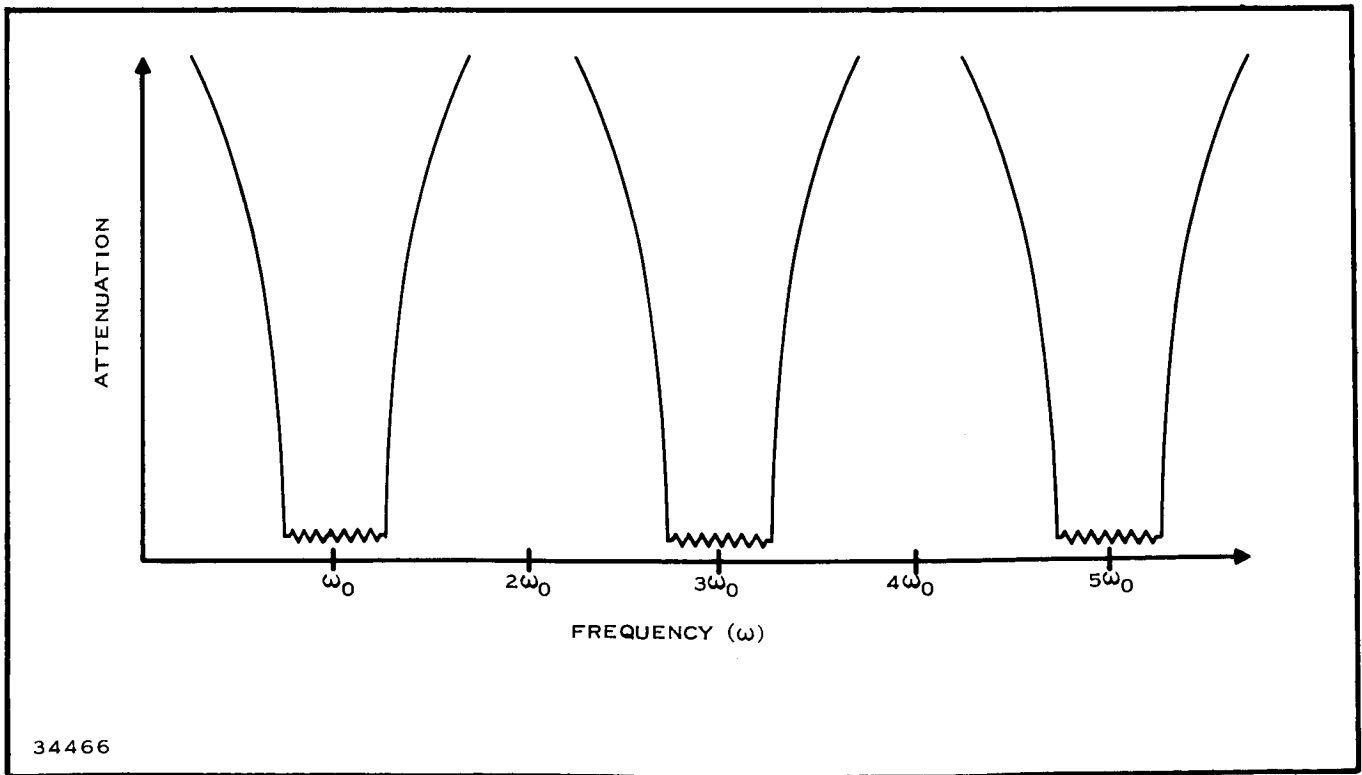


Figure 75. Bandpass Response of Filter Using Stripline Elements

short circuited at one end and open circuited at the other. Coupling is due to the fields between adjacent resonators. Bolljahn and Matthaei<sup>76</sup> have shown that the mathematics describing this filter become quite unwieldy if all the coupling effects are taken into account. Matthaei<sup>77</sup> et al. have a procedure involving several additional simplifying approximations that allow straightforward, easy-to-use design calculations. Although the formulas are approximate, the results of trial designs show that they are sufficiently accurate for most applications. This filter has multiple poles at the even harmonics, can be fabricated without dielectric material (therefore eliminating dielectric losses), and is very compact.

Perhaps the most important filtering problem in microwave applications lies in the basic notion of band-pass operation. One would like to be able to arrange for the transmission of signals within a prescribed finite band of frequencies while at the same time restricting the flow of energy at other frequencies, as shown in Figure 74. This suggests an infinite transmission barrier constructed adjacent to both upper and lower limit frequencies of the pass-band and leaving a pass-band in the spectrum for passage of the desired frequencies. Our concern in the microwave domain cannot be confined to a single, finite desired band of operation such as suggested in Figure 74. We must deal with many discrete bands of unwanted related frequencies whose passage is not inhibited. Therefore, conventional stripline filters are seen to have pass-bands at all odd-harmonic bands, as indicated in Figure 75.

It is evident that special attention to the blocking of the undesired frequencies must be provided in many cases. This usually means, for example, the addition of a different type of structure to reject the third harmonic. In stripline with low dielectric constants (in the range of about 2 to 4), this can be done with efficiency and in an acceptable manner. Apparently, there are no serious reasons to prevent a similar approach being transferred to the higher dielectrics used in semiconductor technology. It should be pointed out that stripline microwave filters are, in general, very sensitive to loading; that is, a close control of the impedances seen on the input and output of the filter must be maintained. If this is not done, the response characteristics both in and out of the pass-band may be deteriorated.

A typical "well-matched" stripline filter built at Texas Instruments (Figure 76) has a pass-band response as shown in Figure 77 and a third harmonic response as shown in Figure 78. These results provide visual evidence of the filter characteristic described above.

Returning to Figure 75, one is likely to think of the stripline filter as having infinite attenuation at all even harmonics of the pass-band. This idealized behaviour is theoretically true for the filter configuration in common use, but is not always easy to achieve in practice. The attenuation functions for different component structures will, in many cases, have their poles and zeros distributed differently throughout the frequency spectrum.

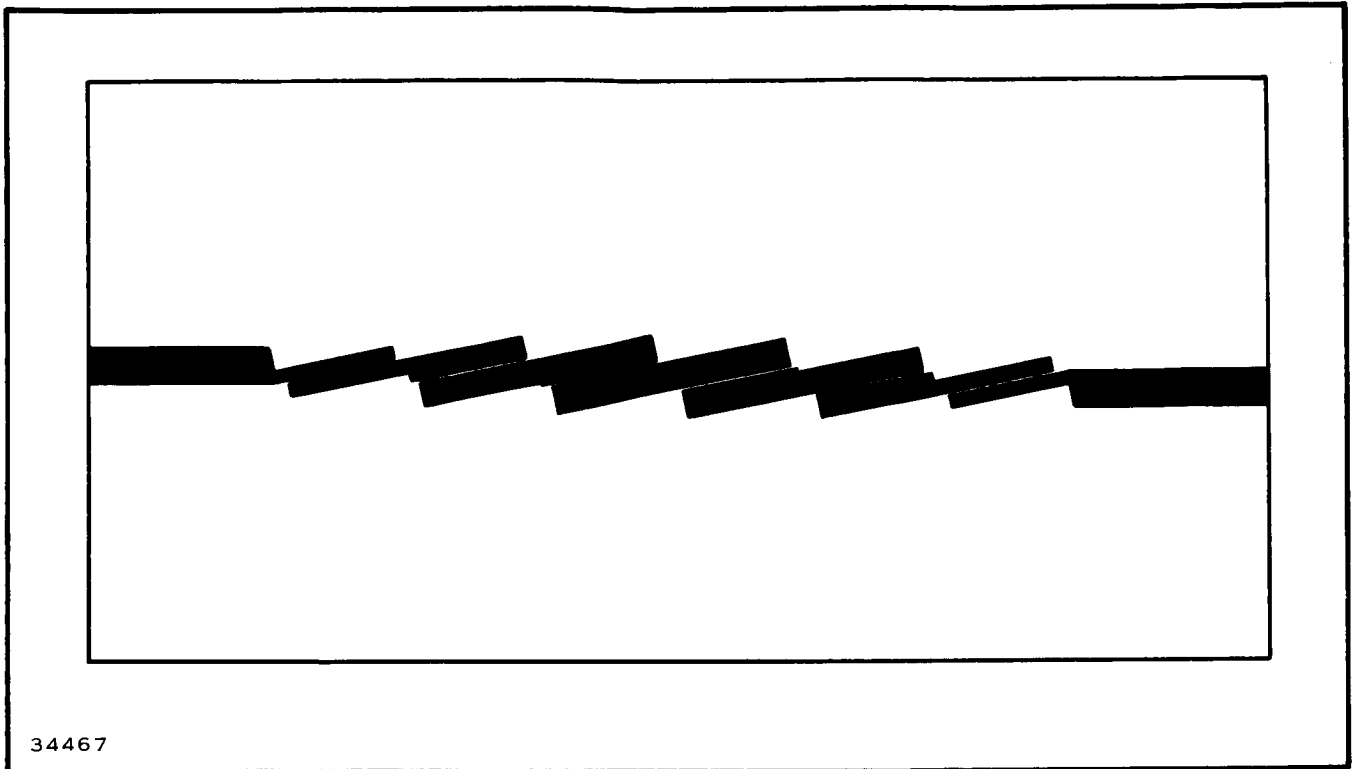
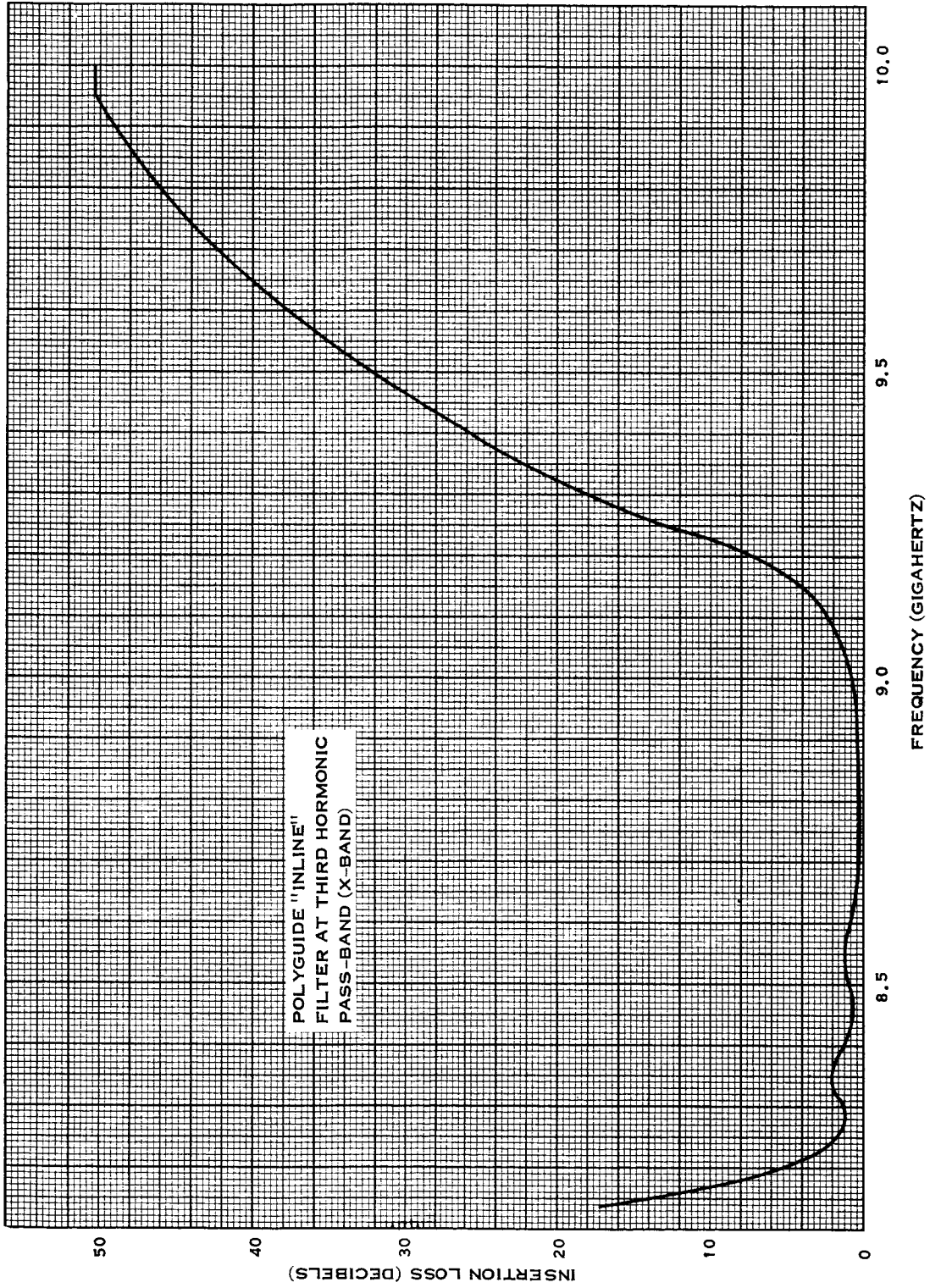


Figure 76. Parallel Resonator Stripline Filter

Thus, the design conceived several years ago by Seymour Cohn at Stanford University has a single pole at the second harmonic; this is one of the most common and least complex designs. Although the pass-band characteristics of this filter are good when it is carefully designed and fabricated, "holes" and spurious response at the second harmonic are almost impossible to avoid. This particular design is important even though it is very simple to build, being constructed essentially of parallel-coupled half-wave resonators etched in copper on a dielectric supporting base.

A more recent design concept uses a somewhat different method of construction to achieve an improved response characteristic. This, the so-called interdigital filter (Figure 79), has multiple poles at the even harmonics. The improvement in operation, however, is not achieved with ease since the construction is difficult to accomplish in practice. This is a consequence of the short-circuited resonators which are a part of the structure and are important to the proper spectral distribution of the attenuation poles.

The two cases described are intended to illustrate the type of problems to be expected in carrying over conventional microwave techniques into integrated circuitry. The stripline RF short circuit is very difficult to achieve in practice, and there is no reason to believe that it will be any easier in integrated circuits. It has been cited here as an example of the kind of problem one may encounter in seeking the best possible filter operation.



34469

Figure 78. Third Harmonic Response of a Well-matched Stripline Filter



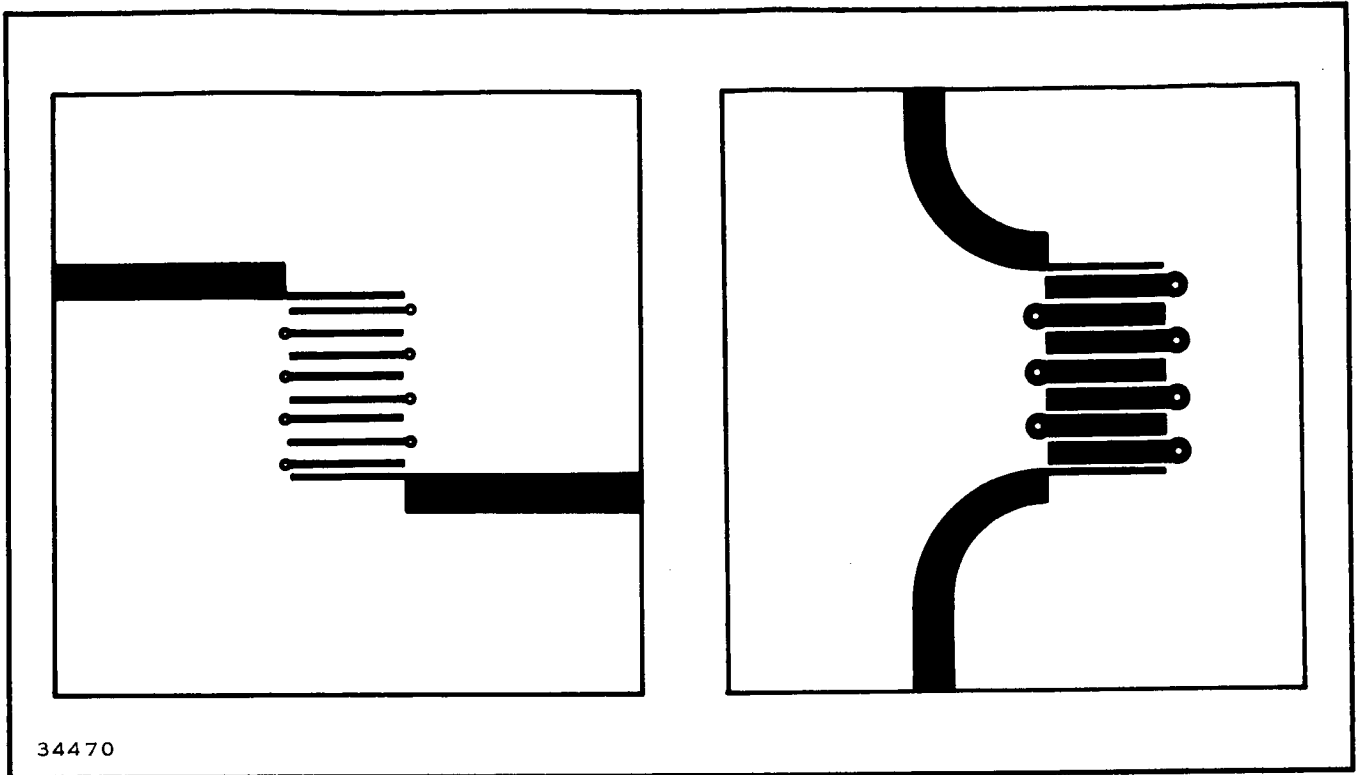
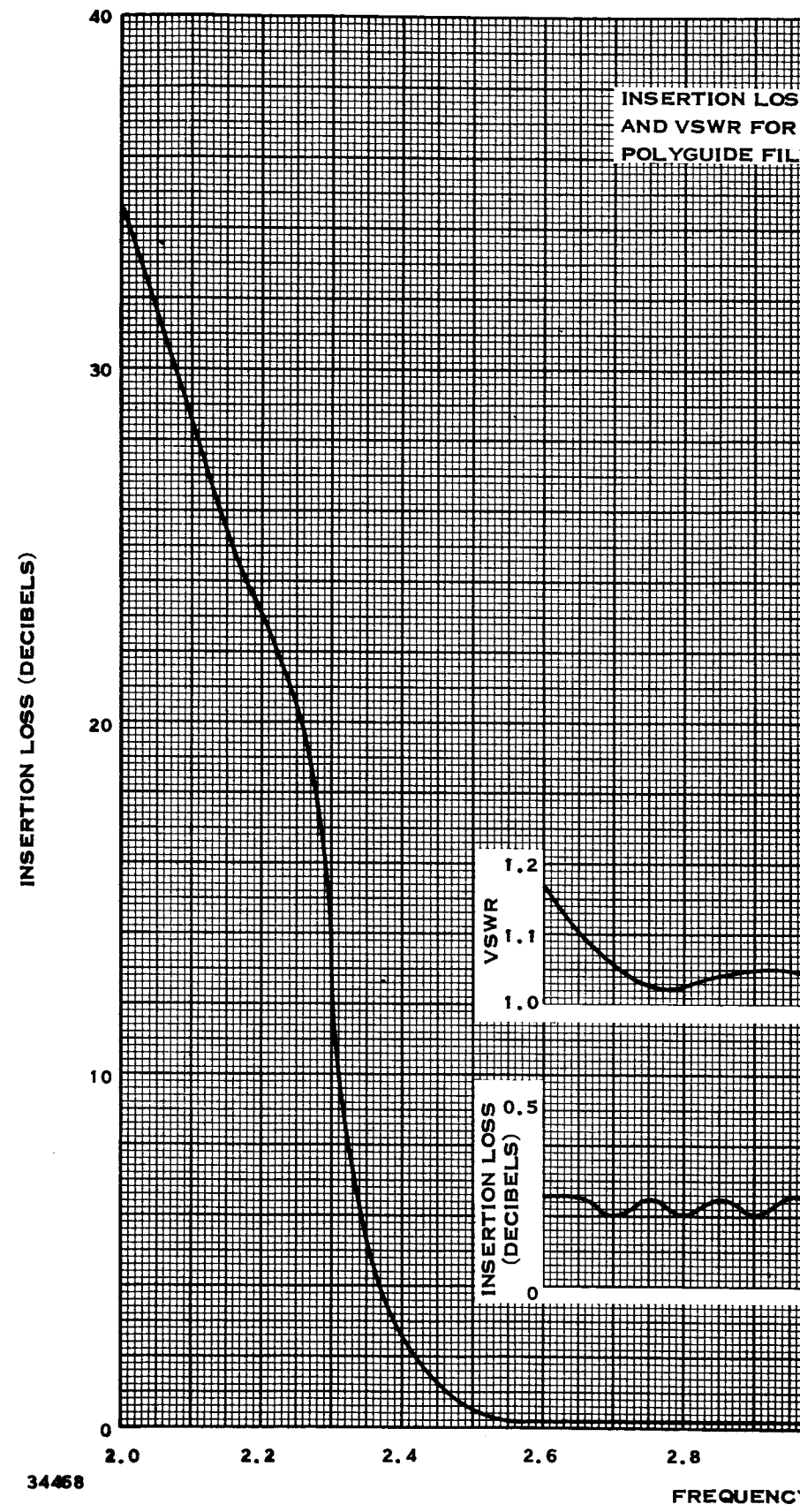


Figure 79. Interdigital Filter

Operational response characteristics are realistically typified by the curves in Figures 80 and 81 which are reproduced from experimental data obtained from a parallel-coupled, half-wave resonator filter and an interdigital filter respectively as discussed previously. Figure 80 shows that the parallel-coupled resonators afford an acceptable pass-band characteristic, but the out-of-band response, being very sensitive to the circuit loading, leaves something to be desired—especially at the second harmonic. On the other hand, the interdigital filter, Figure 81, shows a much better control of the stop-band. The superiority of this configuration in the range of the second harmonic and nearby is obvious. Further, the shape of the pass-band and the slope of the filter "skirts" at the band edges are greatly improved for the interdigital filter as compared to the simpler filter. This is a direct consequence of the multiple poles at the second harmonic of the attenuation function; the poles, in turn, are realized by virtue of the difficult construction of the stripline RF short circuit.



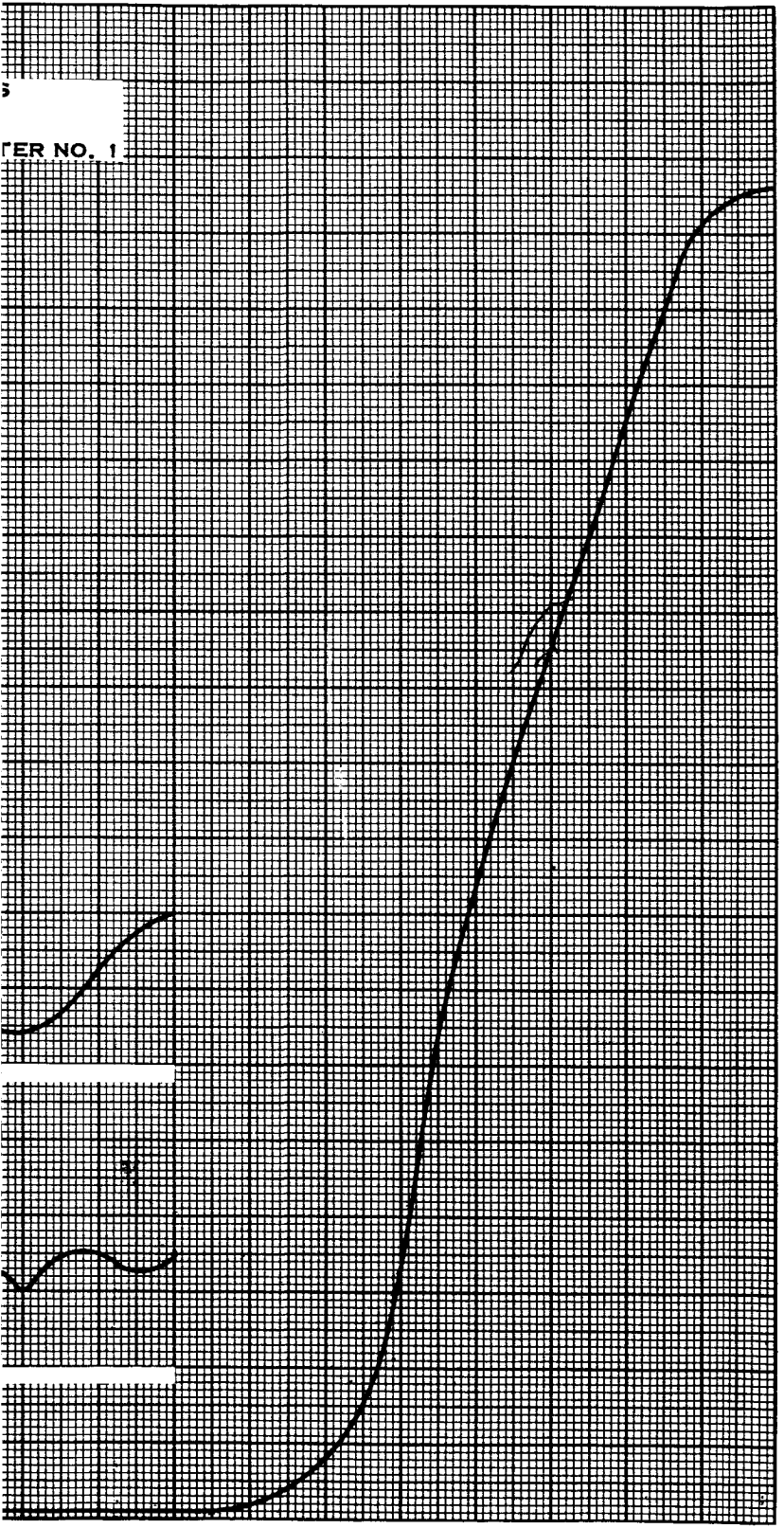
34468

FREQUENCY

Figure 77. Passband Resp

139①

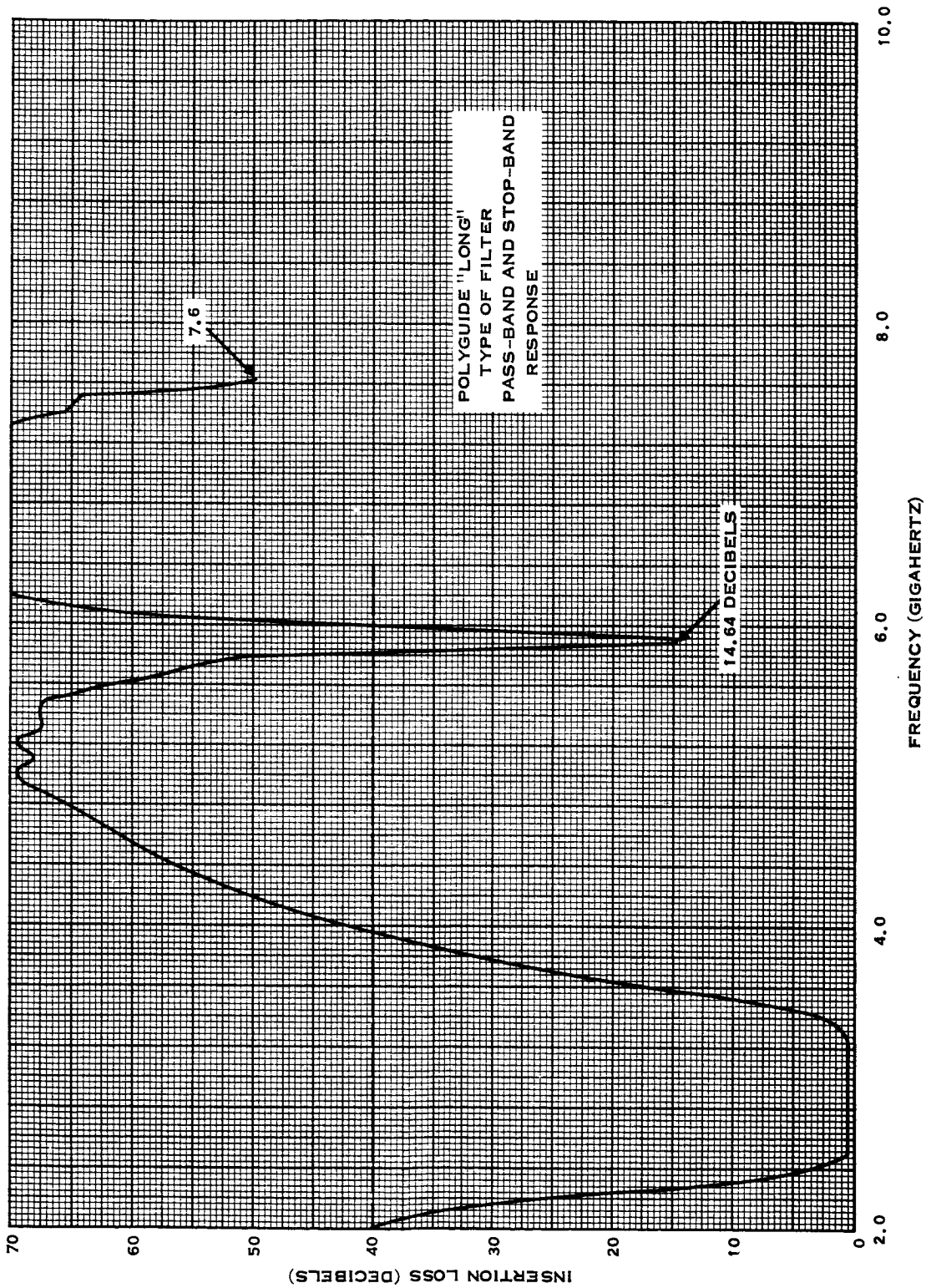
5  
FILTER NO. 1



3.0 3.2 3.4 3.6 3.8 4.0  
f (GIGAHERTZ)

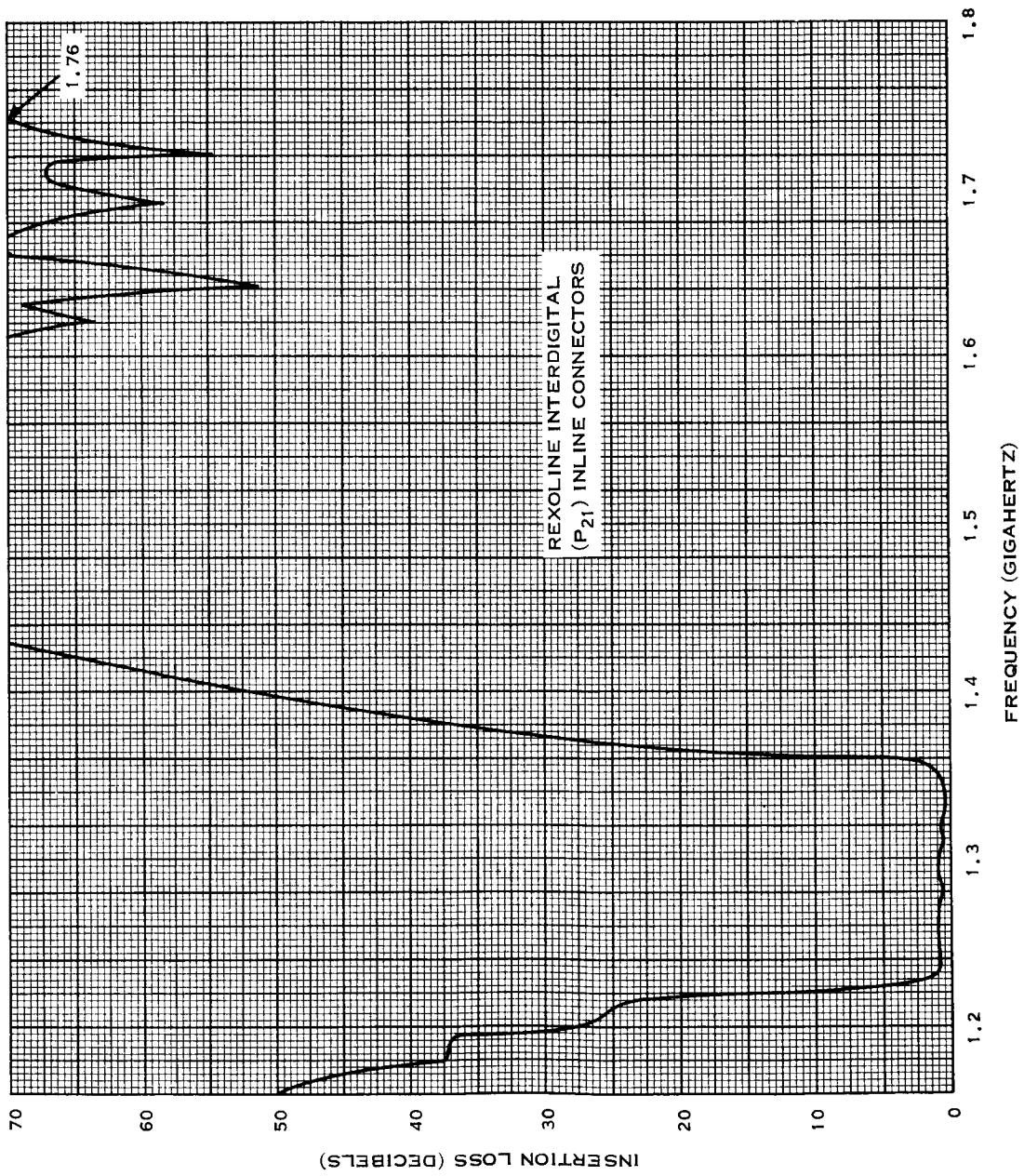
Response of a Well-matched Stripline Filter

140 (3)



34471

Figure 80. Wideband Response of an Experimental Parallel-coupled Half-wave Resonator Stripline Bandpass Filter



34472

Figure 81. Wideband Response of an Experimental Interdigital Stripline Bandpass Filter

SECTION XI  
PROGRAM PERSONNEL

<u>Name</u>	<u>Title</u>
Albert E. Mason, Jr.	Project Engineer
Louis I. Farber	Engineer

## SECTION XII

### CONCLUSION

Under item three of the work statement, an analysis of the technical parameters of the various components and techniques used in the FM telemetry transmitter, defined in item two, will be conducted. At that time, knowledge of the capabilities and limitations of the devices, techniques, and components which are the subject of this study will be required. Because of the rapid progress being made in microwave integrated circuits, it will be necessary to up-date the work covered in this report before finalizing the design of the transmitter. Nevertheless, this study of solid-state microwave devices, techniques, and components with application to integrated circuits has formed a basis for subsequent work to be performed under this contract.

## BIBLIOGRAPHY

1. H. F. Cooke, "Microwave Transistor Circuits," Microwaves, Vol. 3, Aug 1964.
2. E. G. Neilson, "Behavior of Noise Figure in Junction Transistors," Proc. IRE, Vol. 45, Jun 1959.
3. H. F. Cooke, "Transistor Noise Figure," Solid State Design, Vol. 4, Feb 1963.
4. Texas Instruments Incorporated, Molecular Electronics for Radar Applications, by T. M. Hyltin and L. R. Pfeifer, Jr., Interim Engineering Report No. 3, Contract AF 33(615)-1993, BPSN 4-6399-415906 and 5-674159-415906, Jul 1965.
5. Texas Instruments Incorporated, Molecular Electronics for Radar Applications, Research Contract Status Report No. 7, Contract AF 33(615)-1993, BPSN 4-6399-415906 and 5-674159-415906, May 1965.
6. B. T. Vincent, "Microwave Transistor Amplifier Design," G-MTT Symposium, 1965.
7. B. T. Vincent, "Large Signal Operation of Microwave Transistors," Correspondent to Editor, IEEE Trans. on MTT.
8. K. M. Eisele, R. S. Engelbrecht, and K. Kurokawa, "Balanced Transistor Amplifier for Precise Wideband Microwave Applications," Digest of Technical Papers, 1965 International Solid-state Circuits Conference.
9. W. G. Matthei, "Advances in Solid State Microwave Devices," Micro-wave Journal, Jul 1964.
10. J. Hamasaki, "A Wideband High-gain Transistor Amplifier at L-Band," Digest of Technical Papers, 1963 International Solid-state Circuits Conference, Feb 1963.
11. Texas Instruments Microlibrary, Communication Handbook, Pt. II, Chap. 5 and 6, 1965.
12. R. M. Barrett, "Microwave Printed Circuits—A Historical Survey," G-MTT Symposium, Mar 1955.
13. R. H. T. Bates, "Characteristic Impedance of the Shielded Slab Line," IRE PMGTT, Jan 1956.
14. J. M. Dukes, "The Application of Printed Circuit Techniques to the Design of Microwave Components," Inst. Elec. Eng., Aug 1957.
15. F. Assadourian and E. Rimai, "Simplified Theory of Microstrip Transmission Systems," Proc. IRE, Vol. 40, 1952, p. 1651.



16. D. Greig and H. Engelmann, "Microstrip—A New Transmission Technique for the Kilomegacycle Range," Proc. IRE, Vol. 40, Dec 1952, p. 1644.
17. J. A. Kostriza, "Microstrip Components," Proc. IRE, Vol. 40, Dec 1952, p. 1658.
18. J. H. Cash, R. L. Gower, "Fabrication of Microstrip Interconnections for Microwave Hybrid/Monolithic Circuits, Internal Paper, 29 Oct 1965.
19. E. Ginztor, Microwave Measurements, New York, McGraw-Hill, 1957.
20. Texas Instruments Incorporated, "Hybrid Study Task I of the MERA IF and RF Corporate Feed Manifold," Internal Report, 15 Oct 1965.
21. C. Bowness, "Strip Transmission Lines," Electronic Eng., Vol. 28, No. 335, Jan 1956, pp. 2-7.
22. T. M. Hyltin, "Microstrip Transmission on Semiconductor Dielectrics," G-MTT Symposium, 1965.
23. W. E. Fromm, "Characteristics and Some Applications of Stripline Components," G-MTT Symposium, Mar 1955.
24. M. Arditi, "Characteristics and Application of Microstrip for Microwave Wiring," G-MTT Symposium, Mar 1955.
25. M. Arditi and J. Elefant, "Characteristics of Microwave Printed Lines (Microstrip) with Application to the Design of Band-Pass Microwave Filters," IRE-ISU Meeting, 21-24 Apr 1952.
26. M. Arditi, "Characteristics and Application of Microstrip for Microwave Wiring," Proc IRE, Mar 1955.
27. H. E. Green, "The Numerical Solution of Some Important Transmission-Line Problems," IEEE MT&T, Sep 1965.
28. R. S. Clark and D. W. Brooks, "Thin-Film/Monolithic Circuits—How and When to Use Them," Electronic Des, 21 Dec 1964.
29. R. S. Clark, "Reactively Sputtered SiO<sub>2</sub> Capacitors," Trans. Metallurgical Soc. of AIME, Vol. 233, Mar 1965, pp. 592-596.
30. A. E. Feuersanger, "Titanium-Dioxide Dielectric Films Prepared by Vapor Reaction," Proc. IEEE, Vol. 52, Dec 1964, pp. 1463-1465.
31. J. W. Lathrop, "The Status of Monolithic and Thin Film Circuits," Electronic Ind., Vol. 24, Jun 1965, pp. 38-42.
32. Texas Instruments Incorporated, Molecular Electronics for Radar Applications, Research Contract Status Report No. 7, Contract AF 33(615)-1993, BPSN 4-6399-415906 and 5-674159-415906, May 1965.
33. H. G. Dill, "Designing Inductors for Thin-Film Applications," Electronic Des, 17 Feb 1964, p. 52.

34. F.E. Terman, Radio Engineer's Handbook, New York, McGraw-Hill, 1943, pp. 59-60.
35. Texas Instruments Incorporated, Molecular Electronics for Radar Applications, Contract AF 33(615)-1993, BPSN 4-6399-415906 and 5-674159-415906, Jan 1965.
36. L.J. Giacoletto and J. O'Connell, "A Variable Capacitance Germanium Diode for UHF," RCA Review, Mar 1956.
37. L.J. Giacoletto, "Junction Capacitance and Related Characteristics Using Graded Impurity Semiconductors," IRE Trans. on Electron Devices, Vol. ED-4, Jul 1957.
38. T. Fife, et al., "Some Reactive Effects in Forward Biased Junctions," IRE Trans. on Electron Devices, Vol ED-6, Jul 1959.
39. R. Fekete, "Varactors in Voltage Tuning Applications," Microwave J., Jul 1964.
40. C.H. Page, "Frequency Conversion with Positive Nonlinear Resistors," J. Res. NBS, Apr 1956.
41. P. Penfield, Jr., Frequency-Power Formulas, New York, The Technology Press and John Wiley & Sons, 1960.
42. J.M. Manley and H.E. Rowe, "Some General Properties of Nonlinear Elements—Part 1. General Energy Relations," Proc. IRE, Jul 1956.
43. P. Penfield, Jr. and R.P. Rafuse, Varactor Applications, MIT Press, Cambridge, Mass., 1962.
44. Texas Instruments Incorporated, Molecular Electronics for Radar Applications, by T.M. Hylltin and L.R. Pfeifer, Jr., Interim Engineering Report No. 3, Contract AF 33(615)-1993, BPSN 4-6399-415906 and 5-674159-415906, Jul 1965.
45. R.W. Burns and L. Stark, "Pin Diode Advances High-Power Phase Shifting," Microwaves, Nov 1965.
46. W.G. Matthei, "Advances in Solid State Microwave Devices," Microwave J., Jul 1964.
47. W.G. Matthei, "Advances in Solid State Microwave Devices," Microwave J., Aug 1964.
48. D. Leenov, "PIN Diode Microwave Switches and Modulators," Solid State Design/Communications and Data Equipment, Apr 1965.
49. D. Leenov, "PIN Diode Microwave Switches and Modulators," Solid State Design/Communications and Data Equipment, May 1965.
50. A. Ertel, "Surface Oriented Diodes for Microelectronic Applications," Presented to Electro-Chemical Society, 12 May 1965.

51. A. Ertel, "Microwave Evaluation of Surface Oriented Switching Diodes," International Electron Devices Meeting, Washington, D.C., 22 Oct 1965.
52. K. L. Kotzebue, "Optimum Noise Performance of Parametric Amplifier," Proc. IRE, Vol. 48, Jul 1960, pp. 1324-1325.
53. J. C. Sadler and W. E. Wells, "Cryogenically Cooled X-Band Parametric Amplifier," Proc IEEE, Vol. 52, No. 3, Mar 1964.
54. W. E. Wells, et al., "Planar Schottky Barrier Microwave Mixers and Varactors in Gallium Arsenide," Presented at International Electron Device Meeting, Washington, D.C., 20-22 Oct 1965.
55. J. B. Gunn, "Instabilities of Current in III-V Semiconductors," IBM J. Res. Dev., Vol. 8, Apr 1964, pp. 141-159.
56. T. E. Hasty, P. A. Cunningham, and W. R. Wisseman, Microwave Oscillations in Epitaxial Layers of GaAs, Technical Report 08-65-131, 9 Sep 1965.
57. B. W. Hakki and S. Knight, "Phenomenological Aspects of CW Microwave Oscillators in GaAs," Solid State Communications, Vol. 3, 1965, pp. 89-91.
58. N. Braslau, J. B. Gunn, and J. S. Staples, "Continuous Microwave Oscillations of Current in GaAs," IBM J. Res and Dev., Vol. 8 1964, pp. 545-546.
59. W. G. Matthei, "Advances in Solid State Microwave Devices," Microwave J., Aug 1964.
60. E. O. Ammann and R. J. Morris, "Tunable, Dielectric-Loaded Microwave Cavities Capable of High Q and High Filling Factor," IEEE Trans on Microwave Theory and Techniques, Vol. MTT-11, Nov 1963, pp. 528-542.
61. A. Okaya and L. F. Barash, "The Dielectric Microwave Resonator," Proc IRE, Vol. 50, Oct 1962, pp. 2081-2092.
62. S. B. Cohn, "Microwave Filters Containing High-Q Dielectric Resonators," G-MTT Symposium, May 1965, pp. 49-53.
63. A. Okaya, "The Rutile Microwave Resonator," Proc. IRE (correspondence), Vol. 48, Nov 1960, p. 1921.
64. R. V. D'Aiello and H. J. Prager, "Dielectric Resonators for Microwave Applications," IEEE Trans. on Microwave Theory and Techniques (correspondence), Vol. MTT-12, Sep 1964, pp. 549-550.
65. H. Y. Yee, "Natural Resonant Frequencies of Microwave Dielectric Resonators," IEEE Trans. on Microwave Theory and Techniques (correspondence), Vol. MTT-13, Mar 1965, p. 256.

66. D. L. Rebsch, D. C. Webb, R. A. Moore, and J. D. Cowlshaw, "A Mode Chart for Accurate Design of Cylindrical Dielectric Resonators," IEEE Trans. on Microwave Theory and Techniques (correspondence), Vol. MTT-13, Jul 1965, pp. 468-469.
67. L. Thourel, The Use of Ferrites at Microwave Frequencies, New York, The Macmillan Co., 1964.
68. R. F. Soohoo, Theory and Application of Ferrites, New York, Prentice-Hall, 1960.
69. L. S. Nergaard and M. Glicksman, Microwave Solid-State Engineering, New York, D. Van Nostrand, 1964.
70. P. J. B. Clarricoats, Microwave Ferrites, John Wiley and Sons, 1961.
71. B. Lax and K. Button, Microwave Ferrites and Ferrimagnetics, McGraw-Hill, 1962.
72. C. D. Owens, "A Survey of the Properties and Applications of Ferrites Below Microwave Frequencies," Proc. IRE, Oct 1956.
73. C. L. Hogan, "The Elements of Non-reciprocal Microwave Devices," Proc. IRE, Oct 1956.
74. B. Lax, "Frequency and Loss Characteristics of Microwave Ferrite Devices," Proc. IRE, Oct 1956.
75. G. S. Heller, "Ferrites as Microwave Circuit Elements," Proc. IRE, Oct 1956.
76. J. T. Bolljahn and G. L. Matthaei, "A Study of the Phase and Filter Properties of Arrays of Parallel Conductors Between Ground Planes," Proc. IRE, Vol. 50, Mar 1962.
77. G. L. Matthaei, L. Young, and E. M. T. Jones, Microwave Filters, Impedance-Matching Networks, and Coupling Structures, Sec. 10.02, New York, McGraw-Hill, 1964.
78. G. L. Matthaei, "Interdigital Band-Pass Filters," Trans. IRE, PGMTT-10, Nov 1962.

## LIST OF SYMBOLS

BW	bandwidth of bandpass amplifier
C	capacitance or capacitance per unit length
$C_c$	collector to base capacitance
$C_e$	emitter storage capacitance
$C_f$	fringing field capacitance per unit length, pF/m
$C_j$	junction capacitance (for varactors)
$C_{j0}$	junction capacitance at 0 volts (for varactors)
$C_p$	package capacitance (for varactors)
$C_{pp}$	parallel plate capacitance, pF/m
$C_t$	total capacitance measured at diode terminals (for varactors)
$C_t$	capacitance per unit area for a PN junction
D	plate spacing, cm (for striplines)
D	length of a side, mils (for coils)
F	noise figure
f	operating frequency
$f_\alpha$	frequency where $ \alpha  = \alpha_0/\sqrt{2}$
$f_{max}$	maximum frequency of oscillation
$f_o$	center frequency of bandpass amplifier
$f_o$	self-resonant frequency, GHz (for coils)
$f_T$	frequency for which the common emitter current gain is unity
$h_{fe}$	common emitter current gain
$I_{co}$	collector base cutoff current, mA
$I_E$	emitter current, mA
$jK'$	imaginary half period of sn (z)
K	real quarter period of sn (z)
k	modulus of the elliptic functions
L	inductance or inductance per unit length
$L_o$	low frequency inductance

$l$	length of transmission line, cm
$N$	net impurity concentration of lightly doped side of a junction
$N$	number of turns
$PG$	power gain
$P_o$	output power, watts
$Q$	quality factor for a reactive element
$Q_u$	unloaded $Q$
$q$	charge on the electron
$R_g$	source resistance
$r'_b$	base spreading resistance
$r_e$	emitter resistance
$S$	average length of a side, inches (for coils)
$t$	plate thickness, cm (for striplines)
$t$	conductor thickness, microinches (for coils)
$V_{bias}$	dc bias voltage
$V_p$	velocity of propagation
$V_t$	total voltage across a junction
$W$	center conductor strip width, cm
$w$	spiral line width, mils (for coils)
$Z_o$	characteristic impedance, ohms
$Z(z)$	Jacobian zeta function
$\alpha_o$	low-frequency, small-signal current gain for common base configuration
$\epsilon$	dielectric constant (equal to 1 for free space)
$\epsilon_o$	permittivity of free space
$\lambda$	wavelength, cm
$\lambda_o$	wavelength in free space, cm
$\mu$	relative permeability (equal to 1 for free space)
$\mu_o$	permeability of free space
$\mu^*$	complex permeability including loss term
$\sigma$	conductivity, mhos
$\phi$	contact potential